EMERGING INFECTIOUS DISEASES®

U.S. CENTERS FOR DISEASE CONTROL AND PREVENTION

Zoonotic Infections

December 2025

Compilation of Emerging Infectious Diseases covers, various artists, 2025. Digital design by Reginald Tucker.

EMERGING INFECTIOUS DISEASES®

Emerging Infectious Diseases is published monthly by the Centers for Disease Control and Prevention, 1600 Clifton Rd NE, Mailstop H16-2, Atlanta, GA 30329-4018, USA. Telephone 404-639-1960; email eideditor@cdc.gov

EMERGING INFECTIOUS DISEASES®

Zoonotic Infections **December 2025**

On the Cover

Compilation of *Emerging Infectious Diseases* covers, various artists, 2025. Digital design by Reginald Tucker.

About the Cover p. 2347

Synopses

Research

Medscape EDUCATION ACTIVITY

Dispatches

Research Letters

EMERGING INFECTIOUS DISEASES®
December 2025

Comment Letter

About the Cover

Online Report

Reemergence of Yellow Fever, Magdalena Valley, Colombia, 2024–2025

Jerson Andrés Cuéllar-Sáenz, Alfonso J. Rodríguez-Morales, Álvaro A. Faccini-Martínez

Yellow fever, a zoonotic arboviral disease, has re-emerged in Colombia, triggering a major outbreak in the country. During 2024 through mid-2025, a total of 132 human cases and 68 infections in nonhuman primates were confirmed, primarily in the department of Tolima, historically considered a low-risk area. We analyzed the historical and current epidemiology of yellow fever in Colombia, highlighting ecologic, social, and surveillance factors that contributed to the outbreak. Low vaccination coverage, insufficient epizootic and entomological surveillance, deforestation, habitat fragmentation, and limited application of One Health approaches have all exacerbated the situation. The high mortality rate of nonhuman primate species indicated a more profound ecologic crisis. Immediate, comprehensive measures, including mass vaccination, genomic surveillance, and integrated One Health frameworks, are urgently needed. Colombia's experience underscores the need to re-evaluate risk stratification and preparedness strategies across the Americas to prevent future yellow fever outbreaks in previously unaffected regions.

Yellow fever is an acute viral disease caused by an arbovirus (*Orthoflavivirus flavi*) of the genus *Flavivirus*. It is transmitted by vectors, specifically by hematophagous mosquitoes of the genera *Haemagogus* and *Sabethes* for the sylvatic cycle and *Aedes aegypti* for the urban cycle (*1*). As of 2025, there is no specific treatment for the disease; however, vaccination is an effective preventive measure (*2*).

Author affiliations: Universidad Nacional de Colombia, Bogotá, Colombia (J.A. Cuéllar-Sáenz); Pontificia Universidad Javeriana, Bogotá (J.A. Cuéllar-Sáenz); Faculty of Health Sciences, Universidad Científica del Sur, Lima, Peru (A.J. Rodríguez-Morales); Grupo de Investigación Biomedicina, Faculty of Medicine, Fundación Universitaria Autónoma de las Américas-Institución Universitaria Visión de las Américas, Pereira, Colombia (A.J. Rodríguez-Morales); Hospital Militar Central, Bogotá (Á.A. Faccini-Martínez); Universidad Militar Nueva Granada, Bogotá (Á.A. Faccini-Martínez)

DOI: https://doi.org/10.3201/eid3112.251209

Yellow Fever in the 19th and 20th Century

Yellow fever first appeared in Colombia during the 16th and 17th Centuries. The first documented epidemic cases occurred in Cartagena and Santa Marta in 1729; later cases were identified in soldiers arriving on the Atlantic coast from Spain (*3*). During 1830–1900, cases were reported in the Magdalena and Catatumbo Valleys, characterized by notable clinical and epidemiologic descriptions; the populations most affected were farmers, rainforest workers, soldiers, and railway workers. An outbreak in 1830 resulted in 1,800 deaths out of 4,000 inhabitants in Ambalema, Tolima Department (*4*). At the beginning of the 20th Century, outbreaks were reported in Soto's Valley (now in the Santander department) during 1910–1912 and in 1923 (Table 1) (*4*–*7*). Those cases were characterized as a sylvatic outbreak, with the presence of *Haemagogus* spp. mosquitoes (*5*). Until the 1930s, yellow fever cases were associated with *Ae. aegypti* mosquitoes as the vector; the paradigm shifted with Franco's work in Muzo in 1907 (*8*) and Soper's work in 1937 (*3*), which revealed that yellow fever infections in Colombia were part of the sylvatic cycle. In 1929, the last urban cases of the disease, which involves human–vector–human transmission through the bite of the *Ae. aegypti* mosquito, were reported in Socorro, Santander (Figure 1) (*9*).

Gast Galvis (*5*) analyzed 38,275 liver samples collected during 1934–1956, identifying 594 positive cases in the Amazon region, the foothills of the Eastern plains, the Magdalena Valley, and the Catatumbo River basin. The cases were not clinically diagnosed before death. Limited information is available on cases collected during the remaining years of the 20th Century (Table 2) (*10*–*13*).

Table 1. Years of reported cases of yellow fever in Colombia, by department, during the 19th and early 20th Centuries noted in study of reemergence of yellow fever in Colombia, 2024–2025*

Department	Years
Antioquia	1915, 1934–1956
Atlántico	1872, 1889, 1912
Bolívar	1856, 1865, 1866, 1872, 1885, 1912, 1915, 1934–1956
Boyacá	1906, 1907, 1916, 1923, 1924, 1934–1956
Caldas	1915, 1934–1956
Caquetá	1934–1956
Casanare	1919–1923, 1934–1956
Cesar	1934–1956
Cundinamarca	1857, 1865, 1879, 1880, 1884, 1885, 1889, 1910, 1934–1956
Huila	1881
La Guajira	1945
Magdalena	1887
Meta	1934–1956
Norte de Santander	1880, 1883, 1884,1886, 1887, 1888, 1900, 1907, 1934–1956
Putumayo	1934–1956
Quindío	1934–1956
Santander	1900, 1910–1912, 1919, 1923, 1929, 1934–1956
Tolima	1830, 1857, 1858, 1870, 1871, 1872, 1879, 1880, 1881, 1884, 1934–1956
Valle del Cauca	1881, 1907, 1915, 1920

*Sources: Gast Galvis (*4*), Gast Galvis (*5*), Boshell Manrique (*6*), Gast Galvis (*7*). An expanded version of this table showing cases by municipality is available online (https://wwwnc.cdc.gov/EID/article/31/12/25-1209-T1.htm).

Yellow Fever in the 21st Century

During 2000–2023, Colombia reported 216 confirmed cases of yellow fever in the departments of Norte de Santander, Magdalena, Guajira, Vichada, Meta, Caquetá, Putumayo, Guaviare, Chocó, Amazonas, Guainía, Vaupés, and Santander (Table 3) (*14*,*15*). An outbreak occurred in the Catatumbo region of the Norte de Santander department and the Sierra Nevada de Santa Marta region (comprising the César, La Guajira, and Magdalena departments); of 216 cases, 102 (46%) occurred in 2003 and 31(14%) in 2004 (*9*,*16*). The mortality rate was 44% in 2003 and 36% in 2004. Both Colombia and Venezuela used vaccination to control the outbreak on their shared border (*17*).

The Tolima department (within the Magdalena Valley) had no historical reports during 2000–2024; therefore, it was not considered a high-risk region for yellow fever (*2*). Nevertheless, 7 cases were confirmed in October 2024 in neighboring villages in the southwestern part of the Bosque de Galilea Regional Natural Park, which includes areas of 4 municipalities in Tolima (Cunday, Prado, Villarrica, and Purificación) on the border with the Huila and Cundinamarca departments (*18*). The Tolima department was classified as low stratification risk in accordance with the national plan for the prevention and control of yellow fever in Colombia during 2017–2022 (*2*).

As of September 18, 2025, a total of 132 confirmed cases of yellow fever had been reported during 2024–2025 in Colombia, distributed across 10 departments: Tolima (n = 112 cases), Putumayo (n = 8), Meta (n = 3), Caquetá (n = 2), Nariño (n = 2), Vaupés (n = 1), Caldas (n = 1), Cauca (n = 1), Huila (n = 1), and Guaviare (n = 1) (Table 4; Figure 1) (*19*). Those cases represent an estimated incidence of 2.51 cases/1 million population for Colombia (0.25 cases/100,000 population), with higher values for the most affected municipalities (e.g., 382.6 cases/100,000 population in Villarica, Tolima) (Table 4); case-fatality rate was 39.4%, and cumulative mortality rate was 0.99 deaths/1,000,000 population (*19*). Most cases were observed among persons residing in rural areas who have not received the vaccination; median age was 45 years, and sex distribution was 27 women and 105 men (*19*). In contrast, the virus has been confirmed in 68 nonhuman primates (NHPs) in 4 departments: 51 cases in Tolima, 8 in Huila, 8 in Putumayo, and 1 in Meta (*19*). To contain this outbreak, the Ministerio de Salud y Protección Social of Colombia, by Resolution 691 of 2025, declared a health emergency throughout the country and adopted measures for infection prevention and control (*20*). The measures included declaration of a public health emergency, mass vaccination campaigns, intensified vector control, strengthened epidemiologic and epizootic surveillance, and community risk communication, although coverage remained below optimal levels and thus insufficient to fully contain transmission.

Perspectives

For decades, yellow fever has been a public health threat in the Americas because of its emergence and reemergence (*21*). At the same time, it has been recognized that Colombia has an underreported rate, which makes analyzing and controlling cases difficult (*10*). For some time, the importance of improving studies and vigilance regarding vectors (*Aedes* spp., *Haemagogus* spp., and *Sabethes* spp. mosquitoes) and nonhuman primate reservoirs (*Alouatta* spp., *Saimiri* spp., *Ateles* spp., *Aotus* spp., *Callithrix* spp., *Brachyteles* spp., *Callicebus* spp., *Leontopithecus* spp., and *Sapajus* spp. monkeys) has been highlighted, as well as the ecologic characteristics of regions with medium or high risk in Colombia to strengthen vigilance systems (*22*,*23*). Unfortunately, epizootic and vector surveillance are only considered after outbreaks in some cases. Therefore, strong surveillance has been implemented since the ongoing outbreak (*24*).

NHPs are considered natural sentinel species for the early detection of yellow fever epidemics.

NHPs have a clinical course and mortality rate similar to those experienced by humans, and they have a substantial epidemiologic nexus in areas where outbreaks occur. A One Health perspective would consider NHPs' conservation, the ecosystems in which they coexist with humans, and the effects of climate change on vector distribution (*25*). In Colombia, the distribution of *Ae. aegypti* mosquitoes in densely populated urban centers, coupled with the presence of *Haemagogus* and *Sabethes* mosquito species in sylvatic corridors, creates overlapping transmission zones that vary by ecosystem. At the same time, NHPs such as howler monkeys (*Alouatta* spp.), spider monkeys (*Ateles* spp.), and squirrel monkeys (*Saimiri* spp.) act as reservoirs and sentinel hosts; deaths in those animal populations often precede human cases. Those ecologic dynamics are especially evident in departments such as Tolima, Putumayo, and Caquetá, where expanding agricultural frontiers, deforestation, and human settlement bring humans into closer contact with vectors and primate reservoirs, underscoring how ecosystem-specific interactions directly shape the distribution and risk for yellow fever outbreaks across the country. Such outbreaks have been associated with relevant declines in NHP populations, which endanger mammalian biodiversity and influences the epidemiologic behavior of yellow fever (*26*).

In 2025, Brazil, Colombia, Peru, and Bolivia reported cases or outbreaks outside the Amazon region, including cases in other ecologic corridors or ecosystems (*27*). That information is particularly important in the context of the correlation between deforestation, habitat fragmentation, and the destruction of NHPs' habitats because those factors increase contact between humans and NHPs and affect the ecology of emerging infectious diseases (*28*). Approximately 38 species of NHPs are found in Colombia, and 10 of these species are endemic; their populations have declined from deforestation for illegal logging, expansion of the agricultural frontier, use for illicit crops, and mineral extraction, among other factors (*2*,*29*,*30*). At the same time, Colombia has recognized the correlation between deforestation and armed conflict; that social aspect should be studied more deeply (*31*).

As for other emerging infectious diseases, ecologic disruptions could generate changes in the transmission, epidemiology, and distribution of yellow fever in the region (*32*). On the other hand, social determinants play a key role in yellow fever outbreaks, as they do in other neglected tropical diseases. In Colombia, reported cases are correlated with indigenous peoples, agricultural workers, deforested regions, and zones of armed conflict (*2*,*33*).

Since October 2024, Colombia has been experiencing a significant yellow fever outbreak, characterized by sylvatic cycle transmission and a large number of deaths in humans and NHPs in the department of Tolima, compared with the low national vaccination coverage of 64% among persons 1–59 years of age during 1996–2024. In Tolima, vaccination coverage was <50% for the 15–59 age group (*34*). A similar outbreak occurred in Brazil during 2016–2018, which mainly affected unvaccinated persons in areas that were not considered endemic for yellow fever (*35*). That outbreak marked a high number of human and NHP deaths from this virus since 1980 (*35*).

Measures to contain outbreaks of yellow fever include achieving vaccination coverage of >95% in at-risk areas and strengthening entomological and epizootic surveillance, vector control, and risk communication (*36*). Surveillance of epizootics through illness and death rates in NHPs in medium- or high-risk areas is a measure that contributes to the early detection of potential outbreaks before

Figure. Departments of Colombia that have reported cases of yellow fever. Green indicates historical cases of yellow fever during the 19th and early 20th Centuries, yellow indicates cases during the current 2024–2025 outbreak, and orange indicates cases during both periods.

Table 2. Numbers of reported cases of yellow fever in Colombia during 1956–1999 noted in study of reemergence of yellow fever in Colombia, 2024–2025*

Years	Cases
1956–1962	ND
1963	10
1964	10
1965	2
1966	3
1967	5
1968	11
1969	7
1970	7
1971	9
1972	3
1973	16
1974	36
1975	12
1976	22
1977	9
1978	105
1979	51
1980	11
1981	7
1982	2
1983	1
1984	16
1985	4
1986–1999	5

*Sources: Segura et al (*10*), Pan American Health Organization (*11–13*). ND, no data.

human cases appear (*37*). In addition, Brazil has analyzed the importance of genomic epidemiology in understanding the dynamics and spatial corridor of the yellow fever outbreak in southern Brazil (*38*).

Table 3. Numbers of reported cases of yellow fever in Colombia during 2000–2023 noted in study of reemergence of yellow fever in Colombia, 2024–2025*

Year	Cases
2000	5
2001	8
2002	20
2003	102
2004	31
2005	20
2006	5
2007	7
2008	3
2009	5
2010	0
2011	0
2012	0
2013	1
2014	0
2015	0
2016	7
2017	0
2018	1
2019	0
2020	0
2021	0
2022	0
2023	2
Total cases	216

*Source: Instituto Nacional de Salud de Colombia (*14,15*).

Colombia must incorporate genomic surveillance to clarify the circulating lineages of the virus and their relationship with vaccination coverage and eco-epidemiology in different territories. Lessons learned would be applied to other nations in South America also facing similar challenges from ongoing outbreaks of yellow fever (*39*).

To translate those ideas into practice, we propose a package of complementary strategies that health authorities can adopt during and after the current outbreak. First, sustained genomic surveillance of circulating yellow fever strains should be institutionalized to detect viral lineages, mutations, and transmission pathways in real time. Second, permanent One Health monitoring networks that integrate human, primate, and vector data must be established, enabling early detection of epizootics and vector expansion across ecologic corridors (*40*). Third, vaccination strategies should be adapted to include not only historically high-risk areas but also regions newly exposed to yellow fever because of deforestation, migration, and climate change; coverage should be sustained above the 95% threshold. Finally, those measures should be supported by intersectoral collaboration of public health, environmental, and veterinary authorities to provide a coordinated response that strengthens preparedness and resilience.

Discussion

The resurgence of yellow fever in Colombia during 2024–2025, particularly in the Magdalena Valley region, underscores the enduring threat of this arboviral disease in South America. Although yellow fever is a vaccine-preventable illness, the outbreak has exposed major gaps in Colombia's public health infrastructure, especially regarding vaccination coverage, vector and epizootic surveillance, and One Health preparedness. The outbreak through mid-2025, centered in the department of Tolima, represents a significant yellow fever outbreak in Colombia in the 21st Century with 132 confirmed human cases and 68 confirmed infections in NHPs. The crisis reflects both historical patterns and novel ecologic and epidemiologic dynamics shaped by deforestation, habitat disruption, climate change, and sociopolitical factors.

Historically, Colombia has faced recurrent yellow fever outbreaks since colonial times, with notable occurrences in the 19th and 20th Centuries. However, the assumption that some regions, such as Tolima, were at low or negligible risk for yellow fever has proven dangerously misleading. That misclassification hindered preventive measures such as proactive vaccination campaigns, epizootic surveillance, and

vector control programs in areas now recognized as vulnerable. The reappearance of yellow fever in Tolima, a region not historically associated with high yellow fever transmission in the 21st Century, reiterates the critical importance of adopting dynamic, data-driven risk stratification models that reflect ecologic changes and disease emergence patterns.

The current outbreak demonstrates the consequences of delayed and reactive public health responses. Although Colombia's Ministry of Health declared a public health emergency in 2025, the measures came only after widespread transmission among both humans and NHPs. This delayed response highlights a persistent weakness in the integration of One Health approaches, which emphasize early detection through sentinel species monitoring, particularly among NHP populations that share ecologic niches with human communities. The lack of sustained surveillance of illness and deaths in NHPs as well as vector densities is a missed opportunity to anticipate and prevent the current outbreak.

In addition, the intersection of ecologic degradation and yellow fever transmission cannot be ignored. Deforestation, habitat fragmentation, and the displacement of NHPs have brought vectors, wildlife, and humans into closer contact, intensifying the likelihood of spillover events. Those environmental pressures, coupled with the expansion of agricultural frontiers and illicit economies, have drastically altered the eco-epidemiology of yellow fever. Armed conflict further complicates access to vaccination and healthcare in many affected regions, especially in rural and indigenous communities. Those social determinants of health must be addressed as integral components of disease control strategies. We propose an integrated framework that links genomic surveillance, One Health monitoring of NHPs and vectors, and systematic evaluation of socioecologic drivers such as deforestation, land-use change, and armed conflict, thereby offering a robust scientific basis for anticipating, preventing, and more effectively responding to yellow fever outbreaks in Colombia.

The low national yellow fever vaccination coverage—64% among those 1–59 years of age and <50% in Tolima for adults 15–59 years of age—constitutes a major vulnerability. This situation mirrors the Brazil outbreak of 2016–2018, when low immunization in areas previously deemed low-risk enabled widespread transmission. Colombia must urgently reassess its vaccination policies and implement a robust, nationwide campaign targeting not only known endemic areas but also ecologically sensitive regions currently undergoing anthropogenic change.

Table 4. Reported cases of yellow fever in Colombia, by department and municipality, noted in study of reemergence of yellow fever in Colombia, 2024–2025*

Location	No. cases	No. cases/100,000 population
Tolima	112	
Villarica	20	382.6
Cunday	19	215.9
Prado	17	192.8
Ataco	26	129.3
Dolores	4	46.3
Rioblanco	7	29.9
Purificación	7	29.1
Valle de San Juan	1	18.0
Chaparral	8	14.6
Palocabildo	1	10.2
Espinal	1	1.3
Ibagué	1	0.2
Putumayo	8	
Villagarzón	2	7.4
Orito	4	5.3
San Miguel	1	4.6
Valle del Gamuez	1	1.9
Caquetá	2	
El Doncello	1	2.4
Cartagena del Chairá	1	1.2
Nariño	2	
Ipiales	2	1.6
Meta	3	
La Macarena	1	3.4
San Martín	1	3.1
Granada	1	1.3
Vaupés	1	
Mitú	1	2.9
Caldas	1	
Neira	1	4.6
Cauca	1	
Piamonte	1	10.2
Huila	1	
Campoalegre	1	3.0
Guaviare	1	
San José del Guaviare	1	1.8
Total cases	132	

*Source: Instituto Nacional de Salud de Colombia (*19*). Total no. cases is as of September 18, 2025.

Conclusions

Moving forward, Colombia must institutionalize a truly intersectoral One Health approach that integrates ecologic, veterinary, and human health surveillance systems. Strengthening genomic epidemiology capacities is also imperative for tracking yellow fever viral lineages, assessing transmission pathways, and monitoring vaccine escape or mutation events. Those actions, combined with risk communication and community engagement, will enhance outbreak preparedness and foster long-term resilience.

Beyond its human toll, the current outbreak has important economic implications. Many of the affected regions overlap with areas of agricultural production, oil extraction, and mining, sectors that are central to Colombia's national economy. Interruptions in labor productivity caused by illness or

death, combined with restrictions in high-risk zones, can reduce output and generate losses. In addition, tourism, particularly ecotourism in natural parks and forested areas such as Tolima and the Amazon, is susceptible to travel advisories and public perceptions of risk, which could cause declines in both domestic and international visitor numbers. Those effects highlight that yellow fever is not only a health issue but also a threat to economic stability and development. If outbreaks are perceived as undermining income and productivity, particularly in extractive and service industries, political motivation to strengthen vaccination, surveillance, and vector control may increase. Yet, sustained preparedness requires more than reactive measures; it demands continuous allocation of resources from national budgets, complemented by international cooperation and multilateral support, to build resilient One Health infrastructure capable of preventing future crises.

In summary, the current yellow fever outbreak in Colombia is both a public health emergency and a warning. It reflects a failure to learn from historical precedent and to act on mounting ecologic and epidemiologic signals. Colombia, and other South America nations facing similar risks, must prioritize preventive vaccination, entomological and epizootic surveillance, ecologic preservation, and equitable healthcare access. Without decisive action, the cycle of emergence, devastation, and reactive response will persist, putting both human and animal populations at continued risk.

About the Author

Dr. Cuéllar-Sáenz is a veterinarian and researcher in the Veterinary Parasitology Group at the Universidad Nacional de Colombia, as well as a master's degree student in Public Health at Pontificia Universidad Javeriana. His research interests include tropical zoonotic diseases, parasites, and the sociohistorical approach to these topics through a One Health framework.

References

1. World Health Organization. Yellow fever. 2023 [cited 2025 Nov 22]. https://www.who.int/news-room/fact-sheets/detail/yellow-fever
2. Ministerio de Salud y Protección Social de Colombia. Guideline for comprehensive clinical care of yellow fever in Colombia [in Spanish]. 2024 [cited 2025 Nov 22]. https://www.minsalud.gov.co/sites/rid/Lists/BibliotecaDigital/RIDE/VS/PP/ET/lineamiento-atencion-clinica-integral-fiebre-amarilla-2024.pdf
3. Patiño Camargo L. Notes on yellow fever in Colombia [in Spanish]. Rev Fac Med (Caracas). 1937;6:211–81. https://revistas.unal.edu.co/index.php/revfacmed/article/view/23549
4. Gast Galvis A. History of yellow fever in Colombia [in Spanish]. Bogotá: Imprenta del Instituto Nacional de Salud; 1982.
5. Gast Galvis A. Incidence of yellow fever in different areas of Colombia [in Spanish]. Bol Oficina Sanit Panam OSP. 1958;44.
6. Boshell Manrique J. Report on wild yellow fever in the Meta region, from July 1934 to December 1936 [in Spanish]. Rev Fac Med (Caracas). 1938;6:407–27. https://revistas.unal.edu.co/index.php/revfacmed/article/view/24090
7. Gast Galvis A. Examination results of the first 5,000 human liver samples obtained in Colombia for the study of yellow fever [in Spanish]. Rev Fac Med (Caracas). 1941;10:87–112. https://revistas.unal.edu.co/index.php/revfacmed/article/view/25974
8. Corredor Arjona A. Yellow fever in Colombia: a seminal investigation [in Spanish]. Rev Salud Publica (Bogota). 1999;1:137–51.
9. Instituto Nacional de Salud de Colombia. Study of a yellow fever outbreak in Caquetá, 2005 [in Spanish]. Inf Quinc Epidemiol Nac. 2006;11:329–44.
10. Segura ÁM, Cardona D, Garzón MO. Trends in yellow fever mortality, Colombia, 1998–2009 [in Spanish]. Biomedica. 2013;33(Suppl 1):52–62.
11. Pan American Health Organization. Reported cases of notifiable diseases in the Americas, 1964 [in Spanish]. 1966 [cited 2025 Nov 22]. https://iris.paho.org/handle/10665.2/47821
12. Pan American Health Organization. Yellow fever in the Americas. PAHO Epidemiol Bull. 1980 [cited 2025 Nov 22]. https://iris.paho.org/handle/10665.2/46432
13. Pan American Health Organization. Yellow fever in the Americas, 1981–1985. Bol Epidemiol. 1986;7:1–2.
14. Instituto Nacional de Salud de Colombia. Yellow fever in Colombia, 2000–2019 [in Spanish]. Boletín Epidemiológico Semanal. Report no. 4. 2020 [cited 2025 Nov 22]. https://www.ins.gov.co/buscador-eventos/BoletinEpidemiologico/2020_Boletin_epidemiologico_semana_4.pdf
15. Instituto Nacional de Salud de Colombia. Event report: yellow fever [in Spanish]. 2025 Mar 22 [cited 2025 Nov 22] https://www.ins.gov.co/buscador-eventos/Informesdeevento/FIEBRE%20AMARILLA%20PE%20III%202025.pdf
16. Sanchez-Rojas IC, Solarte-Jimenez CL, Chamorro-Velazco EC, Diaz-Llerena GE, Arevalo CD, Cuasquer-Posos OL, et al. Yellow fever in Putumayo, Colombia, 2024. New Microbes New Infect. 2025;64:101572.
17. Pan American Health Organization. National profile of yellow fever in Colombia [in Spanish]. 2022 [cited 2025 Nov 22]. https://iris.paho.org/bitstream/handle/10665.2/56910/OPSFPLIM0039_spa.pdf?sequence=1&isAllowed=y
18. Instituto Nacional de Salud de Colombia. SIVICAP Evaluation of chemical and microbiological risk in drinking water in Colombia, 2023 [in Spanish]. Boletín Epidemiológico Semanal. Report no. 43. 2024 [cited 2025 Nov 22]. https://www.ins.gov.co/buscador-eventos/BoletinEpidemiologico/2024_Boletin_epidemiologico_semana_43.pdf
19. Instituto Nacional de Salud de Colombia. Measles and rubella: epidemiological behavior of integrated surveillance [in Spanish]. Boletín Epidemiológico Semanal. Report no. 37. 2025 [cited 2025 Nov 22]. https://www.ins.gov.co/buscador-eventos/BoletinEpidemiologico/2025_Boletin_epidemiologico_semana_37.pdf
20. Ministerio de Salud y Protección Social de Colombia. Resolution 691 of 2025. Through which a health emergency is

declared throughout the national territory due to the outbreak caused by the yellow fever virus, and measures are adopted for its prevention and control [in Spanish]. 2025 [cited 2025 Nov 22]. https://www.minsalud.gov.co/Normatividad_Nuevo/Resolucion%20No%20691%20de%202025.pdf
21. Perez LJ, Perez-Restrepo LS, Ciuoderis K, Usuga J, Moreno I, Vargas V, et al. Emergence, persistence, and positive selection of yellow fever virus in Colombia. Front Microbiol. 2025;16:1548556.
22. Piedrahita-Cortés J, Soler-Tovar D. Geographical distribution of the red howler monkey (*Alouatta seniculus*) and yellow fever in Colombia. Biomedica. 2016;36:116–24.
23. Hernández-Galvis J, Pizarro AB, Cuestas JA, Castañeda-Cardona C, Rosselli D. Yellow fever in Colombia: from public calamity to neglected disease. Acta Med Peru. 2018;35:55–9.
24. Instituto Nacional de Salud de Colombia. Yellow fever [in Spanish]. Boletín Epidemiológico Semanal. Report no. 4. 2024 [cited 2025 Nov 22]. https://www.ins.gov.co/buscador-eventos/BoletinEpidemiologico/2024_Bolet%C3%ADn_epidemiologico_semana_4.pdf
25. Nederlof RA, Virgilio T, Stemkens HJJ, da Silva LCCP, Montagna DR, Abdussamad AM, et al. Yellow fever in non-human primates: a veterinary guide from a One Health perspective. Vet Sci. 2025;12:339.
26. Berthet M, Mesbahi G, Duvot G, Zuberbühler K, Cäsar C, Bicca-Marques JC. Dramatic decline in a titi monkey population after the 2016–2018 sylvatic yellow fever outbreak in Brazil. Am J Primatol. 2021;83:e23335.
27. Organización Panamericana de la Salud. Epidemiological update on yellow fever in the Americas Region [in Spanish]. 2025 [cited 2025 Nov 22]. https://www.paho.org/sites/default/files/2025-04/2025-abril-24-phe-actualizacion-epidemiologica-fiebre-amarilla-final.pdf
28. Aliaga-Samanez A, Real R, Segura M, Marfil-Daza C, Olivero J. Yellow fever surveillance suggests zoonotic and anthroponotic emergent potential. Commun Biol. 2022;5:530.
29. Cruz-Rodríguez C, Noguera-Urbano E, Olaya-Rodríguez MH. Henao-Díaz LF, Guzmán-Caro DC, Ochoa-Quintero JM, et al. Primates and deforestation in Colombia. Alexander von Humboldt Biological Resources Research Institute. 2019 [cited 2025 Nov 22]. https://reporte.humboldt.org.co/biodiversidad/2019/cap2/204
30. Henao Diaz F, Stevenson P, Carretero-Pinzón X, Castillo-Ayala C, Chacón Pacheco J, Defler T, et al. Biodiversity atlas of Colombia. Primates. Alexander von Humboldt Biological Resources Research Institute. 2020 [cited 2025 Nov 22]. https://biomodelos.humboldt.org.co/atlas/Primates.pdf
31. García Botero R; Instituto Colombo-Alemán para la Paz. Deforestation and armed conflict in Colombia: considerations and recommendations. San Francisco: Academia; 2024.
32. McMichael AJ. Environmental and social influences on emerging infectious diseases: past, present and future. Philos Trans R Soc Lond B Biol Sci. 2004;359:1049–58.
33. Tuells J, Henao-Martínez AF, Franco-Paredes C. Yellow fever: a perennial threat. Arch Med Res. 2022;53:649–57. https://doi.org/10.1016/j.arcmed.2022.10.005
34. Ministerio de Salud y Protección Social de Colombia. Technical and operational guidelines for the national yellow fever vaccination campaign in the susceptible population aged 15 to 18 years in Colombia. 2024 [cited 2025 Nov 22]. https://www.minsalud.gov.co/sites/rid/Lists/BibliotecaDigital/RIDE/VS/PP/PAI/lineamientos-tecnicos-operativos-jonada-nacional-vacunacion-fiebre-amarilla-15-18-anos.pdf
35. Santos JD, Rocha KLS, Amaral CD, Dutra AGS, Figueiredo PO, Rocha-Vieira E, et al. The yellow fever outbreak in Brazil (2016–2018): how a low vaccination coverage can contribute to emerging disease outbreaks. Microorganisms. 2025;13:1287.
36. Pan American Health Organization. Epidemiological alert yellow fever in the Americas Region—31 May 2025. 2025 [cited 2025 Nov 22]. https://www.paho.org/en/documents/epidemiological-alert-yellow-fever-americas-region-31-may-2025
37. Bonilla-Aldana DK, Bonilla-Aldana JL, Castellanos JE, Rodriguez-Morales AJ. Importance of epizootic surveillance in the epidemiology of yellow fever in South America. Curr Trop Med Rep. 2025;12:1–9. https://doi.org/10.1007/s40475-025-00349-z
38. Giovanetti M, Pinotti F, Zanluca C, Fonseca V, Nakase T, Koishi AC, et al. Genomic epidemiology unveils the dynamics and spatial corridor behind the yellow fever virus outbreak in southern Brazil. Sci Adv. 2023;9:eadg9204. https://doi.org/%2010.1126/sciadv.adg9204
39. Rodriguez-Morales AJ, Alhazmi AH, Katime A, Hameed AA, Morales A, Lepetic AC, et al.; SLAMVI, ESGITM, EVASG, ALEIMC, GEPI-SEIMC, SEMEVI, and CMTZMV-ACIN. Yellow fever in South America—a plea for action and call for prevention also in travelers from SLAMVI, ESGITM, EVASG, ALEIMC, GEPI-SEIMC, SEMEVI, and CMTZMV-ACIN. Travel Med Infect Dis. 2025;67:102871. https://doi.org/10.1016/j.tmaid.2025.102871
40. Sanchez-Rojas IC, Bonilla-Aldana DK, Solarte-Jimenez CL, Bonilla-Aldana JL, Belisario-Tovar M, Ortega-Gómez S, et al. Fatal yellow fever among captive non-human primates in southern Colombia, 2025. Front Vet Sci. 2025;12:1655474. https://doi.org/10.3389/fvets.2025.1655474

Address for correspondence: Álvaro A. Faccini-Martínez, Servicio de Infectología, Hospital Militar Central, Tv. 3C No. 49–02, Bogotá, Colombia; email: afaccini@gmail.com, afaccini@homil.gov

Two Concurrent Outbreaks of *Listeria monocytogenes* Infections Linked to Packaged Salads, United States, 2014–2022

Alexandra Palacios,[1] Michael Vasser,[1] Asma Madad, Stranjae' Ivory, Lauren Edwards, Danielle Donovan, Tiffany Greenlee, Tim Muruvanda, Joseph Baugher, Kurt Nolte, Annemarie Buchholz, Karen Blickenstaff, Mabel Low, Grace Pederson, Jasmine Huffman, Carrie Crabtree, Colby Brown, Meghan Hamel, Rima Kandar, Erin Szidonya, Hannah Caird, Katie Cibulskas, Brandi Taylor, Jodi Taylor, Yamir Rosa, Laura Gieraltowski, Amanda Conrad

We describe 2 genetically unrelated outbreaks of *Listeria monocytogenes* infections (outbreak A and outbreak B) linked to packaged salads from 2 different firms that were investigated simultaneously in 2021. Combined, the outbreaks caused 30 illnesses, 27 hospitalizations, and 4 deaths over 8 years. Those investigations led to recalls of product from 2 different firms and highlight how *L. monocytogenes* contamination can persist for long periods and cause illnesses over many years. Outbreak A was investigated 3 times with illnesses occurring over 8 years, whereas illnesses in outbreak B occurred over 5 years. Both outbreaks illustrate the importance of routine and epidemiologically directed sampling by state partners, without which these outbreaks likely would have gone unsolved. The outbreaks were the second and third multistate outbreaks of listeriosis linked to packaged salads, providing further documentation of the potential for *L. monocytogenes* infections from consumption of contaminated packaged salads.

Before 2015, listeriosis outbreaks linked to produce items in the United States were linked to melons, sprouts, and celery. At least 1 sporadic listeriosis case in 2014 and 1 binational listeriosis outbreak in 2015–2016 were linked to packaged salads (*1*). We describe an unusual situation of 2 genetically unrelated outbreaks of *Listeria monocytogenes* infection in the United States (outbreak A and outbreak B), investigated simultaneously in late 2021, that were linked to packaged salads from 2 different firms. Of those outbreaks, 1 also included genetically related cases in Canada. The Centers for Disease Control and Prevention (CDC) and Public Health Agency of Canada (PHAC) regularly exchange information when an outbreak has potential to span national borders.

Listeria can survive in production facilities or environments for long periods. Listeriosis outbreak investigations often span multiple years before a food vehicle is identified because of harborage in a production facility or persistent contamination levels in the environment or product, resulting in seemingly sporadic illnesses over long periods (*2*,*3*). Evidence of contamination in California watersheds connected to a major leafy green production region was described in a 2014 study conducted by the US Department of

Author affiliations: Centers for Disease Control and Prevention, Atlanta, Georgia, USA (A. Palacios, M. Vasser, M. Low, G. Pederson, J. Huffman, L. Gieraltowski, A. Conrad); US Food and Drug Administration, College Park, Maryland, USA (A. Madad, S. Ivory, T. Greenlee, T. Muruvanda, J. Baugher, K. Nolte, A. Buchholz, K. Blickenstaff); Michigan Department of Agriculture and Rural Development, Lansing, Michigan, USA (L. Edwards); Michigan Department of Health and Human Services, Lansing (D. Donovan): Georgia Department of Agriculture, Atlanta (C. Crabtree, C. Brown); Public Health Agency of Canada, Ottawa, Ontario, Canada (M. Hamel, R. Kandar); National Microbiology Laboratory, Winnipeg, Manitoba, Canada (E. Szidonya); British Columbia Centre for Disease Control, Vancouver, British Columbia, Canada (H. Caird); Ohio Department of Health, Columbus, Ohio, USA (K. Cibulskas, B. Taylor); Ohio Department of Agriculture, Reynoldsburg, Ohio, USA (J. Taylor, Y. Rosa)

DOI: https://doi.org/10.3201/eid3112.250989

[1]These first authors contributed equally to this article.

Agriculture (USDA) (*4*) (hereafter referred to as the USDA study), in which investigators found that *L. monocytogenes* was prevalent in 43% of all environmental samples. When water isolates from that study are related to clinical isolates by whole-genome sequencing (WGS), that link gives investigators a clue that leafy greens or other produce grown in that region could be a source of illness.

In listeriosis outbreaks, epidemiologic information is often limited because of relatively low case numbers, long incubation periods, and severity of illness. Patients might be older, have poor food recall, or be too sick to provide food exposure information. Listeriosis outbreaks can take longer to solve than foodborne outbreaks caused by other pathogens and might rely on product or environmental sampling (*5*,*6*). This activity was reviewed by CDC, deemed not research, and conducted consistent with applicable federal law and CDC policy (e.g., 45 C.F.R. part 46.102(l)(2), 21 C.F.R. part 56; 42 U.S.C. §241(d); 5 U.S.C. §552a; 44 U.S.C. §3501 et seq.).

Methods

Case Definition

An outbreak A case was defined as invasive listeriosis in a patient from whom an isolate was collected during August 16, 2014–January 15, 2022, and related to the outbreak A strain within 0–21 allele differences by whole-genome multilocus sequence typing (wgMLST). An outbreak B case was defined as invasive listeriosis in a patient whose isolate was collected during July 26, 2016–October 19, 2021, and related to the outbreak B strain within 0–7 allele differences by wgMLST.

Epidemiologic Data

The *Listeria* Initiative is a national surveillance system coordinated by CDC that collects clinical, demographic, and food exposure data for all listeriosis cases (*7*). State and local health departments interview patients or surrogates about foods eaten in the 28 days before their illness. CDC conducts case–case analyses using SAS version 9.4 (SAS Institute Inc., https://www.sas.com) to compare foods eaten by outbreak patients to foods eaten by sporadic listeriosis patients not associated with an outbreak from the same states. Supplemental questionnaires are deployed to collect more specific product information. Investigators also request records from stores reported by patients for a comprehensive purchase history. PHAC uses similar methods to investigate listeriosis outbreaks (*6*).

Laboratory Methods

PulseNet USA, CDC's national molecular subtyping network for enteric disease surveillance, detects clusters of *L. monocytogenes* when 3 clinical isolates related by 0–25 allele differences by wgMLST occur within 120 days (*8*). For strains with genetic diversity, CDC might narrow the allele range to ≤10 (*9*). Sequencing results and analysis were performed using BioNumerics version 7.6.3 (bioMérieux, https://www.biomerieux.com). All sequenced isolates are uploaded to the National Center for Biotechnology Information (NCBI) Pathogen Detection pipeline (https://www.ncbi.nlm.nih.gov/pathogens). Before the use of wgMLST, pulsed-field gel electrophoresis was performed on isolates uploaded during 2014–2018. Canada uses similar laboratory methods to detect clusters but with narrower criteria (*6*).

Samples of leafy green products, water, or environmental swabs were collected using standard practices and analyzed them for *L. monocytogenes* using the US Food and Drug Administration (FDA) Bacteriological Analytical Manual (https://www.fda.gov/food/laboratory-methods-food/bacteriological-analytical-manual-bam). FDA and firm isolates underwent WGS analysis using the CFSAN SNP Pipeline (*10*).

Sampling

State and local public health partners conduct routine surveillance sampling and epidemiologically directed sampling. Routine sampling is done at regular intervals, independently from outbreak investigations. In Michigan Department of Agriculture and Rural Development (MDARD) routine sampling, inspectional and laboratory staff collect samples for microbiological testing. During a sampling event, inspectors obtain samples of high-risk or empirically driven commodities to test for *Salmonella*, *Listeria*, and Shiga toxin–producing *Escherichia coli*. The Georgia Department of Agriculture (GDA) Retail Risk-Based Surveillance Program uses a set schedule for retail inspectors to obtain samples from retail locations for laboratory testing during routine inspections.

Epidemiologically directed sampling is conducted in multistate outbreaks when investigators suspect a food vehicle as the source of an outbreak but require additional laboratory evidence to link illnesses to a product. Officials visit retail locations reported by patients to sample suspected foods identified through interviews or collected records.

Traceback

The FDA conducts traceback in multistate outbreaks using previously described methods (*11*) to determine

whether suspected food products come from a common source. FDA conducts full-scope Preventive Controls for Human Food inspections at processing facilities of interest, which require facilities to have food safety plans, including hazard analysis and risk-based preventive controls. Inspections also include collecting traceability records and samples.

Results

Outbreak A

2019–2020

On January 28, 2019, PulseNet detected a cluster of *L. monocytogenes* clinical isolates related within 0–10 allele differences by wgMLST. Epidemiologic information was insufficient to identify a source, and the investigation was closed on April 12, 2019; a total of 5 cases were identified in 5 states (Iowa, Maryland, Ohio, Pennsylvania, and Texas).

On December 10, 2019, after PulseNet identified 4 additional cases related within 0–10 allele differences by wgMLST to the previous cases, CDC opened a second investigation. PHAC identified 2 cases highly related to the outbreak strain in 2 Canada provinces. One Canada patient reported consuming brand X packaged coleslaw. Packaged salad exposure information was unavailable for the second case. Grocery store locations were shared with the Canadian Food Inspection Agency, which confirmed that brand X packaged coleslaw, sourced from a US processing facility, was available for purchase before the patient's illness onset.

Packaged salads were the most reported exposure among US patients; a leafy greens supplemental questionnaire was deployed. All 5 patients reported consuming packaged salads. Among 3 patients who recalled the brand names of packaged salad, 2 patients reported brands of packaged salad produced by firm X and 1 reported packaged salad from retail chain K. No patients reported consuming coleslaw. Compared with sporadic cases, a case–case analysis showed outbreak case-patients were more likely to have consumed packaged salads before illness (odds ratio [OR] 24.14 [95% CI 4.33–∞]).

The Ohio Department of Agriculture conducted epidemiologically directed sampling and collected 31 samples of packaged salads at retail locations reported by patients. Sampling did not yield *L. monocytogenes*, but *L. welshimeri* was isolated from retail chain K–brand packaged coleslaw produced by firm X's Ohio facility. The presence of *Listeria* bacteria suggested that conditions were also suitable for survival and growth of *L. monocytogenes* (*12*). On the basis of those sampling results and patient geographic distribution, FDA collected records and samples from firm X facilities in North Carolina and Ohio in January 2020. No food safety observations of concern were noted during the Ohio facility inspection. The North Carolina facility inspection noted issues related to identifying preventive controls, monitoring sanitation controls, written procedures for monitoring process controls, and inadequate design, cleaning, and maintenance of equipment and utensils. *L. monocytogenes* was not detected in samples. One coleslaw sample collected at firm X's Ohio facility yielded *L. welshimeri*.

Epidemiologic data suggested that packaged salads produced by firm X could have been the source of illness but were not confirmed as the cause. Investigators closed the second investigation on February 10, 2020, after no additional illnesses were identified. The outbreak yielded a total of 11 cases from 8 US states (Iowa, Maryland, North Carolina, Ohio, Oregon, Pennsylvania, Texas, and Wisconsin) and 2 Canada provinces with specimen collection dates during August 16, 2014–November 20, 2019.

2021

On October 18, 2021, GDA conducted routine sampling unrelated to the outbreak investigation and identified *L. monocytogenes* in brand X packaged garden salad produced at firm X's North Carolina facility. Firm X voluntarily recalled packaged garden salad products on October 29, 2021 (*13*).

On November 1, 2021, CDC opened the investigation a third time when PulseNet identified 7 additional cases. Interviews and record review showed that 10 of 11 patients with exposure information (91%) reported eating packaged salads. Of 4 patients who had brand information, 3 reported consuming brand X and 1 reported consuming brand Y. On December 3, 2021, sequencing showed the brand X packaged garden salad isolate collected by GDA was highly related to the outbreak strain within 0–18 allele differences by wgMLST. To determine whether contaminated product was still on the market, MDARD conducted epidemiologically directed sampling at retail locations, including a store where a patient purchased packaged salad, and collected 37 samples. On December 21, 2021, MDARD identified *L. monocytogenes* in a bag of brand X packaged iceberg lettuce produced in firm X's Arizona facility. The isolate was highly related to the outbreak strain within 0–18 allele differences by wgMLST.

By investigation closure, the outbreak included 20 cases from 13 states (Iowa, Idaho, Maryland,

Michigan, Minnesota, North Carolina, Nevada, Ohio, Oregon, Pennsylvania, Texas, Utah, and Wisconsin) (Figure 1) and 2 Canadian provinces. Specimens were collected during August 16, 2014–January 15, 2022 (Figure 2). Age range was 50–94 (median 76) years; 17/20 case-patients were women. Seventeen patients were hospitalized, and 3 died. No illnesses were associated with pregnancy.

Traceback and Inspection

Because of limited exposure information, FDA did not conduct formal traceback analysis. Products associated with any single firm X facility could not account for the geographic distribution of patients in the outbreak. On the basis of additional illnesses, *L. monocytogenes*–positive samples collected by GDA and MDARD, and other investigational information, FDA ultimately conducted inspections at firm X facilities in Arizona, California, North Carolina, and Ohio. Firm X also initiated an internal investigation that included collecting product and environmental samples. FDA inspections at the 4 firm X facilities involved collection of 60 product and environmental samples. FDA sampling did not yield *L. monocytogenes*, but *L. welshimeri* and *L. innocua* were detected in 1 environmental sample and *L. innocua* were detected in 1 finished product sample, both collected from the North Carolina facility.

Control Measures

On December 21, 2021, after the sample collected by MDARD yielded *L. monocytogenes*, firm X halted production at their North Carolina and Arizona facilities. On December 22, 2021, firm X voluntarily recalled all brand X and private-label packaged salads processed at the 2 facilities (*14*). CDC and FDA published announcements on December 22, 2021, warning consumers not to eat recalled products (*15*,*16*).

Firm X conducted a root-cause analysis to determine the source of the lettuce contamination and, in particular, to determine how 2 bags of packaged salads, produced 7 weeks apart in separate facilities, could contain the same strain of *L. monocytogenes*. That analysis was further complicated because iceberg lettuce in the salads was sourced from different regions. Firm X identified a common harvest rig used to harvest the iceberg lettuce in both packaged products collected by GDA and MDARD; environmental swab specimens from the harvest rig yielded the outbreak strain. Firm X's root-cause analysis concluded the contaminated harvest rig harbored the outbreak strain and the

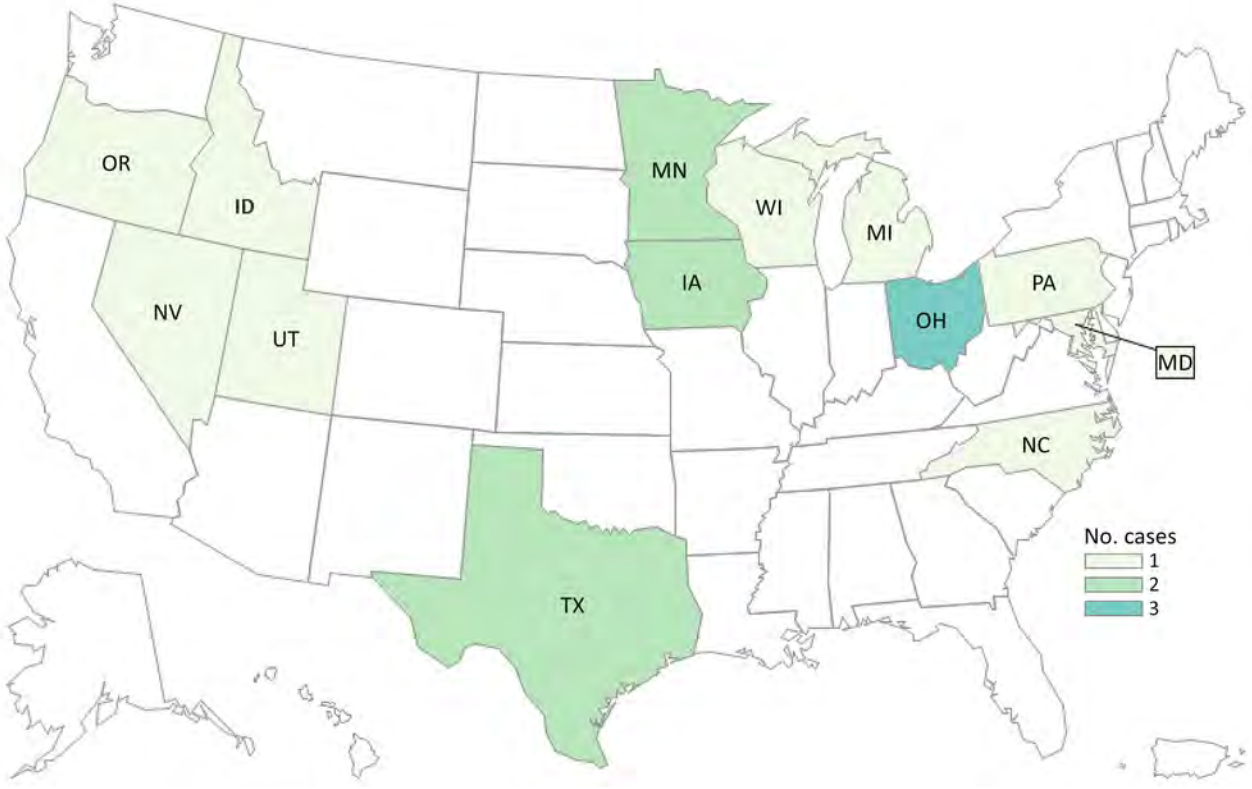

Figure 1. Cases of *Listeria monocytogenes* infection in outbreak A (n = 18), by state of residence, in study of 2 concurrent outbreaks linked to packaged salads, United States, 2014–2022. Colors indicate number of cases per state.

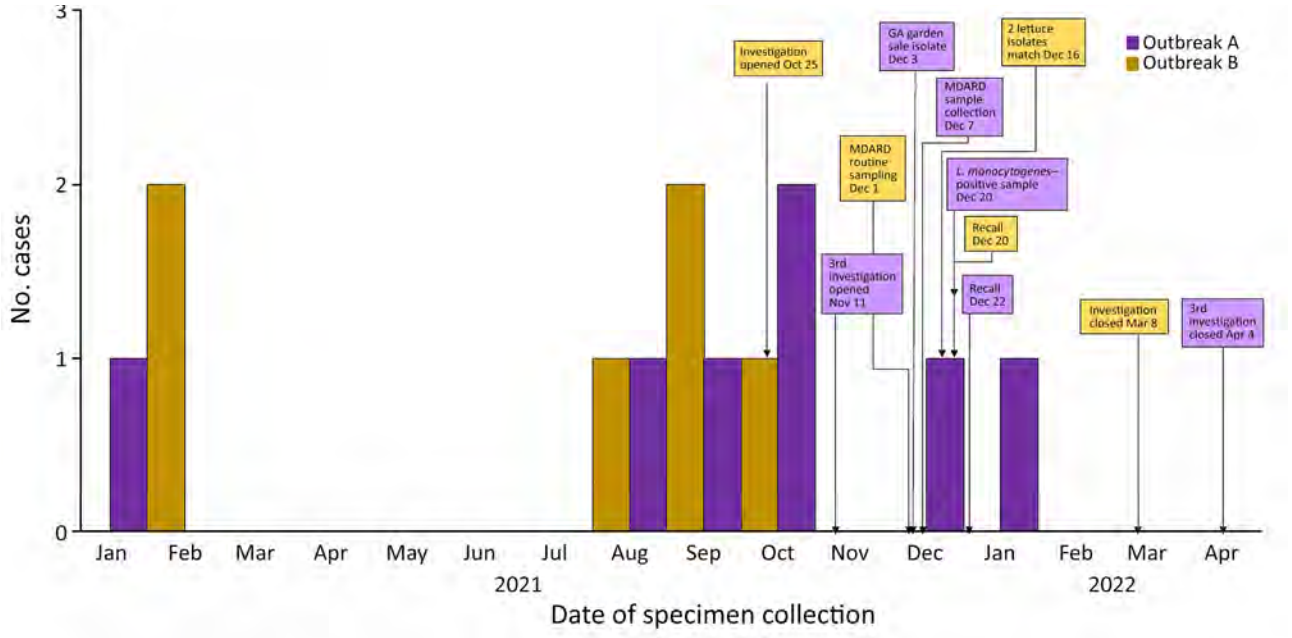

Figure 2. Epidemiologic curve and timeline for 2 outbreaks of *Listeria monocytogenes* infections linked to packaged salads, United States, 2021–2022 (n = 13 cases). Epidemiologic curve only shows US cases from outbreak A and B during 2021–2022. Both cases from Canada occurred in 2019. MDARD, Michigan Department of Agriculture and Rural Development.

harvest process enabled introduction into the supply chain (N. Dyenson, firm X, pers. comm., email, 2023 Apr 21). After the December 2021 recall, firm X conducted product sampling, which yielded the outbreak strain. FDA analysis verified genetic relatedness. On January 7, 2022, after identifying the outbreak strain on the harvest rig, firm X conducted an additional voluntary recall to include all brand X and private-label packaged salads containing iceberg lettuce processed at their Ohio and California facilities (*17*).

Firm X permanently decommissioned the harvest rig, developed enhanced sanitation protocols, and implemented measures to reduce contamination routes. Firm X also implemented WGS as a tool for early surveillance, integrated microbiological surveillance of incoming raw material, and proactively engaged industry colleagues. Firm X played a collaborative role with FDA and CDC during the outbreak investigation by providing regular updates related to their own investigation and sharing isolates and sequencing data.

Additional Laboratory Findings

Several *L. monocytogenes* water-sediment isolates from the USDA study were uploaded to the NCBI Pathogen Detection pipeline in 2020 and 2021 (*4*). Of 635 *L. monocytogenes* isolates identified, 72 were related within 35 alleles by wgMLST to outbreak A.

Outbreak B

2021

On October 22, 2021, PulseNet identified a cluster of 10 clinical isolates related within 1–6 allele differences by wgMLST. Investigators reviewed data in NCBI and found that the clinical isolates were in the same phylogenetic tree as water-sediment isolates collected as part of the USDA study (*4*). That finding led investigators to suspect a produce item as the source of illnesses given the foods grown in the Salinas Valley of California.

CDC conducted a case–case analysis and found exposure to carrots and exposure to herbs were statistically significant (OR 10.78 [95% CI 1.95–∞] for carrots, OR 14.71 [95% CI 1.65–179.39] for herbs). Of 5 patients with information, all reported exposure to carrots and 3 reported exposure to herbs. Packaged salad consumption was reported by 4 of 5 patients and was not significantly higher than the rate of consumption among sporadic cases. No common types or brands were reported. CDC continued to monitor for additional illnesses.

On December 1, 2021, MDARD collected 45 routine retail samples that included packaged salad products. On December 16, 2021, MDARD notified CDC of isolates that were related to the outbreak strain within 0–7 allele differences by wgMLST. The sample was from brand Z packaged romaine and butter lettuce salad

mix sourced from the Salinas Valley and produced by firm Z. At the time, only 1 patient reported consuming brand Z packaged iceberg lettuce. Two patients were reinterviewed using a supplemental questionnaire and their purchase records were collected.

By investigation closure, the outbreak included 10 cases from 8 states (Illinois, Massachusetts, Michigan, New Jersey, New York, Ohio, Pennsylvania, and Virginia) (Figure 3) and 2 food samples with isolates related within 0–7 allele differences by wgMLST. Specimen collection dates were July 16, 2016–October 19, 2021 (Figure 2). Patient age range was 44–95 (median 80) years; 6 of 10 case-patients were women. All 10 patients were hospitalized, and 1 patient died. No illnesses were associated with pregnancy. Four of five patients reported consuming packaged salads; 4 included iceberg and 3 included romaine. Two patients reported consuming brand Z products: 1 reported packaged iceberg lettuce and the other a salad kit containing romaine and baby spinach. No genetically related illnesses were identified in Canada.

Traceback and Inspection

In December 2021, FDA initiated a traceback investigation. Because of limited exposure information, only the positive sample collected by MDARD was included in the traceback analysis. On the basis of harvest date information associated with the production code of the positive sample, 3 growers and their 4 respective fields were identified. Because of comingling at firm Z's Illinois facility, products from each of those fields were used to manufacture the positive sample collected by MDARD.

FDA conducted an environmental investigation at firm Z's Illinois facility focused on environmental swabbing and review of sanitation practices, procedures, records, and corrective actions. During the inspection, 100 swabs were collected; all were negative for *Listeria* spp.

Control Measures

Upon notice of MDARD's positive sample and the related outbreak, firm Z halted production and initiated a complete sanitation review at their Illinois facility. On December 20, 2021, firm Z voluntarily recalled certain varieties of its branded and private-label salad products produced at the Illinois facility (*18*). Recalled product was sent to distributors and wholesalers in the midwestern and northeastern United States and 2 Canada provinces. Product distribution aligned

Figure 3. Cases of *Listeria monocytogenes* infection in outbreak B (n = 10), by state of residence, in study of 2 concurrent outbreaks linked to packaged salads, United States, 2014–2022. Colors indicate number of cases per state.

with geographic location of patients in the outbreak. Firm Z's root cause investigation and environmental monitoring did not identify the source of contamination but informed corrective actions.

CDC and FDA published communications on December 22, 2021, warning consumers not to eat recalled products (*19*). CDC closed the investigation on March 8, 2022, after no new illnesses were identified.

Additional Laboratory Findings

Isolates in outbreak B are a rare *L. monocytogenes* sequence type (ST), 639, and exhibit a propensity for water (*20*). The strain was previously found in watersheds from the Salinas Valley (*4*). ST639 was not previously implicated in outbreaks where a source of illness was identified. Of the 4 fields identified in the traceback investigation, 1 was located in the same county where the strain was identified in California watersheds.

Discussion

Outbreaks A and B, both multistate outbreaks of listeriosis linked to packaged salads, are unique because they were investigated concurrently and highlight how illnesses can occur over multiple years because *L. monocytogenes* contamination can persist for long periods in the natural environment, on harvest equipment, and in the production environment. Outbreak A was investigated 3 times and illnesses occurred over 8 years, whereas illnesses in outbreak B occurred over 5 years. Both outbreaks illustrate the importance of routine and epidemiologically directed sampling by state partners, without which these outbreaks likely would have gone unsolved. Because *Listeria* can form biofilms and survive for extended periods in production facilities, contamination often occurs in the production environment (*12*). Listeriosis outbreak investigations do not commonly identify a root cause of contamination outside of a production environment, such as a specific farm or growing field. The steps firm X took to identify the exact harvest equipment contaminated with the outbreak A strain is a powerful example of data points companies can use to identify points of persistent contamination. Conversely, we speculate that outbreak B was likely caused by environmental contamination at a single production facility. Both outbreaks highlight the ongoing potential for *L. monocytogenes* infections as a result of consuming contaminated packaged salads, especially for high-risk consumers.

Water-sediment isolates collected in the USDA study (*4*) demonstrate the persistence of *Listeria* within an environment where produce is grown (*14*). The genetic relatedness of clinical isolates in the 2 outbreak strains and the California water-sediment isolates provide evidence that *Listeria* could be persistent in growing environments within the Salinas Valley. Environmental sampling and WGS provide insight into the potential source and scope of contamination during outbreaks, which underscores the value of widespread microbiologic sampling of watersheds nationally.

In both outbreaks, leafy green exposure was reported in interviews, but brand information and purchase records needed for regulatory efforts were limited. Relying on available exposure data alone would not have solved these outbreaks. Obtaining complete exposure information is challenging for listeriosis outbreaks because patients are severely ill or may have died. In those instances, a surrogate might be interviewed who has limited knowledge of the patient's food history. Patients themselves might have difficulty recalling food exposures and providing details like brands, purchase locations, and consumption dates when asked about foods eaten weeks or months before their illness. In the outbreaks described, packaged salad exposure was easily identified, but narrowing the source to a single firm was difficult because leafy green processors are often associated with multiple brands and can have similar packaging.

Given those limitations, routine and epidemiologically directed sampling efforts by GDA and MDARD were key to solving both outbreaks and provided laboratory evidence needed to justify regulatory inspections and product actions. Internal sampling, root cause analysis, and information sharing by firm X played a substantial role in outbreak A's investigation. Firm X encourages industry partners to leverage forms of routine early surveillance, including sampling raw materials and using WGS to compare isolates in NCBI. They also emphasize the importance of investigating outside the production facility, such as field or farm investigations, in response to outbreaks (N. Dyenson, firm X, pers. comm., email, 2023 Apr 21).

During 2015–2024, a total of 8 US listeriosis outbreaks were linked to packaged salads (4 suspected and 4 confirmed) (*21*). During January 2015–May 2024, FDA classified (i.e., the final determination of violation and risk) recalls of ≈240 packaged salad products because of potential contamination with *L. monocytogenes* (*22*,*23*). Responsibility for food safety occurs along the entire farm-to-fork continuum of growing, harvesting, processing, distribution, and preparation. Research shows both romaine and iceberg

lettuce can potentially internalize *L. monocytogenes* (*24*,*25*), in addition to the risk associated with colonization of *L. monocytogenes* during and after harvest. Although refrigerated storage supports the survival and growth of *L. monocytogenes* on both packaged and less processed leafy greens, packaged salads might be at higher risk for *L. monocytogenes* contamination than less processed leafy greens because they touch a higher number of surfaces and equipment during processing.

Outbreaks A and B caused 30 illnesses, 27 hospitalizations, and 4 deaths over 8 years. Those outbreaks provide further evidence of the ongoing risk for *Listeria* infections associated with packaged salad. Routine and epidemiologically directed sampling conducted by state partners solved these outbreaks, and the actions taken by both firms likely prevented additional illnesses and deaths. Actions taken by the firms provide examples of measures other producers can implement to identify and prevent contamination from harvest to packaging. Firms should consider WGS as a tool that can be leveraged to prevent illnesses. Sequencing pathogens identified within processing facilities can enhance internal microbial monitoring programs, enabling comparison of strains over time against known isolates or events in NCBI. Firms should consider applying a similar methodology to incoming raw material in processing facilities. Microbiological surveillance of incoming product could enable firms to identify potential risk before introducing pathogens into facilities. If foodborne pathogens are identified, firms should consider conducting internal root cause analysis both at the production facility and further upstream at harvesting sites. Leafy greens are part of a healthy diet, and more research should be done to identify improved production methods for preventing contamination.

Acknowledgments

We thank investigators at departments of health, public health laboratories, departments of agriculture, and departments of environmental health for their contributions from the following states: Idaho, Illinois, Iowa, Maryland, Massachusetts, Michigan, Minnesota, New Jersey, New York, North Carolina, Nevada, Ohio, Oregon, Pennsylvania, Texas, Utah, Virginia, and Wisconsin. We also thank investigators from the FDA Office of Inspections and Investigations. We extend our thanks to analogous agencies in Canada including the Public Health Agency of Canada, local and provincial public health authorities, provincial public health laboratories, the Enhanced National Listeriosis Surveillance Program, and the Canadian Food Inspection Agency.

About the Author

Ms. Palacios and Ms. Vasser are infectious disease epidemiologists in the Division of Foodborne, Waterborne, and Environmental Diseases, National Center for Emerging and Zoonotic Infectious Diseases, Centers for Disease Control and Prevention. Their work focuses on US foodborne outbreak investigation and response, particularly for illnesses caused by *Escherichia*, *Salmonella*, *Listeria*, and *Campylobacter*.

References

1. Jackson KA, Stroika S, Katz LS, Beal J, Brandt E, Nadon C, et al. Use of whole genome sequencing and patient interviews to link a case of sporadic listeriosis to consumption of prepackaged lettuce. J Food Prot. 2016; 79:806–9. https://doi.org/10.4315/0362-028X.JFP-15-384
2. Sullivan G, Orsi RH, Estrada E, Strawn L, Wiedmann M. Whole-genome sequencing-based characterization of *Listeria* isolates from produce packinghouses and fresh-cut facilities suggests both persistence and reintroduction of fully virulent *L. monocytogenes*. Appl Environ Microbiol. 2022;88:e0117722. https://doi.org/10.1128/aem.01177-22
3. Ferreira V, Wiedmann M, Teixeira P, Stasiewicz MJ. *Listeria monocytogenes* persistence in food-associated environments: epidemiology, strain characteristics, and implications for public health. J Food Prot. 2014;77:150–70. https://doi.org/10.4315/0362-028X.JFP-13-150
4. Cooley MB, Quiñones B, Oryang D, Mandrell RE, Gorski L. Prevalence of shiga toxin producing *Escherichia coli*, *Salmonella enterica*, and *Listeria monocytogenes* at public access watershed sites in a California Central Coast agricultural region. Front Cell Infect Microbiol. 2014;4:30. https://doi.org/10.3389/fcimb.2014.00030
5. Conrad AR, Tubach S, Cantu V, Webb LM, Stroika S, Moris S, et al. *Listeria monocytogenes* illness and deaths associated with ongoing contamination of a multiregional brand of ice cream products, United States, 2010–2015. Clin Infect Dis. 2023;76:89–95. https://doi.org/10.1093/cid/ciac550
6. Pereira E, Conrad A, Tesfai A, Palacios A, Kandar R, Kearney A, et al. Multinational outbreak of *Listeria monocytogenes* infections linked to enoki mushrooms imported from the Republic of Korea 2016–2020. J Food Prot. 2023;86:100101. https://doi.org/10.1016/j.jfp.2023.100101
7. Centers for Disease Control and Prevention. About the *Listeria* initiative [cited 2023 Dec 11]. https://www.cdc.gov/listeria/php/surveillance/listeria-initiative.html
8. Tolar B, Joseph LA, Schroeder MN, Stroika S, Ribot EM, Hise KB, et al. An overview of PulseNet USA databases. Foodborne Pathog Dis. 2019;16:457–62. https://doi.org/10.1089/fpd.2019.2637
9. Chen Y, Luo Y, Pettengill J, Timme R, Melka D, Doyle M, et al. Singleton sequence type 382, an emerging clonal group of *Listeria monocytogenes* associated with three multistate outbreaks linked to contaminated stone fruit, caramel apples, and leafy green salad. J Clin Microbiol. 2017;55:931–41. https://doi.org/10.1128/JCM.02140-16
10. Davis S, Pettengill JB, Luo Y, Payne J, Shpuntoff A, Rand H, et al. CFSAN SNP Pipeline: an automated method for constructing SNP matrices from next-generation sequence data. PeerJ Comput Sci. 2015;1:e20. https://doi.org/10.7717/peerj-cs.20

11. Irvin K, Viazis S, Fields A, Seelman S, Blickenstaff K, Gee E, et al. An overview of traceback investigations and three case studies of recent outbreaks of *Escherichia coli* O157:H7 infections linked to romaine lettuce. J Food Prot. 2021;84:1340–56. https://doi.org/10.4315/JFP-21-112
12. Townsend A, Strawn LK, Chapman BJ, Dunn LL. A systematic review of *Listeria* species and *Listeria monocytogenes* prevalence, persistence, and diversity throughout the fresh produce supply chain. Foods. 2021;10:1427. https://doi.org/10.3390/foods10061427
13. US Food and Drug Administration. Dole Fresh Vegetables announces precautionary limited recall of garden classic salads for possible contamination with *Listeria monocytogenes* [cited 2021 Oct 29]. https://www.fda.gov/safety/recalls-market-withdrawals-safety-alerts/dole-fresh-vegetables-announces-precautionary-limited-recall-garden-classic-salads-possible
14. US Food and Drug Administration. Dole Fresh Vegetables announces voluntary recall for salads processed at its Bessemer City, NC and Yuma, AZ facilities due to possible health risk from *Listeria monocytogenes* [cited 2021 Dec 22]. https://www.fda.gov/safety/recalls-market-withdrawals-safety-alerts/dole-fresh-vegetables-announces-voluntary-recall-salads-processed-its-bessemer-city-nc-and-yuma-az
15. Centers for Disease Control and Prevention. *Listeria* outbreak linked to packaged salads produced by Dole [cited 2022 Apr 4]. https://archive.cdc.gov/#/details?url=https://www.cdc.gov/listeria/outbreaks/packaged-salad-mix-12-21/index.html
16. US Food and Drug Administration. Outbreak investigation of *Listeria monocytogenes*: Dole packaged salad (December 2021) [cited 2022 Apr 4]. https://www.fda.gov/food/outbreaks-foodborne-illness/outbreak-investigation-listeria-monocytogenes-dole-packaged-salad-december-2021
17. US Food and Drug Administration. Dole Fresh Vegetables, Inc. announces voluntary recall for certain salads processed at its Springfield, OH and Soledad, CA facilities and containing iceberg lettuce due to possible health risk from *Listeria monocytogenes* [cited 2022 Jan 7]. https://www.fda.gov/safety/recalls-market-withdrawals-safety-alerts/dole-fresh-vegetables-inc-announces-voluntary-recall-certain-salads-processed-its-springfield-oh-and
18. US Food and Drug Administration. Fresh Express announces recall of fresh salad products due to potential health risk [cited 2021 Dec 27]. https://www.fda.gov/safety/recalls-market-withdrawals-safety-alerts/fresh-express-announces-recall-fresh-salad-products-due-potential-health-risk
19. Centers for Disease Control and Prevention. *Listeria* outbreak linked to packaged salads produced by Fresh Express [cited 2022 Mar 8]. https://archive.cdc.gov/#/details?url=https://www.cdc.gov/listeria/outbreaks/packaged-salad-12-21-b/index.html
20. Lee S, Chen Y, Gorski L, Ward TJ, Osborne J, Kathariou S. *Listeria monocytogenes* source distribution analysis indicates regional heterogeneity and ecological niche preference among serotype 4b clones. MBio. 2018;9:e00396-18. https://doi.org/10.1128/mBio.00396-18
21. Centers for Disease Control and Prevention. About the National Outbreak Reporting System [cited 2025 Jul 16]. https://www.cdc.gov/nors/about/index.html
22. US Food and Drug Administration. Recalls background and definitions [cited 2024 May 6]. https://www.fda.gov/safety/industry-guidance-recalls/recalls-background-and-definitions
23. US Food and Drug Administration. Enforcement reports [cited 2024 May 6]. https://www.fda.gov/safety/recalls-market-withdrawals-safety-alerts/enforcement-reports
24. Shenoy AG, Oliver HF, Deering AJ. *Listeria monocytogenes* internalizes in romaine lettuce grown in greenhouse conditions. J Food Prot. 2017;80:573–81. https://doi.org/10.4315/0362-028X.JFP-16-095
25. Guan H, Sun Y, Hou W, Zhao W, Wang P, Zhao S, et al. Infection behavior of *Listeria monocytogenes* on iceberg lettuce (Lactuca sativa var. capitata). Food Res Int. 2023;165:112487. https://doi.org/10.1016/j.foodres.2023.112487

Address for correspondence: Michael Vasser, Centers for Disease Control and Prevention, 1600 Clifton Rd NE, Mailstop H20-3, Atlanta, GA 30329-4018, USA; email: mvasser@cdc.gov

Retrospective Multicenter Study of Human Granulocytic Anaplasmosis, France, 2012–2024

Victor Gerber, Thomas Lemmet, Thomas Bonijoly, Baptiste Hoellinger, Anne Pachart, Amandine Woerly, Dominique De Briel, Emilie Talagrand-Reboul, Martin Martinot, Pierre Boyer, Yves Hansmann

Human granulocytic anaplasmosis (HGA), caused by *Anaplasma phagocytophilum* transmitted through tick bites, remains poorly documented in France. We conducted a retrospective, multicenter study of cases in Alsace during 2012–2024, including 39 HGA episodes in 38 patients PCR positive for *A. phagocytophilum*. Most (63.2%) patients were men, median age was 60.5 years, and 76.3% lived in rural areas. A tick bite was reported in 61.6% of cases. Frequent symptoms included fever (97.4%), fatigue (61.5%), and headache (61.5%). Laboratory findings showed elevated C-reactive protein (100%), thrombocytopenia (94.9%), leukopenia (59.0%), and cytolysis (66.7%). One patient had secondary hemophagocytic lymphohistiocytosis. Most (87.2%) patients were hospitalized; none required intensive care unit admission. Doxycycline was administered in 29 cases, and all patients recovered. HGA should be considered in febrile patients with recent tick exposure and cytopenia. Although often benign, rare severe HGA forms can occur and justify increased clinical awareness, especially in *A. phagocytophilum*–endemic areas.

Human granulocytic anaplasmosis (HGA) is a tickborne zoonosis caused by *Anaplasma phagocytophilum*, an obligate gram-negative intracellular bacterium. *A. phagocytophilum* belongs to the order Rickettsiales, family Anaplasmataceae, genus *Anaplasma*, after its separation from the genus *Ehrlichia* (*1*). For decades, the bacterium was known to be associated with equine and ruminant disease, but in 1994, HGA was described in 6 patients in the United States (*2*).

Clinical manifestations of HGA include febrile illness occurring 7–14 days after a tick bite along with mild and nonspecific symptoms, including malaise, headaches, myalgia, arthralgia, and vomiting (*3*). Rarely, severe and life-threatening manifestations, including pneumonia, hemophagocytosis, septic shock, respiratory distress syndrome, and death, can occur (*3*–*6*). Although uncommon, neurologic manifestations also can occur in HGA, including meningitis, encephalitis, stroke-like symptoms, or actual ischemic and hemorrhagic strokes, and represent a major cause of death among affected patients (*7*). Fatal HGA cases after blood transfusion have also been described (*8*). A combination of cytopenia, mostly thrombocytopenia, and elevated liver enzymes are the most frequent abnormal laboratory findings (*3*,*9*). Diagnostic confirmation is made on the basis of blood PCR, serology, blood smear observation, and culture testing (*3*,*10*). PCR appears to be best-suited diagnostic test and has a sensitivity of 74% and a specificity of 100% for *A. phagocytophilum* (*10*).

Most HGA cases have been reported from the United States, specifically to the Centers for Disease Control and Prevention through the National Notifiable Diseases Surveillance System (https://www.cdc.gov/nndss), but some cases have also occurred in Europe and Asia (*11*). During 2000–2016, the number of HGA cases in the United States increased, rising from 1.4 to 7.27 cases/1 million persons/year, and HGA became the second most frequent tickborne disease after Lyme disease in a few US states (*12*–*15*). A 2024 literature review (*3*) showed that 3,019 anaplasmosis cases have been reported globally, including 2,942 HGA cases, but individual patient data were described in <20% of those cases (*3*).

Author affiliations: Centre Hospitalier Universitaire de Strasbourg, Strasbourg, France (V. Gerber, T. Lemmet, B. Hoellinger, A. Woerly, E. Talagrand-Reboul, P. Boyer, Y. Hansmann); Hôpitaux Civils de Colmar, Colmar, France (V. Gerber, T. Lemmet, A. Pachart, D. De Briel, M. Martinot); Centre National de Référence des Borrelia, Strasbourg (V. Gerber, E. Talagrand-Reboul, P. Boyer, Y. Hansmann); Université de Strasbourg, Strasbourg (V. Gerber, E. Talagrand-Reboul, P. Boyer, Y. Hansmann); Centre Hospitalier de Sélestat, Sélestat, France (T. Bonijoly); Groupe Hospitalier de la Région de Mulhouse Sud-Alsace, Mulhouse, France (B. Hoellinger)

DOI: https://doi.org/10.3201/eid3112.250946

In France, an HGA case was reported in 2003 in which the patient presented with atypical pneumonitis; since then, only a few cases had been described, mostly in the northeastern regions (*4*,*10*,*16*,*17*). Alsace is among the northeastern regions of France where HGA cases have been described and where *Ixodes ricinus* ticks are known to carry *A. phagocytophilum* (*16*,*18*). Thus, we aimed to describe all known cases in Alsace to clarify the epidemiology of HGA by focusing on clinical presentations, laboratory findings, and patient outcomes.

Materials and Methods

Study Design and Setting

We conducted a 12-year, descriptive, retrospective multicenter study of all *A. phagocytophilum* PCR tests performed in the bacteriology laboratory of Strasbourg University Hospital (Strasbourg, France). Patient samples were obtained during January 1, 2012–December 31, 2024, from 4 centers in Alsace: Strasbourg, Sélestat, Colmar, and Mulhouse.

Case Definition and Inclusion Criteria

We included all patients with confirmed HGA, which we defined as an *A. phagocytophilum*–positive PCR test on blood. We only included cases diagnosed in a hospital setting because PCR testing was requested exclusively by hospital physicians for inpatients or patients seen in emergency departments or for hospital-based consultations.

Molecular Testing Methods

During 2012–2022, a simplex real-time PCR test targeting the *msp2/p44* gene of *A. phagocytophilum* was used (*16*). Since 2022, the laboratory has used a biplex PCR for simultaneous detection of *Neoehrlichia mikurensis* and *A. phagocytophilum*, in which the *A. phagocytophilum* target is still the *msp2* gene (*19*).

Data Collection and Ethics

The exclusion criteria were as follows: patients with a positive PCR test performed outside the 4 defined hospital centers, patients under legal protection, or patients objecting to the use of their data or for whom nonopposition to the use of their data could not be obtained. We collected the patients' demographic data (age and sex), outdoor activities (forest activities, hunting, fishing, gardening, and hiking), existence of a tick bite, travel within the previous month, medical history, clinical symptoms, laboratory findings, intensive care unit (ICU) admission, complications (including cardiac complications, kidney and respiratory failure, septic shock, multiorgan failure, secondary hemophagocytic lymphohistiocytosis [HLH] with an HScore, bleeding, splenic rupture, and death), and outcomes (*20*). The study was approved by the Ethical Committee of Medicine Odontology and Pharmacy Faculties and Hospitals, University Hospital of Strasbourg (approval no. CE-2024-104).

Results

Study Population

During the study period, we noted 1,032 PCR analyses for *A. phagocytophilum*, among which 55 (5.3%) were positive, representing 47 patients. Nine patients met exclusion criteria. Thus, the analysis included a total of 38 patients, 1 of whom had 2 distinct *Anaplasma* spp. infections, occurring 11 months apart. Therefore, we analyzed a total of 39 HGA cases (Figure).

Epidemiologic and Exposure Characteristics

The patients' mean age was 60.5 years; 63.2% were men and 36.8% were women (Table 1). The most frequent underlying conditions were high blood pressure (34.2%), tobacco use (10.5%), and a history of immunosuppression (10.5%). No patient had liver disease or was pregnant at the time of diagnosis. Only 42.1% of patients engaged in outdoor activities, but most (76.3%) lived in rural areas (Table 1).

Among the 39 HGA cases, tick bite ≤30 days was reported in 61.5% (n = 24) (Table 2). The median time between tick bite and symptom onset was 7 (range 1–28) days. Only 1 patient traveled outside France, specifically in the United States, and 3 traveled in another region of France, 1 in Brittany and 2 in the south of France (Table 2).

Clinical Presentation and Complications

Among HGA cases, 97.4% (38/39) of patients exhibited fever, 61.5% (24/39) reported related headaches, 61.5% (24/39) reported fatigue, and 38.5% (15/39) reported chills. Of note, in 23 cases (59.0%), patients had ≥1 gastrointestinal symptom, including abdominal pain (25.6%, 10/39), nausea (30.8%, 12/39), vomiting (28.2%, 11/39), diarrhea (12.8%, 5/39), or anorexia (20.5%, 8/39). At the initial assessment, 3 patients had severe symptoms: 2 had hypotension and 1 had hypoxia. One third of patients had complications, the most frequent of which were acute kidney injury in 17.9% (7/39) of cases and rhabdomyolysis in 12.8% (5/39).

Laboratory Findings and Microbiological Tests

The most frequent abnormal laboratory finding was cytopenia; 94.9% (37/39) of cases showed thrombocytopenia and 59.0% (23/39) showed leukopenia.

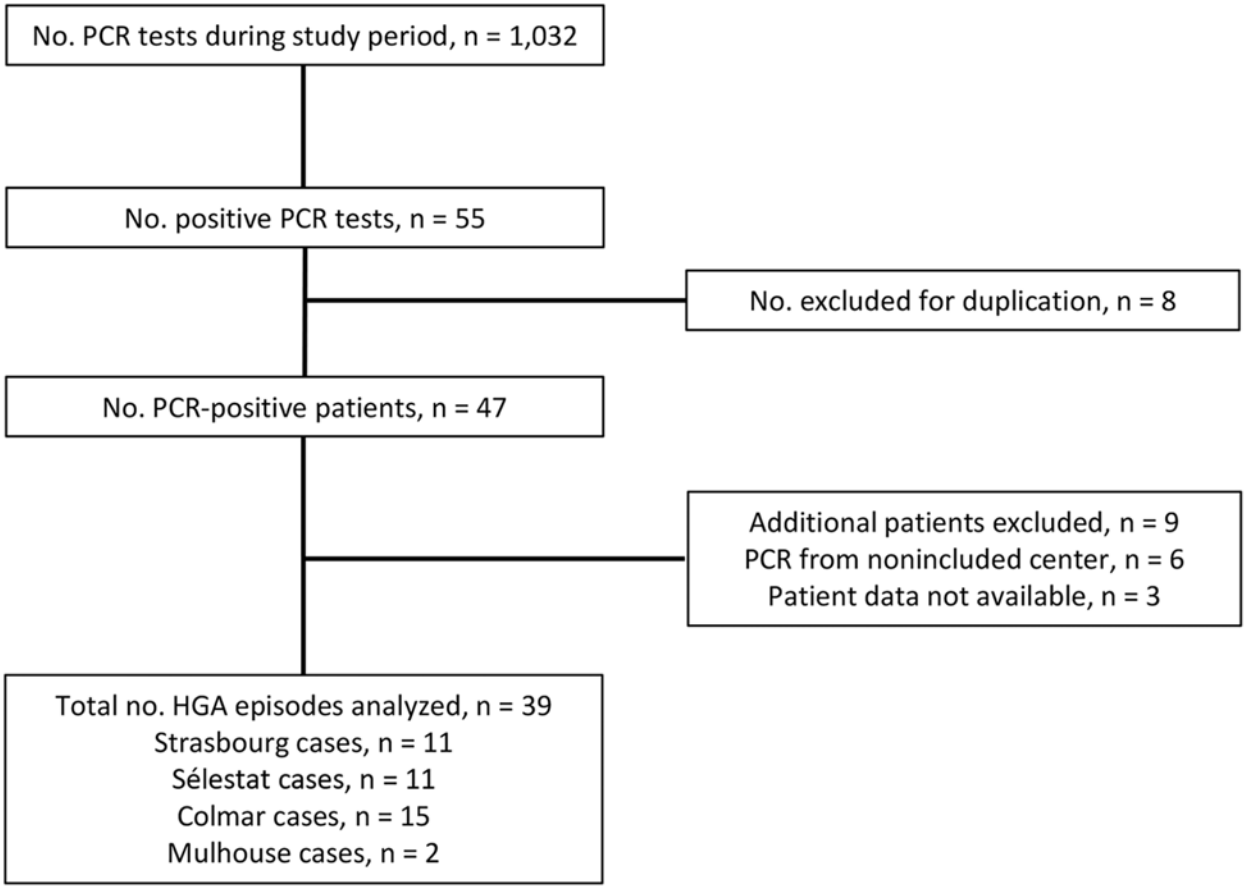

Figure. Flowchart of patient inclusion in a retrospective multicenter study of human granulocytic anaplasmosis, France, 2012–2024.

Other irregular findings included elevated C-reactive protein (CRP) in all 39 cases and elevated liver enzyme levels in 26 (66.6%) cases (Table 3). Among case-patients, 8 had a myelogram performed, from which 1 secondary HLH case was confirmed, and 2 cases had an HScore >169, a threshold that has a sensitivity of 93% and a specificity of 86% for diagnosing secondary HLH.

A positive blood smear was reported in 20.5% (8/39) of cases. *A. phagocytophilum* IgM and IgG indirect immunofluorescence assays were performed in 13 cases by using Focus Diagnostics *Anaplasma phagocytophilum* IFA Test Kit (Focus Diagnostics, https://www.focustechnologies.com) and applying a screening cutoff of 1:64 for IgG and 1:20 for IgM. Positive serum samples were subsequently titrated to determine the exact antibody titer. Nine cases were IgM positive and 7 were IgG positive. One patient had a positive *A. phagocytophilum* PCR result from a cerebrospinal fluid (CSF) sample. CSF analysis showed no leukocytes (0 cells/mL), 10 erythrocytes/mL, a protein level of 0.32 g/L (reference range 0.14–0.45 g/L), and glucose concentration of 0.71 g/L (within reference limits). In the absence of meningitis and because of mild blood contamination in the CSF, a false-positive PCR result was likely, although the patient did have neurologic symptoms, namely confusion.

Treatment and Outcomes

Among the 39 HGA cases, most (87.2%, 34/39) patients were hospitalized, but none were admitted to the ICU (Table 4). Most (74.4%, 29/39 cases) patients were treated with doxycycline for a median duration of 7 (range 1–16) days. In 10 (25.6%) of 39 HGA episodes, patients did not receive doxycycline. Among those cases, 7 patients received no antimicrobial drug therapy, and the other 3 were treated with inappropriate antibiotics, including amoxicillin/clavulanic acid (n = 1), ceftriaxone (n = 1), and a sequential regimen of ceftriaxone and metronidazole followed by amoxicillin/clavulanic acid (n = 1); however, all patients recovered. Persistent asthenia at 3 months after diagnosis was reported in 3 cases.

The patient who experienced 2 distinct infection episodes was not immunocompromised and received appropriate treatment with doxycycline for 14 days during the first episode. However, no

Table 1. Characteristics and underlying conditions among 38 patients in a retrospective multicenter study of human granulocytic anaplasmosis, France, 2012–2024*

Patient characteristics	Value
Mean age, y (range)	60.2 (34–87)
Sex	
F	14 (36.8)
M	24 (63.2)
Participated in outdoor activities	16 (42.1)
Lived in a rural area	29 (76.3)
Underlying conditions	
High blood pressure	13 (34.2)
Tobacco use	4 (10.5)
Immunosuppression	4 (10.5)
Diabetes mellitus	2 (5.3)
Chronic kidney disease, GFR <60 mL/min	1 (2.6)
Chronic respiratory disease	1 (2.6)
Chronic cardiac failure, LVEF <45%	1 (2.6)

*Values are no. (%) except as indicated. One patient had 2 distinct *Anaplasma* spp. infections occurring 11 months apart. GFR, glomerular filtration rate; LVEF, left ventricular ejection fraction.

serologic testing was performed during the first episode, preventing comparison of antibody titers between episodes.

Discussion

In our study, we noted 39 cases of *A. phagocytophilum* infections occurring in 38 patients in 4 hospital centers in northeastern France over a 12-year period. The cases mostly occurred in patients who lived in rural areas and had few underlying conditions. Fever was the most frequent symptom and was often associated with other nonspecific manifestations, including asthenia, headaches, and digestive symptoms. Elevated CRP levels and thrombocytopenia were the most frequent abnormal laboratory findings and were observed in almost all cases. One third of patients had complications develop, including 1 case of HLH, but no patients required ICU admission. All patients recovered, even those who did not receive an appropriate antibiotic therapy.

Globally, most HGA cases have been described in the midwestern and northeastern parts of the United States, mainly in Minnesota, Wisconsin, and Rhode Island (*3*,*12*–*14*). Those cases were reported through a national surveillance system, and since 2000 a gradual increase in HGA incidence was noted, rising from 1.4 cases/1 million persons/year in 2000 to 7.27 cases/1 million persons/year in 2016 (*12*–*14*). In Europe, most HGA cases have been reported in Belgium, Poland, and Slovenia (*3*). However, relatively few confirmed HGA cases with clinical and laboratory findings have been reported, 156 cases from North America and only 46 from Europe. A 2024 systematic literature review reported only 6 published HGA case reports in France (*3*), and only 44 potential infections have ever been described in France, most in Alsace (*4*,*10*,*16*,*17*). Our study cases build on the reported HGA cases in France, and our investigation suggests that Alsace is an HGA hotspot, despite the low *Anaplasma* spp. prevalence rate among ticks (0.4% in nymphs and 1.2% in adults) (*18*,*21*). In addition, *A. phagocytophilum* has been detected in ticks elsewhere in France (*22*,*23*). The apparent absence of HGA cases might reflect regional variation in *A. phagocytophilum* ecotypes, and the human-pathogenic ecotype might be more prevalent in Alsace (*24*). Moreover, the regional difference diagnostic rates might be explained by higher awareness of HGA among clinicians in Alsace.

Among case-patients, we found lower rates of underlying conditions and immunosuppression compared with previously published data (*3*,*9*). The most common suspected route of transmission is a tick bite, reported in up to 95% of confirmed HGA cases (*9*). In our study, a tick bite was reported for 61% (24/39) of cases, which is lower than the theoretical maximum, but remains notably higher than in several other studies on tickborne diseases, where most patients did not recall any tick exposure (*25*). That relatively high percentage might reflect greater awareness among persons in endemic rural areas or improved recognition of tick bites. One of the main risk factors for HGA and tick bite is outdoor activity, which we observed in only 42% (6/38) of our patients. The retrospective nature of the study probably underestimated that factor, especially considering that most patients lived in rural areas.

Blood transfusion is another route of transmission reported in the United States, but we had no cases from blood transfusion in our study (*3*,*9*). The lower incidence in our study cohort in comparison to the cohort from Europe and the systematic leukoreduction treatment of blood bags in France likely explain that difference. Infection though blood transfusion is much more concerning in immunocompromised patients, accounting for approximately half of the HGA cases in those patients (*3*,*9*). Other transmission routes include contact with human or animal body fluids or vertical infection; however, we found no such cases in our study.

Almost all (97.4%, 38/39 cases) patients in our study had fever and thrombocytopenia (94.9%, 37/39 cases), and all had elevated CRP levels within 7 days after tick bite. The symptom frequency was higher in our study than in a previous report (*3*). In addition, of 38 patients in our study, 23 (59%) reported ≥1 gastrointestinal symptom, which is consistent with another literature review (*9*), highlighting the importance of

suspecting HGA in endemic areas when gastrointestinal symptoms are associated with fever, thrombocytopenia, and elevated CRP levels (*9*). The frequencies of liver enzyme elevation (26/39 cases) and leukopenia (23/39 cases) in our study were similar to those of previous cohorts from Europe and North America. Although cytopenia and elevated liver enzyme levels commonly occur in HGA patients, a 2025 study reported that the triad of thrombopenia, leukopenia, and cytolysis occurred in only 23% of HGA cases, but that triad was associated with an increased risk for hospitalization (*26*).

The hospitalization rate for HGA in the United States is 31%, but our study reported an 87.2% hospitalization rate (*13*). That difference could be explained by our study design because we only enrolled hospital-diagnosed cases, whereas the US surveillance data also included milder cases. However, we did not observe many of the known hospitalization risk factors, including altered mental status, older age, underlying conditions, and immunosuppression (*26*), in our cohort. Among the 39 HGA episodes in our study, 13 (33.3%) cases had complications, which was a higher percentage than the complication rate reported in a previous study from Europe but less than that of the US study (*3*,*9*,*13*). That might reflect publication bias and differences in the definition of complication (*3*). Several studies have suggested that the US cases might have been more severe than the cases from Europe because more deaths and ICU transfers occurred in the US cohort (*3*,*9*,*28*). A 1996 study found that 3 (7%) of 41 patients required ICU admission (*27*). Data from US surveillance systems also found an HGA mortality rate of <1% (*12*,*13*). Although most HGA deaths have been reported in the United States, primarily in immunocompromised and older patients, 1 death has been described in Europe (*3*,*5*,*9*,*28*).

Acute kidney injury was the most frequent complication in our cohort and is considered the most frequent complication among HGA cases, possibly in relation to rhabdomyolysis. We found 1 case of confirmed secondary HLH and 2 probable cases among patients with a high HScore (>169). Although rare, HLH is a well-described and potentially life-threatening complication of HGA; the reported HLH mortality rate is 23% among affected patients (*3*,*5*,*29*). HLH has also been increasingly associated with other tickborne infections, particularly *Ehrlichia* spp., *A. phagocytophilum*, and *Rickettsia* spp. infections (*30*). A 2024 review reported that *A. phagocytophilum* accounted for 12.2% of HLH cases linked to tickborne pathogens, following ehrlichiosis (45.9%) and rickettsioses (14.3%) (*30*). Of note, the mortality rate for HLH in that context appears lower than for HLH overall (16.3% vs. 41%), largely because of the availability of effective antimicrobial therapy when initiated promptly (*30*). Doxycycline remains the cornerstone treatment for HGA, but immunosuppressive agents could be considered in severe or refractory cases. In that 2024 review, 43.9% of patients received antimicrobial therapy alone, and 88.4% of those patients recovered without additional immunosuppression (*30*). Therefore, in endemic regions, *A. phagocytophilum* infection should be considered in patients with HLH of unclear origin.

Despite complications, including 1 severe case, none of the patients in our study died, even though only 74.4% received appropriate antibiotic

Table 2. Clinical and epidemiologic characteristics of 39 cases in a retrospective multicenter study of human granulocytic anaplasmosis, France, 2012–2024*

Patient characteristics	Value
Tick bite ≤30 d	24 (61.5)
Median time between tick bite and symptom onset, d (range)	7 (1–28)
Travel history ≤30 d	
Outside France	1 (2.6)†
In France, outside the study region	3 (7.7)
Signs and symptoms	
Fever	38 (97.4)
Fatigue	24 (61.5)
Headache	24 (61.5)
Chills	15 (38.5)
Nausea	12 (30.8)
Vomiting	11 (28.2)
Abdominal pain	10 (25.6)
Myalgia	9 (23.1)
Anorexia	8 (20.5)
Cough	8 (20.5)
Other neurologic signs‡	5 (12.8)
Diarrhea	5 (12.8)
Hepatomegaly	4 (10.3)
Arthralgia	3 (7.7)
Confusion	3 (7.7)
Constipation	2 (5.1)
Splenomegaly	2 (5.1)
Rash	2 (5.1)
Pneumonia	1 (2.6)
Gravity signs	3 (7.7)
Hypotension	2 (5.1)
Hypoxia	1 (2.6)
No. patients with complications	13 (33.3)
Cardiac complications§	1 (2.6)
Pneumonitis	3 (7.7)
Acute kidney injury	7 (17.9)
Rhabdomyolysis	5 (12.8)
Confirmed secondary hemophagocytic lymphohistiocytosis on myelogram	1 (2.6)
Bleeding	1 (2.6)

*Values are no. (%) except as indicated. ARDS, acute respiratory distress syndrome.
†Travel to Pennsylvania, USA.
‡Signs included dizziness, faintness, neuritis, or diadochokinesia.
§Complications included cardiac arrhythmia and heart failure.

Table 3. Laboratory findings for 39 cases a retrospective multicenter study of human granulocytic anaplasmosis, France, 2012–2024*

Laboratory findings	Value	Reference range
Thrombocytopenia, no. (%)	37 (94.9)	
Median cells × 10^3/μL (range)	59 (19–316)	150–400
Leucopenia, no. (%)	23 (59.0)	
Median cells × 10^3/μL (range)	3.2 (1.02–13.01)	4.1–10.5
Anemia	8 (20.5)	
Median hemoglobin, g/dL (range)	13.4 (8.8–15.8)	13–18
No cytopenia, no. (%)	2 (5.1)	
Reactive lymphocytes, no. (%)	7 (17.9)	
Elevated liver enzymes, no. (%)	26 (66.6)	
Median AST, IU/L (range)	103 (24–509)	13–40
Median ALT, IU/L (range)	80.5 (27–829)	7–40
Elevated creatinine, no. (%)	7 (17.9)	
Median creatinine, μmol/L (range)	82 (43–233)	53–97
Elevated CRP	39 (100)	
Median CRP, mg/L (range)	130 (10–286)	0–5
Rhabdomyolysis, no. (%)	5 (12.8)	
Median CK, IU/l (range)	106 (40–1,012)	40–250
Myelogram performed, no. (%)	8 (20.5)	
Median HScore (range)†	76 (19–208)	NA
Anaplasma phagocytophilum testing, no. (%)		
Positive blood smear with morulae	8 (20.5)	NA
Positive IgM at diagnosis	9 (23.1)	Cutoff 1:20
Positive IgG at diagnosis	7 (17.9)	Cutoff 1:64
Other PCR positive, CSF	1 (2.6)	NA
Tickborne disease co-infection, Lyme disease‡	1 (2.6)	NA

*ALT, alanine aminotransferase; AST, aspartate aminotransferase; CRP, C-reactive protein; CK, creatine kinase; CSF, cerebrospinal fluid; NA, not applicable.
†A score used for determining reactive hemophagocytic syndrome.
‡Co-infection data are based on medical records; no further diagnostic details available.

therapy. Indeed, HGA can resolve spontaneously. Furthermore, a previous study showed that only 25% of HGA patients benefitted from antimicrobial drug therapy (*9*). Our study found a higher treatment rate, which was likely related to more severe HGA among our patients, although our patients had a shorter median treatment duration of 7 days compared with 12.9–14 days reported in previous literature (*3*,*9*).

Although retrospective studies are particularly useful for studying rare diseases, such as HGA, they have several limitations. First, our study design was limited by data completeness and might have a selection bias. Systematic HGA screening in febrile patients with tick exposure and cytopenia could improve the detection of the disease. A systematic search in our region during 2010–2012 and resulted in HGA diagnosis in 19 patients from 9 hospitals in Alsace (*10*). Furthermore, we chose to include only patients with a positive PCR test because PCR is the best diagnostic tool for *A. phagocytophilum* (*10*). However, some patients could have had true seroconversion because our study did not include that diagnostic confirmation criteria (*3*,*10*). Finally, a national surveillance system that includes the surveillance of all cases, particularly those with mild symptoms, would provide more precise epidemiologic data.

In conclusion, our study provides additional epidemiologic and clinical insights for HGA in Alsace, a region highly endemic for tickborne diseases. Although HGA is infrequent, it can lead to complications and is likely underdiagnosed. In the northeastern region of France where HGA is endemic, information campaigns targeting patients and healthcare workers could be beneficial. In addition, routine screening of patients with fever, leukopenia, thrombopenia, activation syndrome, or any combination of those signs and symptoms could also be useful.

Table 4. Characteristics and outcomes for 39 cases in a retrospective multicenter study of human granulocytic anaplasmosis, France, 2012–2024*

Patient characteristics	HGA episodes
Median delay between symptom onset and diagnosis, d (range)	8.5 (2–26)
No. hospitalized	34 (87.2)
Median hospitalization duration, d (range)	6 (1–13)
Intensive care unit admission	0
Antimicrobial treatment	
Ineffective therapy before doxycycline	13 (33.3)
No effective antibiotic therapy	10 (25.6)
Treatment with doxycycline	29 (74.4)
Median duration, d (range)	7 (1–16)
Outcomes	
Death ≤30 d after diagnosis	0
Recovered	39 (100)
Sequelae at 3 mo after diagnosis†	3 (7.7)

*Values are no. (%) except as indicated. HGA, human granulocytic anaplasmosis.
†Including asthenia.

Acknowledgments

We thank Benoit Jaulhac for his advice and relevant proofreading. We thank Enago for the English proofreading.

About the Author

Dr. Gerber is an infectious diseases physician at Hôpitaux Civils de Colmar, France, and is a PhD candidate at the National Reference Center for Borrelia in Strasbourg, France. His research interests include tickborne diseases with a focus on Lyme disease in humans.

References

1. Dumler JS, Barbet AF, Bekker CP, Dasch GA, Palmer GH, Ray SC, et al. Reorganization of genera in the families Rickettsiaceae and Anaplasmataceae in the order Rickettsiales: unification of some species of *Ehrlichia* with *Anaplasma*, Cowdria with *Ehrlichia* and *Ehrlichia* with *Neorickettsia*, descriptions of six new species combinations and designation of *Ehrlichia equi* and 'HGE agent' as subjective synonyms of *Ehrlichia phagocytophila*. Int J Syst Evol Microbiol. 2001;51:2145–65. https://doi.org/10.1099/00207713-51-6-2145
2. Chen SM, Dumler JS, Bakken JS, Walker DH. Identification of a granulocytotropic *Ehrlichia* species as the etiologic agent of human disease. J Clin Microbiol. 1994;32:589–95. https://doi.org/10.1128/jcm.32.3.589-595.1994
3. Schudel S, Gygax L, Kositz C, Kuenzli E, Neumayr A. Human granulocytotropic anaplasmosis—a systematic review and analysis of the literature. PLoS Negl Trop Dis. 2024;18:e0012313. https://doi.org/10.1371/journal.pntd.0012313
4. Remy V, Hansmann Y, De Martino S, Christmann D, Brouqui P. Human anaplasmosis presenting as atypical pneumonitis in France. Clin Infect Dis. 2003;37:846–8. https://doi.org/10.1086/377502
5. Tsiodras S, Spanakis N, Spanakos G, Pervanidou D, Georgakopoulou T, Campos E, et al. Fatal human anaplasmosis associated with macrophage activation syndrome in Greece and the public health response. J Infect Public Health. 2017;10:819–23. https://doi.org/10.1016/j.jiph.2017.01.002
6. Malik S, Brucato MF, Faiver L, Phan T, Yassin MH, Bishop JM, et al. Severe fatal ARDS due to untreated human granulocytic anaplasmosis in a 67-year-old man: a case report. Am J Case Rep. 2024;25:e943966. https://doi.org/10.12659/AJCR.943966
7. Cosiquien RJS, Stojiljkovic N, Nordstrom CW, Amadi E, Lutwick L, Dumic I. *Anaplasma phagocytophilum* encephalitis: a case report and literature review of neurologic manifestations of anaplasmosis. Infect Dis Rep. 2023;15:354–9. https://doi.org/10.3390/idr15040035
8. Goel R, Westblade LF, Kessler DA, Sfeir M, Slavinski S, Backenson B, et al. Death from transfusion-transmitted anaplasmosis, New York, USA, 2017. Emerg Infect Dis. 2018;24:1548–50. https://doi.org/10.3201/eid2408.172048
9. Dumic I, Jevtic D, Veselinovic M, Nordstrom CW, Jovanovic M, Mogulla V, et al. Human granulocytic anaplasmosis—a systematic review of published cases. Microorganisms. 2022;10:1433. https://doi.org/10.3390/microorganisms10071433
10. Hansmann Y, Jaulhac B, Kieffer P, Martinot M, Wurtz E, Dukic R, et al. Value of PCR, serology, and blood smears for human granulocytic anaplasmosis diagnosis, France. Emerg Infect Dis. 2019;25:996–8. https://doi.org/10.3201/eid2505.171751
11. Acosta-España JD, Herrera-Yela A, Altamirano-Jara JB, Bonilla-Aldana DK, Rodriguez-Morales AJ. The epidemiology and clinical manifestations of anaplasmosis in humans: a systematic review of case reports. J Infect Public Health. 2025;18:102765. https://doi.org/10.1016/j.jiph.2025.102765
12. Dahlgren FS, Mandel EJ, Krebs JW, Massung RF, McQuiston JH. Increasing incidence of *Ehrlichia chaffeensis* and *Anaplasma phagocytophilum* in the United States, 2000–2007. Am J Trop Med Hyg. 2011;85:124–31. https://doi.org/10.4269/ajtmh.2011.10-0613
13. Dahlgren FS, Heitman KN, Drexler NA, Massung RF, Behravesh CB. Human granulocytic anaplasmosis in the United States from 2008 to 2012: a summary of national surveillance data. Am J Trop Med Hyg. 2015;93:66–72. https://doi.org/10.4269/ajtmh.15-0122
14. Baker A, Wang HH, Mogg M, Derouen Z, Borski J, Grant WE. Increasing incidence of anaplasmosis in the United States, 2012 through 2016. Vector Borne Zoonotic Dis. 2020;20:855–9. https://doi.org/10.1089/vbz.2019.2598
15. Russell A, Prusinski M, Sommer J, O'Connor C, White J, Falco R, et al. Epidemiology and spatial emergence of anaplasmosis, New York, USA, 2010–2018. Emerg Infect Dis. 2021;27:2154–62. https://doi.org/10.3201/eid2708.210133
16. Koebel C, Kern A, Edouard S, Hoang AT, Celestin N, Hansmann Y, et al. Human granulocytic anaplasmosis in eastern France: clinical presentation and laboratory diagnosis. Diagn Microbiol Infect Dis. 2012;72:214–8. https://doi.org/10.1016/j.diagmicrobio.2011.12.005
17. Edouard S, Koebel C, Goehringer F, Socolovschi C, Jaulhac B, Raoult D, et al. Emergence of human granulocytic anaplasmosis in France. Ticks Tick Borne Dis. 2012;3:403–5. https://doi.org/10.1016/j.ttbdis.2012.10.002
18. Ferquel E, Garnier M, Marie J, Bernède-Bauduin C, Baranton G, Pérez-Eid C, et al. Prevalence of *Borrelia burgdorferi* sensu lato and Anaplasmataceae members in *Ixodes ricinus* ticks in Alsace, a focus of Lyme borreliosis endemicity in France. Appl Environ Microbiol. 2006;72:3074–8. https://doi.org/10.1128/AEM.72.4.3074-3078.2006
19. Martinot M, Astrie M, Mohseni-Zadeh M, De Briel D, Jaulhac B, Boyer P. Dual detection of *Neoehrlichia mikurensis* and *Anaplasma phagocytophilum*: how biplex PCR led in France to the diagnosis of neoehrlichiosis in post-tick bite fever. Infect Dis Now. 2024;54:104995. https://doi.org/10.1016/j.idnow.2024.104995
20. Fardet L, Galicier L, Lambotte O, Marzac C, Aumont C, Chahwan D, et al. Development and validation of the HScore, a score for the diagnosis of reactive hemophagocytic syndrome. Arthritis Rheumatol. 2014;66:2613–20. https://doi.org/10.1002/art.38690
21. Sprong H, Fonville M, Docters van Leeuwen A, Devillers E, Ibañez-Justicia A, Stroo A, et al. Detection of pathogens in *Dermacentor reticulatus* in northwestern Europe: evaluation of a high-throughput array. Heliyon. 2019;5:e01270. https://doi.org/10.1016/j.heliyon.2019.e01270
22. Lebert I, Agoulon A, Bastian S, Butet A, Cargnelutti B, Cèbe N, et al. Distribution of ticks, tick-borne pathogens and the associated local environmental factors including small mammals and livestock, in two French agricultural sites: the OSCAR database. Biodivers Data J. 2020;8:e50123. https://doi.org/10.3897/BDJ.8.e50123

23. Chastagner A, Bailly X, Leblond A, Pradier S, Vourc'h G. Single genotype of *Anaplasma phagocytophilum* identified from ticks, Camargue, France. Emerg Infect Dis. 2013;19:825–7. https://doi.org/10.3201/eid1905.121003
24. Jahfari S, Coipan EC, Fonville M, van Leeuwen AD, Hengeveld P, Heylen D, et al. Circulation of four *Anaplasma phagocytophilum* ecotypes in Europe. Parasit Vectors. 2014;7:365. https://doi.org/10.1186/1756-3305-7-365
25. Nigrovic LE, Neville DN, Balamuth F, Bennett JE, Levas MN, Garro AC; for Pedi Lyme Net. A minority of children diagnosed with Lyme disease recall a preceding tick bite. Ticks Tick Borne Dis. 2019;10:694–6. https://doi.org/10.1016/j.ttbdis.2019.02.015
26. Katragadda S, Yetmar ZA, Chesdachai S, Fida M, Pritt BS, Challener DW, et al. Trends in anaplasmosis over the past decade: a review of clinical features, laboratory data and outcomes. Clin Infect Dis. 2025 Apr 3 [Epub ahead of print]. https://doi.org/10.1093/cid/ciaf171
27. Bakken JS, Krueth J, Wilson-Nordskog C, Tilden RL, Asanovich K, Dumler JS. Clinical and laboratory characteristics of human granulocytic ehrlichiosis. JAMA. 1996;275:199–205. https://doi.org/10.1001/jama.1996.03530270039029
28. Bakken JS, Dumler S. Human granulocytic anaplasmosis. Infect Dis Clin North Am. 2008;22:433–48, viii. https://doi.org/10.1016/j.idc.2008.03.011
29. Scribner J, Wu B, Lamyaithong A, Arcega V, Villanueva DD. Anaplasmosis-induced hemophagocytic lymphohistiocytosis: a case report and review of the literature. Open Forum Infect Dis. 2023;10:ofad213. https://doi.org/10.1093/ofid/ofad213
30. Jevtic D, da Silva MD, Haylock AB, Nordstrom CW, Oluic S, Pantic N, et al. Hemophagocytic lymphohistiocytosis (HLH) in patients with tick-borne illness: a scoping review of 98 cases. Infect Dis Rep. 2024;16:154–69. https://doi.org/10.3390/idr16020012

Address for correspondence: Victor Gerber, CHU de Strasbourg, Service de Maladies Infectieuses et Tropicales, 1 place de l'hôpital, 67000 Strasbourg, France; email: victor.gerber@chru-strasbourg.fr

Pregnancy Outcomes after Exposure to Tuberculosis Treatment in Phase 3 Clinical Trial, 2016–2020

Ekaterina V. Kurbatova, William C. Whitworth, Kia E. Bryant, Meredith G. Dixon, Kelly E. Dooley, Nigel A. Scott, Rosanna Boyd, Nicole E. Brown, Kimberley N. Chapman Hedges, Wendy Carr, Lakshmi P. Peddareddy, Grace Muzanyi, Rodney Dawson, Ziyad Waja, Neil Martinson, Jyoti S.V. Mathad, Payam Nahid, Susan Swindells, Richard E. Chaisson, Susan E. Dorman, Patrick P.J. Phillips, AIDS Clinical Trials Group A5349,[1] Tuberculosis Trials Consortium Study 31[2]

Medscape CME Activity

In support of improving patient care, this activity has been planned and implemented by Medscape, LLC and Emerging Infectious Diseases. Medscape, LLC is jointly accredited with commendation by the Accreditation Council for Continuing Medical Education (ACCME), the Accreditation Council for Pharmacy Education (ACPE), and the American Nurses Credentialing Center (ANCC), to provide continuing education for the healthcare team.

Medscape, LLC designates this Journal-based CME activity for a maximum of 1.00 ***AMA PRA Category 1 Credit(s)™***. Physicians should claim only the credit commensurate with the extent of their participation in the activity.

Successful completion of this CME activity, which includes participation in the evaluation component, enables the participant to earn up to 1.0 MOC points in the American Board of Internal Medicine's (ABIM) Maintenance of Certification (MOC) program. Participants will earn MOC points equivalent to the amount of CME credits claimed for the activity. It is the CME activity provider's responsibility to submit participant completion information to ACCME for the purpose of granting ABIM MOC credit.

All other clinicians completing this activity will be issued a certificate of participation. To participate in this journal CME activity: (1) review the learning objectives and author disclosures; (2) study the education content; (3) take the post-test with a 75% minimum passing score and complete the evaluation at http://www.medscape.org/journal/eid; and (4) view/print certificate. For CME questions, see page 2357.

NOTE: It is the policy of Medscape Education to avoid the mention of brand names or specific manufacturers in accredited educational activities. However, trade and manufacturer names in this activity are provided in an effort to provide clarity. The use of brand or manufacturer names should not be viewed as an endorsement by Medscape of any specific product or manufacturer.

Release date: December 29, 2025; Expiration date: December 29, 2026

Learning Objectives

Upon completion of this activity, participants will be able to:

- Compare the efficacy of 4- vs 6-month anti-tuberculosis (TB) regimens among women
- Evaluate the rate of fetal loss among women exposed to anti-TB treatment during pregnancy
- Evaluate the rate of congenital anomaly among women exposed to anti-TB treatment during pregnancy
- Analyze the effects of anti-TB treatment during pregnancy on favorable TB outcomes

CME Editor

Jude Rutledge, BA, Technical Writer/Editor, Emerging Infectious Diseases. *Disclosure: Jude Rutledge, BA, has no relevant financial relationships.*

CME Author

Charles P. Vega, MD, Health Sciences Clinical Professor of Family Medicine, University of California, Irvine School of Medicine, Irvine, California. *Disclosure: Charles P. Vega, MD, has the following relevant financial relationships: consultant or advisor for Boehringer Ingelheim; Exact Sciences.*

Authors

Ekaterina V. Kurbatova, MD, MPH, PhD; William C. Whitworth, MPH; Kia E. Bryant, MPH; Meredith G. Dixon, MD, FAAP; Kelly E. Dooley, MD, PhD; Nigel A. Scott, MS; Rosanna Boyd, PhD; Nicole E. Brown, PhD; Kimberley N. Chapman Hedges, MPH; Wendy Carr, PhD; Lakshmi P. Peddareddy, MBBS, MPH; Grace Muzanyi, MD; Rodney Dawson, MD; Ziyad Waja, MD; Neil Martinson, MD; Jyoti S.V. Mathad, MD, MS; Payam Nahid, MD, MPH; Susan Swindells, MD; Richard E. Chaisson, MD; Susan E. Dorman, MD; Patrick P.J. Phillips, PhD.

A previous study demonstrated noninferior efficacy of 4-month rifapentine/moxifloxacin regimen for tuberculosis (TB) treatment compared with the standard regimen. We analyzed pregnancy outcomes of women who became pregnant during the study. Among 740 women, 97 (13.1%) became pregnant. Of 102 pregnancies (in 97 participants), 30 (29.4%) participants were exposed to study drugs. Fetal loss was reported for 3/13 (23.1%) in the control regimen, 1/9 (11.1%) in the rifapentine/moxifloxacin regimen, and 1/8 (12.5%) in the rifapentine regimen. Among 21 live births in exposed pregnancies (7 in each arm), 1 infant with a congenital anomaly was reported in a participant on the rifapentine regimen. Among women receiving a short rifapentine/moxifloxacin regimen for tuberculosis who became pregnant, we observed no elevated rates of fetal losses or congenital anomalies.

Globally, among pregnant women in 2011, an estimated 216,000 had concurrent active tuberculosis (TB) (*1*). Untreated TB during pregnancy can cause pregnancy complications, nonobstetric maternal death, and infant death (*2*–*8*). Even if treated, TB during pregnancy poses challenges. For treatment of drug-susceptible pulmonary TB, standard treatment regimens containing isoniazid, rifampin, pyrazinamide, and ethambutol are highly efficacious in nonpregnant women, but well-controlled studies in pregnant women are lacking. More generally, data regarding safety, tolerability, and pharmacokinetics of TB drugs during pregnancy have not been collected or reported systematically, leading to inconsistencies in national and international treatment guidelines (*9*). For example, international guidelines recommend the use of pyrazinamide during pregnancy in first-line regimens for drug-susceptible TB (*10*), but US guidelines suggest evaluating the risks and benefits of prescribing pyrazinamide on a case-by-case basis (*11*). The scarcity of high-quality evidence combined with the worldwide occurrence of >200,000 annual cases of active TB disease among pregnant women highlights the need for additional research in this area to expand treatment options for mothers and protect the health of their infants (*9*). A February 2024 consensus statement strongly supports the participation of pregnant women in TB research (*12*), a statement that has been endorsed by community groups (*13*).

Tuberculosis Trials Consortium Study 31/AIDS Clinical Trials Group A5349 (S31/A5349) was a multicenter randomized controlled phase 3 noninferiority open-label trial that examined two 4-month treatment-shortening rifapentine-containing regimens compared with the standard 6-month control regimen for treatment of drug-susceptible pulmonary TB in nonpregnant participants ≥12 years of age (*14*). One investigational regimen contained rifapentine, moxifloxacin, and isoniazid administered for 4 months plus pyrazinamide administered during the first 2 months (rifapentine/moxifloxacin regimen). The other investigational regimen contained rifapentine plus isoniazid administered for 4 months plus pyrazinamide and ethambutol administered during the first 2 months (rifapentine regimen). The trial demonstrated that the 4-month rifapentine/moxifloxacin regimen had efficacy that was noninferior to that of the control and was safe and well-tolerated. The rifapentine regimen did not meet the noninferiority criteria for efficacy (*14*). The World Health Organization and the US Centers for Disease Control and Prevention (CDC) now recommend the 4-month rifapentine/moxifloxacin regimen for treatment of drug-susceptible TB in nonpregnant patients ≥12 years of age (*15*,*16*). The regimen is not recommended in pregnant women because they were not included in enrollment for the S31/A5349 study.

Although pregnant women were not eligible for enrollment in S31/A5349, some participants became pregnant during their participation in the study, some during study treatment, and some in the follow-up period. We conducted a secondary data analysis to describe pregnancy outcomes and safety among S31/A5349 study participants who became pregnant during the trial.

Author affiliations: Centers for Disease Control and Prevention, Atlanta, Georgia, USA (E.V. Kurbatova, W.C. Whitworth, K.E. Bryant, M.G. Dixon, N.A. Scott, R. Boyd, N.E. Brown, K.N. Chapman Hedges, W. Carr, L.P Peddareddy); Vanderbilt University Medical Center, Nashville, Tennessee, USA (K.E. Dooley); Uganda–Case Western Reserve University Research Collaboration, Kampala, Uganda (G. Muzanyi); University of Cape Town Lung Institute, Cape Town, South Africa (R. Dawson); University of the Witwatersrand Perinatal HIV Research Unit, Johannesburg, South Africa (Z. Waja, N. Martinson); Weill Cornell Medical College, New York, New York, USA (J.S.V. Mathad); University of California Center for Tuberculosis, San Francisco, California, USA (P. Nahid, P.P.J. Phillips); University of Nebraska Medical Center, Omaha, Nebraska, USA (S. Swindells); Johns Hopkins University School of Medicine, Baltimore, Maryland, USA (R.E. Chaisson); Medical University of South Carolina, Charleston, South Carolina, USA (S.E. Dorman)

DOI: https://doi.org/10.3201/eid3112.250492

[1]Members of this group are listed at the end of this article.

[2]Members of this group are listed at the end of this article.

Methods

Study Design

Full details of the S31/A5349 study design, eligibility criteria, enrollment and randomization, safety monitoring, and study outcomes have been published previously (*14*,*17*). Pregnant or breastfeeding women were not eligible for enrollment because of uncertainties about the safety of rifapentine, moxifloxacin, and pyrazinamide in those groups (*14*,*17*). We required negative urine or serum pregnancy test results for all women of childbearing potential who were not surgically sterilized or who did not meet the study definition of postmenopausal at or within 7 days before screening. Participants of childbearing potential who were not surgically sterilized had to agree to practice an adequate method of contraception (barrier method or nonhormonal intrauterine device) or abstain from sexual activity that can lead to pregnancy during study treatment, regardless of the study regimen (*17*). Pregnancy tests during study follow-up were not required by the study protocol. We asked participants of childbearing potential during study visits about their last menstrual period, and a pregnancy test could be conducted at the discretion of clinician investigators.

Analysis of Population, Procedures, and Definitions

We included in this secondary analysis all women who were randomized in S31/A5349, took ≥1 dose of assigned treatment, and became pregnant during participation in the trial. We defined a participant of childbearing potential as a woman 15–49 years of age (*18*).

For participants who reported pregnancy or were determined to be pregnant while receiving study therapy, including participants in the control arm, we permanently stopped their study treatment (regardless of assigned regimen) and treated their TB according to their respective national TB program or local guidelines (local standard of care). Pregnant participants continued to receive scheduled study follow-up except for study-specific chest radiographs (*14*,*17*). Those participants were followed by the site until the pregnancy outcome was known. We did not collect nonstudy TB treatment outcomes in this study.

We advised sites to make efforts to estimate a true conception date to the best of their ability and provided sites with guidance on using and prioritizing information available for the estimation of the conception date to determine if conception took place during study treatment and the fetus had been exposed to study drugs (*19*) (Appendix, https://wwwnc.cdc.gov/EID/article/31/12/25-0492-App1.pdf). We considered the participant to be exposed to a study drug during pregnancy if the estimated date of conception (EDC) was on or before the last study dose date. Each pregnancy report was reviewed in real-time by the safety officer (possessing an MD degree) at the Clinical Research Branch, Division of Tuberculosis Elimination, at CDC's National Center for HIV, Viral Hepatitis, STD, and Tuberculosis Prevention.

Sites reported pregnancies on an adverse event (AE) case report form. The form included an EDC as the adverse event onset date. We captured pregnancy outcomes on an AE follow-up case report form and included live birth, fetal death (pregnancy loss at ≥20 weeks of gestation), spontaneous abortion (pregnancy loss at <20 weeks of gestation), or elective abortion. We defined adverse pregnancy outcomes as fetal loss (fetal death or spontaneous abortion) or infants with a congenital anomaly.

The primary efficacy outcome in the parent trial was TB disease-free survival 12 months after randomization. For each participant, we assigned a primary efficacy outcome status of favorable, unfavorable, or not assessable, as described previously; we further classified unfavorable outcomes as TB-related or not TB-related (*14*,*17*). We considered participants with unfavorable and not assessable outcomes to have a not favorable outcome.

The primary safety outcome in the parent trial was the proportion of participants with grade ≥3 AEs during treatment (with onset up to 14 days after the last dose of study medication). Severity of AEs was graded by the site investigators according to the National Cancer Institute common terminology criteria for adverse events version 4.03 (*20*), which requires classification of pregnancy as an AE with a grade of ≥3; therefore, every participant who became pregnant had ≥1 AE that was grade ≥3. We excluded the pregnancy AEs from the analysis of safety outcomes. Tolerability was a secondary safety outcome, which we defined as premature discontinuation of the assigned regimen for any reason other than microbiologic ineligibility.

The trial was approved by CDC's Institutional Review Board and by local ethics committees, and all participants provided written informed consent. The study data were monitored by the Data Safety Monitoring Board.

Data Analysis

We calculated length of exposure to the study drugs as the number of days between EDC and the date of the last study dose. We report frequency of pregnancy outcomes (live birth, fetal loss [death or spontaneous

Table 1. Baseline demographic characteristics of participants who became pregnant during a TB treatment-shortening trial, Tuberculosis Trials Consortium Study 31/AIDS Clinical Trials Group A5349, January 2016–July 2020*

	Exposed to study drugs during pregnancy, N = 30				Unexposed to study drugs during pregnancy, N = 67			
Characteristic	Control, n = 13	RPT/MOX, n = 9	RPT, n = 8	Total, N = 30	Control, n = 22	RPT/MOX, n = 24	RPT, n = 21	Total, N = 67
Age at conception, y, median (range)	24 (19–35)	24 (19–29)	24 (21–33)	24 (19–35)	28 (22–38)	25 (16–44)	23 (18–41)	26 (16–44)
Age at conception group, y								
12–17†	0	0	0	0	0	1 (4.2)	0	1 (1.5)
18–34	11 (84.6)	9 (100.0)	8 (100.0)	28 (93.3)	18 (81.8)	20 (83.3)	17 (81.0)	55 (82.1)
≥35	2 (15.4)	0	0	2 (6.7)	4 (18.2)	3 (12.5)	4 (19.0)	11 (16.4)
Race‡								
Asian	0	0	1 (12.5)	1 (3.3)	2 (9.1)	1 (4.2)	0	3 (4.5)
Black or African American	12 (92.3)	7 (77.8)	5 (62.5)	24 (80.0)	18 (81.8)	19 (79.2)	18 (85.7)	55 (82.1)
White	0	0	0	0	0	2 (8.3)	0	2 (3.0)
≥1 race	0	2 (22.2)	2 (25.0)	4 (13.3)	1 (4.5)	2 (8.3)	3 (14.3)	6 (9.0)
Other	1 (7.7)	0	0	1 (3.3)	0	0	0	0
Not reported	0	0	0	0	1 (4.5)	0	0	1 (1.5)
Geographic region								
Africa	9 (69.2)	7 (77.8)	5 (62.5)	21 (70.0)	12 (54.5)	16 (66.7)	17 (81.0)	45 (67.2)
Asia	0	0	1 (12.5)	1 (3.3)	2 (9.1)	1 (4.2)	0	3 (4.5)
North America	3 (23.1)	2 (22.2)	1 (12.5)	6 (20.0)	7 (31.8)	5 (20.8)	3 (14.3)	15 (22.4)
South America	1 (7.7)	0	1 (12.5)	2 (6.7)	1 (4.5)	2 (8.3)	1 (4.8)	4 (6.0)
HIV-positive§	0	1 (11.1)	0	1 (3.3)	1 (4.5)	3 (12.5)	2 (9.5)	6 (9.0)
CD4 among HIV-positive, median (IQR)	NA	511 (511–511)	NA	511 (511–511)	331 (331–331)	355 (158–678)	382 (374–389)	365 (331–389)
Cavitation on baseline chest radiograph¶								
Absent	5 (38.5)	3 (33.3)	3 (37.5)	11 (36.7)	10 (45.5)	7 (29.2)	7 (33.3)	24 (35.8)
<4 cm	6 (46.2)	3 (33.3)	3 (37.5)	12 (40.0)	7 (31.8)	7 (29.2)	9 (42.9)	23 (34.3)
≥4 cm	2 (15.4)	3 (33.3)	2 (25.0)	7 (23.3)	5 (22.7)	9 (37.5)	5 (23.8)	19 (28.4)
Missing	0	0	0	0	0	1 (4.2)	0	1 (1.5)
WHO sputum smear grade								
Negative	0	0	0	0	1 (4.5)	2 (8.3)	1 (4.8)	4 (6.0)
Scanty or 1–9 AFB	2 (15.4)	2 (22.2)	2 (25.0)	6 (20.0)	5 (22.7)	2 (8.3)	5 (23.8)	12 (17.9)
1+	2 (15.4)	3 (33.3)	1 (12.5)	6 (20.0)	4 (18.2)	4 (16.7)	1 (4.8)	9 (13.4)
2+	7 (53.8)	4 (44.4)	2 (25.0)	13 (43.3)	6 (27.3)	11 (45.8)	7 (33.3)	24 (35.8)
3+	2 (15.4)	0	3 (37.5)	5 (16.7)	6 (27.3)	5 (20.8)	7 (33.3)	18 (26.9)
Participant weight, kg, median (range)	49 (42–80)	49 (43–56)	51 (43–58)	50 (42–80)	51 (42–73)	50 (40–88)	50 (40–70)	50 (40–88)
BMI, kg/m^2, median (range)	19 (18–32)	19 (17–23)	19 (16–22)	19 (16–32)	20 (16–25)	19 (15–32)	19 (15–27)	20 (15–32)
Current smoker	2 (15.4)	0	2 (25.0)	4 (13.3)	3 (13.6)	3 (12.5)	3 (14.3)	9 (13.4)
Diabetes mellitus history	2 (15.4)	0	0	2 (6.7)	2 (9.1)	1 (4.2)	1 (4.8)	4 (6.0)
Prior episode of TB treatment	0	0	1 (12.5)	1 (3.3)	1 (4.5)	2 (8.3)	1 (4.8)	4 (6.0)

*Values are no. (%) except as indicated. Participants who had ≥1 pregnancy during trial are shown by exposure to the study drugs for their first pregnancy. AFB, acid-fast bacillus; ART, antiretroviral therapy; BMI, body mass index; IQR, interquartile range; MOX, moxifloxacin; NA, not applicable; RPT, rifapentine; TB, tuberculosis; WHO, World Health Organization.
†Minimum age of eligibility for the trial was 12 years. No pregnancies were reported in female participants 12–15 years of age.
‡Race was self-reported by trial participants.
§HIV-positive persons were required to be on efavirenz-based ART for a minimum of 30 days at the time of enrollment, or, if not on ART at enrollment, planned initiation of efavirenz-based ART before or at study week 8.
¶Cavity size refers to aggregate diameter of all cavities.

abortion], or elective abortion) among pregnant participants exposed to the study drugs (exposed pregnancies) in the 2 investigational arms compared with the control arm and among participants who became pregnant after study treatment was completed (unexposed pregnancies). We calculated unadjusted risk difference for fetal loss and congenital anomaly comparing investigational regimens to control with exact 95% CIs based on the 2-sided score test. We used SAS 9.4 for those calculations (*21*). We describe study TB treatment outcomes and AEs experienced by pregnant participants.

Results

We enrolled a total of 740 female participants in S31/A5349 during January 25, 2016–October 30, 2018 (we completed study follow-up in July 2020); 97 (13.1%) of those 740 participants became pregnant during study treatment or follow-up. Five (5%) of those 97 participants became pregnant twice during trial participation, resulting in a total of 102 pregnancies. Of 102 pregnancies, 30 (29.4%) were exposed to the study drugs (either investigational or control arms). Median age of those 30 participants was 24 years

Table 2. Duration of study drug exposure during pregnancy and pregnancy and infant outcomes in the TB treatment-shortening trial, Tuberculosis Trials Consortium Study 31/AIDS Clinical Trials Group A5349, January 2016–July 2020*

Drug exposure and outcome	Pregnancies with exposure to study drugs, N = 30				Pregnancies without exposure to study drugs, N = 72			
	Control, n = 13	RPT/MOX, n = 9	RPT, n = 8	Total, N = 30	Control, n = 24	RPT/MOX, n = 26	RPT, n = 22	Total, N = 72
Total no. study drug doses received, median (range)	157 (27–184)	118 (54–133)	107 (81–119)	118 (27–184)	181 (146–195)	119 (55–121)	118 (36–131)	119 (36–195)
Duration of study drug exposure during pregnancy, d, median (range)	39 (11–103)	36 (13–119)	39 (16–114)	37 (11–119)	NA	NA	NA	NA
Pregnancy outcome								
Live birth, no. (%)	7 (53.8)	7 (77.8)	7 (87.5)	21 (70.0)	18 (75.0)	20 (76.9)	16 (72.7)	54 (75.0)
Fetal death, no. (%)	1 (7.7)	0	0	1 (3.3)	1 (4.2)	0	2 (9.1)	3 (4.2)
Spontaneous abortion, no. (%)	2 (15.4)	1 (11.1)	1 (12.5)	4 (13.3)	0	1 (3.8)	2 (9.1)	3 (4.2)
Elective abortion, no. (%)	3 (23.1)	1 (11.1)	0	4 (13.3)	4 (16.7)	4 (15.4)	1 (4.5)	9 (12.5)
Fetal loss by fetal death/spontaneous abortion, no. (%)	3 (23.1)	1 (11.1)	1 (12.5)	5 (16.7)	1 (4.2%)	1 (3.8)	4 (18.2)	6 (8.3)
Unadjusted risk difference† from control in % with fetal loss (95% CI)‡	Referent	−12.0 (−43.8 to 27.7)	−10.6 (−42.7 to 29.8)		Referent	−0.4 (−18.4 to 16.7)	14.0 (−5.9 to 35.4)	
Unknown, no. (%)	0	0	0	0	1 (4.2)	1 (3.8)	1 (4.5)	3 (4.2)
Infant outcomes								
Congenital anomaly, no. (% of live births)	0/7 (0.0)	0/7 (0.0)	1/7 (14.3)	1/21 (4.8)	0/18 (0.0)	1/20 (5.0)	0/16 (0.0)	1/54 (1.9)
Unadjusted risk difference§ (95% CI)‡	Referent	0	14.3 (−26.0 to 53.3)		Referent	5.0 (−13.8 to 24.2)	0	

*MOX, moxifloxacin; NA, not applicable; RPT, rifapentine; TB, tuberculosis.
†Difference from control in percentage with fetal loss.
Exact 95% CI based on a 2-sided score test (*21*).
§Difference from control in percentage of live births with congenital anomaly.

(range 18–35 years); 1 participant was living with HIV (Table 1).

Among 30 pregnancies considered exposed, the median number of days of study drug exposure was 39 days (range 11–103 days) in the control regimen, 36 days (range 13–119 days) in the rifapentine/moxifloxacin regimen, and 39 days (range 16–114 days) in the rifapentine regimen. Outcomes of 30 exposed pregnancies were 21 (70%) live births, 5 (16.7%) fetal loss (fetal death or spontaneous abortion), and 4 (13.3%) elected abortions. Fetal loss was reported for 3/13 (23.1%) pregnancies in the control regimen, 1/9 (11.1%) pregnancies in the rifapentine/moxifloxacin regimen, and 1/8 (12.5%) pregnancies in the rifapentine regimen (unadjusted risk difference [RD] −12.0% [95% CI −43.8% to 27.7%] for rifapentine/moxifloxacin vs. control arm; unadjusted RD −10.6% [95% CI −42.7% to 29.8%] for rifapentine vs. control arm) (Table 2). Four of 5 fetal losses occurred in pregnancies of <20 weeks' gestational age. Among 21 live births in exposed pregnancies (7 in each arm), 1 infant (overall 4.8% of live births) with a congenital anomaly was reported in the rifapentine arm (1/7 live births) (unadjusted RD 14.3% [95% CI −26.0% to 53.3%] for rifapentine vs. control). That infant had congenital musculoskeletal disorder, including clubfeet and myopathy (Table 3).

Table 3. Infants with congenital anomalies born to participants who became pregnant during the TB treatment-shortening trial, Tuberculosis Trials Consortium Study 31/AIDS Clinical Trials Group A5349, January 2016–July 2020*

Case	Description of congenital anomaly	Study regimen	Mother's age at enrollment, y	Total no. study doses mother received	Total no. study doses fetus exposed	EDC calculation method	Infant's gestational age, wks
1	Musculoskeletal disorder, including clubfeet and myopathy	RPT	26	118	41	LMP + 14 d and ultrasound in second trimester	39
2	Umbilical hernia and right inguinal hernia	RPT/MOX	22	121	0	LMP + 14 d	30

*EDC, estimated date of conception; LMP, last menstrual period; MOX, moxifloxacin; RPT, rifapentine; TB, tuberculosis.

Of 72 pregnancies considered unexposed, fetal loss was reported in 1/24 (4.2%) pregnancies in the control regimen, 1/26 (3.8%) pregnancies in the rifapentine/moxifloxacin regimen, and 4/22 (18.2%) pregnancies in the rifapentine regimen. One infant with a congenital anomaly was reported in the rifapentine/moxifloxacin regimen (1/20 live births [5.0%]). That infant had congenital umbilical hernia and right inguinal hernia (Table 3).

Among 29 participants with exposed pregnancies in the microbiologically eligible analysis population, study treatment outcome was assigned as unfavorable for 7/13 (53.8%) participants in the control regimen, 4/9 (44.4%) participants in the rifapentine/moxifloxacin regimen, and 3/7 (42.9%) participants in the rifapentine regimen (Table 4). All 14 unfavorable outcomes in this population were in the not assessable category (all were withdrawn from study treatment because of pregnancy).

Of 30 participants with exposed pregnancies included in the safety analysis population, 5/30 (16.7%) experienced grade ≥3 AEs (excluding pregnancy itself, which was always reported as an AE) during study treatment: 2/13 (15.4%) in the control regimen, 3/9 (33.3%) in the rifapentine/moxifloxacin regimen, and 0/8 (0%) in the rifapentine regimen (Table 5; Appendix Table). No deaths occurred among participants in the study who became pregnant.

Discussion

This analysis examined pregnancy outcomes among women who became pregnant during participation in the S31/A5349 trial of treatment of drug-susceptible pulmonary TB. We observed no excess fetal losses among pregnant participants in the rifapentine/moxifloxacin arm compared with the control arm, although the numbers were small. We noted no infants with congenital anomalies among those considered exposed to study drugs during pregnancy in the rifapentine/moxifloxacin arm. The overall percentages of fetal loss (16.7%) and congenital anomalies (4.8% of live births) in pregnancies exposed to the study drugs we observed in this trial were similar to those estimated for the United States (19.7% for fetal loss and 3% of live births for congenital anomalies) (*22*,*23*).

Because multiple antibiotics are used concomitantly during TB treatment, isolating the effects of individual drugs on pregnancy outcomes is challenging. With regard to rifapentine use in pregnant animals, previous developmental toxicity studies in rats and rabbits suggested that rifapentine produced fetal harm and was teratogenic (*24*). This description is similar to that of rifampin, which was teratogenic in high doses in animal models (*25*); however, on the basis of extensive use and years of clinical experience, the use of rifampin to treat TB during pregnancy has benefits greater than safety concerns with respect to curing TB. Studies of rifapentine during human pregnancy and lactation have been limited. In 6 patients randomized to rifapentine for initial treatment of TB in humans and who become pregnant during this trial, no episodes of teratogenicity occurred; 2 patients had normal deliveries, 2 had first-trimester spontaneous abortions (1 patient had

Table 4. TB treatment outcomes in the microbiologically eligible population of the TB treatment-shortening trial, Tuberculosis Trials Consortium Study 31/AIDS Clinical Trials Group A5349, January 2016–July 2020*

	Pregnancies with exposure to study drugs, N = 29				Pregnancies without exposure to study drugs, N = 67			
Outcome	Control, n = 13	RPT/MOX, n = 9	RPT, n = 7	Total, N = 29	Control, n = 22	RPT/MOX, n = 24	RPT, n = 21	Total, N = 67
Favorable, total†	6 (46.2)	5 (55.6)	4 (57.1)	15 (51.7)	21 (95.5)	23 (95.8)	19 (90.5)	63 (94.0)
Not favorable, total‡	7 (53.8)	4 (44.4)	3 (42.9)	14 (48.3)	1 (4.5)	1 (4.2)	2 (9.5)	4 (6.0)
Unfavorable outcome, total	0	0	0	0	1 (4.5)	0	1 (4.8)	2 (3.0)
TB-related unfavorable outcome, total	0	0	0	0	1 (4.5)	0	0	1 (1.5)
Not seen at month 12; last culture positive	0	0	0	0	1 (4.5)	0	0	1 (1.5)
Not TB-related unfavorable outcome, total	0	0	0	0	0	0	1 (4.8)	1 (1.5)
Treatment changed because of adverse event	0	0	0	0	0	0	1 (4.8)	1 (1.5)
Not assessable outcome, total	7 (53.8)	4 (44.4)	3 (42.9)	14 (48.3)	0	1 (4.2)	1 (4.8)	2 (3.0)
Not seen at month 12; last culture negative	0	0	0	0	0	0	1 (4.8)	1 (1.5)
Withdrawn from treatment because of pregnancy	7 (53.8)	4 (44.4)	3 (42.9)	14 (48.3)	0	1 (4.2)	0	1 (1.5)

*Values are no. (%). Microbiologically eligible analysis population included the subset of all enrolled participants who receive a treatment assignment who, in addition, have culture confirmation of drug-susceptible TB at study entry. MOX, moxifloxacin; RPT, rifapentine; TB, tuberculosis.
†All participants with favorable outcome had culture-negative status at month 12.
‡Participants with unfavorable and not assessable outcomes were considered to have a not favorable outcome.

Table 5. Safety and tolerability among participants with pregnancies in the safety population of the tuberculosis treatment shortening trial, Tuberculosis Trials Consortium Study 31/AIDS Clinical Trials Group A5349, January 2016–July 2020*

Outcome	Pregnancies with exposure to study drugs, n = 30				Pregnancies without exposure to study drugs, N = 67			
	Control, n = 13	RPT/MOX, n = 9	RPT, n = 8	Total, n = 30	Control, n = 22	RPT/MOX, n = 24	RPT, n = 21	Total, n = 67
Primary safety outcome								
Participants with grade ≥3 AE during study treatment†	2 (15.4)	3 (33.3)	0	5 (16.7)	5 (22.7)	2 (8.3)	0	7 (10.4)
Secondary safety outcomes								
Participants with treatment-related grade ≥3 AE during study treatment†	0	1 (11.1)	0	1 (3.3)	2 (9.1)	1 (4.2)	0	3 (4.5)
Other safety outcomes								
Participants with any serious AE during study treatment†	1 (7.7)	1 (11.1)	0	2 (6.7)	3 (13.6)	1 (4.2)	0	4 (6.0)
Participants died	0	0	0	0	0	0	0	0
Participants with any AE resulting in discontinuation of study treatment	0	0	0	0	1 (4.5)	0	1 (4.8)	2 (3.0)
Participants with any grade ≥3 AE during 28 wks after randomization†	3 (23.1)	5 (55.6)	1 (12.5)	9 (30.0)	8 (36.4)	5 (20.8)	5 (23.8)	18 (26.9)
ALT or AST 5-fold ULN‡	0	0	0	0	1 (4.5)	0	0	1 (1.5)
ALT or AST 10-fold ULN	0	0	0	0	0	0	0	0
Serum total bilirubin 3-fold ULN§	0	0	0	0	0	0	0	0
ALT or AST 3-fold ULN plus serum total bilirubin 2-fold ULN (Hy's law)	0	0	0	0	0	0	0	0
AEs during pregnancy¶								
Participants with grade ≥3 AE	1 (7.7)	2 (22.2)	0	3 (10.0)	0	0	0	0
Participants with treatment-related grade ≥3 AE	0	0	0	0	0	0	0	0
Participants with any AE	1 (7.7)	1 (11.1)	0	2 (6.7)	0	0	0	0
Tolerability (microbiologically eligible analysis population)								
Discontinuation of assigned treatment for any reason	7 (53.9)	4 (44.4)	3 (42.9)	14 (50.0)	1 (4.6)	1 (4.2)	2 (9.5)	4 (6.0)

*ALT, alanine aminotransferase; AST, aspartate aminotransferase; MOX, moxifloxacin; RPT, rifapentine; ULN, upper limit of normal range.
†Pregnancies were excluded from this analysis (all pregnancies were reported as grade ≥3 AE in this trial).
‡>5-fold ULN corresponds to grade ≥3.
§>3-fold ULN corresponds to grade ≥3.
¶Includes AEs (other than pregnancy) with onset date from estimated date of conception through date of pregnancy outcome.

alcohol use disorder, and the other patient was living with HIV), 1 had an elective abortion, and 1 was lost to follow-up (*24*). In analysis evaluating safety and pregnancy outcomes among pregnant women who were inadvertently exposed to study medications in 2 Tuberculosis Trials Consortium Study latent tuberculosis treatment trials (PREVENT TB and iAdhere), evaluating 3 months of weekly rifapentine (900 mg) with isoniazid and 9 months of daily isoniazid, fetal loss or congenital anomalies were at similar rates to the general population (*26*). Among 50 women enrolled in the IMPAACT 2001 trial, designed to assess 3 months of weekly rifapentine with isoniazid for TB prevention in pregnant women during the second or third trimester, with or without HIV, no drug-related serious AEs, treatment discontinuations, or TB cases were reported, although 1 case of fetal death was related to maternal physical trauma (*27*). The DOLPHIN-Moms trial, assessing 1 month of daily isoniazid and rifapentine versus 3 months of once-weekly rifapentine and isoniazid in pregnancy, is currently enrolling (*28*).

Concerning fluoroquinolone use in pregnancy, animal studies showed delayed skeletal development in fetal rats and rabbits when exposed to moxifloxacin and toxic cartilage effects in immature dogs when exposed to temafloxacin (*9*,*29*). However, in human studies, a metaanalysis that included 5 studies on use of quinolones during the first trimester of pregnancy did not find an increased risk for major malformations, stillbirths, preterm births, or low birthweight (*30*). A small case series of pregnant women with drug-resistant TB treated with second-line drugs, including fluoroquinolones, suggested that favorable pregnancy outcomes are achievable (*31*–*34*). A systematic review and metaanalysis of outcomes of pregnancies exposed to quinolone and fluoroquinolones, involving 8 cohort and 2 case–control studies, showed no statistically significant increases in rates of major malformations for quinolone and fluoroquinolone exposures (*35*).

Our study expands the scientific literature with additional data on rifapentine, moxifloxacin, pyrazinamide, and isoniazid early in pregnancy. We found that relatively brief exposures to rifapentine and

moxifloxacin early in pregnancy were not associated with adverse fetal or maternal outcomes. However, the effect of longer exposures to rifapentine and moxifloxacin and effect of exposures later in pregnancy on maternal and fetal outcomes remains unknown, given that the trial specified immediate study treatment discontinuation and transition to local standard of care when a pregnancy was recognized. Our findings can help support and accelerate the participation of pregnant women in TB drug trials. In addition, publication of the detailed methodology used in this study to estimate the date of conception and total period of drug exposure during pregnancy might inform other clinical trials and thus help develop much needed harmonized reporting of safety outcomes among pregnant trial participants.

One limitation of our study is that the number of participants who became pregnant during study treatment was small, probably because of rigorous education of study participants of childbearing potential about contraception and preventing pregnancy during study treatment. The small number of pregnant participants limited the ability to detect rare events that can only be detected in larger trials and through pharmacovigilance efforts in the future. In addition, in participants who became pregnant, durations of exposures to study drugs were short, given that the protocol required immediate study treatment discontinuation in pregnancy. Adverse pregnancy events that require a higher cumulative exposure to study drugs to occur might not have been observed, so results should be interpreted in light of the short exposures. However, an average of 30 days of drug exposure during first trimester is a relatively long period of drug exposure and should not be dismissed. Furthermore, because fetal organogenesis primarily occurs in the first trimester, it is reassuring that only 1 infant with a congenital anomaly was observed among pregnancies exposed to rifapentine. In addition, because the study protocol required permanent discontinuation of the study treatment if a participant became pregnant (and transition to local standard of care), most participants who became pregnant during study treatment had their primary study TB treatment efficacy outcome classified as not assessable. Although final pregnancy outcomes were collected in the database for all participants, final TB treatment outcomes (after permanent stop of study treatment and switching to the local standard of care regimen) were not. Moreover, the study did not assess congenital anomalies among fetal deaths or spontaneous abortions. Finally, because study arms contained multiple study drugs, we cannot determine the effect of any single drug on adverse pregnancy outcomes. However, anti-TB drugs are commonly used in pregnancy, given the urgency of providing swift, full treatment for TB as soon as it is diagnosed.

In conclusion, among exposed pregnancies in this large phase 3 drug-susceptible pulmonary TB treatment trial, we did not observe a higher risk for fetal loss or infants with congenital anomalies among those participants who became pregnant while receiving a rifapentine/moxifloxacin regimen compared with the standard 6-month regimen. Those data can be used by clinicians and patients as they engage in shared decision-making and weigh the risks and benefits of using a shorter-duration 4-month rifapentine/moxifloxacin regimen versus a 6-month standard-of-care regimen in pregnancy, especially in the circumstance where an on-treatment pregnancy occurs. Future trials of rifapentine/moxifloxacin-containing regimens should consider allowing reconsent for participants who become pregnant during study treatment so that they can continue these study drugs with careful follow-up if there is potential benefit and there are no contraindications (*36*). The data from our study contribute to the growing body of information about the safety of rifapentine-containing regimens in pregnancy, which should support fuller participation of pregnant women in future TB clinical trials that include these antibiotics.

Members of the AIDS Clinical Trials Group A5349: TASK, South Africa; University of Cape Town Lung Institute, South Africa; Les Centre GHESKIO INLR, Haiti; Parirenyatwa Clinical Research Site, Zimbabwe; South African Tuberculosis Vaccine Initiative, South Africa; Wits Helen Joseph Clinical Research Site Department of Medicine, South Africa; Les Centre GHESKIO IMIS, Haiti; Soweto ACTG Clinical Research Site, South Africa; Byramjee Jeejeebhoy Medical College, India; University of North Carolina Project Tidziwe Centre, Malawi; Kisumu Clinical Research Site, Kenya; Instituto Nacional de Pesquisa Clinica Evandro Chagas, Brazil; Blantyre Clinical Research Site/Johns Hopkins Research Project, Malawi; Family Clinical Research Unit (FAMCRU), South Africa; Durban International Clinical Research Site, South Africa; Moi University Clinical Research Site, Kenya; San Miguel Clinical Research Site, Peru; Asociacion Civil Impacta Salud y Educacion, Peru; Joint Clinical Research Center, Kampala Clinical Research Site, Uganda; Kenya Medical Research Institute/Walter Reed Project Clinical Research Center, Kenya; The Thai Red Cross AIDS Research Centre, Thailand; Chiang Mai University HIV Treatment Clinical Research Site, Thailand; Hospital Conceicao Porto Alegre, Brazil; and University of California San Francisco Clinical Research Site, USA.

Members of the Tuberculosis Trials Consortium Study 31: Uganda-Case Western Reserve University Research Collaboration, Uganda; Vietnam National Tuberculosis Program/University of California San Francisco Research Collaboration, Vietnam; Wits Health Consortium Perinatal HIV Research Unit (PHRU), South Africa; Tuberculosis and Chest Service of Hong Kong, China; San Antonio Veterans Administration Medical Center, USA; Universidad Peruana Cayetano Heredia, Peru; University of North Texas Health Science Center, USA; Columbia University, USA; Austin Tuberculosis Clinic, USA; and Baylor College of Medicine and Affiliated Hospitals/VA, USA.

Acknowledgments

We are grateful to the study participants who contributed their time to this trial and site and local tuberculosis program staff who assisted in the clinical management of study participants.

We are saddened to share that our colleague and coauthor William C. Whitworth passed away prior to the publication of this article. His insight and dedication greatly shaped this work.

Funding support for this trial was provided by the Centers for Disease Control and Prevention, National Center for HIV, Viral Hepatitis, STD, and Tuberculosis Prevention, Division of Tuberculosis Elimination (contract nos. 200-2009-32582, 200-2009-32593, 200-2009-32594, 200-2009-32589, 200-2009-32597, 200-2009-32598, 75D30119C06702, 75D30119C06701, 75D30119C06703, 75D30119C06222, 75D30119C06225, and 75D30119C06010) and by the National Institute of Allergy and Infectious Diseases of the National Institutes of Health (award nos. UM1 AI068634, UM1 AI068636, and UM1 AI106701). Sanofi donated rifapentine and all other study drugs, supported shipping of study drugs to all sites, and provided funding support for pharmacokinetic testing and preparation of the final clinical study in this collaborative study.

Author contributions: study conception and design (E.V.K., W.C.W., P.J.P.P., N.A.S., S.S., R.E.C., S.E.D., and P.N.); data collection (E.V.K., W.C.W., K.E.B., N.A.S., N.E.B., K.H., L.P.P., G.M., R.D., Z.W., W.C., S.S., R.E.C., S.E.D., and P.N.); data analysis (W.C.W., P.J.P.P., N.A.S., and K.E.B.); data interpretation (E.V.K., W.C.W., L.P.P., P.J.P.P., N.A.S., K.E.B., P.J.P.P., W.C., K.E.D., S.S., R.E.C., S.E.D., and P.N.); drafting of the initial manuscript (E.V.K., W.C.W., M.D., K.E.D., and P.J.P.P.); critical review of the final draft of the manuscript (E.V.K., W.C.W., K.E.B., N.A.S., M.D., J.S.V.M., P.J.P.P., R.B., N.E.B., K.H., W.C., L.P.P., G.M., R.D., Z.W., K.E.D., S.S., R.E.C., S.E.D., and P.N.); and access and verification of underlying data (W.C.W., P.J.P.P., N.A.S., and K.E.B.).

The authorship team members have declared any potential conflicts of interest with respect to the research, authorship, or publication of this article. Sanofi commercial interests did not influence the study design; the collection, analysis, or interpretation of data; the preparation of this manuscript; or the decision to submit this manuscript for publication. A Sanofi technical expert served on the protocol team.

About the Author

Dr. Kurbatova is health scientist in the Clinical Research Branch, Division of Tuberculosis Elimination, National Center for HIV, Viral Hepatitis, STD, and Tuberculosis Prevention, Centers for Disease Control and Prevention. Her primary research interests include infectious diseases epidemiology and clinical research, including tuberculosis treatment shortening.

References

1. Sugarman J, Colvin C, Moran AC, Oxlade O. Tuberculosis in pregnancy: an estimate of the global burden of disease. Lancet Glob Health. 2014;2:e710–6. https://doi.org/10.1016/S2214-109X(14)70330-4
2. Zumla A, Bates M, Mwaba P. The neglected global burden of tuberculosis in pregnancy. Lancet Glob Health. 2014;2:e675–6. https://doi.org/10.1016/S2214-109X(14)70338-9
3. Mathad JS, Gupta A. Tuberculosis in pregnant and postpartum women: epidemiology, management, and research gaps. Clin Infect Dis. 2012;55:1532–49. https://doi.org/10.1093/cid/cis732
4. Jana N, Barik S, Arora N, Singh AK. Tuberculosis in pregnancy: the challenges for South Asian countries. J Obstet Gynaecol Res. 2012;38:1125–36. https://doi.org/10.1111/j.1447-0756.2012.01856.x
5. Grange J, Adhikari M, Ahmed Y, Mwaba P, Dheda K, Hoelscher M, et al. Tuberculosis in association with HIV/AIDS emerges as a major nonobstetric cause of maternal mortality in sub-Saharan Africa. Int J Gynaecol Obstet. 2010;108:181–3. https://doi.org/10.1016/j.ijgo.2009.12.005
6. Ahmed Y, Mwaba P, Chintu C, Grange JM, Ustianowski A, Zumla A. A study of maternal mortality at the University Teaching Hospital, Lusaka, Zambia: the emergence of tuberculosis as a major non-obstetric cause of maternal death. Int J Tuberc Lung Dis. 1999;3:675–80.
7. Desai M, Phillips-Howard PA, Odhiambo FO, Katana A, Ouma P, Hamel MJ, et al. An analysis of pregnancy-related mortality in the KEMRI/CDC health and demographic surveillance system in western Kenya. PLoS One. 2013;8:e68733. https://doi.org/10.1371/journal.pone.0068733
8. Pillay T, Khan M, Moodley J, Adhikari M, Coovadia H. Perinatal tuberculosis and HIV-1: considerations for resource-limited settings. Lancet Infect Dis. 2004;4:155–65. https://doi.org/10.1016/S1473-3099(04)00939-9
9. Gupta A, Mathad JS, Abdel-Rahman SM, Albano JD, Botgros R, Brown V, et al. Toward earlier inclusion of pregnant and postpartum women in tuberculosis drug trials: consensus statements from an international expert panel. Clin Infect Dis. 2016;62:761–9. https://doi.org/10.1093/cid/civ991
10. World Health Organization. Treatment of tuberculosis guidelines. 2010 Jul 15 [cited 2025 Aug 18]. https://www.who.int/publications/i/item/9789241547833

11. Nahid P, Dorman SE, Alipanah N, Barry PM, Brozek JL, Cattamanchi A, et al. Official American Thoracic Society/Centers for Disease Control and Prevention/Infectious Diseases Society of America clinical practice guidelines: treatment of drug-susceptible tuberculosis. Clin Infect Dis. 2016;63:e147–95. https://doi.org/10.1093/cid/ciw376
12. SMART4TB Consortium; IMPAACT Network; WHO Global Tuberculosis Programme. Tuberculosis and pregnancy: building consensus on inclusion in research. 2024 Feb [cited 2025 Aug 18]. https://tbcenter.jhu.edu/wp-content/uploads/2024/02/SMART4TB-Pregnancy-and-TB-Report.pdf
13. US Agency for International Development; SMART4TB Consortium. Washington, D.C. community consensus on the earlier inclusion of pregnant women and persons in TB research. 2024 Feb [cited 2025 Aug 18]. https://www.treatmentactiongroup.org/wp-content/uploads/2024/02/pregnancy_consensus_statement_full_final.pdf
14. Dorman SE, Nahid P, Kurbatova EV, Phillips PPJ, Bryant K, Dooley KE, et al.; AIDS Clinical Trials Group; Tuberculosis Trials Consortium. Four-month rifapentine regimens with or without moxifloxacin for tuberculosis. N Engl J Med. 2021;384:1705–18. https://doi.org/10.1056/NEJMoa2033400
15. Carr W, Kurbatova E, Starks A, Goswami N, Allen L, Winston C. Interim guidance: 4-month rifapentine-moxifloxacin regimen for the treatment of drug-susceptible pulmonary tuberculosis—United States, 2022. MMWR Morb Mortal Wkly Rep. 2022;71:285–9. https://doi.org/10.15585/mmwr.mm7108a1
16. World Health Organization. WHO consolidated guidelines on tuberculosis. Module 4: treatment: drug-resistant tuberculosis treatment. 2022 [cited 2025 Aug 18]. https://www.who.int/publications/i/item/9789240063129
17. Dorman SE, Nahid P, Kurbatova EV, Goldberg SV, Bozeman L, Burman WJ, et al.; AIDS Clinical Trials Group and the Tuberculosis Trials Consortium. High-dose rifapentine with or without moxifloxacin for shortening treatment of pulmonary tuberculosis: study protocol for TBTC study 31/ACTG A5349 phase 3 clinical trial. Contemp Clin Trials. 2020;90:105938. https://doi.org/10.1016/j.cct.2020.105938
18. World Health Organization. Women of reproductive age (15–49 years) population (thousands). 2025 [cited 2025 Aug 18]. https://www.who.int/data/gho/indicator-metadata-registry/imr-details/women-of-reproductive-age-(15-49-years)-population-(thousands)
19. American College of Obstetricians and Gynecologists Committee. ACOG committee opinion no. 579: definition of term pregnancy. Obstet Gynecol. 2013;122:1139–40. https://doi.org/10.1097/01.AOG.0000437385.88715.4a
20. US Department of Health and Human Services; National Institutes of Health; National Cancer Institute. Common terminology criteria for adverse events (CTCAE) version 4.03. 2010 Jun 14 [cited 2025 Aug 18]. https://evs.nci.nih.gov/ftp1/CTCAE/CTCAE_4.03/CTCAE_4.03_2010-06-14_QuickReference_8.5x11.pdf
21. Agresti A, Min Y. On small-sample confidence intervals for parameters in discrete distributions. Biometrics. 2001;57:963–71. https://doi.org/10.1111/j.0006-341X.2001.00963.x
22. Rossen LM, Ahrens KA, Branum AM. Trends in risk of pregnancy loss among US women, 1990–2011. Paediatr Perinat Epidemiol. 2018;32:19–29. https://doi.org/10.1111/ppe.12417
23. Hoyert DL, Mathews TJ, Menacker F, Strobino DM, Guyer B. Annual summary of vital statistics: 2004. Pediatrics. 2006;117:168–83. https://doi.org/10.1542/peds.2005-2587
24. US Food and Drug Administration. Priftin (rifapentine) tablets. Highlights of prescribing information. 1998 [cited 2025 Aug 18]. https://www.accessdata.fda.gov/drugsatfda_docs/label/2010/021024s009lbl.pdf
25. Holdiness MR. Teratology of the antituberculosis drugs. Early Hum Dev. 1987;15:61–74. https://doi.org/10.1016/0378-3782(87)90039-9
26. Moro RN, Scott NA, Vernon A, Tepper NK, Goldberg SV, Schwartzman K, et al. Exposure to latent tuberculosis treatment during pregnancy. The PREVENT TB and the iAdhere trials. Ann Am Thorac Soc. 2018;15:570–80. https://doi.org/10.1513/AnnalsATS.201704-326OC
27. Mathad JS, Savic R, Britto P, Jayachandran P, Wiesner L, Montepiedra G, et al. Pharmacokinetics and safety of 3 months of weekly rifapentine and isoniazid for tuberculosis prevention in pregnant women. Clin Infect Dis. 2022;74:1604–13. https://doi.org/10.1093/cid/ciab665
28. ClinicalTrials.gov. Safety and tolerability of 1 month daily (1HP) and 3 Months Weekly (3HP) isoniazid and rifapentine with pharmacokinetics of dolutegravir (DTG) in pregnant people with HIV (DOLPHIN Moms. 2024 Mar 18 [cited 2025 Aug 18]. https://clinicaltrials.gov/study/NCT05122026?term=DOLPHIN-moms&rank=1
29. Krasula RW, Pernet AG. Comparison of organ-specific toxicity of temafloxacin in animals and humans. Am J Med. 1991;91(6A):38S–41S. https://doi.org/10.1016/0002-9343(91)90309-L
30. Bar-Oz B, Moretti ME, Boskovic R, O'Brien L, Koren G. The safety of quinolones—a meta-analysis of pregnancy outcomes. Eur J Obstet Gynecol Reprod Biol. 2009;143:75–8. https://doi.org/10.1016/j.ejogrb.2008.12.007
31. Tabarsi P, Moradi A, Baghaei P, Marjani M, Shamaei M, Mansouri N, et al. Standardised second-line treatment of multidrug-resistant tuberculosis during pregnancy. Int J Tuberc Lung Dis. 2011;15:547–50. https://doi.org/10.5588/ijtld.10.0140
32. Palacios E, Dallman R, Muñoz M, Hurtado R, Chalco K, Guerra D, et al. Drug-resistant tuberculosis and pregnancy: treatment outcomes of 38 cases in Lima, Peru. Clin Infect Dis. 2009;48:1413–9. https://doi.org/10.1086/598191
33. Khan M, Pillay T, Moodley J, Ramjee A, Padayatchi N. Pregnancies complicated by multidrug-resistant tuberculosis and HIV co-infection in Durban, South Africa. Int J Tuberc Lung Dis. 2007;11:706–8.
34. Shin S, Guerra D, Rich M, Seung KJ, Mukherjee J, Joseph K, et al. Treatment of multidrug-resistant tuberculosis during pregnancy: a report of 7 cases. Clin Infect Dis. 2003;36:996–1003. https://doi.org/10.1086/374225
35. Acar S, Keskin-Arslan E, Erol-Coskun H, Kaya-Temiz T, Kaplan YC. Pregnancy outcomes following quinolone and fluoroquinolone exposure during pregnancy: a systematic review and meta-analysis. Reprod Toxicol. 2019;85:65–74. https://doi.org/10.1016/j.reprotox.2019.02.002
36. Gupta A, Hughes MD, Garcia-Prats AJ, McIntire K, Hesseling AC. Inclusion of key populations in clinical trials of new antituberculosis treatments: current barriers and recommendations for pregnant and lactating women, children, and HIV-infected persons. PLoS Med. 2019;16:e1002882. https://doi.org/10.1371/journal.pmed.1002882

Address for correspondence: Ekaterina Kurbatova, Centers for Disease Control and Prevention, 1600 Clifton Road NE, Mailstop H24-4, Atlanta, GA, 30329-4018, USA; email: ies3@cdc.gov

Oral Transmission of Classical Bovine Spongiform Encephalopathy in ARR/ARR Sheep

Alvina Huor,[1], Frederic Lantier,[1] Jean-Yves Douet, Severine Lugan, Naima Aron, Chloe Mesic, Herve Cassard, Tomás Barrio, Hugh Simmons, Isabelle Lantier, Olivier Andreoletti

Selection for the $A_{136}R_{154}R_{171}$ *PRNP* allele is known to curb classical scrapie in sheep, and we expected it to minimize the risk for classical bovine spongiform encephalopathy (c-BSE) propagation. We orally challenged newborn ARR/ARR and ARQ/ARQ lambs with ovine-passaged c-BSE. Contrary to our expectations, prion disease developed in all ARR/ARR lambs after markedly longer incubation times (≈50 months) than ARQ/ARQ controls (≈20 months). Tissue distribution of the abnormal isoform of prion protein (PrP) in clinically affected ARR/ARR sheep largely mirrored tissue distribution seen in ARQ/ARQ animals. Bioassays in bovine- and human-PrP transgenic mice showed that passage through ARR/ARR sheep did not increase the agent's zoonotic potential. Transmission efficiency in human normal cellular isoform PrP-expressing mice remained similar to cattle c-BSE and lower than ARQ-passaged c-BSE. Our data reveal the limitations of breeding exclusively for ARR when the objective is to mitigate c-BSE risk and underscore the need to maintain specific-risk-material removal and surveillance programs.

Prion diseases, or transmissible spongiform encephalopathies (TSE), are fatal neurodegenerative disorders that occur naturally in various mammalian species, including sheep (scrapie), cervids (chronic wasting disease), and humans (Creutzfeldt-Jakob disease [CJD]). A key event in the pathogenesis of TSEs is the conversion of the normal cellular prion protein (PrP^{C}), encoded by the *PRNP* gene, into an abnormal disease-associated isoform (PrP^{Sc}) within the tissues of those affected. PrP^{C} is completely degraded after controlled digestion with proteinase K (PK) under nondenaturing conditions, whereas PrP^{Sc} is N terminally truncated under such conditions, leaving a PK-resistant core termed PrP^{res} (*1*).

In 1985, classical bovine spongiform encephalopathy (c-BSE), a new prion disease affecting cattle, was identified in the United Kingdom (*2*). The number of c-BSE cases in cattle rapidly increased because of the recycling of infected carcasses into the feed chain in the form of meat and bone meal (MBM) (*3*). Over the next 2 decades, c-BSE disseminated to ≥28 countries, mostly in Europe but also in the United States, Canada, and Japan, through the export of infected live animals and contaminated MBM and livestock feed.

Experimental oral or parenteral exposure to c-BSE demonstrated its transmissibility to sheep (*4*). Because MBM was also distributed to small ruminants, the potential spread of c-BSE in the sheep population became a major concern for health authorities. The emergence of variant CJD (vCJD) in humans, because of dietary exposure to the c-BSE agent, further reinforced those concerns, making the prevention of any potential spread of c-BSE to small ruminants a top priority in Europe (*5*,*6*).

In sheep, susceptibility to prion diseases is determined principally by polymorphisms in the *PRNP* gene. The major polymorphic sites influencing susceptibility to classical scrapie are located at codons 136 (A or V), 154 (R or H), and 171 (R, Q, or H) (*7*,*8*), which also strongly influence susceptibility to BSE. Sheep with the AHQ/AHQ and ARQ/ARQ PrP genotypes are highly susceptible to c-BSE

Author affiliations: University of Toulouse, ENVT, INRAE, IHAP, Toulouse, France (A. Huor, J.-Y. Douet, S. Lugan, N. Aron, C. Mesic, H. Cassard, T. Barrio, O. Andreoletti); National Research Institute for Agriculture, Food and Environment, Nouzilly, France (F. Lantier, I. Lantier); Animal and Plant Health Agency, Weybridge, UK (H. Simmons)

DOI: https://doi.org/10.3201/eid3112.250501

[1]These first authors contributed equally to this article.

infection when exposed through intracerebral or oral routes (*4*).

In contrast, intracerebral inoculation of ARR/ARR sheep with cattle c-BSE resulted in an inefficient transmission of the disease (incomplete attack rate), and oral inoculation failed to transmit disease or cause detectable accumulation of prion infectivity or abnormal PrP in the peripheral tissues or central nervous system (*9*). Those findings led to the conclusion that the ARR/ARR PrP genotype confers strong, if not complete, resistance to c-BSE infection in sheep. Selection for the ARR allele was originally conceived as a tool to control classical scrapie in farmed sheep population, but it also appeared to protect against possible c-BSE transmission (*10*). In this study, we experimentally exposed ARQ/ARQ and ARR/ARR newborn lambs orally to c-BSE passaged in ARQ/ARQ sheep to determine transmission efficiency of the disease.

Materials and Methods

Ethics Statement

All animal experiments were performed in compliance with institutional and French national guidelines (directive no. 2010/63/EU). Sheep BSE experimental transmission was approved by the local National Research Institute for Agriculture, Food and Environment committees, and mouse experiments (national registration no. 01734.01) were approved by the Ecole Nationale Veterinaire Toulouse ethics committees.

Lamb Inoculation

We sourced sheep from New Zealand that were considered free of classical scrapie (*11*). ARQ/ARQ and ARR/ARR ewes were produced under TSE-free conditions in the United Kingdom. They were mated with ARQ/ARQ and ARR/ARR rams and exported to France. Lambs were born and raised within an A3 biosecure unit. We sequenced the *PRNP* gene of each sheep and lamb (*12*). We prepared the c-BSE inoculum by using the brainstem of 3 ARQ/ARQ sheep (at the clinical stage of the disease) that were inoculated through the intracerebral route with cattle BSE.

Lambs received 2 doses of inoculum (each equivalent to 2.5 g of brain tissue) through natural suckling. The first inoculation was received within the first 24 hours of life, and the second dose was delivered 14 days after birth. Lambs and ewes of both genotype groups were housed in a single pen. A total of 6 ARQ/ARQ and 8 ARR/ARR lambs were included in the experiment.

Protein Misfolding Cyclic Amplification and Seeding Activity Titration

We used brain tissue from transgenic mice expressing the ovine ARQ PrP variant (tgShXI) (*13*) to prepare the protein misfolding cyclic amplification (PMCA) substrates, as previously described (*14*). We performed PMCA amplification as previously described (*14*). We included 1 to 2 unseeded controls for every 8 seeded reactions in each run. Each PMCA run included a reference ovine BSE sample (1/10 dilution series of a 10% brain homogenate) as a control for amplification efficiency. We analyzed the PMCA reaction products for the presence of PK-resistant PrP by using Western blot.

For each dilution and each sample, we tested ≥4 replicates in 2 independent runs. For each sample, we determined the last dilution showing ≥50% positive replicates (presence of Western blot–detectable PrP^{res}).

We established the seeding activity titer in a reference 10% (wt/vol) frontal cortex homogenate from a clinical c-BSE ARQ/ARQ sheep by endpoint titration (intracerebral route) in bovine PrP expressing (tgBov) mice (*15*). We estimated the infectious titer (median lethal dose [LD_{50}]/g IC in tgBov) by using the Spearman-Kärber method (*16*).

Western Blot Detection of Abnormal PrP

We detected PrP^{res} by using Western blot. We conducted immunodetection by using 2 different PrP-specific monoclonal antibodies: Sha31 (1 μg/mL), which recognizes the amino acid sequences YEDRYYRE (amino acids 145–152) (*17*), and 12B2 (1 μg/mL) (*18*), whose epitope corresponds to amino acid sequence WGQGG (amino acids 89–93).

Mouse Bioassays

We performed mouse inoculations while the mice were under anesthesia. Mice displaying clinical manifestations were anesthetized with isoflurane before being euthanized by using CO_2 inhalation. We conducted bioassays to characterize the c-BSE strain phenotype by using tgBov mice (*15*).

We characterized c-BSE isolates' abilities to propagate in hosts expressing human PrP by using mice expressing the methionine 129 human PrP variant (tg340-tgMet), the valine 129 human PrP variant (tg361-tgVal), and their crossbred (tgMet/Val), as previously described (*19*). We observed the inoculated mice daily and assessed their neurologic status weekly. When clinically progressive TSE symptoms were evident, or at the end of the mice lifespan, we euthanized the mice. We expressed survival time as

the mean number of days postinoculation (dpi) of all the mice scored positive for PrP^{res}, with a corresponding SD. In cages where no clinical signs were observed, mice were euthanized at the end of their natural lifespan (600–800 days). In those cases, incubation periods reported in the table as >600 dpi corresponded to the survival time observed in ≥3/6 mice.

Lesion Profiling

We established vacuolar brain lesion profiles according to methods previously described (*20*). We created each lesion profile on the basis of data obtained from 5–6 animals.

Infectious Titer Estimates

We intracerebrally inoculated (20 µL) a series of 1/10 dilutions of a reference 10% (wt/vol) brain stem homogenate from an ovine-BSE (ARQ/ARQ) isolate into 6 tgBov mice. We estimated the prion infectious titer by using the Spearman-Kärber method (*16*).

Results

BSE Transmission

We exposed 24-hour-old ARQ/ARQ and ARR/ARR lambs to a dose of 2.5 g of infected brain (derived from cattle c-BSE intracerebrally inoculated into ARQ/ARQ sheep) through natural suckling. We administered a second dose of inoculum by the same route at 14 days of age. In each inoculated animal, we collected blood samples at different time points during the incubation phase. We euthanized animals from each genotype at 4 months postinoculation (mpi) (n = 2) and 10 mpi (n = 2 ARQ/ARQ sheep and n = 3 ARR/ARR sheep).

We observed clinical signs compatible with TSE disease in the remaining c-BSE–exposed ARQ/ARQ animals after 19 mpi and ARR/ARR animals after 48 mpi. We euthanized those animals upon showing locomotor difficulties (ARQ/ARQ at 20 mpi, ARR/ARR at 50 mpi). At necropsy, we collected brain, spinal cord, and a panel of lymphoid tissues.

Irrespective of the genotype, Western blotting confirmed the presence of PrP^{res} in the posterior brainstem of each animal. The PrP^{res} Western blot banding profile displayed the typical features of the BSE agent in sheep: a 19-kDa nonglycosylated band, a dominant di-glycosylated PrP^{res} band, and an absence of immunoreactivity to the 12B2 monoclonal antibody (Figure 1).

Ovine c-BSE PMCA Detection

PMCA is an in vitro methodology that mimics prion replication in an accelerated form, enabling

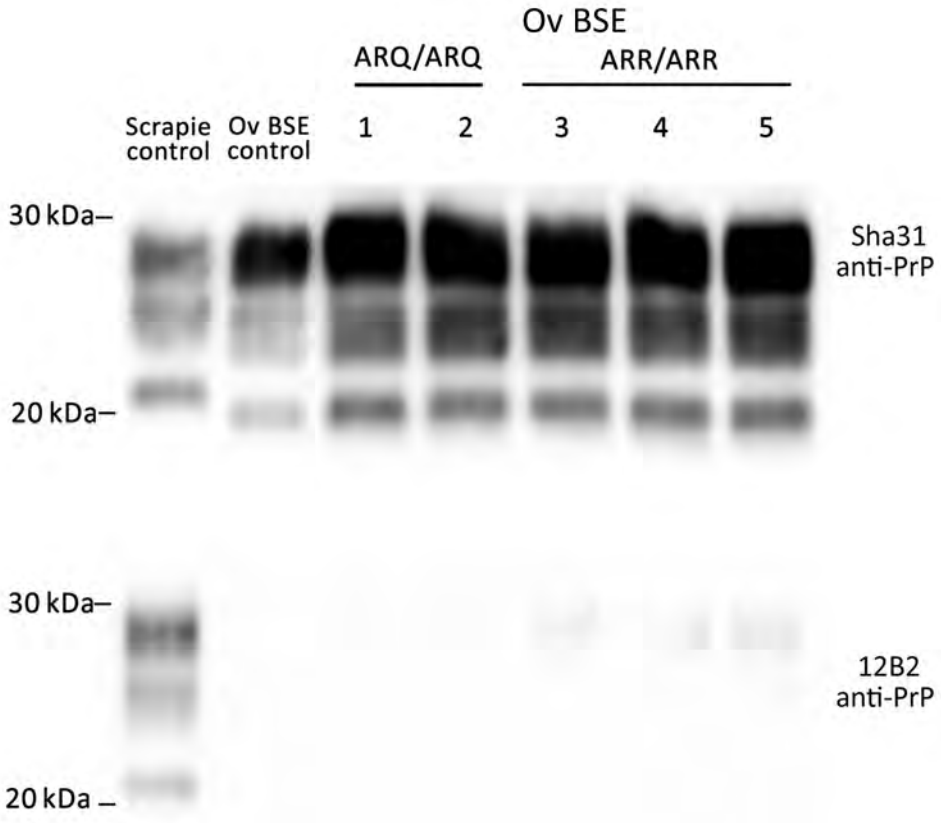

Figure 1. Detection of proteinase K–resistant core PrP in study of oral transmission of classical bovine spongiform encephalopathy in ARR/ARR sheep. Western blot was used for the detection of anti-PrP monoclonal antibodies Sha31 (epitope 145-YEDRYYRE-152) or 12B2 (epitope 89-WGQGG-93). BSE, bovine spongiform encephalopathy; ov, ovine; PrP, prion protein.

amplification of minute amounts of PrP^{Sc} and prion infectivity (*21*). To determine the relative sensitivity of our optimized ovine c-BSE agent amplification PMCA protocol, we endpoint titrated a reference sample (10% cerebral cortex homogenate from an ARQ/ARQ BSE-affected sheep) by using a bioassay in tgBov mice via an intracerebral inoculation route (Appendix Table, http://wwwnc.cdc.gov/EID/article/31/12/25-0501-App1.pdf) and by PMCA by using substrates from ovine ARQ PrP-expressing mice (tgARQ/tgShXI).

The infectious prion titer of the sheep-passaged c-BSE isolate was $\approx 10^{7.2}$ LD_{50}/mL IC in tgBov mice. Amplification of a 10-fold serial dilution of the same sample (12 individual replicates per dilution point) demonstrated that 2 PMCA rounds (24 h/round) were sufficient to reach the maximal sensitivity level of the assay. Additional PMCA rounds neither improved the analytical sensitivity of the assay nor increased the number of positive replicates (Appendix Figure). The estimated prion seeding titer (SA_{50}) was $\approx 10^{10.13}$ SA_{50}/mL by using tgARQ as substrate. Considering that mice were inoculated by using a 4-fold higher amount of material compared with the material used to seed PMCA reactions, this methodology can be considered ≈1,500-fold more sensitive than the bioassay in tgBov mice.

c-BSE Agent Levels in Solid Tissues and Blood

We used the optimized PMCA protocol to characterize the levels of prion seeding activity in the central nervous system (CNS), lymphoid tissues, and blood

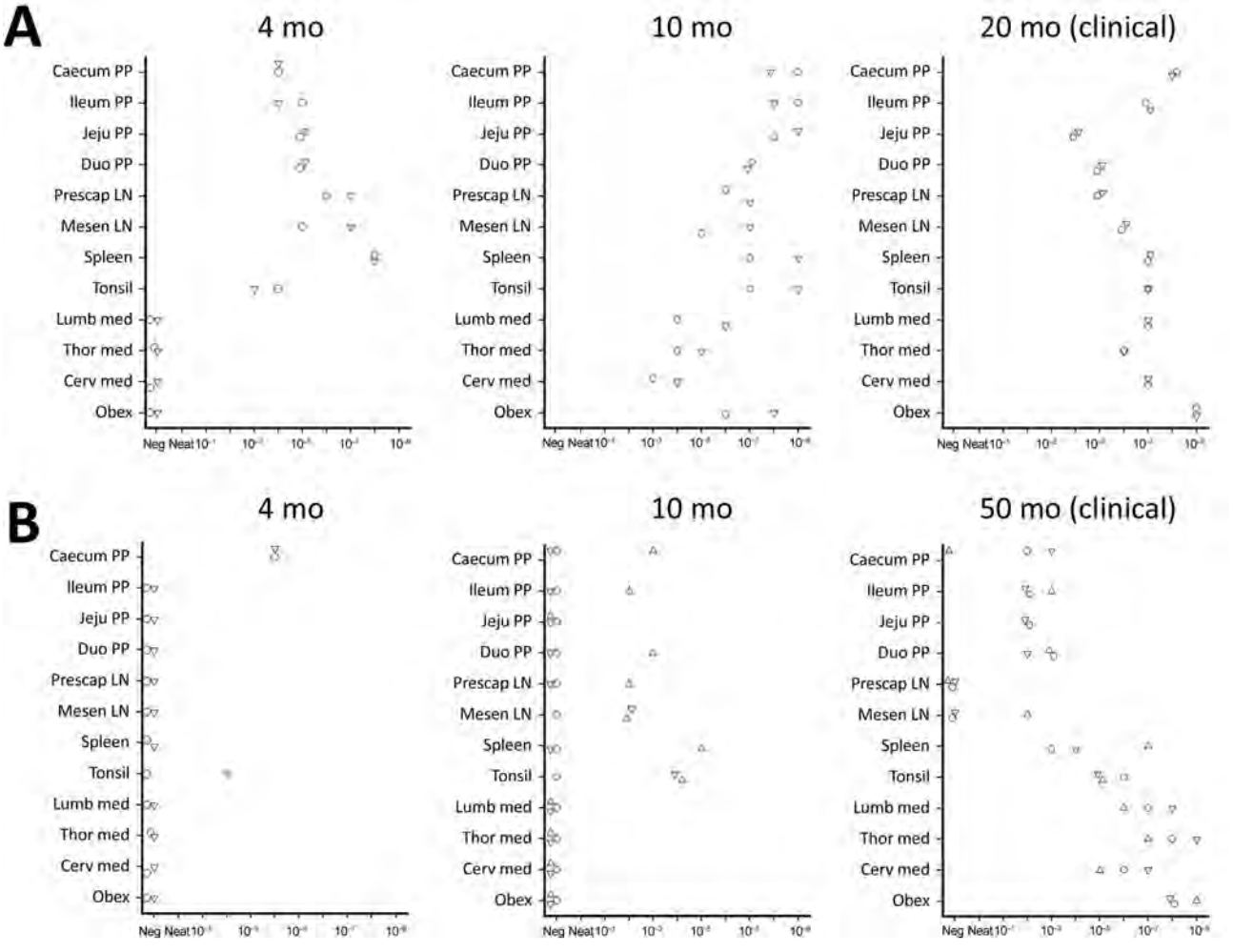

Figure 2. Protein misfolding cyclic amplification (PMCA) seeding activity levels in ARR/ARR and ARQ/ARQ sheep tissues after classical bovine spongiform encephalopathy challenge in study of oral transmission of classical bovine spongiform encephalopathy in ARR/ARR sheep. A) ARQ/ARQ sheep. B) ARR/ARR sheep. Protein misfolding cyclic amplification products were analyzed by using Western blot for proteinase K–resistant core prion protein detection. Each symbol represents a different animal and the associated tissue tested. Cerv, cervical; duo, duodenum; jeju, jejunum; LN, lymph node; lumb, lumbar; med, medial; mesen, mesenteric; Neg, negative; pp, Peyer's patches; prescap, prescapular; thor, thorasic.

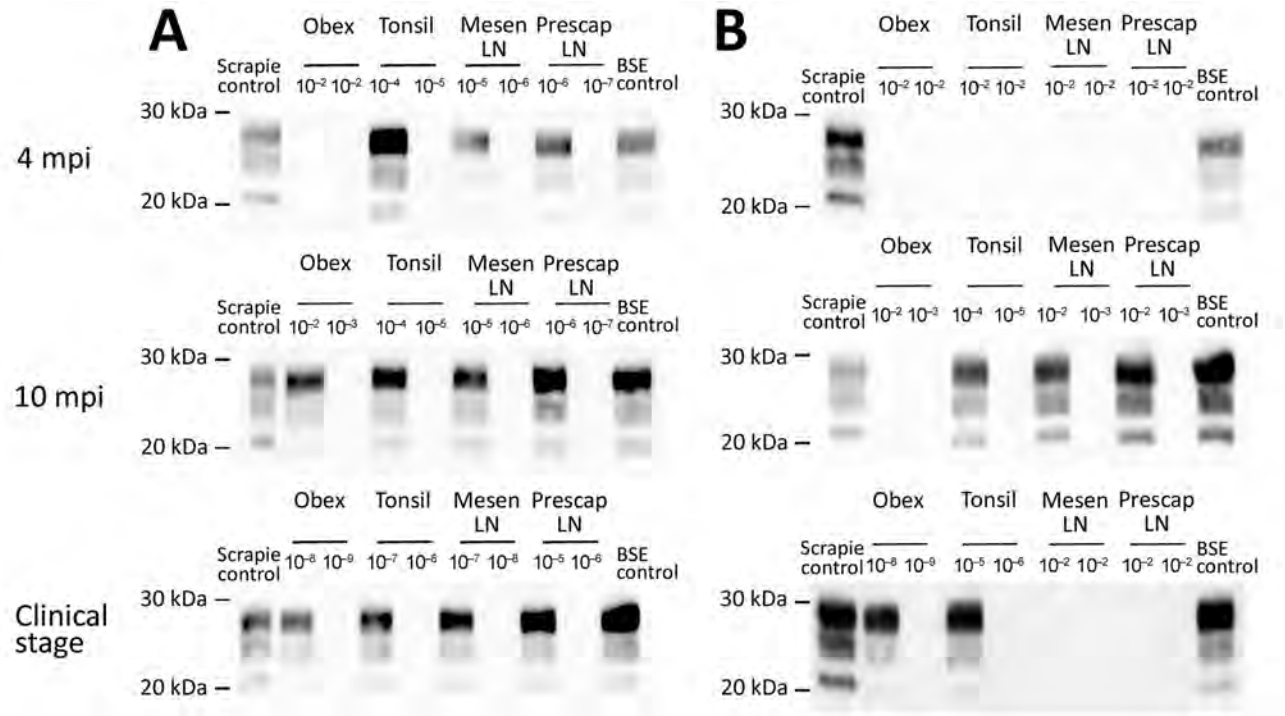

Figure 3. Detection of proteinase K–resistant core prion protein after 2 PMCA rounds of ARR/ARR and ARQ/ARQ sheep tissues after classical BSE challenge in study of oral transmission of BSE in ARR/ARR sheep. A) ARQ/ARQ sheep samples. B) ARR/ARR sheep samples. Western blot results from protein misfolding cyclic amplification products showing a detectable proteinase K–resistant core prion protein in ≥2 of 4 replicates for each tissue and animal. BSE, bovine spongiform encephalopathy; LN, lymph node; mesen, mesenteric; mpi, months postinoculation; prescap, prescapular.

collected from the c-BSE orally challenged lambs. We stored leukocytes isolated from blood samples collected from all the c-BSE-challenged animals during their incubation period (5 mL original blood equivalent) as dry pellets. We prepared 10-fold dilution series from the different samples collected from the ARR/ARR and ARQ/ARQ sheep, either 10% tissue homogenates or leukocyte pellets homogenized in PMCA buffer, and subjected them to 2 rounds of PMCA (Figure 2). We tested the presence of PrP^{res} in the amplification products from each round by Western blot (Figures 3 and 4).

ARQ/ARQ Lambs

We detected seeding activity in all the tested lymphoid organs as early as 4 mpi. In older lambs (10 mpi and clinically affected animals), prion seeding activity in the lymphoid tissues was generally 1–4 $\log_{10}$ higher than those observed in 4-month-old animals. However, in Peyer's patches, spleen, and tonsil, the levels of seeding activity detected at 10 mpi were higher than those measured at the clinical stage of the disease. In the CNS, seeding activity was first observed in lambs euthanized at 10 mpi. The levels of seeding activity in the CNS increased by 1–2 $\log_{10}$ in clinically affected animals (20 mpi). Of note, at the clinical stage of the disease, seeding activity in spleen, tonsil, and lymph nodes was equivalent to activity levels detected in the spinal cord and ≈2 $\log_{10}$ lower than observed in the posterior brainstem. In the blood of some animals, c-BSE seeding activity was detected as early as 2 months of age, and all animals tested at 4 months or older showed detectable levels of prion seeding activity in leukocyte samples.

ARR/ARR Lambs

We observed low but consistent levels of seeding activity in the tonsil or cecal Peyer's patches of the 2 euthanized 4 mpi animals. At 10 mpi, we detected seeding activity in most of the tested lymphoid organs in 2 of 3 lambs. At those stages, we detected no seeding activity in the tested CNS samples. At the clinical stage of the disease (50 mpi), we detected prion seeding activity in the posterior brainstem and spinal cord segments of the 3 tested sheep. We detected no seeding activity in the leukocytes collected at 1–10 months of age. We found positive seeding activity in 3 of 5 animals tested at 10 months of age. In animals ≥20 months of age, BSE seeding activity was detected in all the tested leukocyte samples.

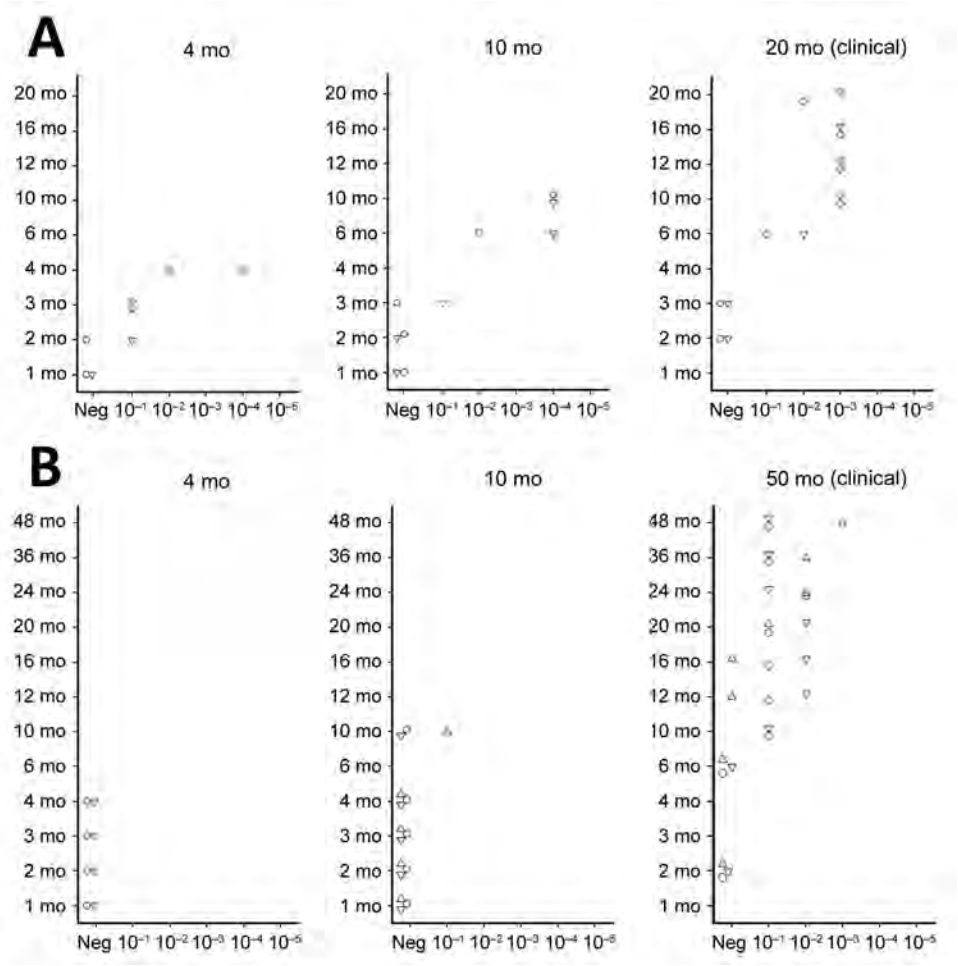

Figure 4. Protein misfolding cyclic amplification seeding activity levels in leukocytes of orally challenged ARR/ARR and ARQ/ARQ sheep in study of oral transmission of classical bovine spongiform encephalopathy in ARR/ARR sheep. A) ARQ/ARQ sheep. B) ARR/ARR sheep. We euthanized sheep at 4 mpi, 10 mpi, or at the clinical stage of infection. Leukocytes from 5 mL of whole blood collected at each month from birth until euthanasia were used to seed quadruplicate protein misfolding cyclic amplification reactions with a 10% wt/vol serial dilution from 10^{-1} to 10^{-5}. Each symbol represents a different animal. mpi, months postinoculation; neg, negative.

Of note, seeding activity in the CNS of the ARR/ARR sheep was similar to those observed in affected ARQ/ARQ animals (20 mpi). At that point, we also detected seeding activity in most of the lymphoid organs. However, the levels of seeding activity were generally 1–3 $\log_{10}$ lower than those observed in the same tissues of the ARQ/ARQ affected animals.

In both ARR/ARR (10 mpi and older) and ARQ/ARQ (3 mpi and older) animals, the level of seeding activity associated with leukocyte displayed a rapid increase and then a plateau that maintained during the clinical phase. At the plateau, the levels of seeding activity in the ARR/ARR sheep leukocyte were generally lower (limit of dilution 10^{-1} to 10^{-2}) than in the ARQ/ARQ sheep (limit of dilution 10^{-2} to 10^{-3}).

Strain Properties and Zoonotic Potential

To characterize the potential effect of passage in ARR/ARR sheep on the strain properties of the original BSE prions, we transmitted 1 ARR/ARR and 1 ARQ/ARQ isolate (both from clinical-stage sheep, prepared as 10% posterior brainstem homogenates) to tgBov mice and performed 2 iterative passages (Table 1). On first passage, we observed some differences in survival time between the mice. However, after second passages, the survival times associated with the 2 ovine

Table 1. Results of intracerebral inoculation of transgenic mice expressing bovine prion protein with a panel of bovine and ovine prion isolates in a study of oral transmission of classical bovine spongiform encephalopathy in ARR/ARR sheep*

	Passage 1		Passage 2	
Inoculum	No. positive/no. tested	Survival, dpi ±SD	No. positive/no. tested	Survival, dpi ±SD
Cattle BSE	6/6	295 ±12	6/6	265 ±35
ARQ Ov-BSE	6/6	229 ±11	6/6	237 ±5
ARR Ov-BSE	6/6	375 ±78	6/6	238 ±9
Negative brain	0/6	>750	0/6	>750
Phosphate buffered saline control	0/6	>750	0/6	>750

*BSE, bovine spongiform encephalopathy; dpi, days postinoculation; ov, ovine.

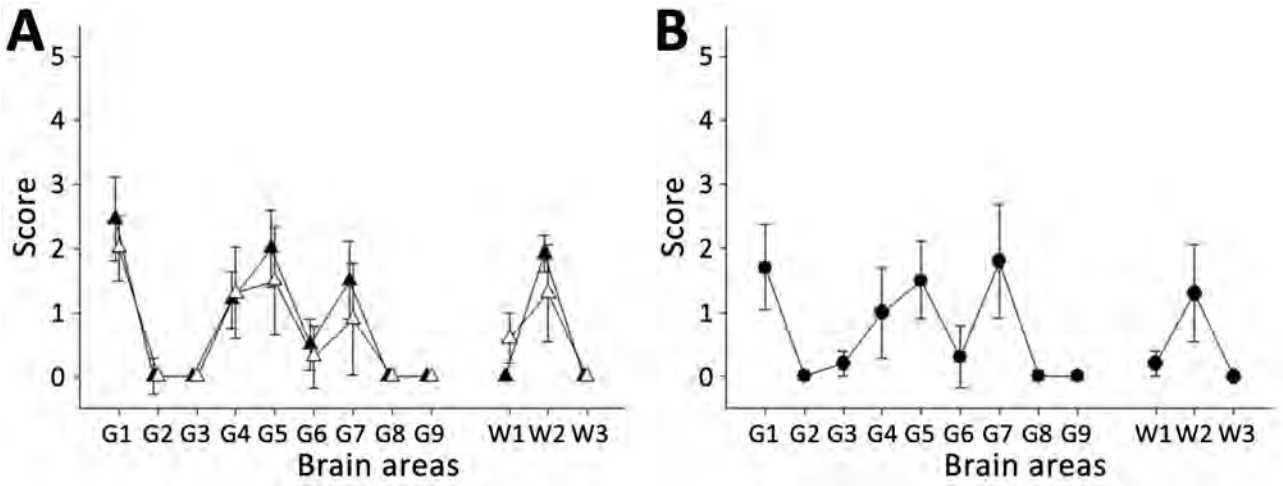

Figure 5. Transmission of ARR/ARR and ARQ/ARQ ovine c-BSE to tgBov mice in study of oral transmission of c-BSE in ARR/ARR sheep. A) Vacuolar lesion profiles in tgBov mice inoculated with ARQ/ARQ and ARR/ARR c-BSE isolates. B) Profiles from tgBov mice inoculated with cattle-derived c-BSE were used as controls. Lesion scoring evaluated 9 grey matter regions and 3 white matter regions. White triangles represent mice inoculated with ARQ/ARQ c-BSE isolates. Black triangles represent mice inoculated with ARR/ARR c-BSE isolates. Black circles represent mice inoculated with cattle-derived c-BSE isolates. c-BSE, classical bovine spongiform encephalopathy; G, grey matter region; tgBov, bovine prion protein–expressing mice; W, white matter region.

BSE isolates converged, and the vacuolar lesion profiles observed in the brains of all inoculated mice were identical to those observed in tgBov mice inoculated with cattle c-BSE isolates (Figure 5). Those results support the conclusion that passage of the c-BSE agent in ARR/ARR sheep did not alter its strain phenotype.

We examined the capacity of c-BSE agents originating directly from cattle or after passage in ARQ/ARQ- and ARR/ARR-genotype sheep to replicate in humanized mice that overexpress the 3 main human PrP codon-129 variants: tgMet (Table 2), tgVal (Table 3), and tgMet/Val (Table 4). We used the same inoculum used for the tgBov experiment. We detected no transmission events (clinical disease or PrP^{res} deposition) in tgVal or tgMet/Val mice after 2 serial intracerebral passages with any of the 3 c-BSE sources. In tgMet mice, first-passage transmission was most efficient with the ARQ/ARQ-derived inoculum (4/6 mice, mean survival 560 ± 83 dpi), whereas only single, very late cases were seen with the cattle (1/6, survival >750 dpi) and ARR/ARR (1/7, survival 737 dpi) isolates. After a second passage the overall attack rate increased for all groups, but subtle kinetic differences remained: ARQ/ARQ BSE produced 100% transmission (6/6, mean survival 569 ± 55 dpi), cattle-derived BSE 50% transmission (3/6, mean survival 572 ± 64 dpi), and ARR/ARR BSE 83% transmission (5/6, mean survival 616 ± 83 dpi). Nevertheless, the PrP^{res} glycoform profile of all positive tgMet brains was indistinguishable across isolates (Figure 6), indicating that strain properties converged after adaptation.

Our observations demonstrate that passage through ARR/ARR sheep does not abolish the zoonotic capacity of c-BSE but appears to impose a modest additional barrier. That barrier is manifested by a lower first-passage attack rate and a slight prolongation of incubation time relative to the ARQ/ARQ derived agent.

Discussion

The efficient transmissions observed in orally challenged ARR/ARR animals demonstrate that this genotype does not provide substantial resistance against

Table 2. Intracerebral inoculation of tgMet humanized mice with a panel of human, bovine, and ovine prion isolates in a study of oral transmission of classical bovine spongiform encephalopathy in ARR/ARR sheep*

	Passage 1		Passage 2	
Isolate	No. positive/no. tested	Survival, dpi ±SD	No. positive/no. tested	Survival, dpi ±SD
Cattle BSE	1/6†	>750	3/6	572 ±64
ARQ Ov-BSE	4/6	560 ±83	6/6	569 ±55
ARR Ov-BSE	1/7	737	5/6	616 ±83
Negative brain	0/12	>750	0/12	>750
Phosphate buffered saline control	0/18	>800	0/12	>650

*BSE, bovine spongiform encephalopathy; dpi, days postinoculation; ov, ovine.
†Abnormal prion protein isoform positive brain in a found dead animal without clinical manifestations of transmissible spongiform encephalopathies.

Table 3. Intracerebral inoculation of tgVal humanized mice with a panel of human, bovine, and ovine prion isolates in a study of oral transmission of classical bovine spongiform encephalopathy in ARR/ARR sheep*

	Passage 1		Passage 2	
Isolate	No. positive/no. tested	Survival, dpi ±SD	No. positive/no. tested	Survival, dpi ±SD
Cattle BSE	0/6	>750	0/6	>750
ARQ Ov-BSE	0/6	>750	0/6	>750
ARR Ov-BSE	0/6	>750	0/6	>750
Negative brain	0/12	>750	0/6	>750
Phosphate buffered saline control	0/12	>750	0/6	>750

*BSE, bovine spongiform encephalopathy; dpi, days postinoculation; ov, ovine.

the ovine c-BSE agent. Our results strongly contrast with those previously obtained in ARR/ARR and ARR/ARQ sheep orally challenged with cattle c-BSE, where no clinical signs and no or limited PrP^{Sc} accumulation has been evidenced, whereas positive transmission occurred in ARQ/ARQ sheep (*22*–*24*).

The inoculation doses used in this study (5 g of brain equivalent material) were similar to those used in studies that concluded the absence of cattle c-BSE transmission through the oral route in ARR/ARR sheep. However, in the absence of an endpoint titration establishing the c-BSE titer in our inoculum, the hypothesis that differences in the infectious titer in the inoculum account for, or at least contribute to, the discrepancies observed between studies cannot be ruled out.

In sheep, the age at the time of inoculation does appear to affect the efficacy of c-BSE transmission in orally exposed ARQ/ARQ sheep (*25*). Transmission efficiency is much higher in animals challenged before weaning (<3 weeks) than in animals inoculated after weaning (≥3 months). In our study, lambs were orally challenged 24 hours after birth and at the age of 2 weeks, whereas in previous studies, where no c-BSE transmission to ARR/ARR animals was observed, the age at inoculation varied from 3–6 months (*26*,*27*) or 5–8 months (*22*).

Experimental oral exposure early after birth is potentially more relevant to a scenario where maternal lateral transmission (via milk and contact with placenta) would play a central role in the disease transmission, as observed in classical scrapie–infected flocks (*28*,*29*). Experimental oral challenge after weaning is certainly a relevant model to mimic a scenario where sheep would be exposed to the c-BSE agent through the ingestion of contaminated feedstuffs (meat and bone meal), as observed in cattle during the c-BSE epidemics.

The last major difference between our transmission experiment and those reported in previous studies was the use of an ovine-adapted c-BSE rather than cattle c-BSE as inoculum. The apparent higher capacity of ARQ/ARQ sheep-passaged c-BSE (when compared with cattle c-BSE) to cross transmission barriers (transmission to porcine and human PrP-expressing hosts) is a well-documented phenomenon. The use of such ovine-passaged c-BSE as inoculum could, at least partly, explain the efficient transmission of the c-BSE agent to ARR/ARR sheep.

During the past 20 years, a breeding for resistance policy relying on the progressive increase of the ARR allele frequency in sheep has been implemented by certain member states of the European Union (EU). That policy's original objectives were to reduce the global incidence of TSEs and to prevent c-BSE emergence and spread in sheep populations. The most recent analysis of the small ruminants' TSE epidemiologic situation in the EU confirmed that the breeding for resistance policy is an efficient means to reduce classical scrapie prevalence in sheep populations (*10*). However, the transmission of the c-BSE agent to ARR/ARR sheep reported in this study suggests that ARR allele selection could have a more limited effect than originally expected on the risk for c-BSE propagation in the sheep population.

At the clinical stage of the disease, the distribution and levels of c-BSE prions in the peripheral tissues of both ARR/ARR and ARQ/ARQ experimentally challenged animals were broadly similar. The main differences observed between both genotypes were a slower dissemination of the c-BSE agent in the

Table 4. Intracerebral inoculation of tgMet/tgVal humanized mice with a panel of human, bovine, and ovine prion isolates in a study of oral transmission of classical bovine spongiform encephalopathy in ARR/ARR sheep*

	Passage 1		Passage 2	
Isolate	No. positive/no. tested	Survival, dpi ±SD	No. positive/no. tested	Survival, dpi ±SD
Cattle BSE	0/6	>750	NA	NA
ARQ Ov-BSE	0/6	>750	NA	NA
ARR Ov-BSE	0/6	>750	0/6	>750
Negative brain	0/12	>750	0/6	>650
Phosphate buffered saline control	0/12	>750	0/6	>650

*BSE, bovine spongiform encephalopathy; dpi, days postinoculation; NA, not available; ov, ovine.

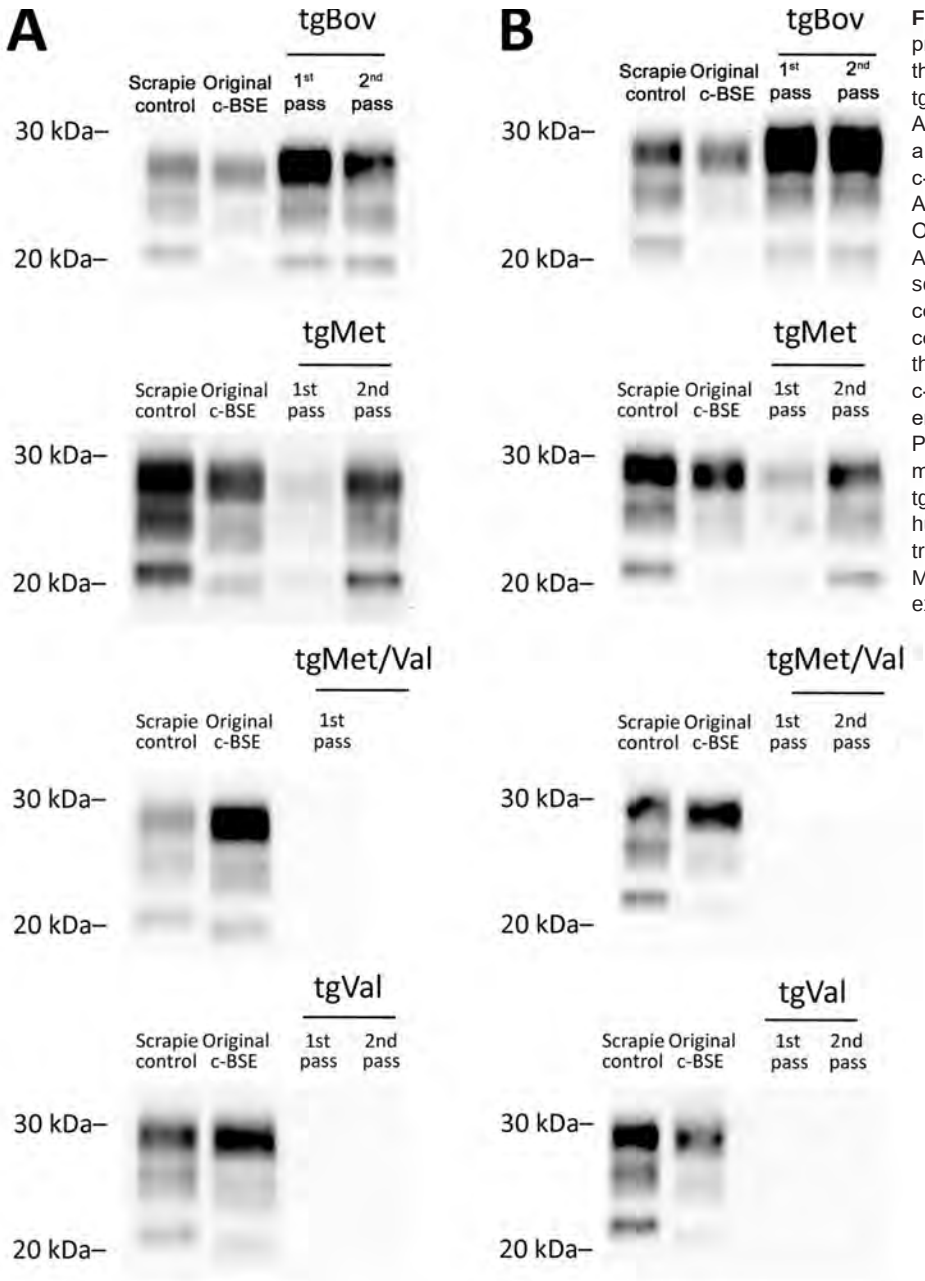

Figure 6. Western blot detection of proteinase K–resistant core PrP in the brains of tgBov, tgMet, (tgVal), or tgMet/Val mice inoculated with ARR/ARR or ARQ/ARQ c-BSE isolates in a study of the oral transmission of c-BSE in ARR/ARR sheep. A) ARQ/ARQ sheep. B) ARR/ARR sheep. Original c-BSE isolates from ARQ/ARQ or ARR/ARR sheep and a scrapie isolate were included as controls. Proteinase K–resistant core PrP was detected by using the monoclonal Sha31 anti-PrP. c-BSE, classical bovine spongiform encephalopathy; pass, passage; PrP, prion protein; tgBov, transgenic mice bovine PrP–expressing mice; tgMet, transgenic mice expressing human Met129; tgMet/Val, transgenic mice expressing human Met/Val129; tgVal, transgenic mice expressing human Val129.

organism and a longer incubation period in the ARR/ARR animals.

In the humanized transgenic mouse panel, both ARR/ARR- and ARQ/ARQ-derived c-BSE remained transmissible to mice expressing methionine 129 human PrP^C, confirming that neither ovine genotype eliminates zoonotic potential. However, the ARR/ARR isolate exhibited modestly reduced transmission efficiency, evident as a lower primary attack rate and longer mean survival times, compared with its ARQ/ARQ counterpart. Those kinetic differences were largely lost after a single adaptation passage, however, suggesting that once the species barrier is crossed, the underlying strain behaves similarly.

In 2001, specific risk material (SRM) measures were implemented throughout the EU, consisting of the systematic removal of cattle and small ruminants' tissues susceptible to contain critical levels of prion infectivity from the food and feed chains. The SRM measures are key for ensuring the protection of consumers against exposure to prions present in farmed animals. Current SRM measures applied to small ruminants in the EU consist of the removal of the spleen and the ileum and, in animals over 12 months of age, the skull (including the eyes and brain), spinal cord,

and tonsils. Because of the large distribution of TSE infectivity in the lymphoid tissues of small ruminants, SRM measures applied to sheep and goats are considered to have a more limited effect on the protection of consumers than they have in the cattle c-BSE context (*30*). However, mathematical modeling of the effect of the SRM measures on the different prion diseases susceptible to occur in small ruminants (atypical scrapie, classical scrapie, and c-BSE) confirmed the strong positive effect of the SRM measures on the final consumer exposure to these different prions (*31*).

In conclusion, although the capacity of the c-BSE agent to propagate in ARR/ARR sheep can be considered unfortunate news, the continuation of the TSE surveillance and SRM measures currently in force for small ruminants in the EU will continue to ensure efficient protection against the risk for exposure to this zoonotic agent. c-BSE infection in ARR/ARR sheep can still pose a public-health risk, but the quantitative probability of successful cross-species transmission might be lower than transmission associated with ARQ/ARQ sheep cases.

This work was supported by the European Union (grant no. QLK-CT 2001-309, program nos. FEDER/INTERREG EFA282/13 TRANSPRION, EFA148/16 REDPRION, and EFA031/01 NEUROCOOP).

About the Author

Dr. Huor is an assistant engineer in the transmissible spongiform encephalopathies research group at the University of Toulouse (UMR 1225 INRAE ENVT unit). Her primary research interests are the pathogenesis of prion diseases and the evolution of prion strain properties, with special emphasis on their iatrogenic and zoonotic risks of transmission.

References

1. McKinley MP, Bolton DC, Prusiner SB. A protease-resistant protein is a structural component of the scrapie prion. Cell. 1983;35:57–62.
2. Wells GA, Scott AC, Johnson CT, Gunning RF, Hancock RD, Jeffrey M, et al. A novel progressive spongiform encephalopathy in cattle. Vet Rec. 1987;121:419–20.
3. Wilesmith JW, Wells GA, Cranwell MP, Ryan JB. Bovine spongiform encephalopathy: epidemiological studies. Vet Rec. 1988;123:638–44.
4. Foster JD, Hope J, McConnell I, Bruce M, Fraser H. Transmission of bovine spongiform encephalopathy to sheep, goats, and mice. Ann N Y Acad Sci. 1994;724:300–3.
5. Bruce ME, Will RG, Ironside JW, McConnell I, Drummond D, Suttie A, et al. Transmissions to mice indicate that 'new variant' CJD is caused by the BSE agent. Nature. 1997;389:498–501.
6. Collinge J, Sidle KC, Meads J, Ironside J, Hill AF. Molecular analysis of prion strain variation and the aetiology of 'new variant' CJD. Nature. 1996;383:685–90.
7. Hunter N, Foster JD, Goldmann W, Stear MJ, Hope J, Bostock C. Natural scrapie in a closed flock of Cheviot sheep occurs only in specific PrP genotypes. Arch Virol. 1996;141:809–24. https://doi.org/10.1007/BF01718157
8. Elsen JM, Amigues Y, Schelcher F, Ducrocq V, Andreoletti O, Eychenne F, et al. Genetic susceptibility and transmission factors in scrapie: detailed analysis of an epidemic in a closed flock of Romanov. Arch Virol. 1999;144:431–45.
9. Houston F, Goldmann W, Chong A, Jeffrey M, González L, Foster J, et al. Prion diseases: BSE in sheep bred for resistance to infection. Nature. 2003;423:498.
10. EFSA Panel on Biological Hazards. Scientific opinion on the scrapie situation in the EU after 10 years of monitoring and control in sheep and goats. EFSA J. 2014;12:3781. https://doi.org/10.2903/j.efsa.2014.3781
11. Simmons HA, Simmons MM, Spencer YI, Chaplin MJ, Povey G, Davis A, et al. Atypical scrapie in sheep from a UK research flock which is free from classical scrapie. BMC Vet Res. 2009;5:8.
12. Moreno CR, Moazami-Goudarzi K, Laurent P, Cazeau G, Andreoletti O, Chadi S, et al. Which PrP haplotypes in a French sheep population are the most susceptible to atypical scrapie? Arch Virol. 2007;152:1229–32.
13. Beck KE, Sallis RE, Lockey R, Vickery CM, Béringue V, Laude H, et al. Use of murine bioassay to resolve ovine transmissible spongiform encephalopathy cases showing a bovine spongiform encephalopathy molecular profile. Brain Pathol. 2012;22:265–79.
14. Douet JY, Lacroux C, Aron N, Head MW, Lugan S, Tillier C, et al. Distribution and quantitative estimates of variant Creutzfeldt-Jakob disease prions in tissues of clinical and asymptomatic patients. Emerg Infect Dis. 2017;23:946–56.
15. Castilla J, Gutiérrez Adán A, Brun A, Pintado B, Ramírez MA, Parra B, et al. Early detection of PrPres in BSE-infected bovine PrP transgenic mice. Arch Virol. 2003;148:677–91.
16. Markus RA, Frank J, Groshen S, Azen SP. An alternative approach to the optimal design of an LD50 bioassay. Stat Med. 1995;14:841–52.
17. Féraudet C, Morel N, Simon S, Volland H, Frobert Y, Créminon C, et al. Screening of 145 anti-PrP monoclonal antibodies for their capacity to inhibit PrPSc replication in infected cells. J Biol Chem. 2005;280:11247–58.
18. Langeveld JP, Jacobs JG, Erkens JH, Bossers A, van Zijderveld FG, van Keulen LJ. Rapid and discriminatory diagnosis of scrapie and BSE in retro-pharyngeal lymph nodes of sheep. BMC Vet Res. 2006;2:19.
19. Cassard H, Torres JM, Lacroux C, Douet JY, Benestad SL, Lantier F, et al. Evidence for zoonotic potential of ovine scrapie prions. Nat Commun. 2014;5:5821.
20. Fraser H, Dickinson AG. The sequential development of the brain lesion of scrapie in three strains of mice. J Comp Pathol. 1968;78:301–11.
21. Saborio GP, Permanne B, Soto C. Sensitive detection of pathological prion protein by cyclic amplification of protein misfolding. Nature. 2001;411:810–3.
22. McGovern G, Martin S, Jeffrey M, Bellworthy SJ, Spiropoulos J, Green R, et al. Influence of breed and genotype on the onset and distribution of infectivity and disease-associated prion protein in sheep following oral infection with the BSE agent. J Comp Pathol. 2015;152:28–40.
23. Jeffrey M, Martin S, Thomson JR, Dingwall WS, Begara-McGorum I, González L. Onset and distribution of tissue

PrP accumulation in scrapie-affected Suffolk sheep as demonstrated by sequential necropsies and tonsillar biopsies. J Comp Pathol. 2001;125:48–57.
24. van Keulen LJ, Vromans ME, Dolstra CH, Bossers A, van Zijderveld FG. Pathogenesis of bovine spongiform encephalopathy in sheep. Arch Virol. 2008;153:445–53.
25. Hunter N, Houston F, Foster J, Goldmann W, Drummond D, Parnham D, et al. Susceptibility of young sheep to oral infection with bovine spongiform encephalopathy decreases significantly after weaning. J Virol. 2012;86:11856–62.
26. Bellworthy SJ, Hawkins SA, Green RB, Blamire I, Dexter G, Dexter I, et al. Tissue distribution of bovine spongiform encephalopathy infectivity in Romney sheep up to the onset of clinical disease after oral challenge. Vet Rec. 2005;156:197–202.
27. McGovern G, Martin S, Jeffrey M, Dexter G, Hawkins SA, Bellworthy SJ, et al. Minimum effective dose of cattle and sheep BSE for oral sheep infection. PLoS One. 2016;11:e0151440.
28. Andréoletti O, Lacroux C, Chabert A, Monnereau L, Tabouret G, Lantier F, et al. PrP(Sc) accumulation in placentas of ewes exposed to natural scrapie: influence of foetal PrP genotype and effect on ewe-to-lamb transmission. J Gen Virol. 2002;83:2607–16.
29. Lacroux C, Simon S, Benestad SL, Maillet S, Mathey J, Lugan S, et al. Prions in milk from ewes incubating natural scrapie. PLoS Pathog. 2008;4:e1000238.
30. European Food Safety Authority. Scientific opinion on BSE/TSE infectivity in small ruminant tissues. EFSA J. 2010;8:92. https://doi.org/10.2903/j.efsa.2010.1875
31. Adkin A, Horigan V, Rajanayagam B, Arnold M, Konold T, Spiropoulos J, et al. Estimating the impact on food and edible materials of changing scrapie control measures: the scrapie control model. Prev Vet Med. 2018;158:51–64.

Address for correspondence: Olivier Andreoletti, École Nationale Vétérinaire de Toulouse, 23 Chemin des Capelles, 31076 Toulouse, France; email: olivier.andreoletti@envt.fr

Silent Propagation of Classical Scrapie Prions in Homozygous K_{222} Transgenic Mice

Natalia Fernández-Borges,[1] Alba Marín-Moreno,[1] Juan Carlos Espinosa, Sara Canoyra, Olivier Andréoletti, Juan María Torres

Classical scrapie affects sheep and goats. To control prevalence in sheep, the European Union initiated breeding programs targeting resilient genotypes. Although certain goat polymorphisms, such as $Q_{222}K$, are linked to resistance, specific breeding programs have not been implemented. Hemizygous transgenic mice carrying the goat K_{222} cellular prion protein (PrP) allele (K_{222}-Tg516) exhibited resistance to several classical scrapie isolates. We inoculated homozygous K_{222}-Tg516 and Q_{222}-Tg501 mice with various scrapie isolates. Homozygous K_{222}-Tg516 mice reached the end of their lifespan without exhibiting clinical signs; we observed brain proteinase K–resistant PrP accumulation in those mice that was lower than in Q_{222}-Tg501 mice. Histologically, K_{222}-Tg516 brains lacked prion-related lesions, except for the presence of few isolated scrapie PrP plaques in cases of isolates highly adapted to the K_{222}-PrP^C environment. Our findings caution against including that polymorphism in breeding programs, because it could lead to emergence of asymptomatic silent prion carriers of classical scrapie among goat populations.

Scrapie is a fatal infectious neurodegenerative disease inherent to sheep and goats that falls within the spectrum of transmissible spongiform encephalopathies (TSEs) or prion diseases. Of note, various mammals, including cattle with bovine spongiform encephalopathy (BSE), mink with transmissible mink encephalopathy, cervids with chronic wasting disease, and humans with Creutzfeldt-Jakob disease, can also succumb to TSEs. The hallmark of those diseases is posttranslational conversion of the host cellular prion protein (PrP), PrP^C, into a misfolded pathologic isoform causing scrapie, $PrPS^C$, which accumulates within the central nervous system of affected individuals (1).

Infection with TSEs in an organism is influenced by 2 main factors: the similarity between the primary PrP sequence of the host (recipient) and the donor (inoculum), and the prion strain (*2*). Together, those factors define the concept of the transmission barrier. Sheep and goats share the same PrP primary sequence, although polymorphisms differ between the animals. In sheep, high susceptibility to classical scrapie is associated with the $V_{136}R_{154}Q_{171}$ and $A_{136}R_{154}Q_{171}$ alleles, whereas the $A_{136}R_{154}R_{171}$ genotype is linked to resistance (*3*–*8*). To control and decrease classical scrapie in sheep, European Union member states have established breeding programs on the basis of the selection of the resistant $A_{136}R_{154}R_{171}$ allele, although the variant does not confer resistance against the atypical/Nor98 scrapie strain (*9*). In goats, some polymorphisms, such as $I_{142}M$ (*10*–*13*) and $N_{146}S$ (*14*), have been associated with resistance to scrapie infection.

The most promising results of studies were in regard to goat-resistant polymorphisms for the goat $Q_{222}K$ polymorphism. The lysine allele (K_{222}) was first reported to confer resistance in Italy (*15*,*16*), and similar results were later found in France (*10*) and Greece (*17*,*18*). Cell-free conversion assays also indicated that K_{222} provides protection against the ME7 scrapie strain (*19*). Experimental studies in goats found that heterozygous Q/K_{222} and homozygous K_{222} goats either showed resistance to classical scrapie or exhibited clear delays in incubation times after intracerebral or oral inoculation (*20*–*23*) and reduced contribution of K_{222} to proteinase K–resistant PrP (PrP^{res}) formation in Q/K_{222} heterozygous goats infected with scrapie (*24*). In addition, Q/K_{222} heterozygous goats were

Author affiliations: Centro de Investigación en Sanidad Animal (CISA-INIA-CSIC), Madrid, Spain (N. Fernández-Borges, A. Marín-Moreno, J.C. Espinosa, S. Canoyra, J.M. Torres); Interactions Hôte Agent Pathogène–École Nationale Vétérinaire de Toulouse, Toulouse, France (O. Andréoletti)

DOI: https://doi.org/10.3201/eid3112.250302

[1]These first authors contributed equally to this article.

found to harbor a relative abundance of the natural α-cleaved PrP^C fragment C1, which has also been detected in classical scrapie-resistant R_{171} sheep (*25*). Furthermore, Q/K_{222} heterozygous goats inoculated with goat BSE showed neither evidence of clinical prion disease nor PrP^{Sc} accumulation in the brain or peripheral tissues (*26*,*27*), but low infectivity was detected after long postinoculation times (*26*). Finally, 1 goat harboring the K_{222}-PrP^C variant tested positive for atypical/Nor98 scrapie, indicating that the genotype may still be susceptible to this scrapie strain (*28*). All those results were replicated using a hemizygous transgenic mouse line expressing the K_{222}-PrP^C allele, which was found to be resistant to several classical scrapie isolates and cattle BSE, while susceptible to goat or sheep BSE and atypical scrapie (*29*,*30*).

We conducted our study on the transgenic homozygous mouse line, along with its control counterpart harboring the wild-type glutamine allele (Q_{222}). We intracranially inoculated the mice with several isolates representative of different categories of classical scrapie strains to test whether animals still remained uninfected, as previously reported (*29*), or if they mimicked the results found in homozygous goats (*22*).

Methods

Ethics Considerations

We performed animal experiments in strict accordance with the recommendations included in the guidelines of European Community Council 2010/63/UE and made all efforts to minimize animal suffering. The Committee on the Ethics of Animal Experiments of the Instituto Nacional de Investigación y Tecnología Agraria y Alimentaria and the General Directorate of the Madrid Community Government approved the study (permit nos. CEEA 2011–050, PROEX 263/15).

Prion Transmission Studies

We intracranially inoculated 20 μL of 10% (wt/vol) brain homogenate from previously characterized classical scrapie isolates (Table 1) into the right parietal lobe of 5–7 transgenic mice (6–7 weeks old), which expressed either the wild-type goat PrP^C (Q_{222}-Tg501) or the K_{222}-PrP^C variant (K_{222}-Tg516) (*29*,*30*) in homozygosity. PrP^C expression levels of both mice lines were 2- to 4-fold the physiologic levels found in goat brain (*29*). We used a 25-gauge disposable hypodermic needle to inoculate animals while they were anesthetized with isoflurane.

After inoculation, we monitored mice daily and assessed their neurologic status twice a week. We euthanized animals when the progression of prion disease was evident, at the end of their lifespan (around 650 days postinoculation), or at previously established endpoints as part of a kinetic study. We harvested mouse brains and sliced them sagittally. We fixed half of each brain in 10% buffered formalin for histopathologic analysis and homogenized the remaining portion as 10% (wt/vol) in 5% glucose to detect PrP^{res} by Western blot.

We calculated survival time as the mean number days postinoculation for all mice that tested positive for PrP^{res} in the brain, with the SD included. We expressed attack rate as the proportion of PrP^{res}-positive mice among all the inoculated mice.

Western Blotting

We homogenized mouse brain tissue in 5% glucose solution in distilled water using grinding tubes (Bio-Rad Laboratories, https://www.bio-rad.com) and adjusted to 10% (wt/vol) using a TeSeE Precess 48TM homogenizer (Bio-Rad) according to the manufacturer's instructions. We determined PrP^{res} presence in transgenic mouse brains by Western blot analysis of 10–100 μL of 10% (wt/vol) brain homogenate, as previously described (*32*). We incubated membranes with the Sha31 monoclonal antibody (mAb) (*33*), which recognizes the $_{148}$YEDRYYRE$_{155}$ epitope of the goat PrP sequence. We detected immunocomplexes with horseradish peroxidase-conjugated mouse IgG (GE HealthCare, https://www.gehealthcare.com) after 1 hour of incubation. We visualized immunoreactivity by chemiluminescence with ECL Select (GE HealthCare). We captured images using ChemiDoc XRS + System (Bio-Rad) and processed them using Image Lab 5.2.1 software (Bio-Rad).

Histologic Analysis

To analyze brain tissue, we trimmed and dehydrated formalin-fixed brains, embedded them in paraffin wax, and cut 4-μm slices. We dewaxed and rehydrated the specimens by standard procedures. We established the vacuolar lesion profile of the brains in accordance with published standard methods and semiquantitatively scored vacuolation on a scale of 0–5 in different brain areas (*34*,*35*).

For immunohistochemical (IHC) demonstration of PrP^{Sc} accumulation, tissue sections underwent antigen retrieval and hydrogen peroxide quenching as previously described (*36*). We incubated the sections with 2A11 mAb (*37*), which recognizes the $_{163}$QVYYRPVDQ$_{171}$ epitope of the goat PrP sequence. Subsequently, we subjected the sections to antigen retrieval and inactivation of endogenous peroxidase activity

before incubating them with the 2A11 mAb. We used a commercial immunoperoxidase technique (VECTASTAIN Elite ABC Kit; Vector Laboratories, https://vectorlabs.com), according to the manufacturer's instructions. Finally, we counterstained the sections with Mayer's hematoxylin. We used the Sha31 mAb (*33*) for paraffin-embedded tissue blotting, as previously described (*38*,*39*).

Results

Homozygous K_{222}-Tg516 Mice and Resistance to Classical Scrapie PrP^{Sc}

We intracranially inoculated homozygous K_{222}-Tg516 with classical scrapie isolates (Table 1) previously characterized as representative of different prion strains circulating in Europe (*31, 40*). Although all mice expressing the wild-type goat PrP (Q_{222}-Tg501) developed recognizable prion disease, K_{222}-Tg516 mice reached the end of their lifespan without showing clinical signs indicative of prion disease (Table 2). After second passage, survival times were still prolonged, even reaching the end of the mice's lifespan again (Table 2). However, in both first and second passages, Western blot analysis showed the presence of PrP^{res} in the brains of K_{222}-Tg516 animals inoculated with the different classical scrapie isolates (Figure 1, panel A). For the 198/9 and S2 isolate, the percentage of PrP^{res}-positive animals in the first passage was not 100% of the inoculated animals (Tables 2, 3). At least for the S2 isolate, 100% of the inoculated mice were PrP^{res}-positive by the completion of the second passage (Tables 2, 3). Comparison between the PrP^{res} signature of the original inoculum and the PrP^{res} obtained molecular mass for the nonglycosylated band, depending on the individual (Figure 1, panel A). In addition, brain PrP^{res} accumulation in K_{222}-Tg516 mice was remarkably reduced compared with that in Q_{222}-Tg501 mice for most of the inoculated isolates, with the exception of F14 and F10 (Figure 1, panel A).

K_{222}-Tg516 PrP^{res}-positive animals exhibited only a few vacuolations that were difficult to distinguish from those resulting from the physiologic aging process (Figure 2). Immunohistochemistry of K_{222}-Tg516 mice inoculated with CP060146/K_{222} goat and F10/K_{222}-Tg516 inocula revealed only a few large and focalized PrP^{Sc} plaques and lacked any other type of deposits affecting neurons or microglia cells (Figures 3, 4). Those PrP^{Sc} deposits were restricted to the mesencephalon, thalamus, and hypothalamus areas (Figures 3, 4). We detected no deposits for the remaining inoculations (data not shown). Consistent with our findings, paraffin-embedded tissue blotting showed clear PrP^{res} deposition only in K_{222}-Tg516 mice inoculated with CP060146/K_{222} goat (Figure 5) and F10/K_{222}-Tg516 inocula (data not shown), with deposition to the exact same brain areas affected by IHC (Figures 3, 4). We detected no deposits for the remaining inoculations (data not shown).

Proteinase K Studies in K_{222}-Tg516 Mice

The differential brain PrP^{res} accumulation observed between K_{222}-Tg516 and Q_{222}-Tg501 mice (Figure 1,

Table 1. Isolates used in study of classical scrapie prions in homozygous K_{222} transgenic mice*

Category	Isolate	Species	Origin	Goat PrP genotype†	Description	Supplier
I	198/9	Sheep	Italy	wt; $S_{240}S$	Classical scrapie isolate from a naturally infected sheep	ISS
II	S2	Goat	Spain	wt; $S_{240}P$	Classical scrapie isolate from a naturally infected goat	UNIZAR
	CP060146 (*22*)	Goat	France	wt	Classical scrapie isolate from an experimentally infected goat	ENVT
	CP060146/K_{222} (*22*)	Goat	France	K_{222}	Classical scrapie isolate from an experimentally infected goat	ENVT
II + III	UKA2	Goat	United Kingdom	wt; $S_{240}P$	Classical scrapie isolate from a naturally infected goat	APHA
	F14	Goat	France	wt; $I_{142}M$, $S_{240}P$	Classical scrapie isolate from a naturally infected goat	INRA
IV	F10	Goat	France	wt; $S_{240}P$	Classical scrapie isolate from a naturally infected goat	INRA
	C1	Goat	Cyprus	wt	Classical scrapie isolate from a naturally infected goat	VS
Negative control	Healthy goat brain	Goat	France	wt	Brain from a noninfected goat	INRA

*Isolates were classified as previously described (*31*) on the basis of prion biochemical features when transmitted in transgenic mice expressing the bovine PrP (Bo-Tg110) and biologic features transmitted in mice expressing the ovine PrP (Q_{222}-Tg501). APHA, Animal and Plant Health Agency, Surrey, United Kingdom; ENVT, École Nationale Vétérinaire de Toulouse, Toulouse, France; INRA, French National Institute for Agricultural Research, Nouzilly, France; ISS, Istituto Superiore di Sanitá Animal, Rome, Italy; UNIZAR, Universidad de Zaragoza, Spain; VS, Veterinary Services, Nicosia, Cyprus; wt, wild-type.

†The wt goat prion protein genotype is $A_{136}R_{154}P_{240}/A_{136}R_{154}P_{240}$. S240S, S240P and I142M refer to polymorphisms at specific codons of the PRNP gene.

Table 2. Transmission of classical scrapie isolates to Q_{222}-Tg501 homozygous mice and survival of mice in study of classical scrapie prions in homozygous K_{222} transgenic mice*

Category	Isolate	1st passage		2nd passage	
		Mean survival time ± SD, d	No. diseased and PrP^{res}-positive/no. inoculated	Mean survival time ± SD, d	No. diseased and PrP^{res}-positive/no. inoculated
I	198/9	592 ± 13	6/6	536 ± 46	5/5
II	S2	228 ± 15	6/6	233 ± 4	6/6
	CP060146	379 ± 31	5/5	ND	NA
	CP060146/K_{222} goat	415 ± 40	6/6	ND	NA
II + III	UKA2	245 ± 36	5/5	252 ± 8	6/6
	F14	526 ± 46	4/4	241 ± 22	4/4
IV	F10	449 ± 19	5/5	372 ± 14	6/6
	F10/K_{222}-Tg516	495 ± 26	3/3	ND	NA
	C1	483 ± 15	4/4	301 ± 10	4/4
Negative control	Healthy goat brain	>650	0/6†	>650	0/6†

*NA, not available; ND, not done; PrP^{res}, proteinase K–resistant PrP.
†Animals were found dead or were euthanized at the end of their lifespan without showing clinical signs of classical scrapie.

panel A) can be attributed to 2 alternative hypotheses. There could be a genuine reduction in PrP^{res} accumulation for these classical scrapie isolates in K_{222}-Tg516 mice. Alternatively, the produced PrP^{res} might be more susceptible to proteinase K treatment, resulting in a weaker Western-blotting signal. To distinguish between those 2 possibilities, we performed proteinase K resistance analyses using different enzyme concentrations in both Q_{222}-Tg501 and K_{222}-Tg516 mice inoculated with F10 (which exhibited similar PrP^{res} accumulation between K_{222}-Tg516 and Q_{222}-Tg501 mice) and CP060146 (which showed reduced PrP^{res} accumulation in K_{222}-Tg516 mice compared with Q_{222}-Tg501 mice) isolates. In all cases, proteinase K consistently acted at a concentration of 50 μg/mL (which falls within the normal proteinase K concentration range for routine Western blotting); we observed the same pattern and signal intensity at a concentration of 500 μg/mL (Figure 6). However, protease action did not achieve proper PrP^{res} resolution at concentrations of 1 μg/mL and 0.1 μg/mL (Figure 6). Those results suggest that both isolates, when replicating in either Q_{222}-PrP^C or K_{222}-PrP^C contexts, retain the same proteinase K sensitivity. Thus, the differences in Western blotting signals detected previously (Figure 1, panel A) truly account for reduced brain PrP^{res} accumulation in K_{222}-Tg516 mice.

Transmission in K_{222}-Tg516 Mice and Host-Induced Reversible Strain Adaptations

After the second passage in K_{222}-Tg516 mice or adaptation in a K_{222} homozygous goat, F10 and CP060146 isolates were transmitted back into Q_{222}-Tg501 mice (Table 3). The purpose of those inoculations was to determine whether replication in the K_{222} context resulted in host-induced reversible adaptations of the

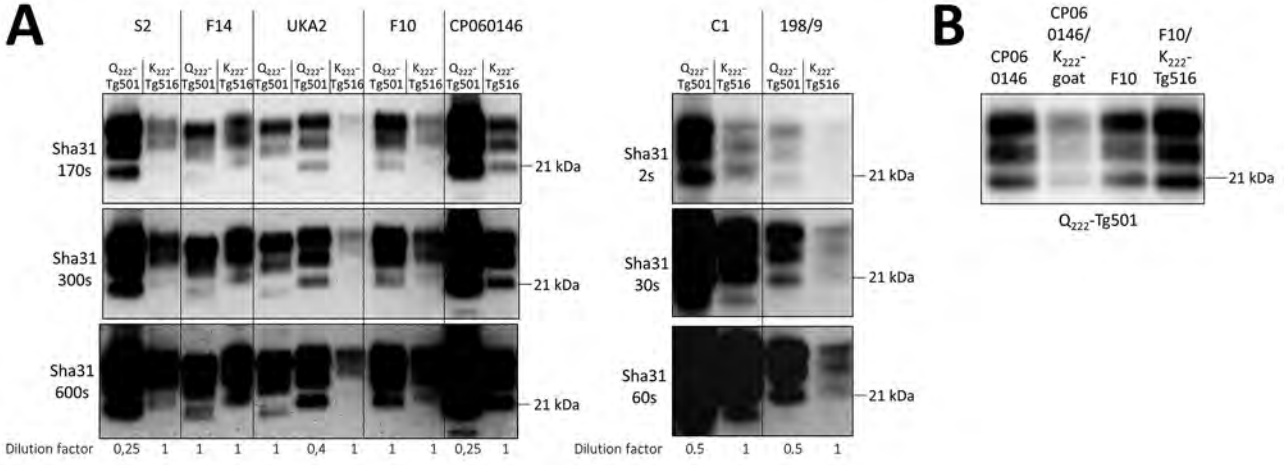

Figure 1. Proteinase K–resistant PrP (PrP^{res}) accumulation in brains of K_{222}-Tg516 and Q_{222}-Tg501 homozygous mice in study of propagation of classical scrapie prions. A) Comparison of the biochemical profile of brain PrP^{res} from classical scrapie isolates in K_{222}-Tg516 mice with that in Q_{222}-Tg501 mice using Sha31 monoclonal antibody. Exposure time and dilution factor are specified. B) Comparison of the biochemical profile of brain PrP^{res} of CP060146 and F10 isolates of classical scrapie, before (left) and after (right) adaptation to the K_{222}-PrP^C context, in Q_{222}-Tg501 mice, using the Sha31 monoclonal antibody. Molecular weight markers are indicated on the right side of each band.

Table 3. Transmission of classical scrapie isolates to K_{222}-Tg516 homozygous mice in study of classical scrapie prions in homozygous K_{222} transgenic mice*

Category	Isolate	1st passage		2nd passage	
		Mean survival time ± SD, d	No. diseased and PrP^{res}-positive/no. inoculated	Mean survival time ± SD, d	No. diseased and PrP^{res}-positive/no. inoculated
I	198/9	>650	1/6†	ND	NA
II	S2	>650	3/4†	>650	7/7†
	CP060146	>650	5/5†	>650	5/5†
	CP060146/K_{222} goat	>650	4/4†	>650	6/6†
II + III	UKA2	>650	4/4†	>650	5/5†
	F14	>650	4/4†	>650	5/5†
IV	F10	>650	6/6†	>650	5/5†
	F10/K_{222}-Tg516	>650	5/5†	>650	6/6†
	C1	>650	7/7†	ND	NA
Negative control	Healthy goat brain	>650	0/6†	>650	0/6†

*NA, not available; ND, not done; PrP^{res}, proteinase K–resistant PrP.
†Animals were found dead or euthanized at the end of their lifespan without showing clinical signs of classical scrapie.

strain, including changes in prion strain characteristics such as biologic properties (mean survival time and proportion of PrP^{res}-positive animals) and biochemical properties (brain PrP^{res} accumulation and PrP^{res} glycosylation pattern). In both cases, the survival times were comparable to those observed for the primary transmission of the same inocula in Q222-Tg501 mice. Specifically, survival time was 449 ± 19 days (5/5) for the original F10 inoculum from a wild-type goat versus 495 ± 26 days (3/3) after adaptation in K_{222}-Tg516 mice and 379 ± 31 days (5/5) for the original CP060146 inoculum from a wild-type goat versus 415 ± 40 days (6/6) after adaptation in a K_{222} goat (Table 2). The PrP^{res} signatures obtained were identical to those observed after the primary transmission of these isolates in Q_{222}-Tg501 mice (Figure 1, panel B).

Differences between K_{222} and Q_{222} PrP^{res} Formation Kinetics

Once we confirmed the lower brain PrP^{res} accumulation in K_{222}-Tg516 mice compared with the Q_{222}-Tg501 control counterparts, we conducted kinetic studies on PrP^{res} formation in both transgenic lines using the goat isolates F10 and CP060146, which had been previously adapted for propagation in a K_{222}-PrP^{C} context. Of interest, both K_{222} and Q_{222}-PrP^{res} appeared at equal levels by 300 days postinoculation (Figure 7). However, Q_{222}-PrP^{res} accumulation continued to increase steadily until the time of death, whereas K_{222}-PrP^{res} remained at low levels throughout the lifespan of the mice (Figure 7).

Discussion

Previous studies conducted in heterozygous Q/K_{222} and homozygous K_{222} goats (*20*–*23*), as well as in hemizygous K_{222}-Tg516 mice (*29*), have highlighted the $Q_{222}K$ polymorphism as one of the most promising candidates for reducing prion disease transmission in goats. Although the K_{222} allele has been consistently reported in certain countries in Europe, such as Italy (*15*,*16*), France (*10*), and Greece (*17*,*42*), in other countries, such as the United Kingdom, the polymorphism has been reported as infrequent (*43*). However, once

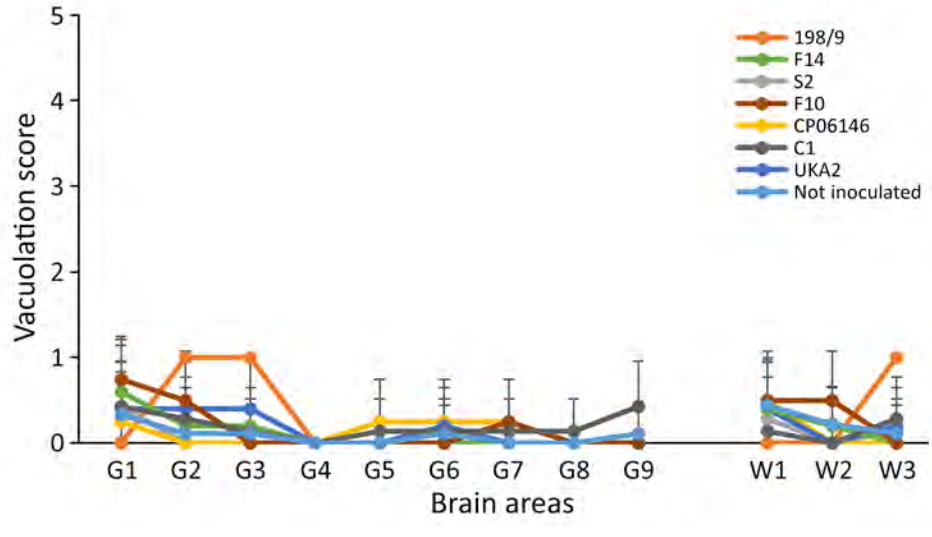

Figure 2. Histologic analysis of brain tissue from K_{222}-Tg516 homozygous mice inoculated with classical scrapie in study of propagation of classical scrapie prions. Comparative analysis shows the vacuolar lesion profile in homozygous K_{222}-Tg516 mice inoculated with different scrapie isolates compared with noninoculated mice. G, gray matter; W, white matter.

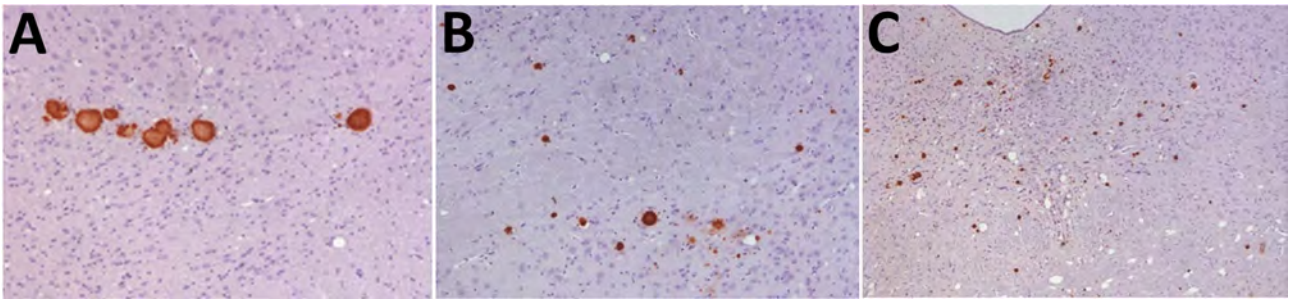

Figure 3. Immunohistochemistry results of brain tissue in study of propagation of classical scrapie prions. Images are of tissue specimens from K_{222}-Tg516 mice inoculated with F10 goat scrapie isolate at second passage. Results are visualized using the Sha31 monoclonal antibody. A) Thalamus specimen. B) Hippocampus specimen. C) Midbrain specimen. Original magnification ×40.

the supposed protective effect against prion diseases is confirmed, the frequency of the K_{222} allele could increase across different countries through selective breeding programs.

Transgenic mice expressing K_{222}-PrP^C in homozygosity emerge as the optimal tool for definitively testing the susceptibility or resistance that allele confers to prions. Our model enables the testing of multiple prion strains more rapidly and cost-effectively than the model using goats. In our study, classical scrapie isolates representing different classical scrapie strains circulating within Europe (*40*–*42*) were selected and used to challenge homozygous K_{222}-Tg516 mice.

Once the expression level is increased, homozygous K_{222}-Tg516 mice become susceptible to all tested classical scrapie isolates (Table 3). The K_{222}-PrP^C variant is capable of sustaining PrP^{Sc} replication even in the absence of the Q_{222}-PrP^C variant, which was identified as responsible for most accumulated brain PrP^{res} in $Q_{222}K$ heterozygous goats (*24*). Furthermore, K_{222}-Tg516 mice exhibit consistently lower brain PrP^{res} accumulation than Q_{222}-Tg501 mice (Figure 1). The explanation that K_{222}-PrP^{res} is more sensitive to proteinase K treatment and so reduced detection of brain PrP^{res} accumulation has been ruled out (Figure 6). Therefore, we recommend careful analysis of the general features and behavior of classical scrapie K_{222}-PrP^{res}.

K_{222}-Tg516 mice inoculated with classical scrapie did not develop typical prion pathology and showed no clinical signs of prion disease, which suggests that classical scrapie K_{222}-PrP^{res} might not be toxic or might not induce the signaling pathways leading to neuronal death. Those conclusions are not only caused by insufficient time for the onset of neuronal death pathways within the animal lifespan; second passages in K_{222}-Tg516 yielded identical results to the first ones.

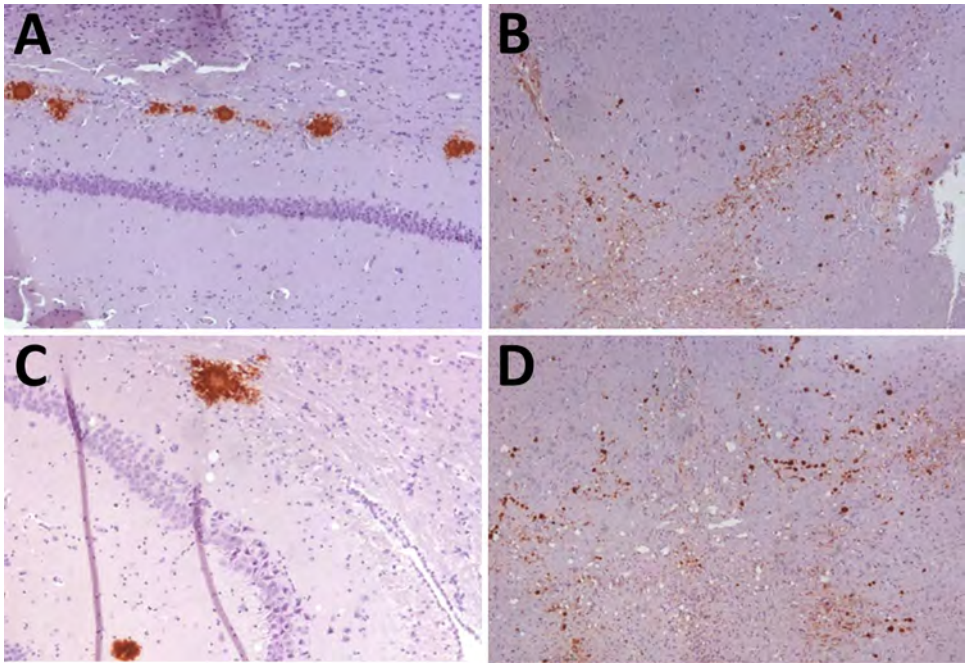

Figure 4. Immunohistochemistry results of brain tissues in study of propagation of classical scrapie prions. Images are of tissue specimens from K_{222}-Tg516 mice inoculated with CP060146/K_{222} goat isolate. Results are visualized using the Sha31 monoclonal antibody. A) Hippocampus specimen tested at first passage. B) Midbrain specimen tested at first passage. C) Hippocampus specimen tested at second passage. D) Midbrain specimen tested at second passage. Original magnification ×40.

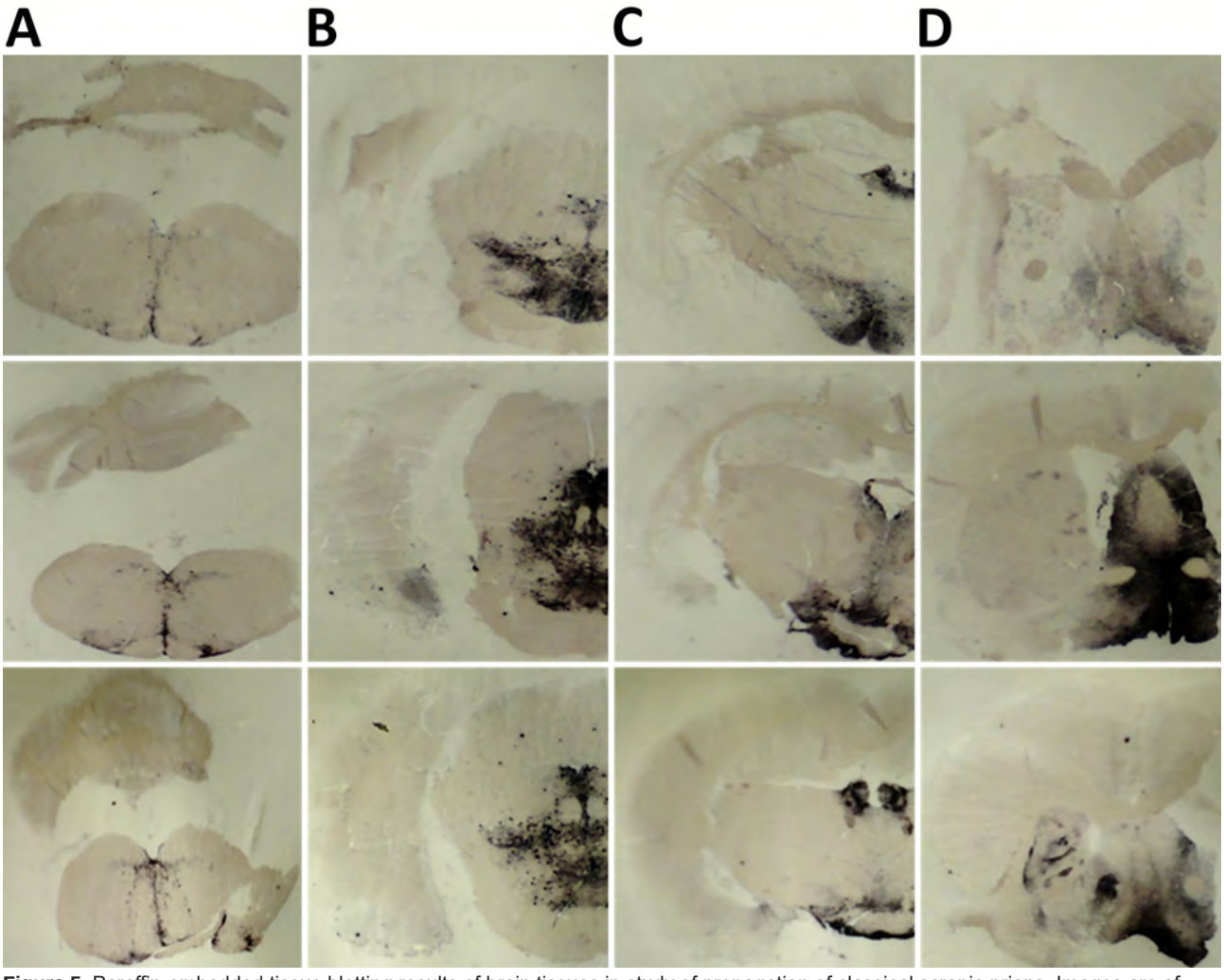

Figure 5. Paraffin-embedded tissue blotting results of brain tissues in study of propagation of classical scrapie prions. Images are of brain specimens from 3 distinct K_{222}-Tg516 mice inoculated with CP060146/K_{222} goat isolate. Results are visualized with the Sha31 monoclonal antibody. A) Cerebellum specimens. B) Thalamus specimens. C) Hippocampus specimens. D) Cerebral cortex specimens. Proteinase K–resistant prion protein is visible as dark staining in similar brain regions in the 3 mice. Original magnification ×20.

However, we noted that the lower brain PrP^{res} accumulation in K_{222}-Tg516 animals could lead to a misinterpretation of those results. The reduced accumulation might reflect insufficient replication within the animal's lifespan, possibly caused by consistently low replication rates, as suggested by our kinetic experiments, or by more efficient clearance of PrP^{res} aggregates. Those factors could explain why transmission does not necessarily result in prion disease, highlighting a dissociation between infectivity and toxicity of classical scrapie K_{222}-PrP^{res}.

All circulating prion strains must be considered in the design of breeding selection programs. Programs aimed at controlling and reducing classical scrapie in sheep, implemented by EU member states, have identified sheep herds that are more susceptible to atypical/Nor98 scrapie (*44*). In our study, K_{222}-Tg516 mice died without exhibiting overt clinical signs after inoculation with different classical scrapie isolates; we found that PrP^{res} accumulated in their brains (Table 1). Of note, K_{222}-derived PrP^{res} retained infectivity when transmitted back to Q_{222}-Tg501 mice, recovering the strain characteristics observed in the original inocula. Our findings suggest that, under the experimental conditions we established, the K_{222} allele does not confer full resistance to classical scrapie agents.

Of interest, the reversibility of strain features observed upon reinoculation of K_{222}-derived PrP^{res} into Q_{222}-Tg501 mice is reminiscent of the phenomenon of nonadaptive prion amplification as described previously (*45*). In that model, PrP^{Sc} can replicate transiently in a nonpermissive host without inducing a permanent

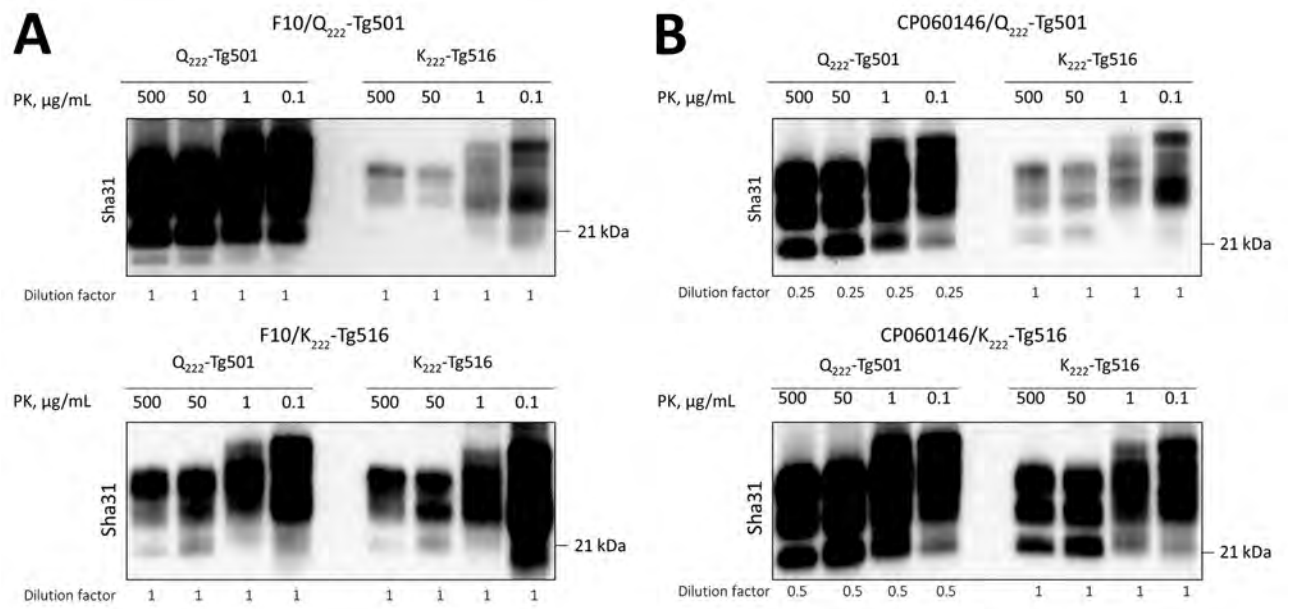

Figure 6. Proteinase K digestion studies conducted as part of study of propagation of classical scrapie prions. K_{222}-Tg516 and Q_{222}-Tg501 homozygous mice were inoculated with classical scrapie. A) Proteinase K–resistant prion protein (PrP^{res}) sensitivity in the brains of Q_{222}-Tg501 and K_{222}-Tg516 mice initially inoculated with F10 scrapie isolate and subsequently reinoculated into both the original model and its counterpart. B) PrP^{res} sensitivity in the brains of Q_{222}-Tg501 and K_{222}-Tg516 mice initially inoculated with CP060146 scrapie isolate and subsequently reinoculated into both the original model and its counterpart. In both cases, proteinase K concentrations of 500, 50, 1 and 0.1 µg/mL were tested. Western blot visualizations were done using the Sha31 monoclonal antibody. Molecular weight markers are indicated on the right side of each band.

adaptation of the strain. Our data are consistent with that concept; the classical scrapie agents replicated in K_{222}-Tg516 mice but reverted to their original biochemical and biologic properties upon passage back into a permissive Q_{222} context. That interpretation reinforces the view that the K_{222} allele may enable subclinical or low-efficiency replication of classical scrapie agents without supporting stable strain selection or adaptation.

It is important to note that the use of transgenic models with PrP overexpression may enhance prion replication efficiency, potentially uncovering low-level or subclinical conversion events that might not occur under physiologic PrP expression in goats. In addition, all animals were inoculated intracerebrally; that route does not mimic natural exposure and bypasses key peripheral barriers such as the gut and

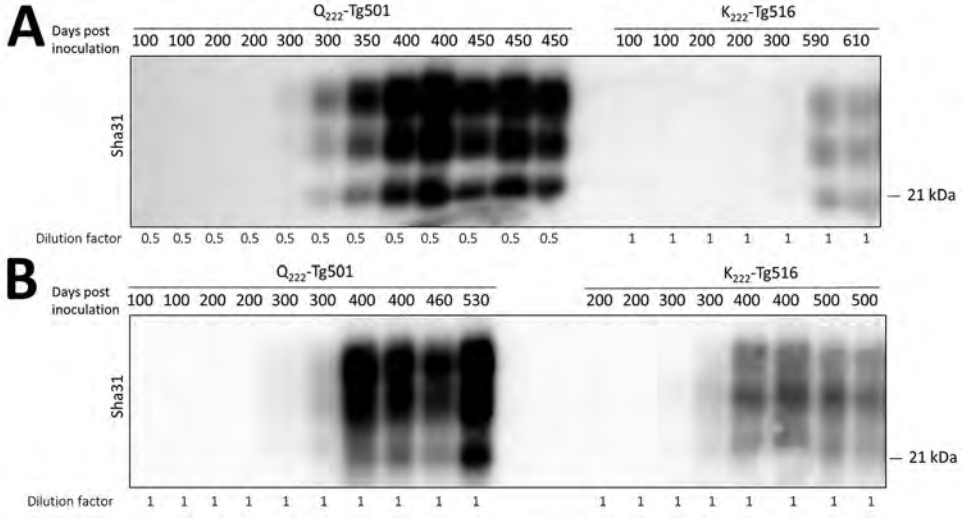

Figure 7. Kinetic studies of proteinase K–resistant prion protein (PrP^{res}) detection in K_{222}-Tg516 and Q_{222}-Tg501 homozygous mice inoculated with classical scrapie in study of propagation of classical scrapie prions. Brain PrP^{res} from mice euthanized at various time points postinoculation were analyzed by Western blotting and visualized using the Sha31 monoclonal antibody. A) Q_{222}-Tg501 and K_{222}-Tg516 mice inoculated with the CP060146 classical scrapie isolate adapted to the K_{222} cellular prion protein (PrP^{C}) context (CP060146/K_{222}-goat). B) Q_{222}-Tg501 and K_{222}-Tg516 mice inoculated with the F10 classical scrapie isolate adapted to the K_{222}-PrP^{C} context (F10/K_{222}-Tg516). Molecular weight markers are indicated on the right side of each band.

associated lymphoid tissues, which play a critical role in determining prion susceptibility and pathogenesis under field conditions. Therefore, although our results highlight the potential for silent propagation of classical scrapie strains in the context of the K_{222} variant, extrapolation to the natural host should be made with caution.

Interest has grown for in-depth characterization of the strains of Q/K_{222} heterozygous goats affected with scrapie, which are abundant in various regions of Greece. The interest lies in determining whether prions propagated under the K_{222} allele can act as potential silent carriers of the disease, as shown in previous studies. Furthermore, understanding whether the presence of the K_{222} allele induces a change in the biologic properties of the strains and their potential transmission to other animal species is crucial.

Overall, our results underscore the need for further in vivo studies using physiologically relevant models or natural hosts to fully evaluate the protective efficacy of the K_{222} allele. Until such evidence becomes available, the inclusion of the K_{222} polymorphism in breeding selection programs should be critically considered, especially in regions where classical scrapie strains with known zoonotic potential remain present. Furthermore, experiments conducted in classical BSE-inoculated Q/K_{222} heterozygous goats have shown at least low infectivity in goat tissues after long postinoculation periods (*26*), whereas heterozygous K_{222}-Tg516 mice were already fully susceptible to goat BSE (*29*). In addition, at least 1 Q/K_{222} heterozygous goat tested positive for atypical/Nor98 scrapie (*28*), and homozygous K_{222}-Tg516 mice were found to be completely susceptible to atypical/Nor98 scrapie (*30*). Taken together, those data suggest that the protective effect of the $Q_{222}K$ polymorphism may be limited, and its use in breeding programs should be carefully evaluated.

Acknowledgments

We thank Patricia Lorenzo, Irene Prieto, and Ana Villa for their technical assistance and the staff of the Biosafety Level 3 animal facility and the biosafety office at the CISA-INIA (Valdeolmos-Madrid) for their excellent animal care and work.

This research was supported by Ministerio de Ciencia, Innovación y Universidades/Agencia Estatal de Investigación (grant PCI2023-143384, funded by MICIU/AEI/10.13039/501100011033) and cofunded by European Union and by grant PID2023-146146NB-I00, funded by MICIU/AEI/10.13039/501100011033 and by Fondo Europeo de Desarrollo Regional, European Union.

About the Author

Dr. Fernández-Borges is a tenured researcher in the Laboratory of Molecular and Cellular Biology of Prions at Centro de Investigación en Sanidad Animal (CISA-INIA-CSIC). Her research interests include prion strain characterization and evolution and the pathogenesis of prion diseases and their effects on human and animal health.

References

1. Prusiner SB. Molecular biology of prion diseases. Science. 1991;252:1515–22. https://doi.org/10.1126/science.1675487
2. Marín-Moreno A, Fernández-Borges N, Espinosa JC, Andréoletti O, Torres JM. Transmission and replication of prions. Prog Mol Biol Transl Sci. 2017;150:181–201. https://doi.org/10.1016/bs.pmbts.2017.06.014
3. Baylis M, Chihota C, Stevenson E, Goldmann W, Smith A, Sivam K, et al. Risk of scrapie in British sheep of different prion protein genotype. J Gen Virol. 2004;85:2735–40. https://doi.org/10.1099/vir.0.79876-0
4. Houston F, Goldmann W, Foster J, González L, Jeffrey M, Hunter N. Comparative susceptibility of sheep of different origins, breeds and PRNP genotypes to challenge with bovine spongiform encephalopathy and scrapie. PLoS One. 2015;10:e0143251. https://doi.org/10.1371/journal.pone.0143251
5. Belt PB, Muileman IH, Schreuder BE, Bos-de Ruijter J, Gielkens AL, Smits MA. Identification of five allelic variants of the sheep PrP gene and their association with natural scrapie. J Gen Virol. 1995;76:509–17. https://doi.org/0.1099/0022-1317-76-3-509
6. Bossers A, Schreuder BE, Muileman IH, Belt PB, Smits MA. PrP genotype contributes to determining survival times of sheep with natural scrapie. J Gen Virol. 1996;77:2669–73. https://doi.org/10.1099/0022-1317-77-10-2669
7. Hunter N, Foster JD, Goldmann W, Stear MJ, Hope J, Bostock C. Natural scrapie in a closed flock of Cheviot sheep occurs only in specific PrP genotypes. Arch Virol. 1996;141:809–24. https://doi.org/10.1007/BF01718157
8. Hunter N, Moore L, Hosie BD, Dingwall WS, Greig A. Association between natural scrapie and PrP genotype in a flock of Suffolk sheep in Scotland. Vet Rec. 1997;140:59–63. https://doi.org/10.1136/vr.140.3.59
9. Benestad SL, Arsac JN, Goldmann W, Nöremark M. Atypical/Nor98 scrapie: properties of the agent, genetics, and epidemiology. Vet Res. 2008;39:19. https://doi.org/10.1051/vetres:2007056
10. Barillet F, Mariat D, Amigues Y, Faugeras R, Caillat H, Moazami-Goudarzi K, et al. Identification of seven haplotypes of the caprine *PrP* gene at codons 127, 142, 154, 211, 222 and 240 in French Alpine and Saanen breeds and their association with classical scrapie. J Gen Virol. 2009;90:769–76. https://doi.org/10.1099/vir.0.006114-0
11. González L, Martin S, Hawkins SA, Goldmann W, Jeffrey M, Sisó S. Pathogenesis of natural goat scrapie: modulation by host PRNP genotype and effect of co-existent conditions. Vet Res. 2010;41:48. https://doi.org/10.1051/vetres/2010020
12. Goldmann W, Ryan K, Stewart P, Parnham D, Xicohtencatl R, Fernandez N, et al. Caprine prion gene polymorphisms are associated with decreased incidence of classical scrapie in goat herds in the United Kingdom. Vet Res (Faisalabad). 2011;42:110. https://doi.org/10.1186/1297-9716-42-110

13. Goldmann W, Martin T, Foster J, Hughes S, Smith G, Hughes K, et al. Novel polymorphisms in the caprine *PrP* gene: a codon 142 mutation associated with scrapie incubation period. J Gen Virol. 1996;77:2885–91. https://doi.org/10.1099/0022-1317-77-11-2885
14. Papasavva-Stylianou P, Windl O, Saunders G, Mavrikiou P, Toumazos P, Kakoyiannis C. *PrP* gene polymorphisms in Cyprus goats and their association with resistance or susceptibility to natural scrapie. Vet J. 2011;187:245–50. https://doi.org/10.1016/j.tvjl.2009.10.015
15. Vaccari G, Bari MAD, Morelli L, Nonno R, Chiappini B, Antonucci G, et al. Identification of an allelic variant of the goat *PrP* gene associated with resistance to scrapie. J Gen Virol. 2006;87:1395–402. https://doi.org/10.1099/vir.0.81485-0
16. Acutis PL, Bossers A, Priem J, Riina MV, Peletto S, Mazza M, et al. Identification of prion protein gene polymorphisms in goats from Italian scrapie outbreaks. J Gen Virol. 2006;87:1029–33. https://doi.org/10.1099/vir.0.81440-0
17. Bouzalas IG, Dovas CI, Banos G, Papanastasopoulou M, Kritas S, Oevermann A, et al. Caprine PRNP polymorphisms at codons 171, 211, 222 and 240 in a Greek herd and their association with classical scrapie. J Gen Virol. 2010;91:1629–34. https://doi.org/10.1099/vir.0.017350-0
18. Fragkiadaki EG, Vaccari G, Ekateriniadou LV, Agrimi U, Giadinis ND, Chiappini B, et al. PRNP genetic variability and molecular typing of natural goat scrapie isolates in a high number of infected flocks. Vet Res (Faisalabad). 2011;42:104. https://doi.org/10.1186/1297-9716-42-104
19. Eiden M, Soto EO, Mettenleiter TC, Groschup MH. Effects of polymorphisms in ovine and caprine prion protein alleles on cell-free conversion. Vet Res (Faisalabad). 2011;42:30. https://doi.org/10.1186/1297-9716-42-30
20. Acutis PL, Martucci F, D'Angelo A, Peletto S, Colussi S, Maurella C, et al. Resistance to classical scrapie in experimentally challenged goats carrying mutation K222 of the prion protein gene. Vet Res (Faisalabad). 2012;43:8. https://doi.org/10.1186/1297-9716-43-8
21. White SN, Reynolds JO, Waldron DF, Schneider DA, O'Rourke KI. Extended scrapie incubation time in goats singly heterozygous for PRNP S146 or K222. Gene. 2012;501:49–51. https://doi.org/10.1016/j.gene.2012.03.068
22. Lacroux C, Perrin-Chauvineau C, Corbière F, Aron N, Aguilar-Calvo P, Torres JM, et al. Genetic resistance to scrapie infection in experimentally challenged goats. J Virol. 2014;88:2406–13. https://doi.org/10.1128/JVI.02872-13
23. Cinar MU, Schneider DA, Waldron DF, O'Rourke KI, White SN. Goats singly heterozygous for PRNP S146 or K222 orally inoculated with classical scrapie at birth show no disease at ages well beyond 6 years. Vet J. 2018;233:19–24. https://doi.org/10.1016/j.tvjl.2017.12.019
24. Mazza M, Guglielmetti C, Pagano M, Sciuto S, Ingravalle F, Martucci F, et al. Lysine at position 222 of the goat prion protein inhibits the binding of monoclonal antibody F99/97.6.1. J Vet Diagn Invest. 2012;24:971–5. https://doi.org/10.1177/1040638712457352
25. Madsen-Bouterse SA, Stewart P, Williamson H, Schneider DA, Goldmann W. Caprine PRNP polymorphisms N146S and Q222K are associated with proteolytic cleavage of PrP^C. Genet Sel Evol. 2021;53:52. https://doi.org/10.1186/s12711-021-00646-x
26. Aguilar-Calvo P, Fast C, Tauscher K, Espinosa J-C, Groschup MH, Nadeem M, et al. Effect of Q211 and K222 PRNP polymorphic variants in the susceptibility of goats to oral infection with goat bovine spongiform encephalopathy. J Infect Dis. 2015;212:664–72. https://doi.org/10.1093/infdis/jiv112
27. Fast C, Goldmann W, Berthon P, Tauscher K, Andréoletti O, Lantier I, et al. Protecting effect of PrP codons M142 and K222 in goats orally challenged with bovine spongiform encephalopathy prions. Vet Res. 2017;48:52. https://doi.org/10.1186/s13567-017-0455-0 10
28. Colussi S, Vaccari G, Maurella C, Bona C, Lorenzetti R, Troiano P, et al. Histidine at codon 154 of the prion protein gene is a risk factor for Nor98 scrapie in goats. J Gen Virol. 2008;89:3173–6. https://doi.org/10.1099/vir.0.2008/004150-0
29. Aguilar-Calvo P, Espinosa JC, Pintado B, Gutiérrez-Adán A, Alamillo E, Miranda A, et al. Role of the goat K222-PrP(C) polymorphic variant in prion infection resistance. J Virol. 2014;88:2670–6. https://doi.org/10.1128/JVI.02074-13
30. Aguilar-Calvo P, Espinosa JC, Andréoletti O, González L, Orge L, Juste R, et al. Goat K_{222}-PrP^C polymorphic variant does not provide resistance to atypical scrapie in transgenic mice. Vet Res. 2016;47:96. https://doi.org/10.1186/s13567-016-0380-7
31. Marin-Moreno A, Aguilar-Calvo P, Espinosa JC, Zamora-Ceballos M, Pitarch JL, Gonzalez L, et al. Classical scrapie in small ruminants is caused by at least four different prion strains. Vet Res. 2021;52:57. https://doi.org/10.1186/s13567-021-00929-7
32. Padilla D, Béringue V, Espinosa JC, Andreoletti O, Jaumain E, Reine F, et al. Sheep and goat BSE propagate more efficiently than cattle BSE in human PrP transgenic mice. PLoS Pathog. 2011;7:e1001319. https://doi.org/10.1371/journal.ppat.1001319
33. Féraudet C, Morel N, Simon S, Volland H, Frobert Y, Créminon C, et al. Screening of 145 anti-PrP monoclonal antibodies for their capacity to inhibit PrPSc replication in infected cells. J Biol Chem. 2005;280:11247–58. https://doi.org/10.1074/jbc.M407006200
34. Marín-Moreno A, Huor A, Espinosa JC, Douet JY, Aguilar-Calvo P, Aron N, et al. Radical change in zoonotic abilities of atypical BSE prion strains as evidenced by crossing of sheep species barrier in transgenic mice. Emerg Infect Dis. 2020;26:1130–9. https://doi.org/10.3201/eid2606.181790
35. Fraser H, Dickinson AG. The sequential development of the brain lesion of scrapie in three strains of mice. J Comp Pathol. 1968;78:301–11. https://doi.org/10.1016/0021-9975(68)90006-6
36. González L, Martin S, Houston FE, Hunter N, Reid HW, Bellworthy SJ, et al. Phenotype of disease-associated PrP accumulation in the brain of bovine spongiform encephalopathy experimentally infected sheep. J Gen Virol. 2005;86:827–38. https://doi.org/10.1099/vir.0.80299-0
37. Brun A, Castilla J, Ramírez MA, Prager K, Parra B, Salguero FJ, et al. Proteinase K enhanced immunoreactivity of the prion protein-specific monoclonal antibody 2A11. Neurosci Res. 2004;48:75–83. https://doi.org/10.1016/j.neures.2003.09.004
38. Andréoletti O, Berthon P, Levavasseur E, Marc D, Lantier F, Monks E, et al. Phenotyping of protein–prion (PrPsc)–accumulating cells in lymphoid and neural tissues of naturally scrapie-affected sheep by double-labeling immunohistochemistry. J Histochem Cytochem. 2002;50:1357–70. https://doi.org/10.1177/002215540205001009
39. Andréoletti O, Simon S, Lacroux C, Morel N, Tabouret G, Chabert A, et al. PrPSc accumulation in myocytes from sheep incubating natural scrapie. Nat Med. 2004;10:591–3. https://doi.org/10.1038/nm1055

40. Langeveld JPM, Pirisinu L, Jacobs JG, Mazza M, Lantier I, Simon S, et al. Four types of scrapie in goats differentiated from each other and bovine spongiform encephalopathy by biochemical methods. Vet Res. 2019;50:97. https://doi.org/10.1186/s13567-019-0718-z
41. Nonno R, Marin-Moreno A, Carlos Espinosa J, Fast C, Van Keulen L, Spiropoulos J, et al. Characterization of goat prions demonstrates geographical variation of scrapie strains in Europe and reveals the composite nature of prion strains. Sci Rep. 2020;10:19. https://doi.org/10.1038/s41598-019-57005-6
42. Kanata E, Humphreys-Panagiotidis C, Giadinis ND, Papaioannou N, Arsenakis M, Sklaviadis T. Perspectives of a scrapie resistance breeding scheme targeting Q211, S146 and K222 caprine PRNP alleles in Greek goats. Vet Res. 2014;45:43. https://doi.org/10.1186/1297-9716-45-43
43. Goldmann W, Marier E, Stewart P, Konold T, Street S, Langeveld J, et al. Prion protein genotype survey confirms low frequency of scrapie-resistant K222 allele in British goat herds. Vet Rec. 2016;178:168. https://doi.org/10.1136/vr.103521
44. Fediaevsky A, Tongue SC, Nöremark M, Calavas D, Ru G, Hopp P. A descriptive study of the prevalence of atypical and classical scrapie in sheep in 20 European countries. BMC Vet Res. 2008;4:19. https://doi.org/10.1186/1746-6148-4-19
45. Bian J, Khaychuk V, Angers RC, Fernández-Borges N, Vidal E, Meyerett-Reid C, et al. Prion replication without host adaptation during interspecies transmissions. Proc Natl Acad Sci U S A. 2017;114:1141–6. https://doi.org/10.1073/pnas.1611891114

Address for correspondence: Juan Maria Torres Trillo, Centro de Investigación en Sanidad Animal (CISA-INIA-CSIC), 28130 Valdeolmos, Madrid, Spain; email: jmtorres@inia.es

Guinea Pig Model for Lassa Virus Infection of Reproductive Tract and Considerations for Sexual and Vertical Transmission

Josilene N. Seixas, Joy M. Gary,[1] Stephen R. Welch, Sarah C. Genzer, JoAnn D. Coleman-McCray, Jessica R. Harmon, Christina F. Spiropoulou, Luciana Silva-Flannery, Georgia Ficarra, Elizabeth Lee, Julu Bhatnagar, Jessica R. Spengler, Jana M. Ritter

Lassa virus (LASV) causes Lassa fever; mortality rates are higher in pregnant women, and fetal infection and death are possible. Sexual transmission after recovery from Lassa fever has occurred. Using virus strains that are lethal (Josiah) or nonlethal (NJ2015) in guinea pigs, we characterized LASV-associated pathology and reproductive tissue tropism in male and female animals. Uterus, ovary, and epididymis were the earliest and most affected tissues; perivascular lymphocytic inflammation was prominent at lethal timepoints and persisted in survivors after clinical disease. LASV-Josiah RNA was detected in reproductive tissues by 4 days postinfection (dpi). Virus localized by immunohistochemistry and in situ hybridization predominantly within vascular smooth muscle and interstitial mesenchymal cells and was widespread in reproductive tissues in lethal infections (12–25 dpi) but not detected in survivors (41–42 dpi). Using a physiologically relevant model, we describe reproductive tissue targets to further elucidate LASV infection and effects on reproductive health and virus transmission.

Lassa virus (LASV) is a zoonotic arenavirus that causes Lassa fever (LF), a hemorrhagic disease endemic to West Africa, where seasonal outbreaks result in an estimated 1–3 million illnesses and up to 5,000 deaths annually (*1*). After an incubation period of 6–21 days, the disease manifests as fever, weakness, and malaise, followed by musculoskeletal, respiratory, gastrointestinal, or other signs. Long-term ocular (*2*,*3*) and auditory (*4*–*6*) complications can occur. In severe cases, hemorrhagic fever with shock causes death within 14 days (*7*). Mortality rates in pregnant women are disproportionately high, especially in the third trimester, in which reported mortality rates were >2 times those observed in nonpregnant women (*8*). Fetal loss rates are 75%–100% (*9*,*10*), and vertical transmission has been reported (*9*–*12*).

Most LF is caused by rodent-to-human transmission through direct contact with infected animals or their excreta (*13*–*17*). Horizontal human transmission, mostly nosocomial, has also been reported through contact with infected blood, urine, or other body fluids (*18*). Sexual transmission of LASV has been postulated (*19*), and persistence of LASV in seminal fluid for >3 months has been documented; however, studies describing the dynamics and infectivity of LASV in semen or other reproductive tract secretions are sparse (*12*,*20*).

Autopsies are rarely performed on LF patients, and reproductive tissues are not routinely collected; thus, descriptions of fatal LF pathology and tissue virus distribution are limited overall, and particularly for reproductive tissues (*21*). In 1 human study, pathology associated with LASV infection was described for 6 complete autopsies, 15 cases with postmortem biopsies of tissues other than liver, and 7 fetuses from infected women (*22*). The authors mentioned that careful examination of ovary, uterus, placenta, and breast demonstrated no specific pathologic alterations (*22*). Another study of postmortem tissue samples from 12 confirmed LF cases reported LASV antigens and viral particles in multiple reproductive

Author affiliation: Centers for Disease Control and Prevention, Atlanta, Georgia, USA

DOI: https://doi.org/10.3201/eid3112.250396

[1]Current affiliation: StageBio, Frederick, Maryland, USA.

organ and cell types, including breast ductal epithelial cells, ovarian thecal and stromal cells, and placental trophoblasts (*21*). To address gaps in knowledge of reproductive tract effects of LASV infection and to learn more about potential for sexual transmission, we investigated LASV pathology and tissue tropism in the female and male reproductive tracts of experimentally infected strain 13/N guinea pigs, a well-characterized model of LASV disease (*2*,*3*,*23*,*24*) and an applicable model of human pregnancy and fetal growth (*23*).

Materials And Methods

Biosafety and Ethics

Work with infectious virus or infected animals was conducted in a Biosafety Level 4 laboratory at the Centers for Disease Control and Prevention (CDC; Atlanta, GA, USA). Recombinant virus work was approved by the CDC Institutional Biosafety Committee. Animal experiments were approved by the CDC Institutional Animal Care and Use Committee (approval nos. 2833, 3073) and performed in an AAALAC-accredited facility.

Virus and Virus Detection

Recombinant LASV-Josiah is based on the sequence of an isolate obtained in 1976 from the serum of a 40-year-old man hospitalized at Songo Hospital in Sebgwena, Sierra Leone (*24*,*25*). We rescued LASV-Josiah in BSR-T7/5 cells and passaged 2 times in Vero-E6 cells (GenBank accession nos. HQ688673.1, HQ688675.1). Recombinant LASV 812673-LBR-USA-2015 (LASV-NJ2015) is based on the sequence of an isolate obtained in 2015 from a 55-year-old man who died of LF in New Jersey after returning from Liberia. We rescued LASV-NJ2015 in BSR-T7/5 cells and passaged 2 times in Vero-E6 cells (*26*) (GenBank accession nos. MG812650 and MG812651). We sequence-verified viral stocks and confirmed them to be mycoplasma-free. We determined titers (as focus-forming units [FFU] or 50% tissue culture infectious dose per milliliter) on Vero-E6 cells by immunofluorescence assays using an in-house anti-LASV monoclonal antibody mix (SPR628) targeting nucleoprotein (NP) and glycoprotein (GP) 2 and calculated them using the method of Reed and Muench (*27*). Further information on virus detection in tissues by quantitative reverse transcription PCR (qRT-PCR), immunohistochemistry (IHC), and in situ hybridization (ISH) are provided (Appendix, https://wwwnc.cdc.gov/EID/article/31/12/25-0396-App1.pdf).

Guinea Pigs

We examined tissues from 57 strain 13/N guinea pigs (26 male and 31 female, age range 165–1,433 days at challenge) previously reported in pathogenesis (*26*,*28*–*30*) or vaccine (*31*) studies. We inoculated all animals subcutaneously between the scapulae with 10^4 FFU (equivalent to $\approx 2 \times 10^4$ 50% tissue culture infectious dose/mL) of recombinant LASV-Josiah (n = 51 [23 male, 28 female]) or LASV-NJ2015 (n = 6 [3 male, 3 female]). Fifteen of 51 LASV-Josiah–inoculated animals were included in a viral replicon particle (VRP) vaccine study (*31*), in which animals were vaccinated subcutaneously with 10^7 FFU of VRP under these conditions: VRP followed by challenge 28 days later (n = 5); replication incompetent VRP (treated with 5×10^6 rads of gamma-irradiation) followed by challenge 28 days later (n = 5); and VRP 1 day after challenge (n = 5) (Figure 1). All remaining animals (n = 42) inoculated with either LASV-NJ2015 (n = 6) or LASV-Josiah (n = 36) were unvaccinated. Animals were housed individually in a climate-controlled laboratory (68–79°F, 30%–70% humidity) on a 12-hour light/dark cycle in individually ventilated cages (Thoren Caging Systems Inc., https://thoren.com) with deep, soft bedding (soft pellets, Carefresh [Healthy Pet, https://www.healthy-pet.com], and Enviro-Dri [Shepherd Specialty Papers, https://www.ssponline.com]). Animals received daily fresh vegetable enrichment and Timothy hay, and Certified Guinea Pig Diet 5026 (LabDiet, https://www.labdiet.com) and water were provided ad libitum. For individual identification and body temperature monitoring, we implanted BMDS IPTT-300 microchip transponders (Avidity Science, https://www.avidityscience.com) subcutaneously in the interscapular region. We monitored animals daily, as previously reported (*26*,*30*,*31*) and humanely euthanized them with isoflurane vapors followed by intracardiac sodium pentobarbital injection upon meeting euthanasia criteria or at study completion.

Results

Widespread Reproductive Tract Infection during Lethal LASV Disease in Guinea Pigs

To investigate reproductive tract infection histologically in lethal disease, we collected tissues from strain 13 guinea pigs at terminal endpoint after subcutaneous LASV-Josiah inoculation, which caused severe disease warranting euthanasia 14–28 days postinfection (dpi) (median 23 days) in 11 animals (6 female, 5 male). Inflammatory changes were identified in ≥1 reproductive tissue from all (6/6) female and 3/5 male

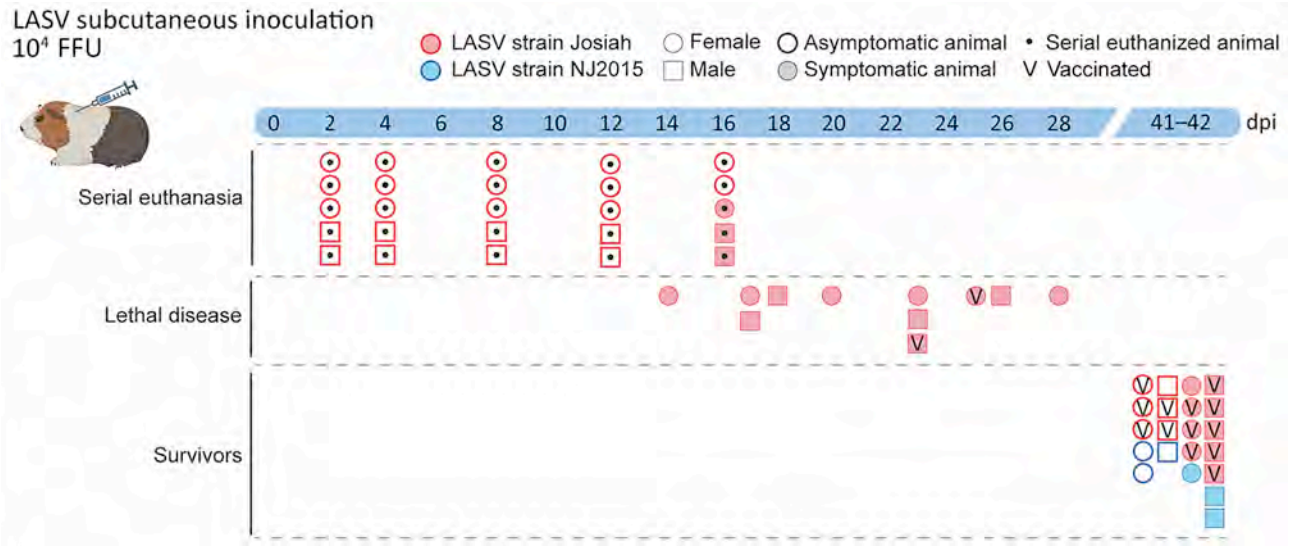

Figure 1. Study design to evaluate reproductive tissue pathology and tissue tropism in strain 13/N guinea pig model of Lassa virus infection. Tissues collected from a total of 57 adult strain 13/N guinea pigs inoculated subcutaneously with a target dose of 10^4 FFU of LASV (equivalent to ≈2 × 10^4 50% tissue culture infectious dose), representing 3 independent studies, were examined by PCR, hematoxylin and eosin, immunohistochemistry, or in situ hybridization. Animals were separated into 3 study groups on the basis of time of sampling and clinical outcome: those serially euthanized at predetermined study endpoints (2, 4, 8, 12, or 16 dpi [n = 5 at each timepoint]) to investigate early infection with highly pathogenic LASV-Josiah strain; terminal animals that reached endpoint criteria because of disease after LASV-Josiah infection (unvaccinated [n = 9] or vaccinated with γ-irradiated viral replicon particle [VRP] [n = 2]); and survivors euthanized at 41–42 dpi. Survivors were 15 animals infected with LASV-Josiah (vaccinated preexposure with VRP [n = 5] or gamma-irradiated VRP [n = 3], vaccinated postexposure with VRP [n = 5], or unvaccinated [n = 2] and 6 animals infected with strain NJ2015 [all unvaccinated (n = 6)]). Shaded symbols indicate animals that exhibited overt signs (defined as weight loss ≥10%, temperature ≥39.5°C for ≥2 consecutive days, or presence of clinical signs [i.e., clinical score ≥1 on ≥1 days). dpi, days postinfection; FFU, focus-forming units; LASV, Lassa virus; V, vaccinated.

animals, including ovary, oviduct, uterus, cervix/vagina, epididymis, seminal vesicle, and penis/prepuce; inflammation was not seen in testes (Table; Figures 2, 3; Appendix Table 1). Those tissues had mild to moderate, multifocal inflammation, which formed perivascular cuffs with occasional vascular mural infiltration. We noted more inflammation at 20–26 dpi than at 14–17 dpi; less inflammation was present at the latest lethal timepoint (28 dpi; 1 female). Infiltrates were predominately lymphocytic and presence of plasma cells and histiocytes was variable; heterophils were rare (Table).

Among 6 female animals with lethal disease, we detected viral antigen, RNA, or both in ovary, oviduct, and uterus of all 5 animals that were euthanized on days 14–25 and in the cervix/vagina in 3/5 animals tested (Figure 2, panel A; Appendix Table 1). Staining was most frequent in the vascular smooth muscle and perivascular mesenchymal cells including fibroblasts, as well as in the uterine muscle and endometrial stroma (Table, Figure 4). We saw similar distribution and intensity of staining in all positive animals; 1 female animal euthanized at 28 dpi had only very mild inflammation and no antigen was detected in reproductive tissues, although in situ hybridization (ISH) was positive in uterus.

Among male animals with lethal disease, viral antigen was detected in the epididymis of 4/5 animals euthanized at 17–26 dpi (Figure 2, panel B; Appendix Table 1). Epididymal staining was focally extensive and within interstitial stromal and inflammatory cells, as well as tubular epithelium, endothelium, vascular smooth muscle cells, and intratubular cells including spermatozoa (Table; Figure 5). We detected no antigen in any testis from lethally infected male animals, and only 2/5 had rare granular ISH staining in very few seminiferous epithelial or interstitial cells. In addition, staining by immunohistochemistry (IHC) or ISH occurred very rarely in 3 accessory sex glands (2 seminal vesicles, 1 prostate) of lethally infected male animals at 17–23 dpi.

We quantified viral RNA (vRNA) using qRT-PCR on ovary and testis samples from a subset (3 female, 3 male) of lethally infected animals. Testing revealed vRNA in all: up to 2.2 × 10^7 copies/μL in ovaries and up to 4.3 × 10^3 copies/μL in testes.

We evaluated mammary tissues in 3/6 female and 1/5 male animals with lethal disease. Two female and 1 male animals had mild glandular interstitial or dermal lymphocytic infiltrates and edema (Table;

Table. Pathologic findings and virus localization by immunohistochemistry or in situ hybridization in reproductive and mammary tissues of LASV-Josiah or LASV-NJ2015 strain–infected guinea pigs at different timepoints in study of guinea pig model for LASV infection of reproductive tract and considerations for sexual and vertical transmission*

			Hematoxylin and eosin		Immunohistochemistry or in situ hybridization	
Sex	Tissue	Group†	n/N (%)‡	Lesion/change	n/N (%)‡	Cellular location
F	Ovary	Early	1/15 (7)	PILPI, PE	7/15 (47)	TIC, GC
		Lethal	5/6 (83)	PILPI, PE	5/6 (83)	TIC, GC, IMC, VSMC, ENDC
		Survivor	2/10 (20)	PILPI	0/10 (0)	ND
	Oviduct	Early	1/15 (7)	PILPI	3/15 (20)	IMC
		Lethal	5/6 (83)	PILPI, PE, congestion	5/6 (83)	PV/IMC, VSMC, OSMC, intravascular inflammatory cells
		Survivor	3/10 (30)	PILPI	0/10 (0)	ND
	Uterus	Early	6/15 (40)	PILPI, PIE, congestion	10/15 (67)	Endometrial stromal, epithelial cells, IFMC, ENDC
		Lethal	6/6 (100)	PILPI, PIE, congestion, vasculitis	6/6 (100)	PV/IMC, IFMC, ENDC, VSMC, OSMC, endometrial stromal
		Survivor	4/10 (40)	PILPI, PIE, congestion	0/10 (0)	ND
	Cervix/ vagina	Early	2/12 (17)	PILPI, PIE	8/12 (67)	IMC, VSMC, epithelial cells, intraluminal debris, FMC
		Lethal	3/6 (50)	PILPI, PIE	3/6 (50)	IMC, VSMC, epithelial cells, ENDC, intraluminal debris, IFMC
		Survivor	4/10 (4)	PILPI, PIE	0/10 (0)	ND
M	Testis	Early	0/10 (0)	None	2/10 (20)	IMC, ENDC, intravascular
		Lethal	0/5 (0)	None	2/5 (40)	IMC, seminiferous tubule
		Survivor	0/11 (0)	None	0/11 (0)	ND
	Epididymis	Early	1/10 (10)	PILPI, epithelial necrosis, intratubular debris	3/10 (30)	IMC, peritubular, tubular epithelium, intraluminal cells (including spermatozoa)
		Lethal	3/5 (60)	PILPI, epithelial necrosis, intratubular heterophils	4/5 (80)	IMC, VSMC, ENDC, tubular epithelium, intraluminal cells/debris (including spermatozoa)
		Survivor	3/11 (27)	PILPI, PIE, intratubular heterophils, MXI, loss of tubules	0/11 (0)	ND
	Seminal vesicle/ prostate	Early	0/10 (0)	None	3/10 (30)	PV/IMC
		Lethal	1/5 (20)	PILPI, PE	3/5 (60)	IMC, intraluminal debris, VSMC
		Survivor	0/11 (0)	None	0/11 (0)	ND
	Penis/ prepuce	Early	NS	NS	NS	NS
		Lethal	1/3 (33)	MXI (preputial gland duct)	0/3 (0)	ND
		Survivor	2/7 (29)	PLPI	0/7 (0)	ND
Both	Mammary tissue	Early	8/20 (40)	PILPI (glands and skin), histiocytic infiltrates, PIE (glands), epidermal necrosis	11/20 (55)	IMC, dermis, follicular wall, epidermis, IFMC
		Lethal	3/4 (75)	PILPI, PIE (glands and skin)	2/4 (50)	IMC, ENDC, glandular epithelial cells, IFMC, intraluminal debris, epidermis, follicular wall
		Survivor	4/13 (31)	PILPI (glands and skin), PIE, congestion, MXI (glands)	0/13 (0)	ND

*dpi, days postinfection; ENDC, endothelial cells; GC, granulosa cells; IFMC, inflammatory cells; IMC, interstitial mesenchymal cells; LASV, Lassa virus; MXI, mixed inflammatory infiltrate; ND, not detected; NS, not sampled; PE, perivascular edema; PIE, perivascular and interstitial edema; PILPI, perivascular and interstitial lymphoplasmacytic inflammation; PLPI, perivascular lymphoplasmacytic inflammation; PV, perivascular; OSMC, other (nonvascular) smooth muscle cells; TIC, Theca-interstitial cells; VSMC, vascular smooth muscle cells.
†Early refers to animals serially euthanized 2–16 dpi after infection with LASV-Josiah-strain. Lethal refers to animals lethally infected with LASV-Josiah-strain and euthanized because of severity of clinical disease 14–28 dpi. Survivor refers to animals that survived LASV-Josiah-strain or LASV-NJ2015 strain infection and were euthanized 41–42 dpi.
‡n indicates number of animals with pathologic changes or staining in the tissue; N represents total number of animals evaluated in the group; percentage indicates percentage of animals evaluated that had the histopathologic finding present or with positive staining by immunohistochemistry or in situ hybridization in that tissue; not all tissues were evaluated or tested by immunohistochemistry or in situ hybridization for all animals (Appendix Tables 1–3, https://wwwnc.cdc.gov/EID/article/31/12/25-0396-App1.pdf).

Figure 6). We detected antigen or RNA in mammary tissue from the 2 female animals, localized to rare endothelial cells and perivascular cells including stromal and inflammatory cells, glandular epithelium and intraluminal cells, and epidermal and follicular epithelium (Table; Figure 6).

Detection of LASV-Josiah in Reproductive Tissues before Onset of Clinical Signs

After LASV-Josiah challenge, we collected tissues for histologic and virologic (qRT-PCR) investigation in animals serially euthanized at 2, 4, 8, 12, or 16 dpi to characterize early reproductive tract infection. In

female animals, we detected vRNA by qRT-PCR in mammary tissue as early as 4 dpi and in ovary (and in urogenital swab specimens, as previously reported [*30*]) from 8–16 dpi. In male animals, we detected vRNA by qRT-PCR in testis, epididymis, mammary tissue, and genital swabs from 8–16 dpi. At 8 dpi,

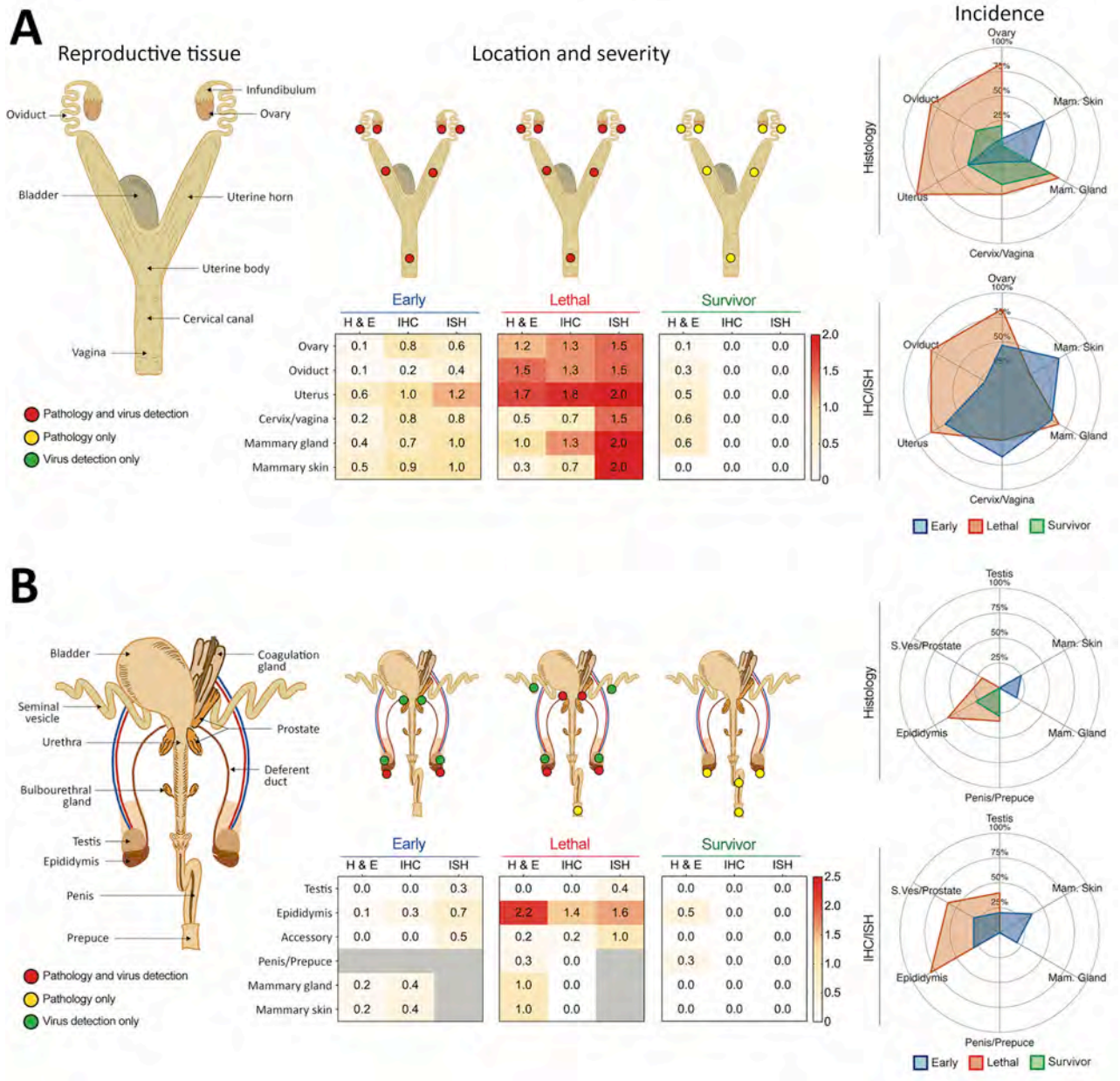

Figure 2. Localization and severity of histopathologic changes and Lassa virus (LASV) detection in reproductive tissues of strain 13/N guinea pigs experimentally infected with LASV strain Josiah or NJ2015 in study of guinea pig model for LASV infection of reproductive tract and considerations for sexual and vertical transmission. Female (A) and male (B) guinea pig reproductive tract anatomy, histopathology, and virus detection (antigen by IHC or viral RNA by ISH) after subcutaneous infection with LASV strain Josiah or NJ-2015 (target dose, 10^4 focus-forming units). Anatomic localization, severity, and incidence are depicted and delineated by stage of infection: early (≤16 dpi), lethal (meeting endpoint criteria at 14–28 dpi), and survivor (41 or 42 dpi). Histopathologic changes (H&E) and viral detection (IHC or ISH) were scored semiquantitatively for each tissue as absent (0), minimal (1), mild (2), moderate (3), or severe (4). Not all analyses were performed for all animals (Appendix Tables 1–3, https://wwwnc.cdc.gov/EID/article/31/12/25-0396-App1.pdf). H&E, IHC, and ISH scores represent mean severity values for each tissue across all animals tested. An asterisk (*) indicates that only 1 animal was evaluated in the group; gray boxes indicate tissues that were not available or not evaluated. Relative incidence of histopathologic change or virus detection in early, lethal, and survivor cohorts with sufficient group sizes (n ≥3) is shown in radar plots; only a single male animal in the lethal cohort was excluded, as it was the sole animal evaluated and test results were positive in both mammary gland and skin. H&E, hematoxylin and eosin; IHC, immunohistochemistry; ISH, in situ hybridization.

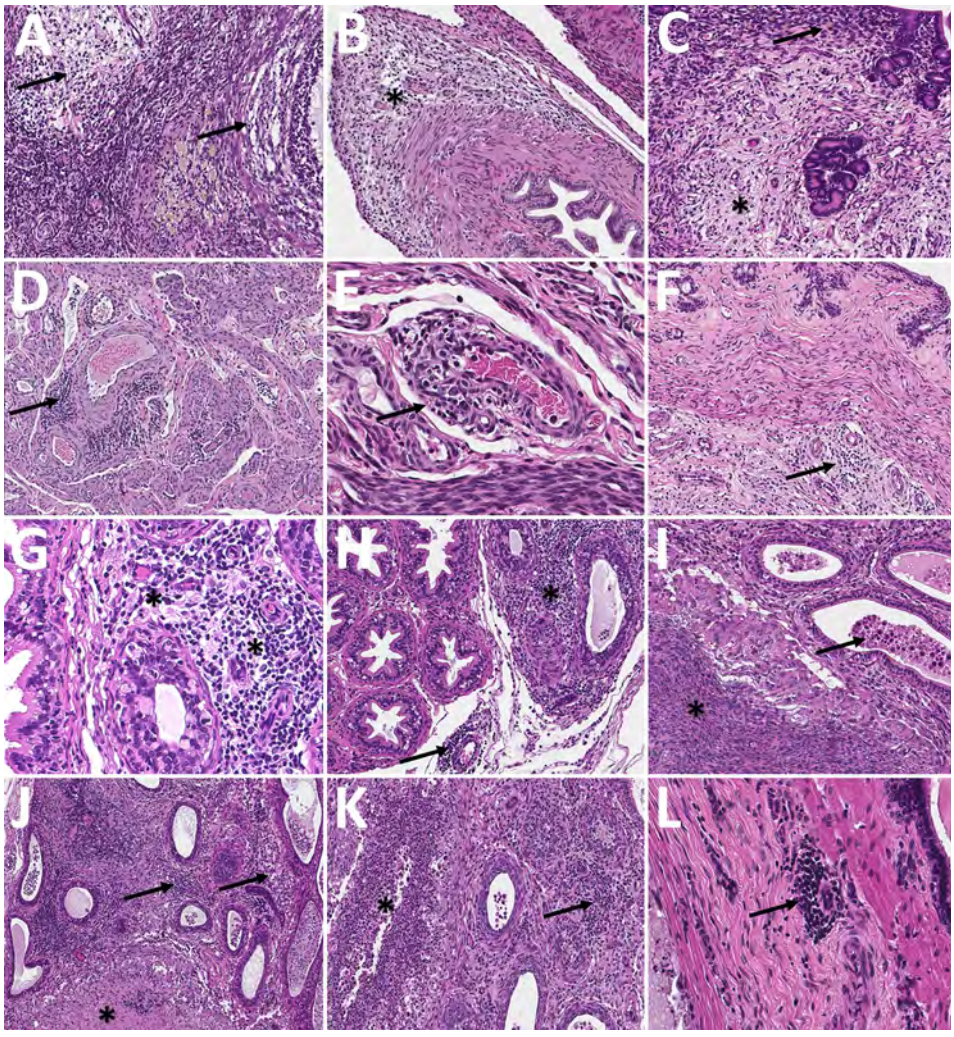

Figure 3. Histopathologic findings in reproductive tissues of strain 13/N guinea pigs with lethal disease after Lassa virus (LASV) strain Josiah infection in study of guinea pig model for LASV infection of reproductive tract and considerations for sexual and vertical transmission. Panels A–F depict samples from female guinea pigs; panels G–L depict samples from male guinea pigs. A) Ovary (25 days postinfection [dpi]) with moderate perivascular and interstitial inflammation (arrows). B) Oviduct (20 dpi) with focal interstitial inflammation and edema (asterisk) within the serosa. C) Uterus (23 dpi) with mild endometrial inflammation and edema (asterisk) and hemosiderin-laden macrophages (arrow). D) Uterus (25 dpi) with multifocal mononuclear inflammatory cells (arrow) forming partial cuffs around vessels in the myometrium. E) Uterine vessel (23 dpi) with mural infiltration by lymphocytes and plasma cells (arrow). F) Cervix (23 dpi) with multifocal, mild, perivascular inflammation (arrow). G) Epididymis (26 dpi) with moderate perivascular inflammation (asterisks). H) Epididymis (23 dpi) with multifocal interstitial inflammation around tubules (asterisk) and a vessel (arrow). I) Epididymis (26 dpi) with marked epididymitis with tubular dilation by inflammatory cells (arrow) and rupture, associated with sperm granuloma formation (asterisk). J) Epididymis (23 dpi) with marked epididymitis, with interstitial inflammation (arrows), and intratubular heterophils associated with rupture and granuloma formation (asterisk). K) Epididymis (26 dpi) with marked interstitial inflammation (arrow) and tubular epithelial necrosis with heterophils (asterisk). L) Prostate (23 dpi) with mild focal lymphocytic, perivascular inflammation (arrow). Hematoxylin and eosin stain. Original magnifications ×20 (panels A, E, G, I, K), ×15 (panels B, H), and ×10 (panels C, D, F, J, L).

vRNA was detected by qRT-PCR in the gonads and associated reproductive tissues of all serially euthanized animals (ovaries, ≤7.3 × 105 copies/μL; uteri, ≤5.5 × 104 copies/μL; testes, ≤1.0 × 105 copies/μL; and epididymides, ≤3.4 × 104 copies/μL).

Histopathologic changes were absent in reproductive tissues of serially euthanized animals at earlier timepoints (female at 2–8 dpi, male at 2–12 dpi); we detected only subtle changes, similar but overall milder than seen in lethal disease, in 6/6 uteri and rarely in other tissues (1 ovary, 1 oviduct, 2 cervix/vagina) of female animals euthanized at later timepoints (12–16 dpi). One of 2 male animals had lymphoplasmacytic inflammation with rare epithelial necrosis and intratubular debris in the epididymis at 16 dpi (Table; Figures 2, 7; Appendix Table 2). We saw no other notable histopathologic lesions in the male reproductive tracts in serially euthanized animals.

In serially euthanized female animals, 10/15 had staining by IHC or ISH in ≥1 reproductive tissue (Table; Figures 2, 8; Appendix Table 2). We observed staining in 7/9 ovaries at 8–16 dpi, the most widespread at 12 dpi. At 8 dpi, focal staining was in a corpus luteum, mainly in granulosa lutein cells, but also in capillary endothelial and few thecal cells. At later time points (at and after 12 dpi), staining was in theca-interstitial cells and granulosa cells. We noted scattered staining in interstitial cells in 3/6 oviducts at 12 and 16 dpi. During 4–16 dpi, 10/12 uteri demonstrated staining. At 4

and 8 dpi, staining was multifocal and rare within endometrial stromal cells. At 12 and 16 dpi, staining in the uterus was similarly distributed in endometrial stromal and epithelial cells but increased overall at 12 dpi and decreased again at 16 dpi. At those later timepoints, staining within inflammatory or endothelial cells in areas with perivascular inflammation was rare. Of available cervix/vagina tissues, 8/11 from 4–16 dpi showed multifocal staining throughout the superficial subepithelial stroma, within endothelial cells and vascular smooth muscle cells, in the myometrium, and, less frequently (2 animals at 12 and 16 dpi), in the cervical epithelium, but not in the vaginal epithelium (Appendix Table 2).

In serially euthanized male animals, 2/10 testes (at 12 dpi) and 3/10 accessory sex glands (at 12 and 16 dpi) showed rare viral detection by ISH but not by IHC. Staining was in interstitial and intravascular cells in those tissues and was unaccompanied by pathologic changes. Epididymides showed multifocal LASV staining by ISH in 3/6 animals tested at 8–16 dpi; only 1 of those 6 also showed staining by IHC at 16 dpi. Staining was in epididymal interstitial cells at 8 dpi and in tubular epithelial and intraluminal cells (including spermatozoa) at 16 dpi. We saw no staining in any tested male tissue before 8 dpi (Table; Figures 2, 8; Appendix Table 2).

Mammary tissues from serially euthanized animals of both sexes had no or minimal histopathologic

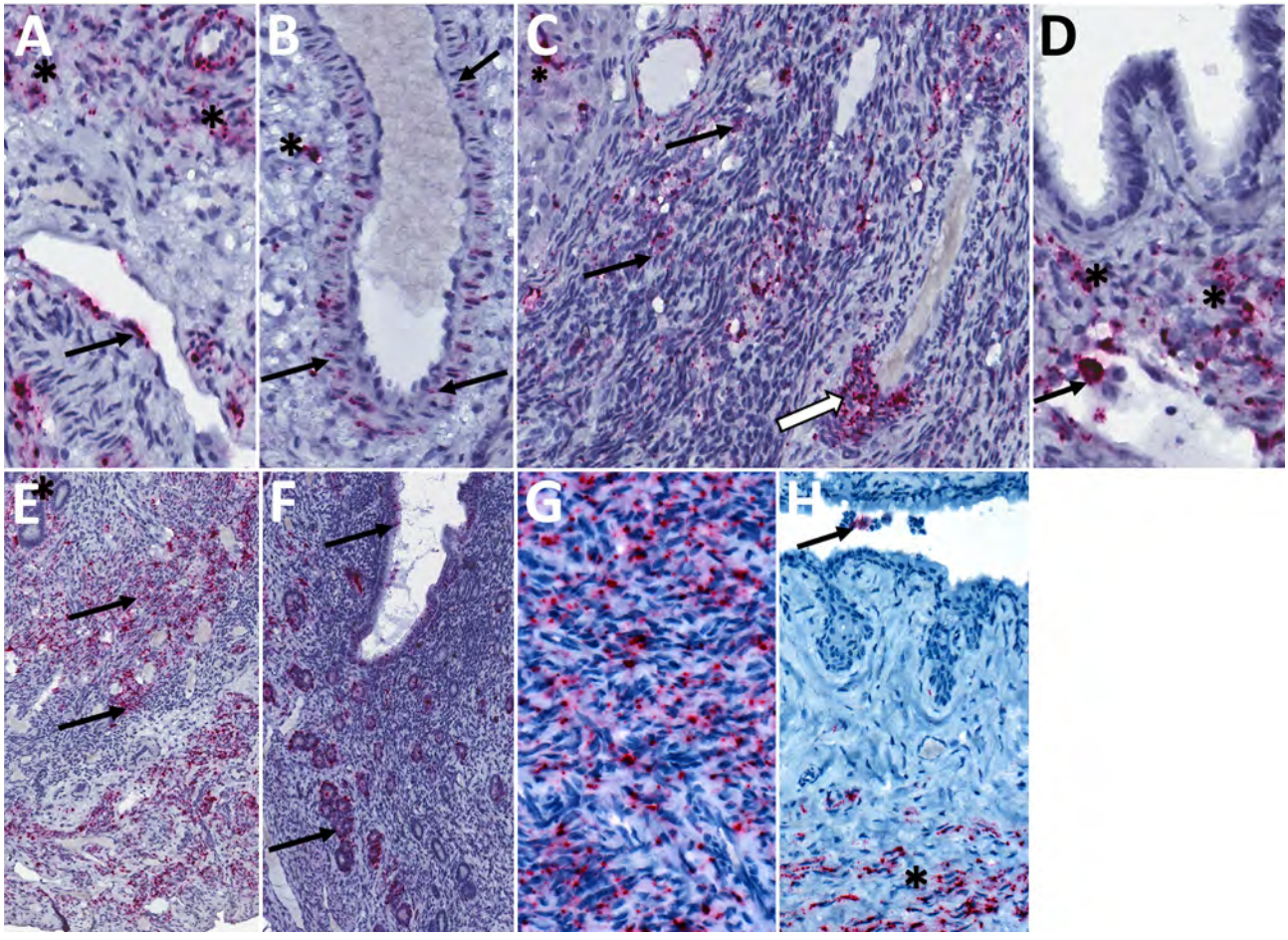

Figure 4. Detection of Lassa virus (LASV) antigens and RNA in reproductive tissues by immunohistochemistry (IHC) and in situ hybridization (ISH) in strain 13/N female guinea pigs lethally infected with LASV strain Josiah in study of guinea pig model for LASV infection of reproductive tract and considerations for sexual and vertical transmission. IHC and ISH chromogens are red. A) Uterus (25 dpi), ISH. Staining in interstitial mesenchymal cells (asterisks) and rare endothelial cells (arrow). B) Uterus (23 dpi), ISH. Staining in vascular smooth muscle cells (arrows) and perivascular interstitial mesenchymal cells (asterisk). C) Ovary (23 dpi), ISH. Staining within a corpus luteum (asterisk), in theca-interstitial cells (arrows), and in inflammatory cells within and around a vascular wall (white arrow). D) Oviduct (23 dpi), ISH. Staining in mesenchymal interstitial cells (asterisk) and intravascular inflammatory cells (arrow). E) Uterus (23 dpi), ISH. Extensive staining in the endometrial stroma (asterisk) and myometrial smooth muscle cells (arrows). F) Uterus (23 dpi), ISH. Extensive staining in the endometrial glandular epithelial cells (arrows). G) Endocervix (23 dpi), IHC. Extensive staining in mesenchymal cells. H) Vagina (23 dpi), IHC. Staining in submucosal mesenchymal cells (asterisk) and intraluminal cellular debris (arrow). Original magnifications ×40 (panels A, B, D, G, H), ×30 (panel C), ×20 (panels E, F).

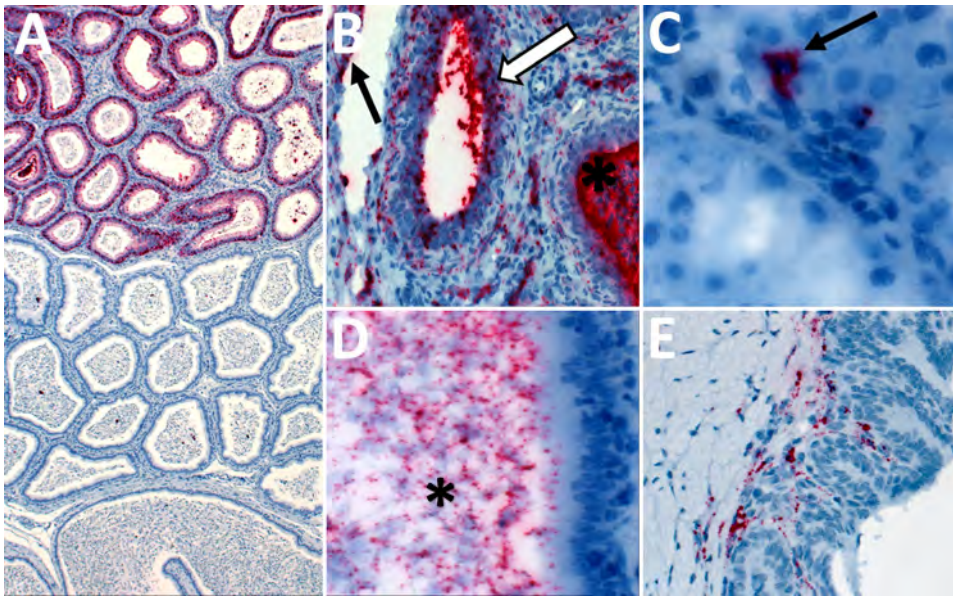

Figure 5. Detection of Lassa virus (LASV) antigens and RNA in reproductive tissues by immunohistochemistry (IHC) and in situ hybridization (ISH) in strain 13/N male guinea pigs lethally infected with LASV strain Josiah in study of guinea pig model for LASV infection of reproductive tract and considerations for sexual and vertical transmission. A) Epididymis (18 dpi), ISH. Regionally extensive staining in epididymal epithelial cells. B) Epididymis (26 dpi), ISH. Staining in interstitial mesenchymal cells, endothelium (arrow), tubular epithelium (white arrow), and intratubular inflammatory cells (asterisk). C) Testis (18 dpi), ISH. Focal intracellular staining in the interstitium (arrow). D) Epididymis (23 dpi), ISH. Intraluminal staining including spermatozoa (asterisk). E) Seminal vesicle (17 dpi), ISH. Focal staining in subepithelial stromal cells. Original magnifications ×5 (panel A), ×40 (panels B, D), ×63 (panel C), ×20 (panel E).

changes at all timepoints, including minimal mononuclear or mixed inflammatory infiltrates and mild periglandular edema in 5/17 animals (at 12–16 dpi) for which mammary glandular tissue was evaluated. Mammary skin occasionally showed mild dermal lymphohistiocytic inflammation, epidermal keratinocyte degeneration, and single cell death. Although vRNA was detected by qRT-PCR in mammary gland as early as 4 dpi, staining by IHC or ISH was seen in mammary gland or skin in 8/12 tested female animals (8–16 dpi) and 3/8 tested male animals (12–16 dpi), characterized by multifocal staining with similar

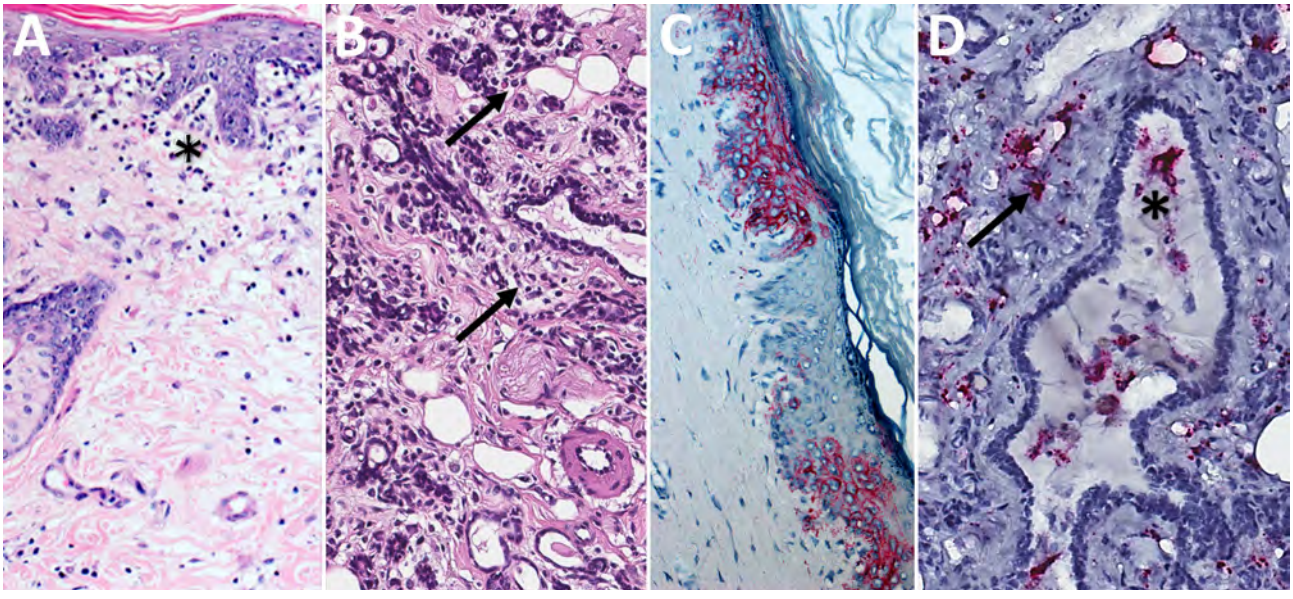

Figure 6. Histopathologic findings and detection of Lassa virus (LASV) antigens and RNA in mammary tissues by immunohistochemistry (IHC) and in situ hybridization (ISH) in strain 13/N guinea pigs lethally infected with LASV strain Josiah in study of guinea pig model for LASV infection of reproductive tract and considerations for sexual and vertical transmission. A) Mammary skin (23 dpi), hematoxylin and eosin stain. Mild interstitial lymphoplasmacytic infiltrates and edema (asterisk) in the superficial dermis. B) Mammary gland (25 dpi), hematoxylin and eosin stain. Mild interstitial lymphoplasmacytic infiltrates (arrows) in the periglandular stroma. C) Mammary skin (23 dpi), IHC. Staining in keratinocytes of the epidermis. D) Mammary gland (23 dpi), ISH. Staining around vessels and within the stroma between glands (arrow) and within cells in a mammary duct lumen (asterisk). Original magnifications ×10 (panels A–C), ×20 (panel D).

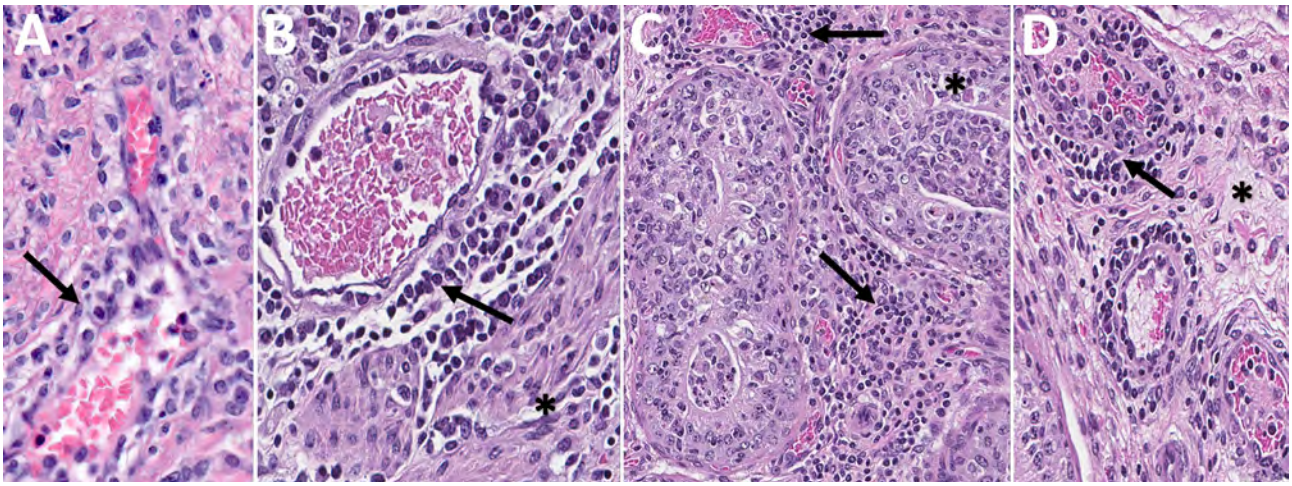

Figure 7. Histopathologic findings in reproductive tissues from strain 13/N guinea pigs serially euthanized 4–16 days postinfection (dpi) after Lassa virus strain Josiah infection in study of guinea pig model for infection of reproductive tract and considerations for sexual and vertical transmission. A) Perivascular mononuclear infiltrates (arrow) in oviduct (12 dpi). B) Perivascular (arrow) and interstitial (asterisk) lymphoplasmacytic infiltrates within the myometrium in uterus (16 dpi). C) Interstitial and perivascular lymphoplasmacytic infiltrates (arrows), with rare single cell necrosis of the tubular epithelial cells (asterisk) in epididymis (16 dpi). D) Mild perivascular and vascular inflammation (arrow) and interstitial edema (asterisk) in epididymis (16 dpi). Hematoxylin and eosin stain. Original magnifications ×40 (panels A, B, D), ×20 (panel C).

distribution as described for the mammary tissues of lethally infected animals (Table; Appendix Table 2).

Reduced Pathology and No LASV Detection in Surviving Guinea Pigs

To assess reproductive tissue pathology and viral persistence in LASV survivors, we histologically examined tissues from 21 LASV-infected guinea pigs (strain Josiah or NJ2015) euthanized at 41–42 dpi. Animals represented 2 outcomes: survival after overt clinical disease or survival without overt clinical disease (Appendix Table 3). Overt disease was defined as weight loss ≥10%, temperature ≥39.5°C for ≥2 consecutive days, or a clinical score of ≥1 on ≥1 days. Both untreated and vaccinated surviving animals were included, because animals with and without clinical intervention are clinically relevant for these investigations. Among 12 survivors of overt clinical disease, similar but generally less severe perivascular and interstitial inflammatory changes described for animals in other groups (<28 dpi) were variably present at 41–42 dpi (Table). All animals with inflammation had been infected with LASV-Josiah; those included 4/5 female animals with effects in 2 ovaries, 3 oviducts, 4 uteri, and 4 cervix/vagina and 3 mammary glands and 3/7 male animals with inflammation in 1 tissue each, including 2 epididymides and 1 penis/prepuce. No histopathologic changes were seen in testes or accessory sex glands of surviving male animals (Table; Figures 2, 9; Appendix Table 3). Among 9 surviving animals without overt clinical disease, 1/5 female animals had minimal inflammation in mammary glandular tissue but no inflammation in other reproductive tissues. One of 4 male animals had minimal epididymal inflammation only, and another male survivor had minimal inflammation in the penis/prepuce. Neither viral antigen nor RNA were detected by IHC or ISH in any female or male reproductive tissue tested from surviving animals, regardless of clinical course. We evaluated tissues from 14 survivors (all infected with LASV-Josiah) by qRT-PCR targeting the nucleoprotein; vRNA was not detected in ovaries or testes from 5 survivors without overt signs, whereas low levels of vRNA were detected in 4/4 ovaries (78.4–270 copies/μL) and 4/5 testes (15–50 copies/μL) of 9 survivors after overt disease.

Discussion

Using guinea pig models of both lethal and nonlethal LF, we characterized reproductive tissue tropism and associated histopathologic changes. In lethal cases, we found widespread reproductive tract infection, but pathology was often subtle or nonspecific, whereas survivors exhibited minimal pathology and no ISH or IHC staining. Furthermore, after infection with a known lethal strain, vRNA was detected in reproductive tract tissues early in infection, preceding the onset of clinical signs or tissue inflammation.

The overall paucity of inflammation in LASV infection could reflect the ability of LASV to replicate in dendritic cells and macrophages and create immune-privileged reservoirs that enable unchecked LASV

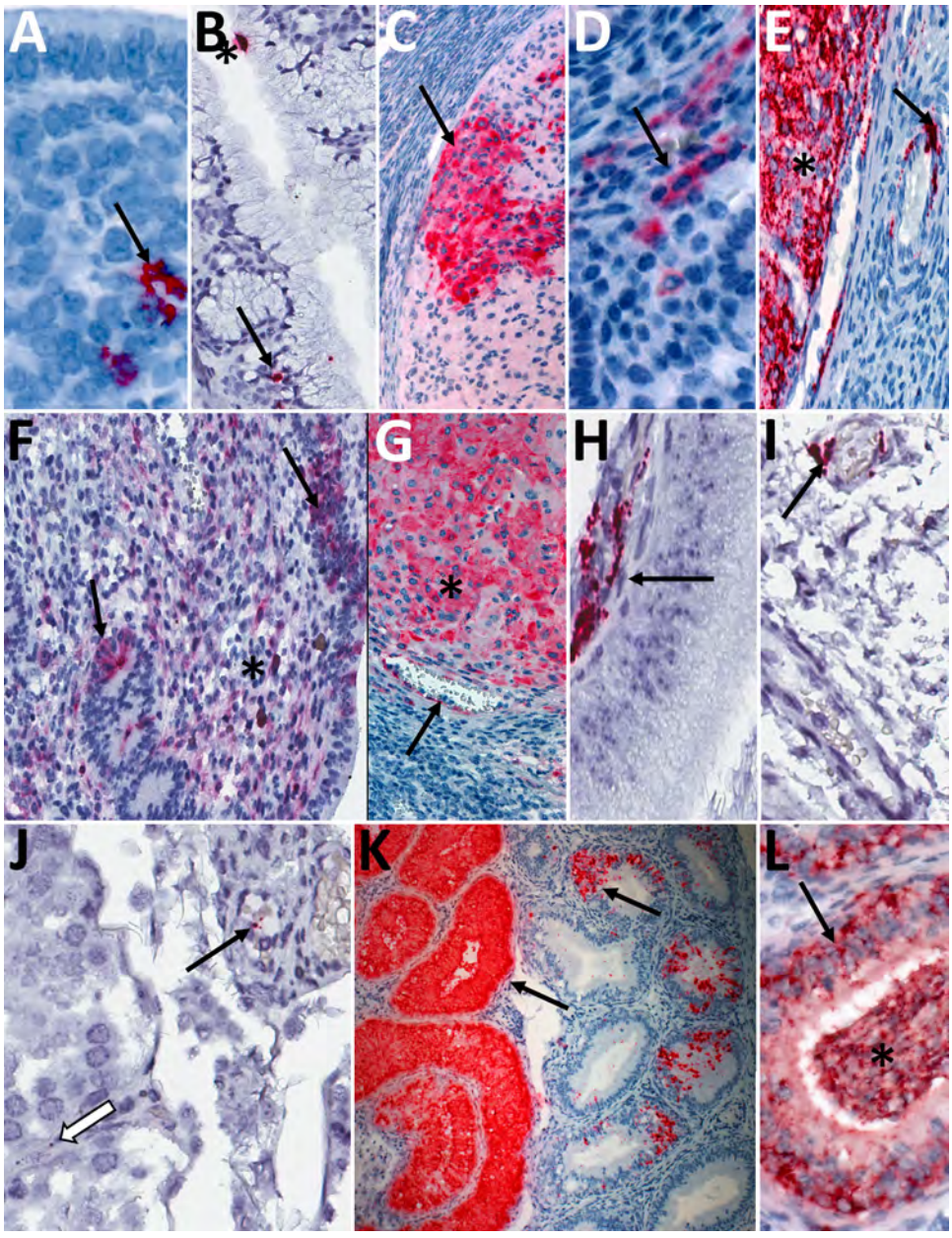

Figure 8. Detection of viral antigens and RNA by immunohistochemistry (IHC) and in situ hybridization (ISH) in reproductive tissues from strain 13/N guinea pigs serially euthanized 4–16 dpi after LASV strain Josiah infection in study of guinea pig model for infection of reproductive tract and considerations for sexual and vertical transmission. IHC and ISH chromogens are red. Panels A–G depict samples from female guinea pigs; panels H–L depict samples from male guinea pigs. A) Uterus (4 dpi), ISH. Rare staining in the endometrial stroma (arrow), without inflammation. B) Endocervix (4 dpi), ISH. Staining of the apical surface of an endocervical epithelial cell (asterisk) and beneath the basilar epithelium (arrow), without inflammation. C) Ovary (8 dpi), IHC. Staining in granulosa lutein cells (arrow) of a corpus luteum without inflammation. D) Uterus (8dpi), IHC. Staining in endometrial stromal cells (arrow) without inflammation. E) Ovary (12 dpi), ISH. Staining in theca interstitial cells (asterisk) and endothelium (arrow). F) Uterus (12 dpi), IHC. Endometrial stromal lymphoplasmacytic infiltrates and staining in endometrial stromal (asterisk) and epithelial (arrows) cells. G) Ovary (16 dpi), IHC. Staining in granulosa cells (asterisk) and endothelium (arrow). H) Epididymis (8 dpi), IHC. Staining in peritubular interstitial mesenchymal cells (arrow). I) Seminal vesicle (12 dpi), ISH. Staining in the wall of a small interstitial vessel (arrow). J) Testis (12 dpi), ISH. Rare granular staining of viral RNA in the interstitium (white arrow) and in a vascular lumen (arrow). K, L) Epididymis (16 dpi), ISH. Extensive staining in tubular epithelium (arrows) and within tubular lumens, including spermatozoa (asterisk). Original magnifications ×40 (panels A, C, D, F, G, H, J, L), ×63 (panels B, I), ×10 (panel E), ×4 (panel K).

replication early in infection and subsequent systemic spread, including to the reproductive tract (*28*,*32*,*33*). We detected viral antigen and RNA in multiple reproductive tissues and cell types in male and female animals, including in tissue and cell types previously described for guinea pigs (*32*). ISH, which detects vRNA, was more sensitive than IHC, which detects viral protein; among 36 positive tissues on which both IHC and ISH were performed, results were ISH positive and IHC negative for 18 (50%). That finding indicates that viral RNA might persist or be detectable in tissues even when protein expression is below the threshold of IHC detection. In female animals, vRNA detection was earliest and most abundant in uteri and ovaries; for male animals, vRNA detection was earliest and most extensive in epididymides. Whether LASV has a specific tropism for these tissues or whether their apparent preferential infection is the result of hemodynamic factors during viremia is unclear. At peak viremia, staining was predominantly,

but not exclusively, localized in tissues with inflammatory changes; however, staining was also seen in tissues without overt pathology. Mesenchymal cells (interstitial stromal cells and smooth muscle cells) were affected earlier and more commonly than epithelial cells (granulosa cells, endometrial glands, mammary glands, epididymal epithelium and endothelial cells), suggesting that infected fibroblasts could be involved in immune activation and modulation in LASV infection (*34*).

Conversely, in surviving animals, mild inflammation was sometimes present, but vRNA and antigen were not detected by ISH and IHC. However, low-level vRNA was detected by qRT-PCR in about half of survivor gonadal tissues, exclusively in animals that had exhibited overt clinical signs. Those findings suggest substantial viral clearance from reproductive tissues by 42 dpi, although clearance may be incomplete, particularly in more severe cases. Shedding of LASV by humans can be prolonged; even after recovery, virus remains infective in body fluids, including semen, vaginal fluid, urine, and breast milk for long periods (*12*,*19*,*20*). Although we did not directly test genital fluids in this study, IHC or ISH staining was detected in tissues that contribute to genital fluids (testes, epididymides, male accessory sex glands, cervix/vagina) at the latest timepoints examined (23–26 dpi) in lethally infected animals. Altogether, our findings indicate a window of potential risk for sexual transmission of as early as 4 dpi, before the onset of clinical signs, and extending up to 3–4 weeks, or possibly longer, after infection, underscoring the

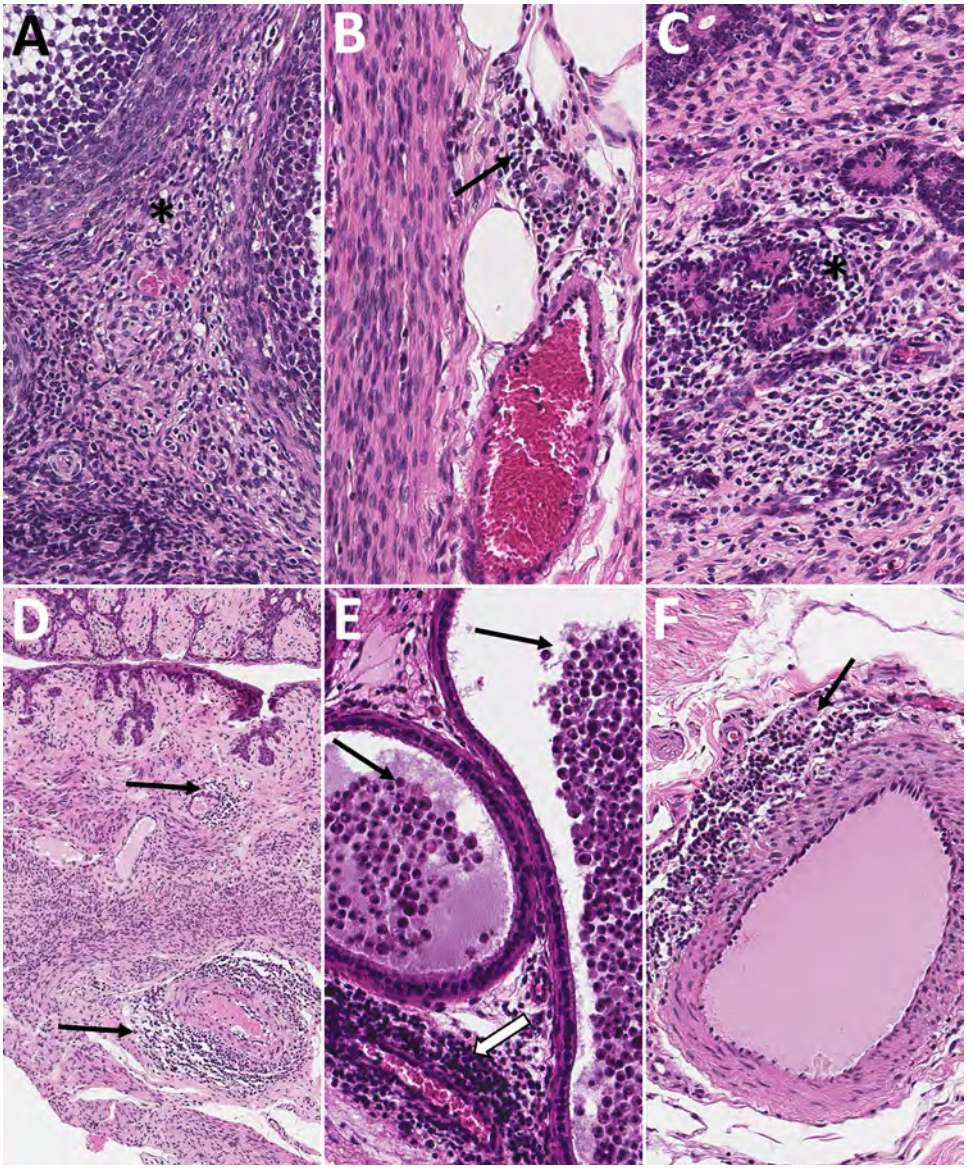

Figure 9. Histopathologic findings in reproductive tissues from strain 13/N guinea pig survivors of Lassa virus strain Josiah infection at 42 days postinfection (dpi) in study of guinea pig model for Lassa virus infection of reproductive tract and considerations for sexual and vertical transmission. Panels A–D depict samples from female guinea pigs; panels E–F depict male samples from male guinea pigs. A) Ovary (42 dpi) with lymphoplasmacytic inflammation in the stroma (asterisk). B) Oviduct (42 dpi) with focal perivascular and interstitial inflammation (arrow). C) Uterus (42 dpi) with endometrial stromal lymphoplasmacytic inflammation (asterisk) around glands. D) Vagina (42 dpi) with lymphocytic inflammation (arrows) around vessels in the vaginal wall. E) Epididymis (42 dpi) with dense perivascular lymphoplasmacytic inflammation around a vessel (white arrow) and heterophils within tubular lumens (black arrows). F) Penile connective tissue (42 dpi) with perivascular lymphocytic inflammation (arrow). Hematoxylin and eosin stain. Original magnification ×40 (panels A–C, E, F) ×10 (panel D).

need for continued research on LASV persistence in reproductive tissues and factors influencing the duration of detection.

Our findings have implications for reproductive health, including fertility and pregnancy outcomes, and suggest the potential for both sexual and vertical LASV transmission. We detected LASV in ovarian thecal and granulosa cells, which are the cells that differentiate into the corpus luteum and secrete progesterone that is essential for early pregnancy maintenance in both guinea pigs and humans (*23*). Ovarian infection might lead to early pregnancy loss because of virus-induced progesterone insufficiency and to detrimental effects not only on a current pregnancy but on future fertility (*35*). In uteri, we observed uterine vascular, stromal, and epithelial LASV staining, which has also been previously reported in guinea pigs for LASV and filoviral infections (*32*,*36*). We did not investigate placentas, but others have reported high human placental viral LASV titers and demonstrated viral antigen in trophoblasts (*21*,*22*). Our data indicating LASV predilection for the uterus suggest high risk for direct placental infection, with potential for placental compromise and transplacental transmission to the fetus.

Male reproductive tract infections can also be related to infertility and fetal infection. In our study, viral detection in testes was limited to rare interstitial cells and occurred without associated pathology, possibly because LASV does not principally target the testes or possibly because of the restriction of viral replication by testicular cells with innate antiviral properties (*37*). Epididymides showed more consistent pathology and LASV staining, including epididymal epithelial and interstitial mesenchymal cell staining, as well as apparent staining of leukocytes and intraluminal spermatozoa. Together with occasional staining observed in seminal vesicle and prostate, those findings indicate potential for infection of both spermatozoa and seminal fluid. Although the immune-privileged environment of the testis and epididymis is capable of local defense against microbial pathogens, it also provides a microbial escape from immune surveillance and could prevent or delay clearance; potentially, adverse effects on male fertility, as well as sexual transmission, even after long periods postinfection, could be possible (*38*,*39*).

Breastfeeding poses another potential risk for LASV transmission to infants. Shedding in milk and high viral titers with viral immunostaining in mammary glandular tissue has been demonstrated in humans (*21*,*22*). In addition, natural and experimental infections through skin exposure have been reported (*13*–*17*,*40*). We found viral antigen and RNA localized to both mammary glandular epithelium and overlying epidermis, indicating that both milk and skin contact might be possible sources of infant infection during breastfeeding. However, no specific study links breastfeeding to LASV transmission, and our findings only highlight the need for additional interdisciplinary research and surveillance efforts to understand these risks.

In conclusion, our findings in a guinea pig model demonstrate that LASV infects both female and male reproductive tracts as early as 4 dpi, indicating a potential risk for early sexual and vertical transmission, including through breastfeeding, even during the incubation period before clinical signs are apparent. This model further suggests that transmission risk could persist for at least 4 weeks and possibly longer, warranting additional studies of human cases to better inform evidence-based guidance for survivors regarding abstinence or protected-sex practices as part of behavioral interventions to reduce transmission, considerations that are particularly relevant given the current lack of available LASV-specific vaccines or therapeutics. More broadly, this study highlights critical gaps in our understanding of long-term sequelae and tissue reservoirs for LASV and other viral hemorrhagic fevers in survivors, as well as the need for focused investigation into infection during pregnancy and its effects on maternal, placental, and fetal health. Such knowledge is essential for refining survivor counseling, infection prevention strategies, and public health preparedness in LASV-endemic settings.

Acknowledgments

We thank members of the Centers for Disease Control and Prevention (CDC) Comparative Medicine Branch, Office of Laboratory Systems and Response, for assisting with care for the animals and Tatyana Klimova for assistance editing the manuscript.

This work was supported in part by Defense Threat Reduction Agency (DTRA) grant number HDTRA1241740 made to the Emory Institute for Drug Development and CDC (CB11079, Evaluation of the anti-arenavirus activity of EIDD small molecules, both in vitro and in vivo, and investigation of mechanisms of action and resistance profiles); by DTRA contract MCDC2005-005 to EIDD (Identification and Development of Broadly Active Antiviral Countermeasures for Alphavirus, Arenavirus, and Other Biodefense Threats); and CDC Emerging Infectious Disease Research Core Funds.

About the Author

Dr. Seixas is a veterinary pathologist in the Infectious Diseases Pathology Branch, Division of High-Consequence Pathogens and Pathology, National Center for Emerging and Zoonotic Infectious Diseases, at CDC. Her research interests include animal models of human infectious disease caused by high-consequence pathogens.

References:

1. Ahmad M, Ahmed I, Satapathy P, Asumah MN, Padhi BK. Re-emergence of the Lassa virus in Africa: a global health concern. Int J Surg. 2023;109:1044–5. https://doi.org/10.1097/JS9.0000000000000248
2. McCormick JB, King IJ, Webb PA, Johnson KM, O'Sullivan R, Smith ES, et al. A case-control study of the clinical diagnosis and course of Lassa fever. J Infect Dis. 1987;155:445–55. https://doi.org/10.1093/infdis/155.3.445
3. White HA. Lassa fever. A study of 23 hospital cases. Trans R Soc Trop Med Hyg. 1972;66:390–401. https://doi.org/10.1016/0035-9203(72)90269-6
4. Okokhere PO, Ibekwe TS, Akpede GO. Sensorineural hearing loss in Lassa fever: two case reports. J Med Case Rep. 2009;3:36. https://doi.org/10.1186/1752-1947-3-36
5. Mateer EJ, Huang C, Shehu NY, Paessler S. Lassa fever-induced sensorineural hearing loss: a neglected public health and social burden. PLoS Negl Trop Dis. 2018;12:e0006187. https://doi.org/10.1371/journal.pntd.0006187
6. Cummins D, McCormick JB, Bennett D, Samba JA, Farrar B, Machin SJ, et al. Acute sensorineural deafness in Lassa fever. JAMA. 1990;264:2093–6. https://doi.org/10.1097/INF.0000000000000849
7. World Health Organization. Lassa fever [cited 2024 Nov 8]. https://www.who.int/news-room/fact-sheets/detail/lassa-fever
8. Keane E, Gilles HM. Lassa fever in Panguma Hospital, Sierra Leone, 1973–6. Br Med J. 1977;1:1399–402. https://doi.org/10.1136/bmj.1.6073.1399
9. Kayem ND, Benson C, Aye CYL, Barker S, Tome M, Kennedy S, et al. Lassa fever in pregnancy: a systematic review and meta-analysis. Trans R Soc Trop Med Hyg. 2020;114:385–96. https://doi.org/10.1093/trstmh/traa011
10. Okogbenin S, Okoeguale J, Akpede G, Colubri A, Barnes KG, Mehta S, et al. Retrospective cohort study of Lassa fever in pregnancy, southern Nigeria. Emerg Infect Dis. 2019;25:1494–500. https://doi.org/10.3201/eid2508.181299
11. Murphy HL, Ly H. Pathogenicity and virulence mechanisms of Lassa virus and its animal modeling, diagnostic, prophylactic, and therapeutic developments. Virulence. 2021;12:2989–3014. https://doi.org/10.1080/21505594.2021.2000290
12. Thielebein A, Ighodalo Y, Taju A, Olokor T, Omiunu R, Esumeh R, et al. Virus persistence after recovery from acute Lassa fever in Nigeria: a 2-year interim analysis of a prospective longitudinal cohort study. Lancet Microbe. 2022;3:e32–40. https://doi.org/10.1016/S2666-5247(21)00178-6
13. Garnett LE, Strong JE. Lassa fever: with 50 years of study, hundreds of thousands of patients and an extremely high disease burden, what have we learned? Curr Opin Virol. 2019;37:123–31. https://doi.org/10.1016/j.coviro.2019.07.009
14. Lecompte E, Fichet-Calvet E, Daffis S, Koulémou K, Sylla O, Kourouma F, et al. *Mastomys natalensis* and Lassa fever, West Africa. Emerg Infect Dis. 2006;12:1971–4. https://doi.org/10.3201/eid1212.060812
15. Mari Saez A, Cherif Haidara M, Camara A, Kourouma F, Sage M, Magassouba N, et al. Rodent control to fight Lassa fever: evaluation and lessons learned from a 4-year study in Upper Guinea. PLoS Negl Trop Dis. 2018;12:e0006829. https://doi.org/10.1371/journal.pntd.0006829
16. Monath TP, Newhouse VF, Kemp GE, Setzer HW, Cacciapuoti A. Lassa virus isolation from *Mastomys natalensis* rodents during an epidemic in Sierra Leone. Science. 1974;185:263–5. https://doi.org/10.1126/science.185.4147.263
17. Olayemi A, Cadar D, Magassouba N, Obadare A, Kourouma F, Oyeyiola A, et al. New hosts of the Lassa virus. Sci Rep. 2016;6:25280. https://doi.org/10.1038/srep25280
18. Dan-Nwafor CC, Ipadeola O, Smout E, Ilori E, Adeyemo A, Umeokonkwo C, et al. A cluster of nosocomial Lassa fever cases in a tertiary health facility in Nigeria: description and lessons learned, 2018. Int J Infect Dis. 2019;83:88–94. https://doi.org/10.1016/j.ijid.2019.03.030
19. Richmond JK, Baglole DJ, Baglole DJ, Baglole DJ. Lassa fever: epidemiology, clinical features, and social consequences. BMJ. 2003;327:1271–5. https://doi.org/10.1136/bmj.327.7426.1271
20. Salu OB, Amoo OS, Shaibu JO, Abejegah C, Ayodeji O, Musa AZ, et al. Monitoring of Lassa virus infection in suspected and confirmed cases in Ondo State, Nigeria. Pan Afr Med J. 2020;36:253. https://doi.org/10.11604/pamj.2020.36.253.22104
21. Shieh W-J, Demby A, Jones T, Goldsmith CS, Rollin PE, Ksiazek TG, et al. Pathology and pathogenesis of Lassa fever: novel immunohistochemical findings in fatal cases and clinico-pathologic correlation. Clin Infect Dis. 2022;74:1821–30. https://doi.org/10.1093/cid/ciab719
22. Walker DH, McCormick JB, Johnson KM, Webb PA, Komba-Kono G, Elliott LH, et al. Pathologic and virologic study of fatal Lassa fever in man. Am J Pathol. 1982;107:349–56.
23. Morrison JL, Botting KJ, Darby JRT, David AL, Dyson RM, Gatford KL, et al. Guinea pig models for translation of the developmental origins of health and disease hypothesis into the clinic. J Physiol. 2018;596:5535–69. https://doi.org/10.1113/JP274948
24. Wulff H, Johnson KM. Immunoglobulin M and G responses measured by immunofluorescence in patients with Lassa or Marburg virus infections. Bull World Health Organ. 1979;57:631–5.
25. Albariño CG, Bird BH, Chakrabarti AK, Dodd KA, Erickson BR, Nichol ST. Efficient rescue of recombinant Lassa virus reveals the influence of S segment noncoding regions on virus replication and virulence. J Virol. 2011;85:4020–4. https://doi.org/10.1128/JVI.02556-10
26. Welch SR, Scholte FEM, Albariño CG, Kainulainen MH, Coleman-McCray JD, Guerrero LW, et al. The S genome segment is sufficient to maintain pathogenicity in intra-clade Lassa virus reassortants in a guinea pig model. Front Cell Infect Microbiol. 2018;8:240. https://doi.org/10.3389/fcimb.2018.00240
27. Reed LJ, Muench H. A simple method for estimating fifty percent endpoints. Am J Epidemiol. 1938;27:493–7.
28. Gary JM, Welch SR, Ritter JM, Coleman-McCray J, Huynh T, Kainulainen MH, et al. Lassa virus targeting of anterior uvea and endothelium of cornea and conjunctiva in eye of guinea pig model. Emerg Infect Dis. 2019;25:865–74. https://doi.org/10.3201/eid2505.181254
29. Huynh T, Gary JM, Welch SR, Coleman-McCray J, Harmon JR, Kainulainen MH, et al. Lassa virus antigen distribution and inflammation in the ear of infected strain 13/N

guinea pigs. Antiviral Res. 2020;183:104928. https://doi.org/10.1016/j.antiviral.2020.104928
30. Welch SR, Genzer SC, Coleman-McCray JD, Harmon JR, Scholte FEM, Montgomery JM, et al. Viral RNA and infectious virus in mucosal specimens from guinea pigs modelling early phases of lethal and non-lethal Lassa fever. Emerg Microbes Infect. 2022;11:1390–3. https://doi.org/10.1080/22221751.2022.2071637
31. Kainulainen MH, Spengler JR, Welch SR, Coleman-McCray JD, Harmon JR, Scholte FEM, et al. Protection from lethal Lassa disease can be achieved both before and after virus exposure by administration of single-cycle replicating Lassa virus replicon particles. J Infect Dis. 2019;220:1281–9. https://doi.org/10.1093/infdis/jiz284
32. Bell TM, Shaia CI, Bearss JJ, Mattix ME, Koistinen KA, Honnold SP, et al. Temporal progression of lesions in guinea pigs infected with Lassa virus. Vet Pathol. 2017;54:549–62. https://doi.org/10.1177/0300985816677153
33. Cornish EF, Filipovic I, Åsenius F, Williams DJ, McDonnell T. Innate immune responses to acute viral infection during pregnancy. Front Immunol. 2020;11:572567. https://doi.org/10.3389/fimmu.2020.572567
34. Davidson S, Coles M, Thomas T, Kollias G, Ludewig B, Turley S, et al. Fibroblasts as immune regulators in infection, inflammation and cancer. Nat Rev Immunol. 2021;21:704–17. https://doi.org/10.1038/s41577-021-00540-z
35. Tomac J, Mazor M, Lisnić B, Golemac M, Kveštak D, Bralić M, et al. Viral infection of the ovaries compromises pregnancy and reveals innate immune mechanisms protecting fertility. Immunity. 2021;54:1478–1493.e6. https://doi.org/10.1016/j.immuni.2021.04.020
36. Cooper TK, Huzella L, Johnson JC, Rojas O, Yellayi S, Sun MG, et al. Histology, immunohistochemistry, and in situ hybridization reveal overlooked Ebola virus target tissues in the Ebola virus disease guinea pig model. Sci Rep. 2018;8:1250. https://doi.org/10.1038/s41598-018-19638-x
37. Zhao S, Zhu W, Xue S, Han D. Testicular defense systems: immune privilege and innate immunity. Cell Mol Immunol. 2014;11:428–37. https://doi.org/10.1038/cmi.2014.38
38. Zhao H, Yu C, He C, Mei C, Liao A, Huang D. The immune characteristics of the epididymis and the immune pathway of the epididymitis caused by different pathogens. Front Immunol. 2020;11:2115. https://doi.org/10.3389/fimmu.2020.02115
39. Wang F, Zhang J, Wang Y, Chen Y, Han D. Viral tropism for the testis and sexual transmission. Front Immunol. 2022;13:1040172. https://doi.org/10.3389/fimmu.2022.1040172
40. Port JR, Wozniak DM, Oestereich L, Pallasch E, Becker-Ziaja B, Müller J, et al. Severe human Lassa fever is characterized by nonspecific t-cell activation and lymphocyte homing to inflamed tissues. J Virol. 2020;94:e01367-20. https://doi.org/10.1128/JVI.01367-20

Address for correspondence: J.M. Ritter, Centers for Disease Control and Prevention, 1600 Clifton Rd NE, Mailstop H18-SB, Atlanta, GA 30329-4018, USA; email: vtr0@cdc.gov

etymologia revisited

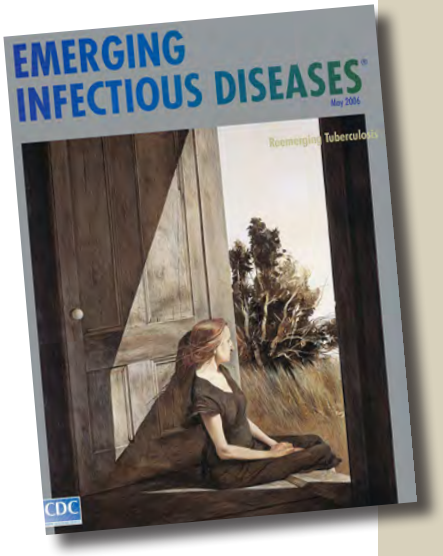

Originally published in May 2006

Tuberculosis

[too-ber′′ku-lo′sis]

Any of the infectious diseases of humans or other animals caused by bacteria of the genus *Mycobacterium*. From the Latin tuberculum, "small swelling," the diminutive form of tuber, "lump." Tuberculosis has existed in humans since antiquity; it is believed to have originated with the first domestication of cattle. Evidence of tuberculosis has been shown in human skeletal remains and mummies from as early as 4000 BC. *Mycobacterium bovis* bacillus Calmette-Guérin has been successfully used to immunize humans since 1921, and treatment (rather than prevention) of tuberculosis has been possible since the introduction of streptomycin in 1946. Hopes of completely eliminating the disease, however, have been diminished since the rise of drug-resistant *M. tuberculosis* strains in the 1980s.

Reference

1. Dorland's illustrated medical dictionary. 30th ed. Philadelphia: Saunders; 2003;
2. Merriam-Webster's collegiate dictionary. 11th ed. Springfield (MA): Merriam-Webster Incorporated; 2003.
3. http://www.wikipedia.org

https://wwwnc.cdc.gov/eid/article/12/5/et-1205_article

Novel Highly Pathogenic Avian Influenza A(H5N1) Virus, Argentina, 2025

Ralph E.T. Vanstreels, Martha I. Nelson, María C. Artuso, Vanina D. Marchione, Luana E. Piccini, Estefania Benedetti, Alvin Crespo-Bellido, Agostina Pierdomenico, Thorsten Wolff, Marcela M. Uhart, Agustina Rimondi

Genomic sequencing of reemerging highly pathogenic avian influenza A(H5N1) virus detected in Argentina in February 2025 revealed novel triple-reassortant viruses containing gene segments from Eurasian H5N1 and low pathogenicity viruses from South and North American lineages. Our findings highlight continued evolution and diversification of clade 2.3.4.4b H5N1 in the Americas.

Highly pathogenic avian influenza (HPAI) viruses were introduced to South America in 2022 by migratory birds from North America. The viruses belonged to the 2.3.4.4b clade of HPAI A(H5N1) virus that became widespread in Europe in 2020 and spread to North America in 2021. The trajectory of H5N1 in South America has differed from H5N1 in North America in several critical ways. First, nearly all South America outbreaks stem from a single introduction of H5N1 viruses from North America (*1*,*2*), whereas the North America epizootic was reseeded by multiple independent introductions from Europe and Asia (A1–A6) (*3*,*4*). Second, South America H5N1 outbreaks were driven by a single genotype (B3.2) that was introduced from North America and remained genetically stable during its spread across South America. In contrast, H5N1 viruses in North America underwent frequent reassortment with low pathogenicity avian influenza (LPAI) viruses, prompting new genotype nomenclature (using B, C, D) (*3*). Third, South America's H5N1 epizootic is unique in establishing mammal-to-mammal transmission in marine mammals, enabled by the H5N1 (B3.2) virus acquiring mammalian-adaptive polymerase basic (PB) 2 mutations (Q591K and D701N) (*1*,*2*). That pattern has not occurred in North America, where H5N1 spillover into terrestrial and marine mammals was transient, except in United States dairy cattle (*3*).

Beyond the ecologic devastation among coastal wildlife, in 2023, H5N1 (B3.2) virus spread widely in birds across mainland South America, leading to poultry and wild bird outbreaks (*5*–*8*). Although in 2024 HPAI outbreaks occurred in Brazil and Peru (World Organisation for Animal Health, https://wahis.woah.org), there were no detections in Argentina during March 2024–January 2025.

The Study

On February 11, 2025, Servicio Nacional de Sanidad y Calidad Agroalimentaria (SENASA; Buenos Aires, Argentina), Argentina's national organization for agricultural health and safety, was notified of an outbreak in a mixed backyard flock (chickens, ducks, and turkeys) in Chaco Province, northern Argentina. The flock experienced high mortality (33/81 chickens, 37/99 ducks) in just 1 week. When we inspected the living flock, two thirds of the remaining 48 chickens had diarrhea and 1 of the remaining 62 ducks was lethargic; 2 turkeys were asymptomatic. The household was located within a remnant fragment of the Dry Chaco biome, a hot and semi-arid tropical dry forest, surrounded by agriculture cropland. The affected flock had free access to a small pond frequently visited by wild waterfowl (Appendix 1, http://wwwnc.

Author affiliations: University of California Davis School of Veterinary Medicine, Davis, California, USA (R.E.T. Vanstreels, M.M. Uhart); National Institutes of Health, Bethesda, Maryland, USA (M.I. Nelson, A. Crespo-Bellido); Servicio Nacional de Sanidad y Calidad Agroalimentaria, Martínez, Buenos Aires, Argentina (M.C. Artuso, V.D. Marchione, L.E. Piccini); Instituto Nacional de Enfermedades Infecciosas Dr. Carlos G. Malbrán, Buenos Aires (E. Benedetti); Servicio Nacional de Sanidad y Calidad Agroalimentaria, Buenos Aires (A. Pierdomenico); Robert Koch-Institut, Berlin, Germany (T. Wolff, A. Rimondi)

DOI: https://doi.org/10.3201/eid3112.250783

cdc.gov/EID/article/31/12/25-0783-App1.pdf). We depopulated and disinfected the area. We inspected backyard poultry within the 3 km perifocal zone (1 household) and the 3–10 km surveillance zone (7 households) and detected no illness or death. We did not find any affected wildlife on site.

We collected oropharyngeal and cloacal swab samples from 8 birds to test for influenza A virus. We tested and subtyped the samples by real-time PCR at SENASA. We performed next-generation sequencing on positive samples as previously described (*6*) (Appendix 1). We deposited full and partial genome sequences in the GISAID database (https://gisaid.org; accession nos. EPI_ISL_19752381 and EPI_ISL_19823059–68).

We inferred global avian influenza virus (AIV) phylogenies (including both HPAI and LPAI virus sequences) independently for each of the 8 gene segments to determine the genetic composition of H5N1 viruses from this outbreak (H5N1-Arg_Feb2025 viruses). The phylogenies indicated the H5N1-Arg_Feb2025 viruses are novel 4:3:1 triple reassortants (Figure 1; Appendix 1). Four gene segments (PB2, PB1, polymerase [PA], and nonstructural [NS]) belong to the South American LPAI lineage (Figure 1) that has circulated regionally in wild birds for decades (*9*–*12*). Three gene segments (hemagglutinin [HA], neuraminidase [NA], and matrix protein [MP]) clustered with H5N1 viruses of the B3.2 genotype and belong to the original Eurasian H5N1 lineage introduced to North America (Figure 2). We identified novel amino acid changes in the HA and NA segments of H5N1-Arg_Feb2025 viruses (Table) (*13*); the functional relevance of those changes is unknown but might merit further investigation if consistently detected in future outbreaks. One segment, nucleoprotein (NP), did not cluster with any previously known South American viruses and instead grouped with North American LPAI viruses (Figure 3). Because of limited surveillance in South America, where ≈90% of full-genome

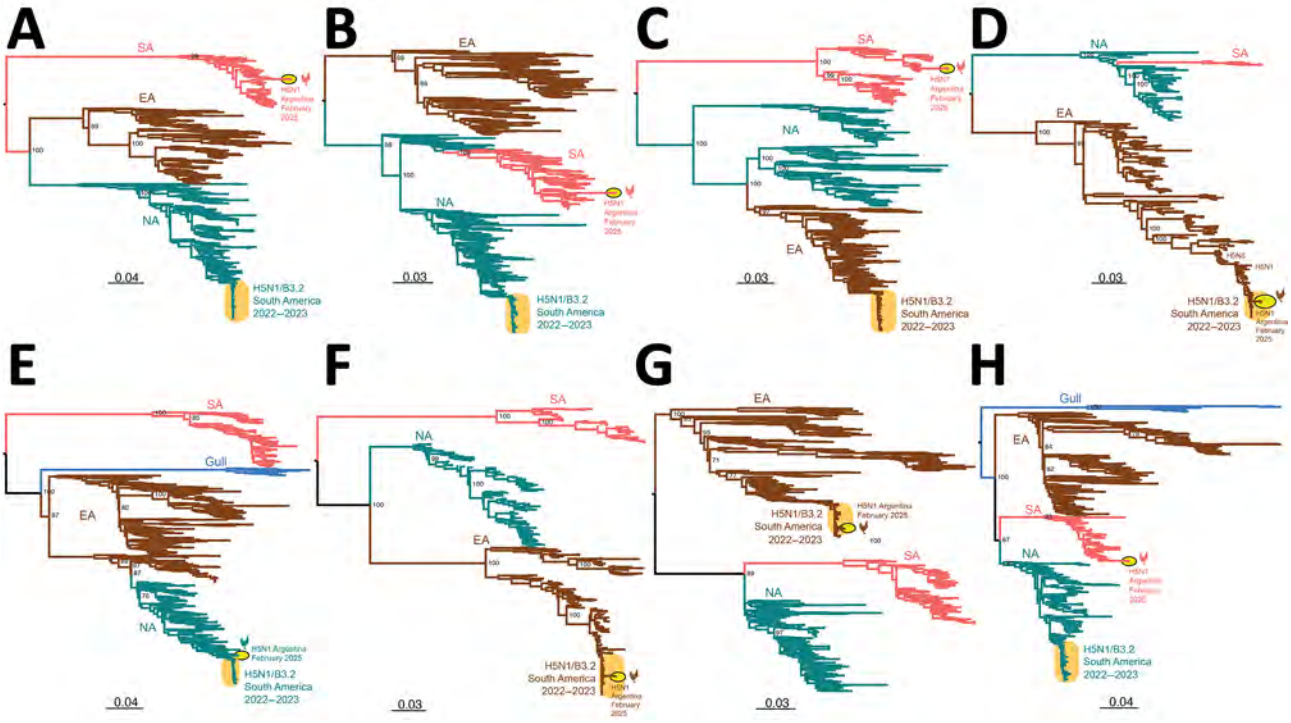

Figure 1. Maximum-likelihood trees inferred for the 8 genome segments sequenced in this study of novel triple reassortant highly pathogenic avian influenza A(H5N1) virus, Argentina, 2025. Phylogenetic trees were inferred by using IAVs collected globally in avian hosts. A) Gene segment PB2. B) Gene segment PB1. C) Gene segment PA. D) Gene segment H5. E) Gene segment NP. F) Gene segment N1. G) Gene segment MP. H) Gene segment NS; only A allele is shown. The number of sequences used to construct each tree was 676 for PB2, 667 for PB1, 686 for PA, 271 for H5, 682 for NP, 443 for N1, 639 for MP, and 506 for NS (Appendix 2, http://wwwnc.cdc.gov/EID/article/31/12/25-0783-App2.xlsx). Trees are midpoint rooted for clarity. Key node bootstrap values are shown. Teal shading represents NA lineage, brown shading represents EA lineage, pink shading represents SA lineage, and blue shading represents gull lineage. Orange oval represents previously reported SA H5N1 clade B3.2 genotype virus. Yellow oval with black outline and chicken silhouette represents the novel H5N1 virus found in Argentina. Branch lengths are drawn to scale. Scale bars represent nucleotide substitutions per site. EA, Eurasian; MP, matrix protein; NA, North American; NP, nucleoprotein; NS, nonstructural protein; PA, polymerase; PB, polymerase basic; SA, South American.

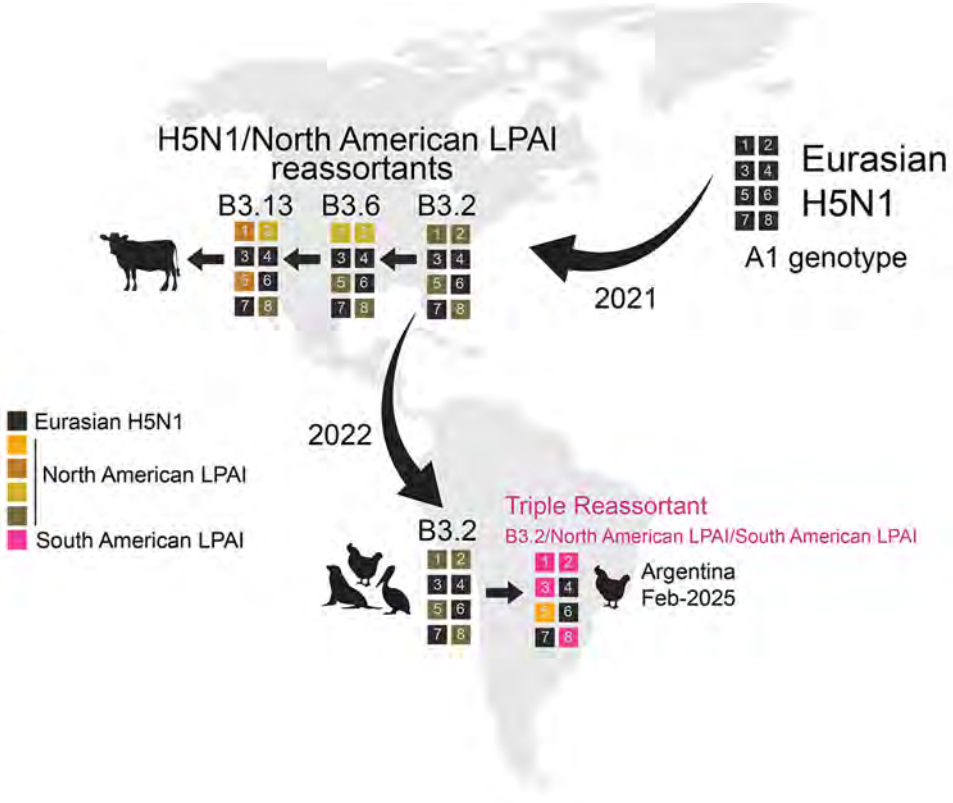

Figure 2. Key reassortment and migration events leading to the novel triple reassortant influenza A(H5N1) viruses in February 2025, Argentina. Each box represents 1 of the 8 segments of the influenza A virus genome, numbered in order of longest to shortest length: 1, polymerase basic protein 2; 2, polymerase basic protein 1; 3, polymerase acidic protein; 4, hemaggultinin; 5, nucleoprotein; 6, neuraminidase; 7, matrix protein; and 8, nonstructural protein. Curved black arrows indicate the direction of major geographic migration events. Straight black arrows indicate sequential reassortment events of interest. LPAI, low pathogenicity avian influenza.

sequences are from Argentina and Chile, it was difficult to determine how the North America–derived NP segment became part of the triple reassortant H5N1 viruses we identified.

Conclusions

We have documented a reassortment event between HPAI H5N1 and endemic South America LPAI viruses. South American PB2 and PA segments are divergent from global AIV diversity (*9*) (Figure 1), indicating reassortment has expanded H5N1 polymerase diversity. Although the H5N1-Arg_Feb2025 viruses have exchanged 5 gene segments, they retained the original Eurasian MP segment (Figure 2), which remains conserved in most reassortant H5N1 viruses in North America. That segment conservation suggests the Eurasian MP segment might confer a selective advantage in HPAI H5 viruses. To date, we found no evidence of those novel 4:3:1 triple reassortant viruses in other South America countries; however, if future detections confirm wider spread, designation of a new H5N1 genotype would be warranted. Of consequence, genotyping tools such as the US Department of Agriculture's GenoFlu should be expanded to include South American lineage genes for systematic classification of new virus genotypes.

Table. Amino acid differences in hemagglutinin and neuraminidase of novel triple reassortant influenza A(H5N1) virus from Argentina, 2025, compared with previously reported South American highly pathogenic avian influenza A(H5N1) viruses

Protein (subunit)	Position*	Amino acid in previous viruses	Mutated amino acid in reassortant virus	Protein domain
Hemagglutinin (HA1)	64	E	D	Vestigial esterase domain
	172	L	Y	Receptor-binding domain
	181	S	P	Receptor-binding domain
	208	T	K	Receptor-binding domain
	235	P	S	Receptor-binding domain
Hemagglutinin (HA2)	493	E	K	Helical globule
	510	V	I	Transmembrane domain
	532	M	I	Cytoplasmic tail
Neuraminidase	35	S	V	Stalk domain
	49	C	R	Stalk domain
	68	N	Y	Head domain
	454	G	S	Stalk domain

*HA positions refer to H5 numbering.

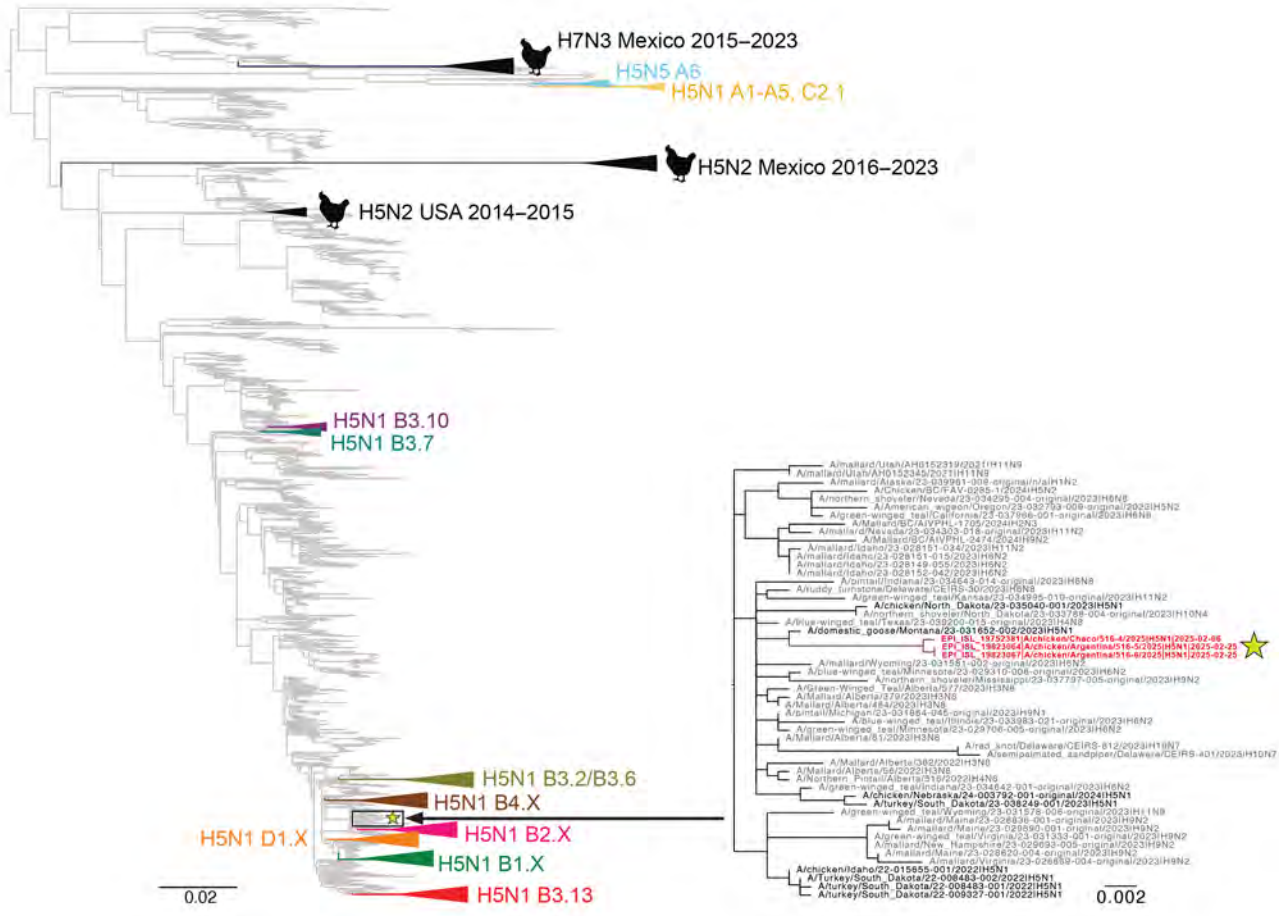

Figure 3. Phylogenetic tree showing how North American low pathogenicity avian influenza (LPAI) lineage contributed nucleoprotein (NP) genes by reassortment to novel influenza A(H5N1) viruses from Argentina, 2025. We inferred the phylogenetic tree by using the maximum-likelihood method for 11,820 North American LPAI and highly pathogenic avian influenza (HPAI) NP sequences collected during 2015–2025. Gray indicates LPAI viruses. HPAI H5N1 clades are collapsed and shaded in different colors and labeled according to corresponding H5 clade 2.3.4.4b genotypes. Black indicates prior H5N2 and H7N3 outbreaks in poultry. The 3 H5N1 viruses collected from poultry in Argentina in February 2025 are indicated in red and with a yellow star. A more detailed subsection of the tree containing those 3 viruses is shown, with tip labels. Branch lengths are drawn to scale. Scale bar represents nucleotide substitutions per site.

Reassortment is a key mechanism in the evolution and host adaptation of AIV, often enabling their emergence in new animal communities and contributing to the development of strains with panzootic or pandemic potential (*14*,*15*). The genomic constellation of the H5N1-Arg_Feb2025 viruses parallels patterns found in North America, where clade 2.3.4.4b H5N1 viruses have also incorporated primarily internal LPAI genes. H5N1-Arg_Feb2025 viruses replaced the PB2, PB1, NP, and NS segments from the parental B3.2 genotype, a reassortment pattern observed in North American genotypes B3.6 and B3.13 (Figure 2), both derived from B3.2. However, the H5N1-Arg_Feb2025 viruses also replaced the Eurasian PA segment with a segment from South American LPAI viruses. Despite substantial genomic changes, the novel reassortant viruses from Argentina caused illness and death rates comparable to those previously observed for the B3.2 genotype. The primary clinical manifestation in this outbreak was diarrhea, affecting nearly two thirds of chickens. During H5N1 poultry outbreaks in Argentina in 2023, diarrhea was less common (reported in 29.7% of outbreaks), whereas high death rates (81.2%), lethargy (65.4%), cyanotic comb (57.4%), and neurologic signs (30.7%) were more frequent (n = 101 outbreaks) (SENASA, unpub. data). The predominance of gastrointestinal signs suggests possible shifts in tissue tropism or virulence. Also, the detection of a North American NP segment not previously identified in LPAI viruses from Argentina or elsewhere in South America highlights the need to strengthen regional AIV surveillance, even in

the absence of active HPAI circulation. There is a lack of information on avian species and flyways involved in introductions of North American gene segments to South American LPAI viruses. Moreover, investigating the functional role of the North America–derived NP gene within the South American internal genes could clarify its potential contribution to the distinct gastrointestinal phenotype observed in this outbreak.

Further research on the diversity of LPAI viruses circulating in Neotropical wildlife will be essential to understand potential interactions between H5N1 and South American lineage strains and to assess the long-term consequences of the introduction of HPAI viruses into the region. Our findings underscore the critical importance of sustained influenza surveillance coupled with whole-genome sequencing to track the evolution of HPAI H5N1 and support efforts to control and mitigate its effect on domestic animals, wildlife, and human health.

Acknowledgments

We thank the specific agreement between the Administración Nacional de Laboratorios e Institutos de Salud and the Servicio Nacional de Sanidad y Calidad Agroalimentaria in Argentina, which enabled the genome sequencing of the influenza virus strains detected.

This work was partially supported by the Department of Health and Human Services, Centers of Excellence for Influenza Research and Response (contract no. 75N93021C00014), and by the Intramural Research Program of the National Institutes of Health. Additional support for M.M.U. was provided by the US National Science Foundation Center for Pandemic Insights (award no. 2412522).

The contributions of the National Institutes of Health authors are considered Works of the United States Government.

About the Author

Dr. Vanstreels is a veterinarian and an associate researcher with the Karen C. Drayer Wildlife Health Center at the University of California, Davis. His research interests include South American and Antarctic wildlife health, with a special interest in the ecology and effects of highly pathogenic avian influenza H5N1 on wild bird and marine mammal populations.

References

1. Uhart MM, Vanstreels RET, Nelson MI, Olivera V, Campagna J, Zavattieri V, et al. Epidemiological data of an influenza A/H5N1 outbreak in elephant seals in Argentina indicates mammal-to-mammal transmission. Nat Commun. 2024;15:9516.
2. Pardo-Roa C, Nelson MI, Ariyama N, Aguayo C, Almonacid LI, Gonzalez-Reiche AS, et al. Cross-species and mammal-to-mammal transmission of clade 2.3.4.4b highly pathogenic avian influenza A/H5N1 with PB2 adaptations. Nat Commun. 2025;16:2232.
3. Tawidian P, Torchetti MK, Killian ML, Lantz K, Dilione KE, Ringenberg JM, et al. Genotypic clustering of H5N1 avian influenza viruses in North America evaluated by ordination analysis. Viruses. 2024;16:1818.
4. Nguyen TQ, Hutter CR, Markin A, Thomas M, Lantz K, Killian ML, et al. Emergence and interstate spread of highly pathogenic avian influenza A(H5N1) in dairy cattle in the United States. Science. 2025;388:eadq0900.
5. Ariyama N, Pardo-Roa C, Muñoz G, Aguayo C, Ávila C, Mathieu C, et al. Highly pathogenic avian influenza A(H5N1) clade 2.3.4.4b virus in wild birds, Chile. Emerg Infect Dis. 2023;29:1842–5.
6. Artuso MC, Marchione VD, Benedetti E, Bonastre P, Alvarez AM, Piccini L, et al. Detection and characterization of highly pathogenic avian influenza A (H5N1) clade 2.3.4.4b virus circulating in Argentina in 2023. Rev Argent Microbiol. 2024:S0325-7541(24)00115-9.
7. Marandino A, Tomás G, Panzera Y, Leizagoyen C, Pérez R, Bassetti L, et al. Spreading of the high-pathogenicity avian influenza (H5N1) virus of clade 2.3.4.4b into Uruguay. Viruses. 2023;15:1906.
8. Sevilla N, Lizarraga W, Jimenez-Vasquez V, Hurtado V, Molina IS, Huarca L, et al. Highly pathogenic avian influenza A (H5N1) virus outbreak in Peru in 2022–2023. Infect Med (Beijing). 2024;3:100108.
9. Rimondi A, Gonzalez-Reiche AS, Olivera VS, Decarre J, Castresana GJ, Romano M, et al. Evidence of a fixed internal gene constellation in influenza A viruses isolated from wild birds in Argentina (2006–2016). Emerg Microbes Infect. 2018;7:194.
10. Jiménez-Bluhm P, Karlsson EA, Freiden P, Sharp B, Di Pillo F, Osorio JE, et al. Wild birds in Chile harbor diverse avian influenza A viruses. Emerg Microbes Infect. 2018;7:44.
11. Nelson MI, Pollett S, Ghersi B, Silva M, Simons MP, Icochea E, et al. The genetic diversity of influenza A viruses in wild birds in Peru. PLOS ONE. 2016;11(1):e0146059.
12. Araujo ADC, Cho AY, Silva LMN, Port D, Demoliner M, Gularte JS, et al. Whole genome sequencing of low pathogenicity avian influenza virus (H6N2) detected from a Brazilian teal (Amazonetta brasiliensis) in Brazil, 2023. Microbiol Resour Announc. 2024;13(7):e00158–24.
13. Carter T, Iqbal M. The influenza A virus replication cycle: a comprehensive review. Viruses. 2024;16:316.
14. Dugan VG, Chen R, Spiro DJ, Sengamalay N, Zaborsky J, Ghedin E, et al. The evolutionary genetics and emergence of avian influenza viruses in wild birds. PLoS Pathog. 2008;4(5):e1000076.
15. Youk S, Torchetti MK, Lantz K, Lenoch JB, Killian ML, Leyson C, et al. H5N1 highly pathogenic avian influenza clade 2.3.4.4b in wild and domestic birds: introductions into the United States and reassortments, December 2021–April 2022. Virology. 2023;587:109860.

Address for correspondence: Agustina Rimondi, Robert Koch-Institut, Seestr. 10, 13353, Berlin, Germany; email: rimondia@rki.de

Case of Congenital Tularemia with Neuroinvasive Disease, Utah, USA

Brent D. Nelson, Amara Finch, Krow Ampofo, Elizabeth L. Ryals, Andrew T. Pavia, Anne J. Blaschke, Jody L. Lin, Benjamin Kalm, Angie White, Kacy D. Nowak, Julian A. Villalba, Julu Bhatnagar, Bert Lopansri, Elizabeth D. Knackstedt

We diagnosed neuroinvasive tularemia in a neonate in Utah who had culture-negative pleocytosis in cerebrospinal fluid, rim-enhancing lesions on brain magnetic resonance imaging, and blood microbial cell-free DNA *Francisella tularensis* detection. Maternal history, serologic testing, and *Francisella* sp. identified in the fallopian tube by immunohistochemistry and 16S rRNA gene PCR strongly support congenital infection.

Tularemia, caused by *Francisella tularensis*, is a bacterial illness endemic to the Northern Hemisphere (*1*). Tularemia classically presents as ulceroglandular, glandular, oculoglandular, oropharyngeal, pneumonic, or typhoidal disease; other manifestations have been described (*1*–*4*). Neuroinvasive disease, although rare and difficult to diagnose, has also been reported (*5*–*7*).

Rarely, vertically transmitted tularemia in animals with histopathological and immunohistochemical (IHC) confirmation of *F. tularensis* in aborted fetuses (*8*,*9*) has been reported. One presumed case of human congenital infection has been reported. In 1947, Lide (*10*) reported delivery of a stillborn infant after tularemia was diagnosed in the mother. Gram-negative bacilli were observed in placental and fetal tissues without confirmatory testing (*10*).

We recently diagnosed congenital, neuroinvasive tularemia in a neonate after a positive blood test for microbial cell-free DNA (cfDNA) (Karius, https://kariusdx.com). IHC staining and 16S rRNA gene PCR identified *F. tularensis* in the mother's fallopian tube.

University of Utah School of Medicine, Salt Lake City, Utah, USA (B.D. Nelson, A. Finch, K. Ampofo, A.T. Pavia, A.J. Blaschke, J.L. Lin, B. Kalm, B. Lopansri, E.D. Knackstedt); Primary Children's Hospital, Salt Lake City (E.L. Ryals); Bear River Health Department, Logan, Utah, USA (A. White); Utah Department of Health and Human Services, Salt Lake City (K.D. Nowak); Centers for Disease Control and Prevention, Atlanta, Georgia, USA (J.A. Villalba, J. Bhatnagar); Intermountain Medical Center, Murray, Utah, USA (B. Lopansri)

DOI: https://doi.org/10.3201/eid3112.250703

The Study

A 2-week-old infant was admitted to a hospital in Salt Lake City, Utah, USA, with lethargy, poor feeding, and pallor. The mother had ulcerative colitis in remission on infliximab therapy. One week after her infliximab dose at 34 weeks' gestation, she experienced fever, sore throat, conjunctivitis, and cervical lymphadenopathy. After 6 days, a computed tomography scan of the neck revealed cervical lymphadenitis (Figure 1). An otolaryngologist evaluated and treated her with ceftriaxone and dexamethasone. She was evaluated by obstetrics 4 days later for decreased fetal movement. A biophysical profile score of 8 was reassuring. She underwent incision and drainage of her cervical lymph node. During the procedure, purulent fluid was encountered and sent for routine and acid-fast bacilli culture; no growth was noted at 4 days on routine culture or 42 days on acid-fast bacilli culture. She completed 10 days of amoxicillin/clavulanate.

The infant was born at 37 weeks' gestation by cesarean section because of gestational hypertension and ongoing maternal illness. At delivery, the infant required 15 minutes of respiratory support but weaned to room air and was discharged home on day of life (DOL) 2. On DOL 16, he was seen in the emergency department for lethargy and decreased oral intake. He was tachycardic but afebrile. Complete blood count, complete metabolic panel, C-reactive protein, procalcitonin, and blood, urine, and cerebral spinal fluid (CSF) cultures were obtained; results were notable for marked peripheral leukocytosis, elevated C-reactive protein, hepatitis, and lymphocytic CSF pleocytosis (Table 1). The infant received ampicillin and ceftazidime.

Increasing lethargy and new oxygen requirement prompted transfer to the pediatric intensive care unit. At arrival, he was febrile to 39.6°C. Results of blood PCR testing for adenovirus, parvovirus B19, and cytomegalovirus were negative. A multiplex PCR panel (BioFire, https://www.biofiredx.com) detected

human rhinovirus/enterovirus on a nasopharyngeal swab specimen. Results of multiplex PCR testing of the CSF (BioFire Filmarray Meningitis/Encephalitis Panel) were negative. During hospitalization, the infant developed thrombocytopenia to 115 K/μL. Bacterial blood cultures remained negative, and laboratory abnormalities improved (Table 1). He was observed for 24 hours off antibiotics, then discharged home.

He returned to the emergency department 9 days later, DOL 30. Vital signs were unremarkable, although he appeared unwell. He was transferred to our institution for further evaluation and infectious disease consultation.

Repeat lumbar puncture showed persistent lymphocytic CSF pleocytosis, and he underwent brain magnetic resonance imaging (MRI) with contrast. The MRI revealed 3 lesions, 2–7 mm in diameter, located in the left subthalamic nucleus, right thalamus, and left parietal cortex (Figure 1). Results of PCR testing of the CSF for toxoplasmosis were negative. Because of persistent illness and previously nondiagnostic evaluation, blood cfDNA testing (Karius) was performed, and results were positive for 804 molecules of microbial cfDNA/μL of *F. tularensis* DNA most aligned with subspecies *holartica* (Table 2). Treatment with intravenous (IV) ciprofloxacin and gentamicin was initiated.

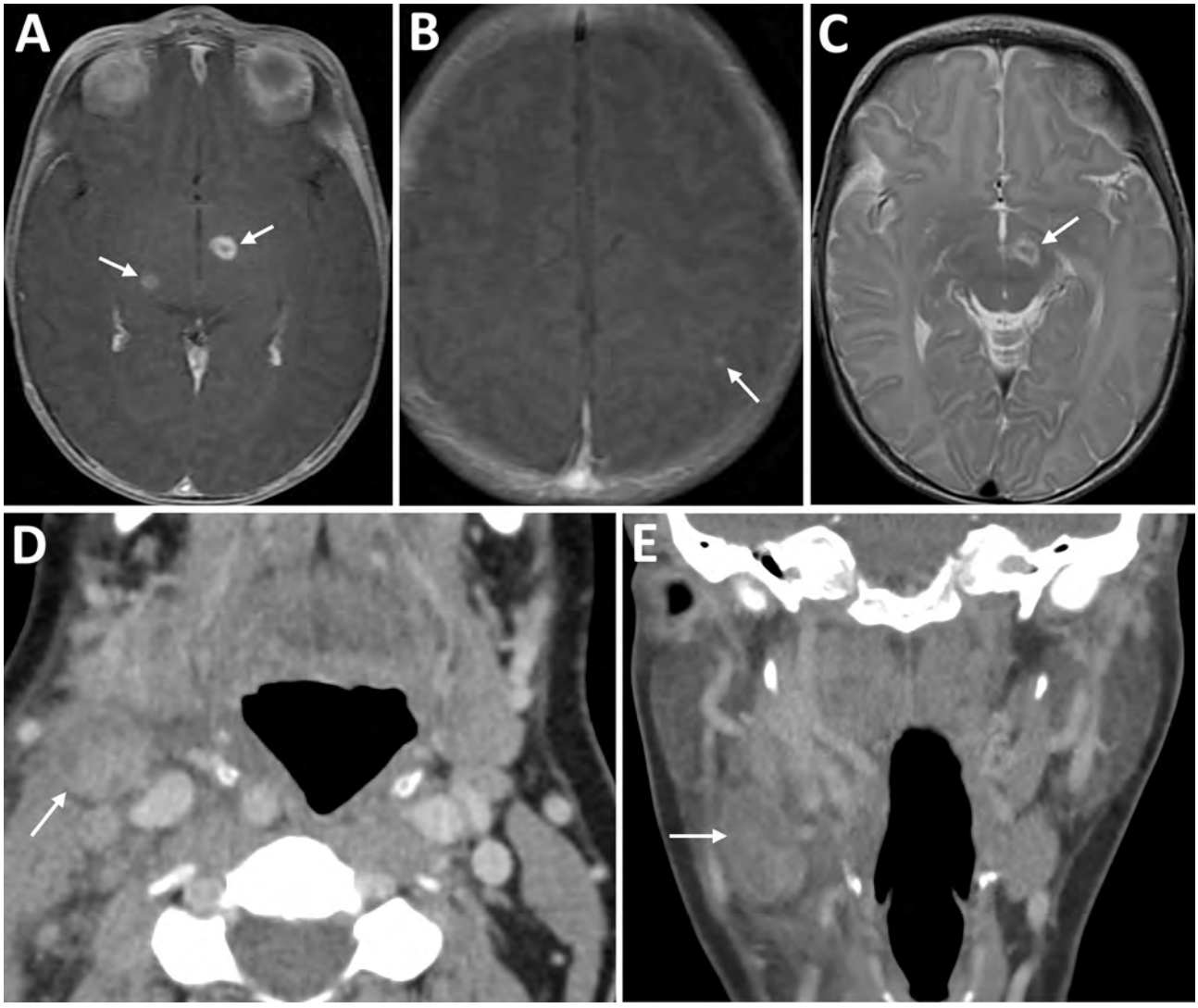

Figure 1. Imaging from infant and mother in case of congenital tularemia with neuroinvasive disease, Utah, USA. A, B) Axial T1 post-contrast images showing the infant's initial magnetic resonance imaging findings of rim enhancing lesions near the left subthalamic nucleus and right inferior thalamus (arrows, panel A), as well as a punctate enhancing lesion in the left parietal lobe (arrow, panel B). C) Axial T2 image demonstrating T2 hyperintense edema along the margins of the largest lesion near the left subthalamic nucleus (arrow). D, E) Axial (D) and coronal (E) images from the mother's computed tomography scan with intravenous contrast showing an enlarged, heterogeneous right cervical chain lymph node with inflammatory stranding in the adjacent soft tissues (arrows).

Table 1. Pertinent results of laboratory tests taken during hospitalization of infant in case of congenital tularemia with neuroinvasive disease, Utah, USA*

Test	Hospitalization 1		Hospitalization 2
	Admission: DOL 16	Discharge: DOL 21	Admission: DOL 30
Complete blood count			
Hemoglobin, K/μL	13.8	12.6	13.1
Hematocrit, g/dL	39.8	**36.7**	39.6
Leukocyte, K/μL	**56.8**	17.6	**25.2**
Neutrophils, K/μL	**29.0**	3.3	**4.8**
Lymphocytes, K/μL	**19.9**	11.3	**15.4**
Monocytes, K/μL	**4.5**	**3.0**	**3.5**
Platelets, K/μL	206	**149**	**584**
Chemistry			
Sodium, mmol/L	**129**	144	137
Total bilirubin, mg/dL	1.3	1.1	0.9
ALP, unit/L	205	139	335
AST, unit/L	**898**	**144**	57
ALT, unit/L	**316**	**96**	26
Lactic acid, mmol/L	**2.4**		1.8
Inflammatory/infectious markers			
C-reactive protein, mg/dL	**17.1**	**6.8**	**4.7**
Procalcitonin, ng/mL	**3.02**		**0.15**
Cerebrospinal fluid			
Glucose, mg/dL	44	NA	**36**
Total protein, mg/dL	**114**	NA	81
Leukocytes, cells/μL	**48**	NA	**31**
Neutrophils, %	3	NA	4
Lymphocytes, %	81	NA	71
Monocytes, %	16	NA	25
Erythrocytes, cells/μL	<1	NA	**7**
Gram stain	Negative	NA	Negative
BioFire Respiratory 2.1 panel	**Positive for rhinovirus**		**Positive for rhinovirus**
Cultures			
Blood	No growth × 5 d	NA	No growth × 5 d
Urine	1,000 colony-forming units of *Staphylococcus lugdunensis*	NA	No growth × 2 d
CSF	No growth × 4 d	NA	No growth × 4 d

*Abnormal values in bold. ALP, alkaline phosphatase; ALT, alanine transaminase; AST, aspartate aminotransferase; DOL, day of life; NA, not applicable.

The family lives on a multiple-acre property supplied by well water with nearby irrigation canals and a beaver population. Pets consisted of 1 rabbit, 2 hunting dogs, and a cat. The family had bred rabbits until ≈2 years before. The cat hunted mice and voles and was frequently in close physical contact with the mother. The cat had been "vomiting up worms" and, 2 days before the infant's second hospitalization, was run over by a tractor and died.

On day 40 postpartum, the mother was seen by an infectious disease physician because of the infant's tularemia diagnosis. She had continued to experience night sweats, fatigue, and anorexia, and new, diffuse arthralgias had developed, most prominently in her hands. Throat culture results were negative, but tests for *F. tularensis* IgG and IgM were positive (Table 2). She received 14 days of ciprofloxacin and subsequently returned to her baseline state of health.

The county health department investigated the home. The well water had increased coliform counts, but well water PCR test results for *F. tularensis* were negative. All other family members tested negative for *F. tularensis* antibodies. Their rabbit had been euthanized and was unavailable for further testing, as was the cat.

The infant received 1 week of IV gentamicin and 4 weeks of IV ciprofloxacin. Near the end of therapy, repeat microbial cfDNA testing (Karius) demonstrated a marked decline in *F. tularensis* microbial cfDNA levels (Table 2). Repeat brain MRI with contrast showed near complete resolution of the previous lesions with only "trace residual focus of enhancement in the left subthalamic region." He remains well, last evaluated at 15 months of age.

The mother underwent elective tubal ligation during her cesarean section. Extensive left-sided subacute suppurative salpingitis with serositis incidentally was noted. Once the diagnosis of congenital tularemia was suspected, remaining formalin-fixed paraffin-embedded tissue were sent to the Centers for Disease Control and Prevention, where results of an IHC assay for *F. tularensis* were positive for bacterial antigens with coccobacilli in the left fallopian tube, along with necroinflammatory debris (Figure 2) (*11*). In addition, a gram-negative bacteria 16S rRNA gene

Table 2. Infant and maternal testing for *Francisella tularensis* in study of congenital tularemia with neuroinvasive disease, Utah, USA*

Test, specimen source	Infant	Mother
Microbial cell free DNA metagenomic sequencing (Karius), plasma†	4 weeks: 804 MPM *F. tularensis* subsp. *holartica* cfDNA (Appendix, https://wwwnc.cdc.gov/EID/article/31/12/25-0703-App1.pdf) 7 weeks: 11 MPM *F. tularensis subsp. holartica* cfDNA (Appendix)	NA
F. tularensis IgM, serum	4 weeks: negative 8 weeks: negative	6 weeks postpartum: positive
F. tularensis IgG, serum	4 weeks: positive 8 weeks: negative	6 weeks postpartum: positive
Culture data	(Table 1)	Neck abscess (35 weeks' gestation): no growth × 5 d Throat culture (6 weeks postpartum): no growth × 5 d
Next-generation metagenomic sequencing, CSF‡	4 weeks: negative	NA
Multiplex PCR panel (BioFire), serum	4 weeks: negative	NA
Multiplex PCR panel, (BioFire); meningitis/encephalitis panel (Filmarray), CSF	4 weeks: negative	NA
Francisella tularensis immunohistochemistry, FFPE maternal fallopian tube tissue§	NA	*Francisella* spp. antigens detected (Figure 2)
Gram-negative bacteria 16S rRNA gene PCR test, FFPE maternal fallopian tube tissue§	NA	Positive for *Francisella* spp.

*cfDNA, cell-free DNA; CSF, cerebrospinal fluid; FFPE, formalin-fixed paraffin-embedded; MPM, molecules per microliter; NA, not applicable.
†Testing performed at Karius (https://kariusdx.com).
‡Testing performed at University of California, San Francisco (San Francisco, CA, USA).
§Testing performed at Centers for Disease Control and Prevention (Atlanta, GA, USA).

PCR performed on DNA extracts from a formalin-fixed paraffin-embedded tissue block containing tissue of the left fallopian tube was positive for *Francisella* spp.

Conclusions

We report vertical transmission of tularemia, resulting in congenital infection with neuroinvasive disease in a neonate. The findings of CSF lymphocytic

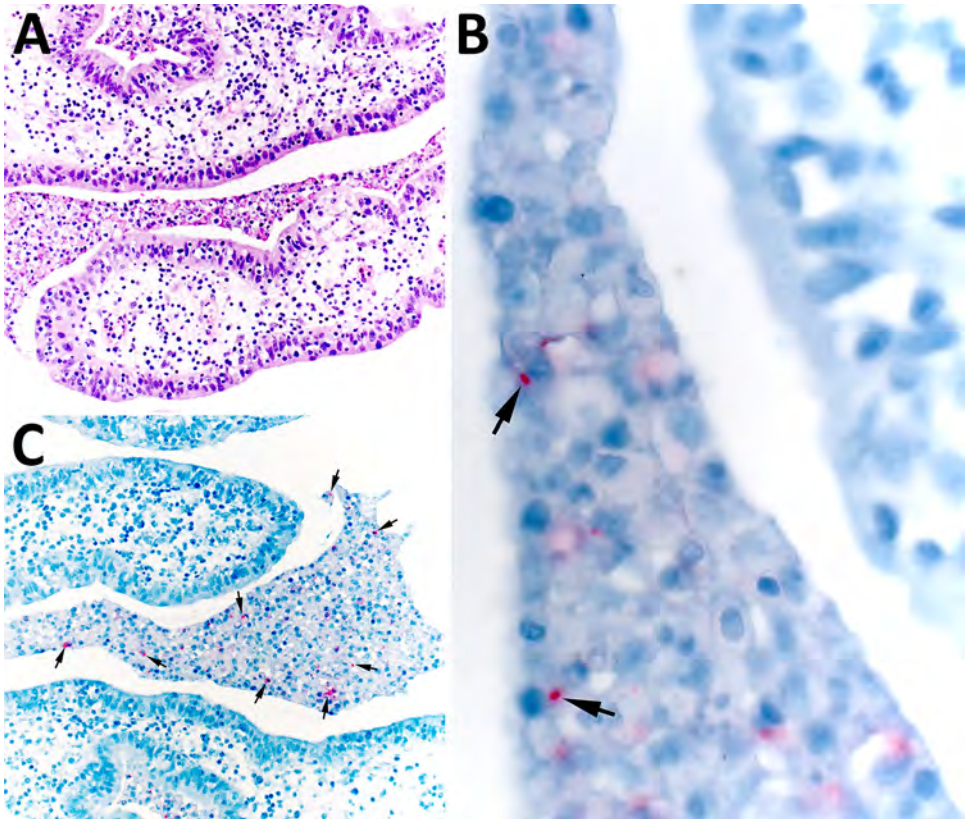

Figure 2. Histopathology in study of congenital tularemia with neuroinvasive disease, Utah, USA. Histopathological evaluation revealed the presence of subacute suppurative salpingitis with serositis. A) Hematoxylin and eosin–stained tissue showing abundant necroinflammatory debris in the lumen of the left fallopian tube. The endosalpinx was edematous, and infiltrating neutrophils and mononuclear cells were seen in the lamina propria and tubal epithelium. Original magnification ×200. B) Higher-power microphotograph highlights immunostaining within intracellular coccobacilli (arrows). Original magnification ×630. C) *Francisella tularensis* immunohistochemistry showing immunoreactive granular forms of bacterial antigens (arrows) within areas of the luminal necroinflammatory infiltrate. Original magnification ×200.

pleocytosis, 3 discrete brain lesions, and positive blood cfDNA testing for *F. tularensis* on 2 separate samples, with resolution of brain lesions after therapy, support this diagnosis. The mother's illness at 34 weeks' gestation was consistent with oropharyngeal tularemia and supported by serologic testing 40 days postpartum. The detection of *F. tularensis* and 16S rRNA gene by PCR in the fallopian tube confirm tularemia-induced salpingitis and presumed vertical transmission.

Neuroinvasive tularemia is uncommon; lymphocytic meningitis is the most common manifestation. Rare reports exist of discrete brain lesions (*5*). Various antibiotic medications have been described in treatment of neuroinvasive tularemia, such as streptomycin, gentamicin, doxycycline, chloramphenicol, and ciprofloxacin, often in combination (*5*).

This case of vertical transmission of *F. tularensis* in humans, supported with microbiological confirmation by histopathological and molecular methods, is unique. Complications of tularemia in pregnancy have been reported previously (*10*,*12*–*14*). The source of maternal infection remains unclear. A concurrent zoonotic outbreak of tularemia among beavers occurred in neighboring counties, and the mother had multiple other potential exposures. However, we found no clear linkage (*15*).

This case highlights the possibility of vertical transmission of tularemia, as well as neurologic manifestations in neonates. Diagnosis can be challenging and require assistance from state health departments and specialized commercial and Centers for Disease Control and Prevention national reference laboratories.

Acknowledgments

We thank Jana Ritter, Roosecelis B. Martines, and Jennifer Kasten for assisting in the pathological evaluation of the tissues and Pamela Fair and Marlene DeLeon Carnes for performing immunohistochemical and molecular assays. We also thank Sarah Park and Shivkumar Venkatasubrahmanyam for their detailed analysis of cfDNA genetic sequences.

About the Author

Dr. Nelson is a pediatric infectious diseases fellow at the University of Utah. His research interests are congenital infections and clinical microbiology.

References

1. Auwaerter PG, Penn RL. *Francisella tularensis* (tularemia). In: Bennett JE, Dolin R, Blaser MJ, editors. Mandell, Douglas, and Bennett's principles and practice of infectious diseases, 9th edition. Amsterdam: Elsevier; 2020. p. 2759–2773.
2. Sharma R, Patil RD, Singh B, Chakraborty S, Chandran D, Dhama K, et al. Tularemia—a re-emerging disease with growing concern. Vet Q. 2023;43:1–16. https://doi.org/10.1080/01652176.2023.2277753
3. Seles M, Altziebler J, Gorkiewicz G, Kriegl L, Hatzl S, Ahyai S, et al. Human tularemia epididymo-orchitis caused by *Francisella tularensis* subspecies *holartica*, Austria. Emerg Infect Dis. 2023;29:2105–7. https://doi.org/10.3201/eid2910.230436
4. Byington CL, Bender JM, Ampofo K, Pavia AT, Korgenski K, Daly J, et al. Tularemia with vesicular skin lesions may be mistaken for infection with herpes viruses. Clin Infect Dis. 2008;47:e4–6. https://doi.org/10.1086/588843
5. Cash-Goldwasser S, Beeson A, Marzec N, Ho DY, Hogan CA, Budvytiene I, et al. Neuroinvasive *Francisella tularensis* infection: report of 2 cases and review of the literature. Clin Infect Dis. 2024;78(Suppl 1):S55–63. https://doi.org/10.1093/cid/ciad719
6. Blech B, Christiansen M, Asbury K, Orenstein R, Ross M, Grill M. Polyneuritis cranialis after acute tularemia infection: a case study. Muscle Nerve. 2020;61:E1–2. https://doi.org/10.1002/mus.26725
7. Gangat N. Cerebral abscesses complicating tularemia meningitis. Scand J Infect Dis. 2007;39:258–61. https://doi.org/10.1080/00365540600823243
8. O'Toole D, Williams ES, Woods LW, Mills K, Boerger-Fields A, Montgomery DL, et al. Tularemia in range sheep: an overlooked syndrome? J Vet Diagn Invest. 2008;20:508–13. https://doi.org/10.1177/104063870802000417
9. Giannitti F, Dorsch MA, Schild CO, Caffarena RD, Sverlow K, Armién AG, et al. Pathologic and immunohistochemical evidence of possible Francisellaceae among aborted ovine fetuses, Uruguay. Emerg Infect Dis. 2023;29:141–4. https://doi.org/10.3201/eid2901.220698
10. Lide TN. Congenital tularemia. Arch Pathol (Chic). 1947;43:165–9.
11. Guarner J, Zaki SR. Histopathology and immunohistochemistry in the diagnosis of bioterrorism agents. J Histochem Cytochem. 2006;54:3–11. https://doi.org/10.1369/jhc.5R6756.2005
12. Fleck-Derderian S, Davis KM, Winberg J, Nelson CA, Meaney-Delman D. Systematic review of tularemia during pregnancy. Clin Infect Dis. 2024;78(Suppl 1):S47–54. https://doi.org/10.1093/cid/ciad686
13. Saranovic M, Milic M, Radic I, Katanic N, Vujacic M, Gasic M, et al. Tularemia in pregnant woman, Serbia, 2018. Emerg Infect Dis. 2023;29:806–8. https://doi.org/10.3201/eid2904.221318
14. Yeşilyurt M, Kiliç S, Çelebi B, Gül S. Tularemia during pregnancy: report of four cases. Scand J Infect Dis. 2013;45:324–8. https://doi.org/10.3109/00365548.2012.720027
15. Utah Division of Wildlife Resources. DWR confirms beavers killed by disease; urges public to report any dead beavers [cited 2024 Nov 19]. https://wildlife.utah.gov/news/utah-wildlife-news/1869-dwr-confirms-beavers-killed-by-tularemia-and-urges-public-to-report-any-dead-beavers.html

Address for correspondence: Brent D. Nelson, Division of Pediatric Infectious Diseases, Department of Pediatrics, University of Utah School of Medicine, 30 N Mario Capecchi Dr, Salt Lake City, UT 84112, USA; email: brent.d.nelson@hsc.utah.edu

West Nile Virus–Associated Hemophagocytic Lymphohistiocytosis, Switzerland

Clemente Lascano, Lena Groenendijk, Benjamin Bruno, Enrico Meduri, Ariane Malclès, Florian Laubscher, Francisco Javier Pérez-Rodriguez, Manuel Schibler, Christophe Marti, Aude Nguyen

A 62-year-old patient was hospitalized in Geneva, Switzerland, with an atypical manifestation of West Nile virus infection. Initially, he sought care for febrile diarrhea and vomiting; his condition deteriorated and hemophagocytic lymphohistiocytosis and meningoencephalitis developed. Corticosteroids improved his condition. We used high-throughput sequencing and ophthalmologic findings to diagnose West Nile virus.

West Nile virus (WNV) is an enveloped, single-stranded positive-sense RNA virus belonging to the genus *Orthoflavivirus*, family *Flaviviridae*. First isolated from a patient in Uganda in 1937, this mosquitoborne virus has spread worldwide, causing sporadic infections and outbreaks on every continent except Antarctica (*1*). Birds, the natural reservoir, act as amplifying hosts and play a major role in the spread of WNV (*2*). Since the late 1990s, an increasing number of outbreaks have been reported in Southern and Central Europe, suggesting a trend to an endemic presence in various regions of Europe (*3*). That trend might be partly explained by modifications of ecosystems and climate change. Rising temperature and fluctuating rainfall can influence mosquito activity, bird migration patterns and their abundance and of consequence, the expansion of vector habitat that can contribute to increased virus transmission (*4*,*5*). To date, 9 phylogenetic lineages of WNV have been identified, of which only lineages 1 and 2 are associated with major outbreaks in humans (*3*,*4*).

Author affiliations: Geneva University Hospitals, Geneva, Switzerland (C. Lascano, L. Groenendijk, E. Meduri, A. Malclès, F. Laubscher, F.J. Pérez-Rodriguez, M. Schibler, C. Marti, A. Nguyen); Centre Hospitalier de Wallonie Picard, Tournai, Belgium (B. Bruno); University of Geneva, Geneva (A. Malclès, M. Schibler)

DOI: https://doi.org/10.3201/eid3112.250776

The WNV incubation period ranges from 2–15 days after a mosquito bite. Approximately 20% of infected persons will experience an acute systemic illness, known as West Nile fever, characterized generally by fever, malaise, headaches, myalgias, arthralgias, maculopapular rash, and gastrointestinal symptoms. Neuroinvasive disease will develop in <1% of infected persons, manifesting as meningitis, encephalitis, or acute flaccid paralysis, a poliomyelitis-like syndrome (*6*). Among those with neuroinvasive disease, the mortality rate ranges from 10–30%, which represents <0.1% of all infected cases (*1*,*6*).

Hemophagocytic syndromes or hemophagocytic lymphohistiocytosis (HLH) are rare, underdiagnosed, and often life-threatening conditions because of an overstimulation of the immune system, leading to systemic inflammation (activated cytotoxic T cells and natural killer cells), cytokine storm, and multiorgan failure. Those syndromes can be divided into primary HLH, associated with genetic factors and usually seen in children, and secondary HLH, also called reactive hemophagocytic syndrome (RHS), which can be triggered by malignancy, autoimmune diseases, or infections (*7*,*8*). The most common infectious triggers are herpes viruses, in the case of primary infection or reactivation, although many other viruses, such as HIV, hepatitis viruses, parvovirus B19, and influenza virus, have been reported (*9*). In adults, the average age of diagnosis is 50, and more women are affected than men (*8*). Diagnosis is currently made on the basis of various diagnostic criteria, such as HLH-2004 criteria (commonly used) and the HScore (specifically developed for adult RHS) (*10*). Those criteria include a constellation of clinical manifestations and biologic or cytological findings: fever, hepatosplenomegaly, cytopenia, elevated plasmatic ferritin, high lactate dehydrogenase and triglycerides, low fibrinogen, hepatic cytolysis and cholestasis, and

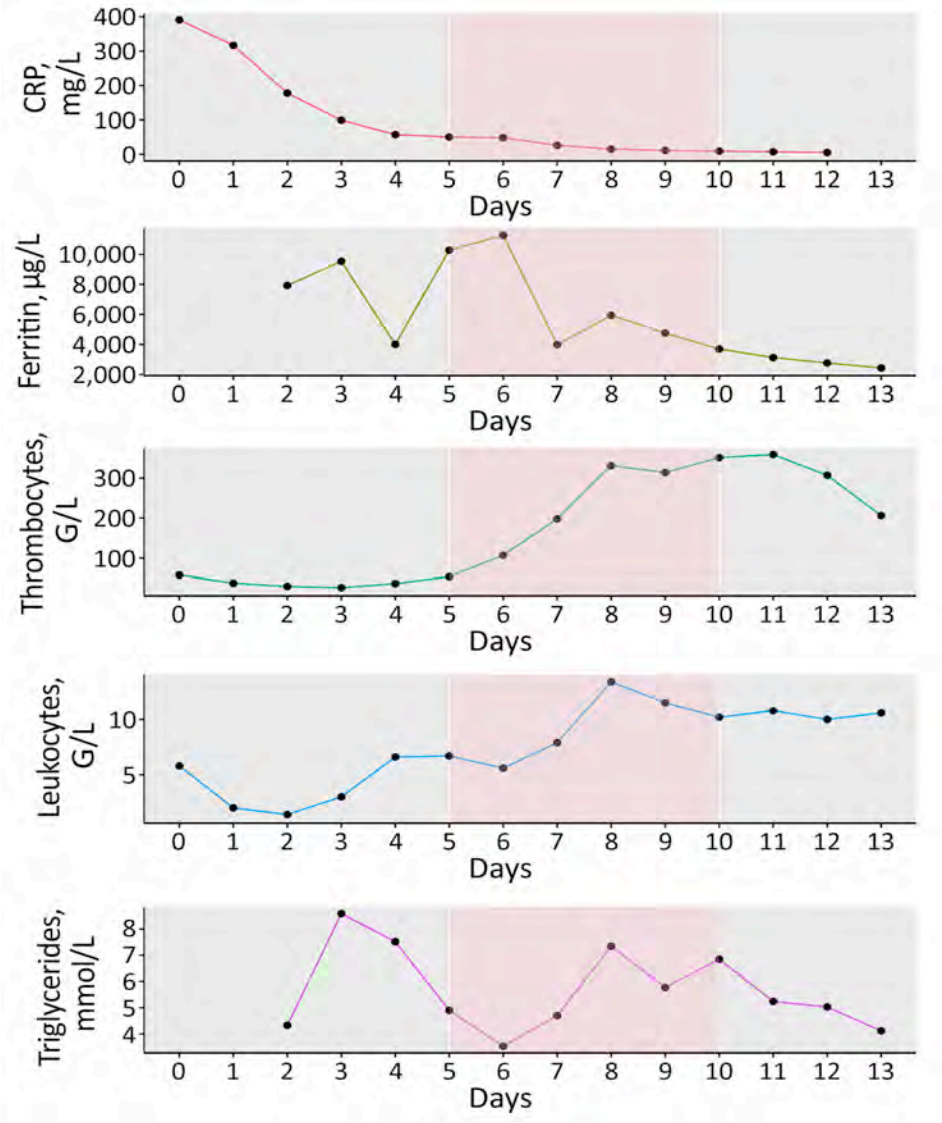

Figure 1. Evolution of laboratory data for a patient with West Nile virus–associated hemophagocytic lymphohistiocytosis during hospitalization, Geneva, Switzerland. Results include C-reactive protein, ferritin, thrombocytes, leukocytes, and triglycerides. Pink shading indicates corticosteroid treatment.

hemophagocytosis in bone marrow biopsy (*7*,*8*). However, none of those criteria are pathognomonic alone. An HLH diagnosis can be made even in the absence of hemophagocytosis in bone marrow biopsy (*6*). We report a case of WNV-associated hemophagocytic lymphohistiocytosis in a man in Switzerland.

The Case

A 62-year-old man with a history of prostate adenocarcinoma under close follow-up by urologists since 2022 was admitted to Geneva University Hospitals (Geneva, Switzerland) in August 2024 with complaints of a 48-hour history of fever, watery diarrhea, and vomiting. He had recently returned from a trip to Toulon on the south coast of France. He also reported moderate bitemporal headache for 1 week without photophobia or phonophobia.

In the emergency department, the patient was febrile with signs of septic shock but had an otherwise unremarkable physical examination. Initial workup revealed thrombocytopenia (58×10^9 cells/L, reference range $150–400 \times 10^9$ cells/L), lymphocytopenia (0.12×10^9 cells/L, reference $4–11 \times 10^9$ cells/L), elevated C-reactive protein (391 mg/L, reference <0.9 mg/L), and acute kidney injury (KDIGO stage 2 [https://kdigo.org/guidelines/acute-kidney-injury]). Abdominal contrast-enhanced computed tomography scan revealed hepatosplenomegaly. We admitted the patient to a monitored care unit for presumed bacterial sepsis of enteric origin and provide empirical antimicrobial therapy (ceftriaxone 2 g/d and metronidazole 500 mg/8 h), along with intensive intravenous fluid therapy. We performed a microbiological diagnostic workup, including serology for

viral hepatitis, cytomegalovirus, Epstein-Barr virus, HIV, parvovirus B19, syphilis, and leptospirosis; all results were negative for acute infection. Results of a gastrointestinal multiplex molecular assay were positive for enteropathogenic *Escherichia coli*, which we believed reflected colonization.

During the patient's hospitalization, a persistent fever developed and kidney failure worsened; profound pancytopenia, hyperferritinemia (11,272 mcg/L, reference 12–200 mcg/L), hypertriglyceridemia (7.35 mmol/L, reference <2 mmol/L), and isolated aspartate aminotransferase elevation occurred (Figures 1, 2). Hematology consultation led to the suspicion of an HLH secondary to a concurrent yet undetermined infection. That suspicion was supported by an HScore of 244 points (high temperature; organomegaly; cytopenia; elevated ferritin, triglycerides, and aspartate aminotransferase; reference fibrinogen levels; and absence of hemophagocytosis features on bone marrow), translating to an HLH diagnostic probability >99%. Total body positron emission tomography–computed tomography revealed no malignancy. Bone marrow biopsy showed no evidence of hematological neoplasia or hemophagocytosis. The infectious workup showed no herpetic infection or reactivation; blood PCR results were negative for herpes simplex virus 1 and 2, human herpesvirus 6, Epstein-Barr virus, and cytomegalovirus. Dengue virus was also not detected.

On day 4 of hospitalization, the patient experienced altered mental status, psychomotor slowing, and disorientation. Cerebrospinal fluid (CSF) analysis revealed mixed pleocytosis (leukocyte count 327 mol/L, 48% lymphocytes and 46% polymorphonuclear cells), proteinorachia, and hypoglycorrhachia. Suspecting neurolisteriosis, we changed the antimicrobial therapy to meropenem (2 g/12 h). Results of a multiplex molecular panel for meningitis and encephalitis and a CSF culture were negative. Brain MRI showed mesial temporal hyperintensity, and electroencephalogram indicated no epileptic activity. Soluble CD25 serum concentration on day 5 of hospitalization was elevated at 4 ng/mL (reference <2 ng/mL). We started the patient on dexamethasone (20 mg 1×/d) for possible HLH-related central nervous system involvement; the treatment led to fever resolution, slow neurologic status improvement, and normalization of ferritin and triglyceride values (Figures 1, 2). We discontinued meropenem and continued corticotherapy for a total of 5 days. Ophthalmological evaluation for new onset myodesopsia revealed uveitis and scattered chorioretinal lesions with a targetoid appearance, findings highly suggestive of WNV chorioretinitis (Appendix Figure 1, https://wwwnc.cdc.gov/EID/article/31/12/25-0776-App1.pdf).

An unbiased high-throughput sequencing performed on the initial serum sample to identify a viral HLH trigger identified WNV sequences (4 reads on 2 separate genomic regions, enabling classification in WNV lineage 2) (Appendix Figure 2). We isolated RNA by using TRIzol (Invitrogen, https://www.invitrogen.com) according to the manufacturer's instructions. We prepared libraries by using the TruSeq (Illumina, https://www.illumina.com) total RNA preparation protocol and then sequenced on a MiSeq platform (Illumina) by using the 2 × 75 bp paired-end protocol. We analyzed reads by using a bioinformatics pipeline designed to detect all vertebrate viruses on the basis of the Virosaurus database as previously described (*11*). Subsequent serology and blood PCR confirmed the viral diagnosis, whereas CSF WNV reverse transcription PCR was negative.

Conclusions

We report an atypical manifestation of WNV infection with features of meningoencephalitis, ophthalmological involvement, and secondary HLH. Of

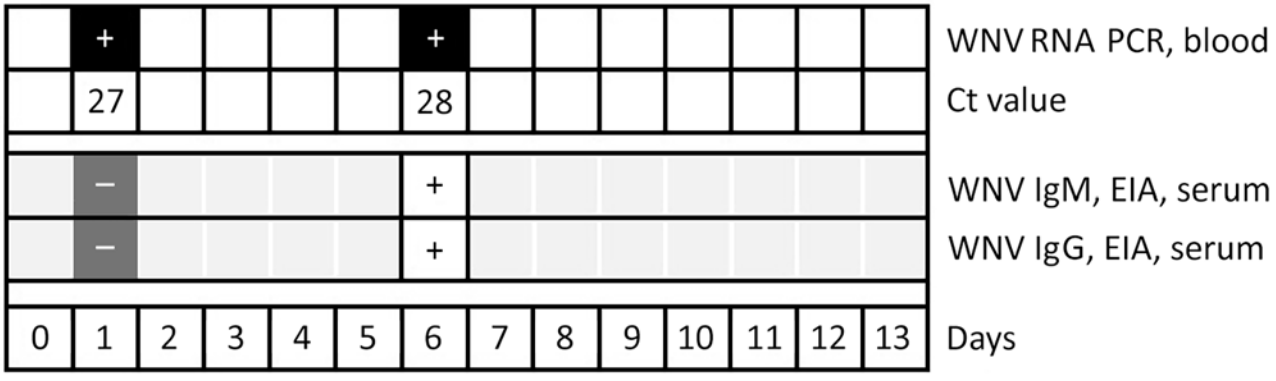

Figure 2. WNV testing results of a patient with WNV-associated hemophagocytic lymphohistiocytosis during hospitalization, Geneva, Switzerland. Ct, cycle threshold; EIA, enzyme immunoassay; WNV, West Nile virus.

note, the pathognomic chorioretinal findings provided the first hint pointing toward a viral etiology. The infection was likely acquired on the south coast of France, where multiple infections were reported at the time. Although cases of HLH secondary to other flaviviruses such as dengue virus have been reported, RHS triggered by WNV infection is unusual (*12*,*13*). The diagnosis of RHS was established despite the absence of hemophagocytosis in the bone marrow biopsy, consistent with current diagnostic standards (*8*,*10*). Corticosteroid treatment led to clinical improvement. Because of the ongoing effects of climate change and the increasing incidence of WNV infections, clinicians should be aware of potential clinical manifestations and WNV's possible complications, such as secondary HLH, which might affect patient prognosis.

Acknowledgments

We thank the staff involved in the care of this patient at Geneva University Hospitals and the patient for providing permission to publish this case report.

Author contributions: study conception, data interpretation, manuscript drafting, C.L. and A.N.; data collection, manuscript revision, final approval of the submitted version, accountability for all aspects of the data and research, C.L., A.N., L.G, B.B., E.M., A.M., F.L., F.J.P-R., M.S, and C.M.

About the Author

Mr. Lascano is a medical resident in internal medicine at the University Hospitals of Geneva, Switzerland. His research interests include clinical research with a focus on antimicrobial resistance and stewardship.

References

1. Naveed A, Eertink LG, Wang D, Li F. Lessons learned from West Nile Virus infection: vaccinations in equines and their implications for one health approaches. Viruses. 2024;16:781.
2. Simonin Y. Circulation of West Nile virus and Usutu virus in Europe: overview and challenges. Viruses. 2024;16:599.
3. Lu L, Zhang F, Oude Munnink BB, Munger E, Sikkema RS, Pappa S, et al. West Nile virus spread in Europe: phylogeographic pattern analysis and key drivers. PLoS Pathog. 2024;20:e1011880.
4. Paz S. Climate change impacts on West Nile virus transmission in a global context. Philos Trans R Soc Lond B Biol Sci. 2015;370:20130561.
5. Singh P, Khatib MN, Ballal S, Kaur M, Nathiya D, Sharma S, et al. West Nile Virus in a changing climate: epidemiology, pathology, advances in diagnosis and treatment, vaccine designing and control strategies, emerging public health challenges—a comprehensive review. Emerg Microbes Infect. 2025;14:2437244.
6. Sejvar JJ. Clinical manifestations and outcomes of West Nile virus infection. Viruses. 2014;6:606–23.
7. Hayden A, Park S, Giustini D, Lee AYY, Chen LYC. Hemophagocytic syndromes (HPSs) including hemophagocytic lymphohistiocytosis (HLH) in adults: a systematic scoping review. Blood Rev. 2016;30:411–20.
8. Ramos-Casals M, Brito-Zerón P, López-Guillermo A, Khamashta MA, Bosch X. Adult haemophagocytic syndrome. Lancet. 2014;383:1503–16.
9. Koumadoraki E, Madouros N, Sharif S, Saleem A, Jarvis S, Khan S. Hemophagocytic lymphohistiocytosis and infection: a literature review. Cureus. 2022;14:e22411.
10. Cox MF, Mackenzie S, Low R, Brown M, Sanchez E, Carr A, et al.; HiHASC group. Diagnosis and investigation of suspected haemophagocytic lymphohistiocytosis in adults: 2023 Hyperinflammation and HLH Across Speciality Collaboration (HiHASC) consensus guideline. Lancet Rheumatol. 2024;6:e51–62.
11. Gleizes A, Laubscher F, Guex N, Iseli C, Junier T, Cordey S, et al. Virosaurus a reference to explore and capture virus genetic diversity. Viruses. 2020;12:1248.
12. Chung SM, Song JY, Kim W, Choi MJ, Jeon JH, Kang S, et al. Dengue-associated hemophagocytic lymphohistiocytosis in an adult: a case report and literature review. Medicine (Baltimore). 2017;96:e6159.
13. See KC. Dengue-associated hemophagocytic lymphohistiocytosis: a narrative review of its identification and treatment. Pathogens. 2024;13:332.

Address for correspondence: Aude Nguyen, Geneva University Hospitals, Rue Gabrielle-Perret-Gentil 4, 1211 Genève 14, Geneva, Switzerland; email: aude.nguyen@hug.ch

Human Infection by Zoonotic Eye Fluke *Philophthalmus lacrymosus*, South America

Thomas Weitzel, Esteban M. Cordero,[1] Trinidad Mujica,[1] Carolina Aravena, Brianne E. Phillips, Michael J. Yabsley, Gregory A. Lewbart, Diego Páez-Rosas, María Isabel Jercic, Sofía Capasso

We report a case of severe conjunctivitis in a traveler infected with a *Philophthalmus lacrymosus* eye fluke, probably acquired on the Galápagos Islands in Ecuador. This zoonotic parasite is endemic in Brazil and Venezuela, where it has been reported in birds and capybaras.

Philophthalmus spp. parasites are cosmopolitan digeneans, typically inhabiting the conjunctival sac of waterbirds. The trematodes, known as avian eye flukes, have a complex lifecycle, which includes freshwater and marine snails as intermediate hosts and waterbirds as final hosts. Birds are infected by ingestion of infective metacercariae that are encysted on aquatic plants (*1*). After thermally triggered excystation in the pharynx, the parasite migrates through the lacrimal ducts to the orbital cavity. Ocular infections of mammals have been reported in capybaras (*Hydrochoerus hydrochaeris*) from Brazil, Galapagos sea lions (*Zalophus wollebaeki*) in Ecuador, and rarely other mammals, including humans (*2*–*6*). The mode of infection in nonavian hosts is uncertain; both ingestion and direct contact with cercariae or metacercariae have been proposed (*2*,*7*).

Globally, >50 nominal *Philophthalmus* spp. trematodes have been described; however, recent evidence suggests that only ≈10 species are valid (*1*,*5*). In South America, *Philophthalmus* spp. flukes have been reported from Brazil, Peru, Venezuela, and Ecuador's Galápagos Islands (*1*,*3*,*8*,*9*). Further geographic spread of *Philophthalmus* spp. trematodes by invasive snail species is probable (*9*,*10*).

Since 1939, a total of 12 human philophthalmiasis cases have been published. Infections were acquired in Asia, Europe, and North America and mostly identified to the genus level, but cases compatible with philophthalmiasis already were known in the 19th Century (Appendix 1, https://wwwnc.cdc.gov/EID/article/31/12/25-1126-App1.pdf). We describe a case of philophthalmiasis caused by a *Philophthalmus lacrymosus* eye fluke in a traveler from Europe, probably acquired on the Galápagos Islands.

The Study

A 26-year-old woman from England sought care in Santiago, Chile, for a 9-day history of intense pain, swelling, and a moving foreign body sensation in her right eye. Before symptom onset, she had visited Colombia (4-week stay); Ecuador, including Galápagos Islands (2.5-week stay); and Peru (1-week stay). Ocular examination showed eyelid edema, intense chemosis and follicular reaction of the inferior fornix, and superior tarsal conjunctiva. Results of cornea examination, anterior segment findings, and fundus examination were unremarkable. After a thorough examination, we removed an elongated mobile structure located on the upper tarsal conjunctiva by using a moist cotton swab. After removal, the foreign body sensation disappeared. Follow-up over the following weeks showed a complete recovery without complications.

We performed detailed morphologic studies of the extracted structure on a temporary wet mount by

Author affiliations: Charité–Universitätsmedizin Berlin, Berlin, Germany (T. Weitzel); Clínica Alemana, Universidad del Desarrollo, Santiago, Chile (T. Weitzel, C. Aravena); Instituto de Salud Pública, Santiago (E.M. Cordero, M.I. Jercic), Fundación Instituto Professional Duoc UC, Santiago (T. Mujica); Zoo New England, Boston, Massachusetts, USA (B.E. Phillips); University of Georgia, Athens, Georgia, USA (M.J. Yabsley); North Carolina State University, Raleigh, North Carolina, USA (G.A. Lewbart), Universidad San Francisco de Quito, Puerto Baquerizo Moreno, Ecuador (D. Páez-Rosas); Galápagos Conservancy, Puerto Ayora, Ecuador (D. Páez-Rosas); Oniris, INRAE, BIOPAR, Nantes, France (S. Capasso)

DOI: https://doi.org/10.3201/eid3112.251126

[1]These authors contributed equally to this article.

using an Olympus SZ61 stereo microscope (https://www.olympus-global.com), an Olympus DP22 digital camera, and Olympus cellSens software version 2.3 (https://evidentscientific.com). Our analyses confirmed the specimen as a *P. lacrymosus* fluke (Figure 1). The single mature ovigerous specimen had an elongated oval shape, smooth surface, no spines, and constriction at the level of the ventral sucker. Maximum width was always posterior to ventral sucker, oral sucker subterminal, pharynx muscular, esophagus bifurcating posteriorly to pharynx, and ceca extending to posterior margin of posterior testis. The acetabulum was larger than the oral sucker and preequatorial; testes were in tandem, smooth and spherical, located in the posterior portion of the body, in an intercecal position; cirrus sac was elongated, slightly surpassing posterior margin of acetabulum (cirrus not visible), and genital pore median, at level of cecal bifurcation. Ovary was spherical, located pretesticular in the intercecal area; the uterus was long and coiled, occupying the space between the ventral sucker and the level of anterior margin of the anterior testis; the vitellarium was follicular and eggs nonoperculated, containing a fully formed miracidium with a dark eyespot in most eggs. We morphometrically compared the sample with previously reported *P. lacrymosus* specimens (Appendix 1).

We confirmed species diagnosis by molecular analyses using PCR and bidirectional Sanger sequencing of nuclear internal transcribed spacer (ITS) 2 and mitochondrial cytochrome c oxidase I (Cox1) (Appendix 2, https://wwwnc.cdc.gov/EID/article/31/12/25-1126-App1.xlsx). We compared amplicons with sequences from GenBank and *Philophthalmus zalophi* ocular trematodes from Galápagos sea lions.

An 861-bp ITS-2 consensus sequence from the human sample was identical to the consensus *P. zalophi* sequence (M.J. Yabsley, unpub. data) and showed 98.6% identity with *P. lacrymosus* and 95.9% identity with *P. lucipetus*, both fluke species found in gulls (*Larus* spp.) from Portugal, and 95.6% identity with *P. gralli* sequences from invasive red-rimmed melania snails (*Melanoides tuberculata*) from Costa Rica and small passerines from Peru (Figure 2). The 396-bp Cox1 consensus sequence had 99.73% (single transition) and 99.45% identity with *P. lacrymosus* sequences from kelp gulls (*Larus dominicanus*) in Brazil, whereas similarities with *P. lacrymosus* sequences from Portugal were 91.90%–92.15%. We observed identity values ranging from 87.34% to 87.09% with *P. lucipetus* sequences from Portugal. An 87.12% identity was shared with a specimen annotated as *Philopthalmus* sp., which was isolated from a Japanese snail (*Semisulcospira libertina*) (Figure 2). We constructed additional Bayesian-inferred phylogenetic trees from 17 ITS-2 sequences and 16 Cox1 sequences (Appendix 1 Figure).

Conclusions

The epidemiology of human philophthalmiasis is poorly understood. Cases have been reported from Asia, Europe, and North America (Appendix 1 Table 1). Some reports suggest infection by direct inoculation of metacercariae during swimming (Appendix 1), whereas others suggest oral ingestion of metacercaria with food or direct inoculation during food preparation (Appendix 1). Of note, the parasite can survive for several months in the human host (Appendix 1). Nearly all cases were caused by single worms and involved unilateral irritation, sensation of a foreign body, and conjunctivitis. Vision impairment has not been reported, except for historical cases in the 18th Century with high worm loads (Appendix 1).

The number of species causing human philophthalmiasis is uncertain, given that most extracted worms were identified only to genus. In North

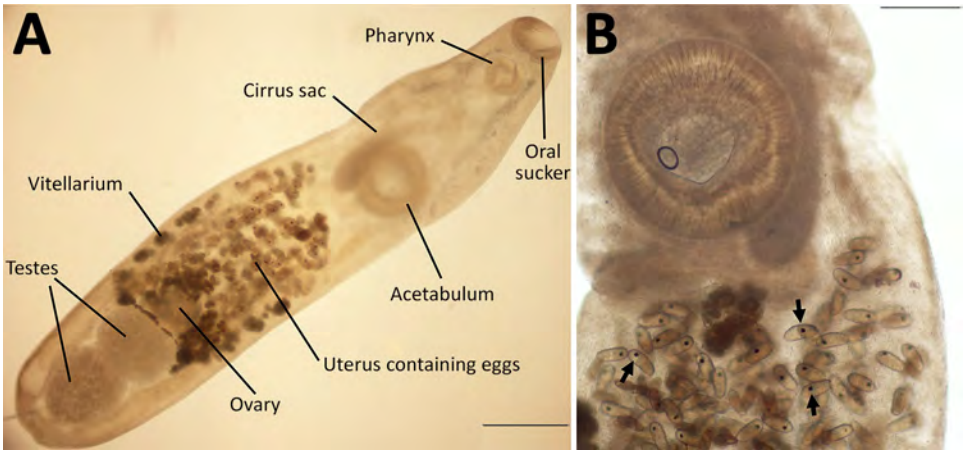

Figure 1. Specimen of *Philophthalmus lacrymosus* fluke extracted from conjunctiva of a female traveler from England in Chile. A) Full view of the unstained specimen showing oral sucker, pharynx, cirrus sac, acetabulum, uterus containing eggs, ovary, testes, and vitellarium. B) Intrauterine eggs showing fully formed miracidia with eyespots (arrows). Scale bars: panel A, 500μm; panel B, 200μm.

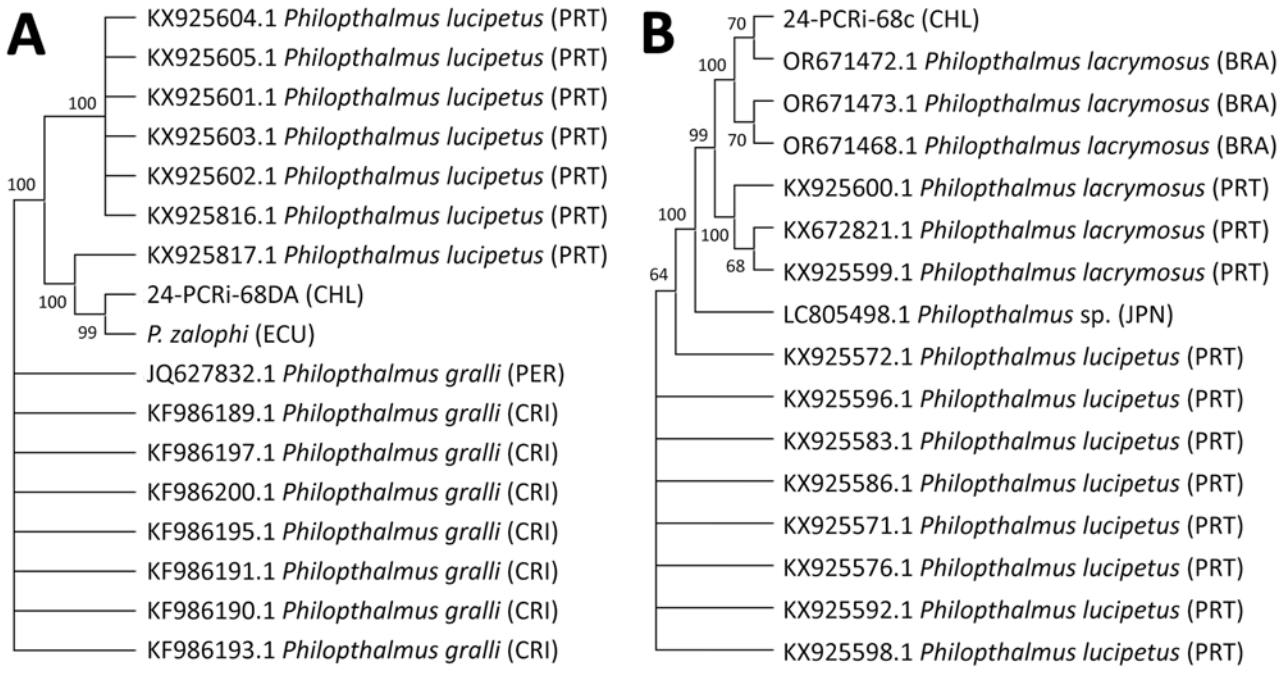

Figure 2. Maximum-likelihood phylogenetic tree constructed from 17 internal transcribed spacer 2 sequences (trimmed alignment 673 bp) (A) and 16 cytochrome c oxidase I sequences (trimmed alignment 365 bp) (B) of *Philophthalmus lacrymosus* fluke extracted from conjunctiva of a female traveler from England in Chile. Consensus trees were inferred from 1,000 replicates by using the Kimura 2-parameter test in MEGA 11 (https://www.megasoftware.net). Bootstrap values at the nodes indicate the percentages of replicates in which the sequences clustered together. Sequence codes include GenBank accession numbers and parasite information. In parentheses, letter codes indicate the country of origin. Sequences from this case report are 24-PCRi-68DA_CHL (GenBank accession no. PX240011) and 24-PCRi-68c_CHL (accession no. PX238763). BRA, Brazil; CHL, Chile; CRI, Costa Rica; ECU, Ecuador; JPN, Japan; PER, Peru; PRT, Portugal.

America, the *P. lacrymosus* fluke (recorded as *P. lacrimosus*) was diagnosed in a human case from Mexico (*11*). In South America, *P. lacrymosus* flukes have exclusively been diagnosed in waterbirds in Brazil and Venezuela and capybaras in Brazil (*5*). The patient reported here had only direct contact with natural water environments on the Galápagos Islands, where *P. zalophi*, a new fluke species defined by morphologic criteria, has been reported in Galapagos sea lions (*3*,*4*). Considering that *Philophthalmus* parasites can inhabit the human eye for several months, a previous case from Ohio, USA, might plausibly have also been acquired on the Galápagos Islands, which the patient had visited 5 months before symptom onset (*12*). Marine snails of the Batillariidae family, present on the Galápagos Islands, could serve as potential intermediate hosts; that family includes the West Indian false cerith (*Lampanella minima*), a known intermediate host of *P. lacrymosus* flukes (*13*,*14*).

The patient's exposure on Galápagos Islands remains inferential, requiring studies of infected intermediate hosts or environmental larval stages. However, our molecular data indicate that *P. zalophi* flukes from Galápagos might be conspecific with *P. lacrymosus* flukes. Probable spillover of *P. lacrymosus* flukes from a bird host to sea lions could explain morphologic differences, which can occur during adaptation to the mammalian host as reported in capybaras (*2*). Similarly, host-related plasticity or different development stages could explain certain morphologic deviations of our sample from previous *P. lacrymosus* specimens (Appendix 1). The specimen we report shared several traits with *P. zalophi* flukes, including a similar oral sucker to pharynx ratio and a body length <6 mm.

Further comparative genomic analyses are required to clarify taxonomic uncertainty of *Philophthalmus* spp. flukes infecting humans, as recently shown in Japan (*15*). The *P. lacrymosus* species might be paraphylectic or represent a complex of geographically and host-related lineages with South American isolates forming a genetically cohesive clade that is taxonomically distinct from forms of *P. lacrymosus* flukes in Europe and Asia.

In conclusion, our clinical and epidemiologic findings show that the zoonotic eye fluke *P. lacrymosus* can infect humans in South America. The findings also suggest that the parasite might be endemic on the Galápagos Islands in Ecuador.

Acknowledgments

We thank James Flowers for the field work on the Galápagos Islands and Armin Araya and Kayla Garrett for laboratory assistance.

About the Author

Dr. Weitzel is a tropical medicine and parasitology expert at Clínica Alemana, Universidad del Desarrollo, Santiago, Chile. His research interests include vectorborne, parasitic, and travel-associated infections.

References

1. Nollen PM, Kanev I. The taxonomy and biology of philophthalmid eyeflukes. Adv Parasitol. 1995;36:205–69. https://doi.org/10.1016/S0065-308X(08)60492-3
2. Pinto RM, dos Santos LC, Tortelly R, Menezes RC, de Moraes W, Juvenal JC, et al. Pathology and first report of natural infections of the eye trematode *Philophthalmus lachrymosus* Braun, 1902 (Digenea, Philophthalmidae) in a non-human mammalian host. Mem Inst Oswaldo Cruz. 2005;100:579–83.
3. Dailey M, Ellin R, Parás A. First report of parasites from pinnipeds in the Galapagos Islands, Ecuador, with a description of a new species of *Philophthalmus* (Digenea: Philophthalmidae). J Parasitol. 2005;91:614–7.
4. Phillips BE, Páez-Rosas D, Flowers JR, Cullen JM, Law JM, Colitz C, et al. Evaluation of the ophthalmologic disease and histopthologic effects due to the ocular trematode *Philophthalmus zalophi* on juvenile Galápagos sea lions (*Zalophus wollebaeki*). J Zoo Wildl Med. 2018;49:581–90.
5. Hernández DL, Somma AT, Steuernagel A, Vieira TSWJ, Moore B, Reifur L, et al. A molecular phylogenetic study of the eye fluke *Philophthalmus lacrymosus* (Trematoda: Philophthalmidae) found in *Larus dominicanus* (Aves: Laridae) from Brazil. Acta Parasitol. 2024;69:1027–34.
6. Meise K, Garcia-Parra C. Behavioral and environmental correlates of *Philophthalmus zalophi* infections and their impact on survival in juvenile Galapagos sea lions. Mar Biol. 2015;162:2107–17. https://doi.org/10.1007/s00227-015-2740-7
7. Rajapakse RD, Wijerathne KMS, S de Wijesundera M. Ocular infection with an avian trematode (*Philophthalmus* sp). Ceylon Med J. 2009;54:128–9.
8. Pulido-Murillo EA, Tkach VV, Pinto HA. The life cycle of *Philophthalmus aylacostoma* n. sp. (Trematoda: Philophthalmidae), a new eye fluke species transmitted by *Aylacostoma* spp. (Gastropoda: Thiaridae) in Brazil. Parasitol Res. 2022;121:933–44.
9. Literák I, Heneberg P, Sitko J, Wetzel EJ, Cardenas Callirgos JM, Čapek M, et al. Eye trematode infection in small passerines in Peru caused by *Philophthalmus lucipetus*, an agent with a zoonotic potential spread by an invasive freshwater snail. Parasitol Int. 2013;62:390–6.
10. Metz DCG, Turner AV, Nelson AP, Hechinger RF. Potential for emergence of foodborne trematodiases transmitted by an introduced snail (*Melanoides tuberculata*) in California and elsewhere in the United States. J Infect Dis. 2023;227:183–92.
11. Lamothe-Argumedo R, Diaz-Camacho SP, Nawa Y. The first human case in Mexico of conjunctivitis caused by the avian parasite, *Philophthalmus lacrimosus*. J Parasitol. 2003;89:183–5.
12. Gutierrez Y, Grossniklaus HE, Annable WL. Human conjunctivitis caused by the bird parasite *Philophthalmus*. Am J Ophthalmol. 1987;104:417–9.
13. Heneberg P, Casero M, Waap H, Sitko J, Azevedo F, Těšínský M, et al. An outbreak of philophthalmosis in *Larus michahellis* and *Larus fuscus* gulls in Iberian Peninsula. Parasitol Int. 2018;67:253–61.
14. Charles Darwin Foundation. Galapagos species database [cited 2025 Jul 12]. https://datazone.darwinfoundation.org/en/checklist/?species=9355
15. Sasaki M, Miura O, Nakao M. *Philophthalmus hechingeri* n. sp. (Digena: Philophthamidae), a human-infecting eye fluke from the Asian mud snail, *Batillaria attramentaria*. J Parasitol. 2022;108:44–52.

Address for correspondence: Thomas Weitzel, Laboratorio Clínico, Clínica Alemana, Av. Vitacura 5951, Santiago, Chile; email: thomas.weitzel@gmail.com

Highly Pathogenic Avian Influenza A(H5N1) Clade 2.3.4.4b Virus Infection in Poultry Farm Workers, Washington, USA, 2024

Yasuko Hatta,[1] Juan A. De La Cruz,[1] Theresa Murray, Brian Hiatt, Yunho Jang, Julia C. Frederick, Kristine A. Lacek, Juliana C. DaSilva, Dan Cui, Paul Carney, Jimma Liddell, Kay W. Radford, Natasha Burnett, Sabrina Schatzman, Pauline Trinh, Anna Unutzer, Elizabeth A. Pusch, Monique Johnson, Ha T. Nguyen, Benjamin L. Rambo-Martin, Larisa Gubareva, James Stevens, C. Todd Davis, Marie K. Kirby, Allison Black, Han Di

Poultry workers in Washington, USA, were infected with highly pathogenic avian influenza A(H5N1) virus and recovered. The viruses were clade 2.3.4.4b genotype D1.1, closely related to viruses causing poultry outbreaks. Continued surveillance and testing for influenza A(H5) clade 2.3.4.4b viruses remain essential for risk assessment and pandemic preparedness of zoonotic influenza viruses.

The global spread of A/goose/Guangdong/96-lineage highly pathogenic avian influenza (HPAI) virus of the A(H5) subtype has resulted in numerous clades, subclades, and genotypes because of continuous genetic drift and reassortment. HPAI H5N1 clade 2.3.4.4b virus is the most widespread globally; since December 2021, that clade has circulated in wild birds in the United States, affecting millions of poultry, mammalian wildlife, domestic livestock, and companion animals (*1*,*2*). In 2024, two distinct genotypes were mainly responsible for ongoing outbreaks in the United States, B3.13 mostly in dairy cattle and D1.1 mostly in poultry, but outbreaks of both genotypes were reported in cattle and poultry (*3*,*4*).

Sporadic human infections with clade 2.3.4.4b viruses have also been reported in the United States. During April 1, 2024–June 30, 2025, a total of 70 human cases were reported, including 41 cases after dairy cattle exposure, 24 after exposure to commercial poultry flocks, 2 after exposure to backyard flocks, and 3 with an unknown exposure source (*5*,*6*). In response to reported human infections with clade 2.3.4.4b viruses in the United States and other countries, several 2.3.4.4b A(H5) prepandemic candidate vaccine viruses (CVVs) have been made available for pandemic influenza preparedness (*7*).

In late 2024, the Washington State Public Health Laboratory detected influenza A(H5) virus by real-time reverse transcription PCR among specimens from poultry workers experiencing influenza symptoms. We investigated virus isolates from human cases in Washington to determine virus receptor-binding preference and cross-reactivity with existing CVVs.

The Study

During October 23–November 5, 2024, the Centers for Disease Control and Prevention (CDC; Atlanta, GA, USA) received multiple presumptive influenza A(H5)–positive human clinical specimens from the Washington State Public Health Laboratory. Testing at CDC confirmed HPAI A(H5) virus in 8 poultry farm workers. All 8 cases occurred in adults exposed to H5N1 virus–infected poultry during depopulation efforts to control an outbreak among poultry in

Author affiliations: Centers for Disease Control and Prevention, Atlanta, Georgia, USA (Y. Hatta, J.A. De La Cruz, Y. Jang, J.C. Frederick, K.A. Lacek, J.C. DaSilva, D. Cui, P. Carney, J. Liddell, K.W. Radford, N. Burnett, S. Schatzman, E.A. Pusch, M. Johnson, H.T. Nguyen, B.L. Rambo-Martin, L. Gubareva, J. Stevens, C.T. Davis, M.K. Kirby, H. Di); Washington State Department of Health, Shoreline, Washington, USA (T. Murray, B. Hiatt, P. Trinh, A. Unutzer, A. Black)

DOI: https://doi.org/10.3201/eid3112.251118

[1]These authors contributed equally to this article.

Washington. Each affected person reported conjunctivitis, and some also reported respiratory symptoms (*6*). The mean cycle threshold (Ct) value to detect influenza A matrix gene from the H5-positive specimens was 33 (range 25–36.9).

After multiple genetic sequencing attempts at CDC, we obtained complete hemagglutinin (HA) gene sequences from 5 confirmed cases and partial or complete neuraminidase (NA) gene sequences from 4 confirmed cases. On the basis of the available HA and NA sequences, the viruses in the specimens belonged to HPAI H5N1 clade 2.3.4.4b. Sequences of the internal gene segments were only available from 4 human cases at various levels of completion. We observed minimal genetic variation among human cases; we submitted all available gene sequences to GISAID (https://www.gisaid.org) and GenBank (Appendix Table 1, https://wwwnc.cdc.gov/EID/article/31/12/25-1118-App1.pdf).

We attempted virus isolation by inoculating the positive specimens in 10–11-day-old embryonated chicken eggs, MDCK cells, or both. We isolated A/Washington/239/2024 from a conjunctival specimen in MDCK cells and isolated A/Washington/254/2024 and A/Washington/255/2024 from the conjunctival specimens in eggs. We also isolated A/Washington/240/2024 in eggs from both conjunctival and nasopharyngeal specimens (Table).

Since late 2021, at least 6 distinct introductions of clade 2.3.4.4b A(H5) viruses from Europe and Asia (genotypes A1–A6) have occurred in the United States. Each introduction was followed by reassortment events that generated many different genotypes (*8*,*9*). Phylogenetic analysis of the 8 gene segments from H5N1 viruses in the specimens of the Washington human cases determined that they belonged to genotype D1.1. That genotype derived from the Eurasian genotype A3 and acquired North American wild bird lineage polymerase basic (PB) 2 (am24 group), polymerase acidic (am4 group), nucleoprotein (am13 group), and NA (am4N1 group) gene segments (Figure 1; Appendix Figures 1–6). Genotype D1.1 is different from genotype B3.13, which derived from the Eurasian genotype A1 after acquiring North American wild bird lineage PB2 (am2.2 group), PB1 (am4 group), nucleoprotein (am8 group), and nonstructural (am1.1 group) gene segments after reassortment.

Phylogenetically, HA sequences from the Washington human cases belonged to the Eurasian ea3 group and were closely related to viruses detected from the Washington poultry outbreak. Those HA sequences also resembled sequences from wild birds detected in British Columbia, Canada, during 2024 (Figure 1, panel A). The HA sequences from the Washington D1.1 human cases did not contain mutations known to be associated with increased infectivity or transmissibility among humans (FluSurver, https://flusurver.bii.a-star.edu.sg). The NA gene segments of H5N1 clade 2.3.4.4b viruses circulating in the United States have been predominantly Eurasian lineage since their introduction (*8*). However, the D1.1 viruses detected in the Washington cases all contained North American lineage N1 NA genes closely related to those of H5N1 viruses detected in poultry and wild birds in British Columbia in 2024 and H1N1 viruses detected in wild birds in the United States and Canada in 2023 (Figure 1, panel B). The available NA and internal gene sequences from the Washington D1.1 human cases lacked changes associated with

Table. Hemagglutination inhibition testing of highly pathogenic avian influenza A(H5N1) clade 2.3.4.4b genotype D1.1 viruses isolated from poultry farm workers, Washington, USA, 2024*

Antigens	Subtype	Clade	Hemagglutination inhibition titer†						
			CDC-RG	RG71A	RG71A	RG78A	RG78A	NIID-002	TX/37
Reference antigens									
CDC-RG, A/Vietnam/1203/2004	H5N1	1	**2,560**	<10	<10	<10	<10	<10	<10
IDCDC-RG71A, A/Astrakhan/3212/2020	H5N8	2.3.4.4b	10	**160**	**160**	80	80	40	<10
IDCDC-RG78A, A/American Wigeon/South Carolina/22-000345-001/2021	H5N1	2.3.4.4b	10	160	160	**160**	**320**	80	80
NIID-002, A/Ezo red fox/Hokkaido/1/2022	H5N1	2.3.4.4b	10	160	320	160	160	**80**	80
A/Texas/37/2024	H5N1	2.3.4.4b	10	80	80	160	160	80	**80**
Test antigens									
A/Washington/239/2024, conjunctival‡	H5N1	2.3.4.4b	10	80	160	160	160	80	80
A/Washington/240/2024, conjunctival§	H5N1	2.3.4.4b	10	80	80	160	160	40	40
A/Washington/240/2024, nasopharyngeal§	H5N1	2.3.4.4b	10	80	80	320	320	80	80
A/Washington/254/2024, conjunctival§	H5N1	2.3.4.4b	10	80	40	160	160	80	80
A/Washington/255/2024, conjunctival§	H5N1	2.3.4.4b	10	40	40	160	160	80	40

*Bold indicates homologous titers. TX/37, A/Texas/37/2024.
†Two different lots of ferret antiserum against RG71A or RG78A were used in this test.
‡Isolated on MDCK cells.
§Isolated in 10–11-day-old embryonated chicken eggs.

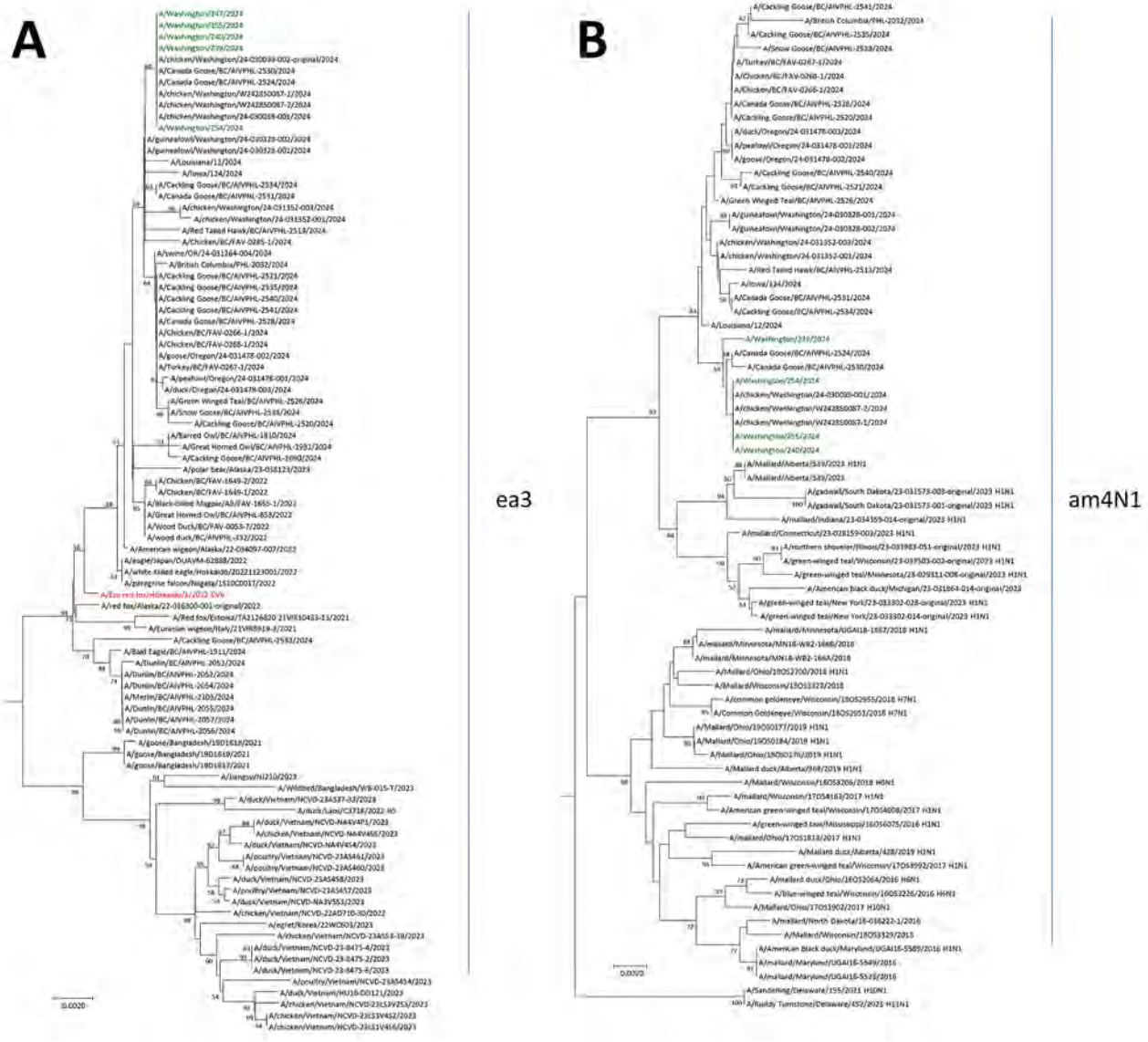

Figure 1. Neighbor-joining phylogenetic trees of highly pathogenic avian influenza A(H5N1) clade 2.3.4.4b viruses isolated from poultry farm workers, Washington, USA, 2024. A) Hemagglutinin gene segment; B) neuraminidase gene segment. Green font indicates influenza A(H5N1) D1.1 viruses from Washington human cases; red font indicates prepandemic candidate vaccine virus A/Ezo red fox/Hokkaido/1/2022. Bootstrap values >50, generated from 1,000 replicates, are labeled on branch nodes. Scale bars indicate nucleotide substitutions per site.

reduced antiviral susceptibility or mammalian adaptation. They also lacked PB2-M631L mutation that was detected in most B3.13 viral sequences (*10*–*12*).

The HA sequences from the Washington D1.1 viruses also lacked changes previously associated with increased binding to mammalian-like α2,6 sialic acid receptors. Glycan microarray analysis of the representative virus isolate A/Washington/240/2024 suggested that the Washington D1.1 H5N1 virus retained preferential binding to avian-like α2,3 sialic acid receptors (Figure 2). We used 3 A(H5) clade 2.3.4.4b prepandemic CVVs in this study: IDCDC-RG78A (A/American wigeon/South Carolina/22-000345-001/2021), NIID-002 (A/Ezo red fox/Hokkaido/1/2022), and IDCDC-RG71A (A/Astrakhan/3212/2020). Compared with the most closely related CVV, NIID-002 (HA group ea3), the HA sequences from Washington H5N1 D1.1 viruses (also HA group ea3) all carried 2 amino acid differences at T36A and N476D (mature H5 numbering); neither substitution was located within putative antigenic sites. The HA from Washington H5N1 D1.1 viruses also had 3 amino acid differences relative to IDCDC-RG71A (HA group ea3) and 6 relative to IDCDC-RG78A (HA group ea1), and 1 difference

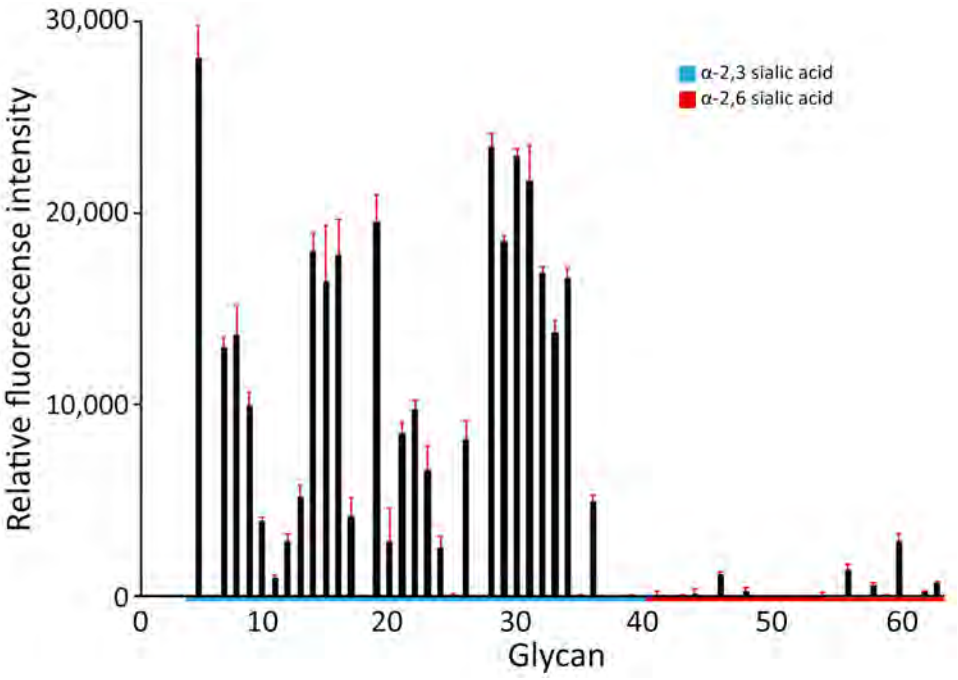

Figure 2. Glycan microarray analysis of highly pathogenic avian influenza A(H5N1) clade 2.3.4.4b virus isolated from poultry farm workers, Washington, USA, 2024. Clade 2.3.4.4b genotype D1.1 H5N1 virus A/Washington/240/2024 was isolated from a confirmed Washington human case. Glycans containing α-2,3 sialic acid and α-2,6 sialic acid are shown. Error bars reflect SDs from 6 independent replicates on the microarray. Details of the glycan structures are listed in Appendix Table 2 (https://wwwnc.cdc.gov/EID/article/31/12/25-1118-App1.pdf).

was in the putative antigenic site D (Appendix Table 3). Hemagglutination inhibition (HI) assays indicated that all available Washington H5N1 D1.1 virus isolates cross-reacted well with ferret antisera raised against each of the 3 clade 2.3.4.4b CVVs. Ferret antiserum raised to NIID-002 and IDCDC-RG78A cross-reacted with the D1.1 viruses at heterologous HI titers equal to or within 2-fold of the homologous HI titer (Table). Ferret antisera raised against IDCDC-RG71A cross-reacted with the D1.1 viruses at heterologous HI titers 2- to 4-fold lower than the homologous HI titer. Ferret antiserum raised against A/Texas/37/2024, the virus isolated from an H5N1 human case in 2024 associated with a dairy cattle outbreak (genotype B3.13), also cross-reacted well with the Washington D1.1 H5N1 virus isolates at heterologous HI titers ≤2-fold of the homologous HI titer (Table).

Conclusions

We detected human cases of HPAI H5N1 clade 2.3.4.4b genotype D1.1 in poultry farm workers in Washington. Additional human cases of H5N1 D1.1 virus infection have been subsequently reported, including a fatal human case detected in Louisiana, USA (*13*), and 2 severe human cases, 1 detected in British Columbia, Canada (*14*), and 1 in Wyoming, USA (*15*). Among the virus genomes detected in the Washington cases, we noted no changes that are known to be associated with mammalian adaptation, increased infectivity, or transmissibility among humans. Washington H5N1 D1.1 virus retained avian-like α2,3 sialic acid receptor binding preference and cross-reacted well with ferret antiserum raised against A(H5) clade 2.3.4.4b prepandemic CVVs available to vaccine manufacturers. Nonetheless, continued surveillance and testing of clade 2.3.4.4b A(H5) viruses remain essential for influenza pandemic preparedness.

Acknowledgments

We thank the persons who provided specimens and information for this investigation. We also thank Trent Bullock for his editorial assistance.

This study was supported by the Influenza Division, National Center for Immunization and Respiratory Diseases, Centers for Disease Control and Prevention.

About the Author

Dr. Hatta is a senior service fellow in the Influenza Division, National Center for Immunization and Respiratory Diseases, Centers for Disease Control and Prevention, Atlanta, GA, USA. Her research interests focus on improving influenza vaccine effectiveness by developing new vaccine platforms and performing antigenic characterizations.

References

1. Abdelwhab EM, Beer M. Panzootic HPAIV H5 and risks to novel mammalian hosts. Npj Viruses. 2024;2:22. https://doi.org/10.1038/s44298-024-00039-z
2. Caliendo V, Lewis NS, Pohlmann A, Baillie SR, Banyard AC, Beer M, et al. Transatlantic spread of highly pathogenic avian influenza H5N1 by wild birds from Europe to North America

in 2021. Sci Rep. 2022;12:11729. https://doi.org/10.1038/s41598-022-13447-z
3. Caserta LC, Frye EA, Butt SL, Laverack M, Nooruzzaman M, Covaleda LM, et al. Spillover of highly pathogenic avian influenza H5N1 virus to dairy cattle. Nature. 2024;634:669–76. https://doi.org/10.1038/s41586-024-07849-4
4. Krammer F, Hermann E, Rasmussen AL. Highly pathogenic avian influenza H5N1: history, current situation, and outlook. J Virol. 2025;99:e0220924. https://doi.org/10.1128/jvi.02209-24
5. Centers for Disease Control and Prevention. H5 bird flu: current situation [cited 2025 Sep 24]. https://www.cdc.gov/bird-flu/situation-summary/index.html
6. Garg S, Reinhart K, Couture A, Kniss K, Davis CT, Kirby MK, et al. Highly pathogenic avian influenza A(H5N1) virus infections in humans. N Engl J Med. 2025;392:843–54. https://doi.org/10.1056/NEJMoa2414610
7. World Health Organization. Zoonotic influenza: candidate vaccine viruses and potency testing reagents [cited 2025 Sep 24]. https://www.who.int/teams/global-influenza-programme/vaccines/who-recommendations/zoonotic-influenza-viruses-and-candidate-vaccine-viruses
8. Youk S, Torchetti MK, Lantz K, Lenoch JB, Killian ML, Leyson C, et al. H5N1 highly pathogenic avian influenza clade 2.3.4.4b in wild and domestic birds: Introductions into the United States and reassortments, December 2021–April 2022. Virology. 2023;587:109860. https://doi.org/10.1016/j.virol.2023.109860
9. Tawidian P, Torchetti MK, Killian ML, Lantz K, Dilione KE, Ringenberg JM, et al. Genotypic clustering of H5N1 avian influenza viruses in North America evaluated by ordination analysis. Viruses. 2024;16:1818. https://doi.org/10.3390/v16121818
10. Nguyen T-Q, Hutter CR, Markin A, Thomas M, Lantz K, Killian ML, et al. Emergence and interstate spread of highly pathogenic avian influenza A(H5N1) in dairy cattle in the United States. Science. 2025;388:eadq0900. https://doi.org/10.1126/science.adq0900
11. Nguyen HT, Chesnokov A, De La Cruz J, Pascua PNQ, Mishin VP, Jang Y, et al. Antiviral susceptibility of clade 2.3.4.4b highly pathogenic avian influenza A(H5N1) viruses isolated from birds and mammals in the United States, 2022. Antiviral Res. 2023;217:105679. https://doi.org/10.1016/j.antiviral.2023.105679
12. Signore AV, Joseph T, Ranadheera C, Erdelyan CNG, Alkie TN, Raj S, et al. Neuraminidase reassortment and oseltamivir resistance in clade 2.3.4.4b A(H5N1) viruses circulating among Canadian poultry, 2024. Emerg Microbes Infect. 2025;14:2469643. https://doi.org/10.1080/22221751.2025.2469643
13. Centers for Disease Control and Prevention. First H5 bird flu death reported in United States [cited 2025 Jan 6]. https://www.cdc.gov/media/releases/2025/m0106-h5-birdflu-death.html
14. Jassem AN, Roberts A, Tyson J, Zlosnik JEA, Russell SL, Caleta JM, et al. Critical illness in an adolescent with influenza A(H5N1) virus infection. N Engl J Med. 2025;392:927–9. https://doi.org/10.1056/NEJMc2415890
15. Centers for Disease Control and Prevention. CDC A(H5N1) bird flu response update [cited 2025 Feb 26]. https://www.cdc.gov/bird-flu/spotlights/h5n1-response-02262025.html

Address for correspondence: Han Di, Centers for Disease Control and Prevention, 1600 Clifton Rd NE, Mailstop H23-6, Atlanta, GA 30329-4027, USA; email: nnu7@cdc.gov

Bat Reovirus as Cause of Acute Respiratory Disease and Encephalitis in Humans, Bangladesh, 2022–2023

Sharmin Sultana,[1] Ariful Islam,[1] James Ng, Sunil Kumar Dubey, Manjur Hossain Khan, Cheng Guo, Mohammed Ziaur Rahman, Joel M. Montgomery, Syed Moinuddin Satter, Tahmina Shirin, W. Ian Lipkin, Lisa Hensley,[2] Nischay Mishra[2]

We report 5 patients in Bangladesh presumed to have Nipah virus infections after consuming raw date palm sap. PCR and serology for Nipah virus were negative, but high-throughput sequencing identified *Pteropine orthoreovirus* in archived throat swab samples and virus cultures. This batborne virus should be considered in differential diagnosis of Nipah-like illnesses.

Bats are the natural reservoir of numerous known and novel zoonotic viruses, including rabies, Nipah, Hendra, Marburg, and severe acute respiratory syndrome viruses (*1*). In Bangladesh, Nipah virus (NiV) outbreaks are seasonal, and cases peak during December–April annually. In 2006, the Institute of Epidemiology, Disease Control and Research, Bangladesh (Dhaka, Bangladesh); icddr,b (Dhaka); and US Centers for Disease Control and Prevention (Atlanta, GA, USA) collaboratively established a hospital-based national sentinel surveillance program to address public health risks posed by NiV (*2*). During 2006–2022, the program enrolled >22,000 patients with symptoms of NiV infection. We report detection of *Pteropine orthoreovirus* (PRV) from 5 NiV-negative patients with acute respiratory disease and encephalitis during a 2022–2023 outbreak.

The Study

PRV is an emerging batborne orthoreovirus previously linked to acute respiratory infections in humans, especially in Southeast Asia (*4*–*6*). PRV is classified under the genus *Orthoreovirus*, family Reoviridae, which includes Nelson Bay virus (NBV), identified in Australia in 1968 (*7*). Zoonotic potential of NBV was confirmed in 2006, when a human case occurred in Melaka, Malaysia (*8*).

PRVs are nonenveloped, fusogenic viruses with double-stranded RNA genomes composed of 10 segments (S1, S2, S3, S4, M1, M2, M3, L1, L2, and L3). The S1 segment is tricistronic, encoding 3 proteins: cell-attachment protein, fusion-associated small transmembrane protein, and nonstructural protein p17 of unknown function (*9*).

The Bangladesh surveillance program uses quantitative PCR on throat swab samples to test for NiV RNA and on serum for NiV IgG or IgM. During December 2022–March 2023, five patients with presumptive NiV infection diagnoses were admitted to hospitals in Bangladesh but tested NiV-negative (Table). Three patients were admitted to Faridpur Medical College Hospital (MCH) (Faridpur, Bangladesh), and 1 patient each was admitted to Rajshahi MCH (Rajshahi, Bangladesh) and Khulna MCH (Khulna,

Author affiliations: Institute of Epidemiology, Disease Control and Research (IEDCR), Dhaka, Bangladesh (S. Sultana, A. Islam, M. Hossain Khan, T. Shirin); Gulbali Research Institute, Charles Sturt University, Wagga Wagga, New South Wales, Australia (A. Islam); Center for Infection and Immunity, Mailman School of Public Health, Columbia University, New York, New York, USA (J. Ng, S. Kumar Dubey, C. Guo, W.I. Lipkin, N. Mishra); icddr,b, Dhaka (M.Z. Rahman, S. Moinuddin Satter); Centers for Disease Control and Prevention, Zoonotic Atlanta, Georgia, USA (J.M. Montgomery) and Emerging Disease Research Unit, National Bio and Agro-Defense Facility, USDA Agricultural Research Service Manhattan, Kansas, USA (L. Hensley)

DOI: https://doi.org/10.3201/eid3112.250797

[1]These first authors contributed equally to this article.

[2]These last authors contributed equally to this article.

Bangladesh). All patients had clinical signs and symptoms, including fever, disorientation, altered mental status, abnormal gait, and difficulty breathing. Four patients had a primary diagnosis of encephalitis, and 1 pediatric case had mild symptoms and a primary diagnosis of febrile convulsions (Table). All patients reported consuming raw date palm sap within 2 weeks of symptoms developing.

Patients originated from different geographic regions of Bangladesh. Case-patients BDB047, BDB051, and BDB052 were from Faridpur and Rajbari, within a 30-mile radius of central Bangladesh, near the Padma River Basin (Figure 1). Those 3 patients and pediatric case-patient BDB113 from Khulna (≈180 km south of Faridpur and Rajbari) were hospitalized within the same 2-week period in late December 2022 and early January 2023 (Table). Case-patient BDB040 was admitted in Sirajganj (≈150 km north of Faridpur and Rajbari) during March–April 2023. That patient had a history of chronic mental illness and also consumed raw date palm sap while hospitalized.

All patients were discharged after 2–3 weeks. During telehealth follow-up >15 months after discharge, case-patients BDB047 and BDB052 reported persistent fatigue, disorientation, and breathing and walking difficulties. Case-patients BDB051 and BDB113 fully recovered, but case-patient BDB040 died in August 2024, following deteriorating health and unexplained neurologic issues (Table).

We conducted viral discovery by using a capture-based agnostic viral sequencing method, VirCap Seq-VERT (VCS) (*3*), on total nucleic acid extracted from archived throat swab samples collected in

Table. Characteristics of patients in study of bat reovirus as cause of acute respiratory disease and encephalitis in humans, Bangladesh, 2022–2023*

	Patient identification no.				
Geographic and clinical data	BDB047	BDB051	BDB052	BDB113	BDB040†
Age, y/sex	65/M	17/F	65/M	2/M	56/M
District	Rajbari	Faridpur	Rajbari	Khulna	Sirajganj
Diagnosis at admission	Encephalitis	Encephalitis	Encephalitis	Febrile convulsions	Encephalitis
Symptom onset date	2022 Dec 27	2023 Jan 3	2023 Jan 5	2023 Jan 2	2023 Mar 31
Date palm sap consumption	Y	Y	Y	Y	Y
Frequency, no. times	1	4	1	1	1
Date first consumed	2022 Dec 14	2023 Jan 1	2022 Dec 27	2022 Dec 31	2023 Apr 4
Throat swab collection date	2022 Dec 29	2023 Jan 3	2023 Jan 7	2023 Jan 2	2023 Apr 6
Hospitalization data					
Duration of hospital stay, d	9	2	9	8	14
Symptons at admission					
Fever	Y	Y	Y	Y	Y
Difficulty in breathing	Y	N	N	N	N
Disorientation	Y	Y	Y	N	Y
Vomiting	N	N	Y	N	N
Diarrhea	N	N	Y	N	N
Altered mental status	Y	N	Y	N	Y
Headache	N	Y	Y	N	Y
Stiff neck	Y	N	N	N	Y
Convulsions	N	N	N	Y	N
Unconscious	Y	N	N	Y	N
Salivation	N	N	Y	N	N
Mental status‡	Moderate	Mild	Moderate	Moderate	Mild
Neurologic details, motor	Abnormal gait movements	Mild, abnormal tone	Moderate; abnormal gait, movements	Moderate; abnormal gait, movements	Normal
qPCR and virus culture					
PRV viral load, Ct	24.50	19.17	30.48	33.40	Undetected
Positive virus culture	Y	Y	N	Y	N
Discharge health status	Alive	Alive	Alive	Alive	Alive
Telehealth followup§					
Health status	Alive	Alive	Alive	Alive	Dead
Date of follow	2024 May 21	2024 May 21	2024 May 21	2024 May 21	2024 Oct 30
Condition recorded	Difficulty walking; weakness, disorientation, occasional respiratory distress	Fully recovered; healthy	Generalized weakness and musculoskeletal pain	Fully recovered; healthy	Died in August 2024

*Ct, cycle threshold; PRV, *Pteropine orthoreovirus*.
†Patient had prior history of mental disorder and other cognitive disabilities before the onset of Nipah virus–like illness in April 2023. He also consumed date palm sap while hospitalized. The patient later died in August 2024 due to unexplained neurological disease.
‡Moderate: lethargic, decreased response; mild: confused, disoriented, or agitated.
§Telehealth followup was conducted >15 mo after hospital discharge.

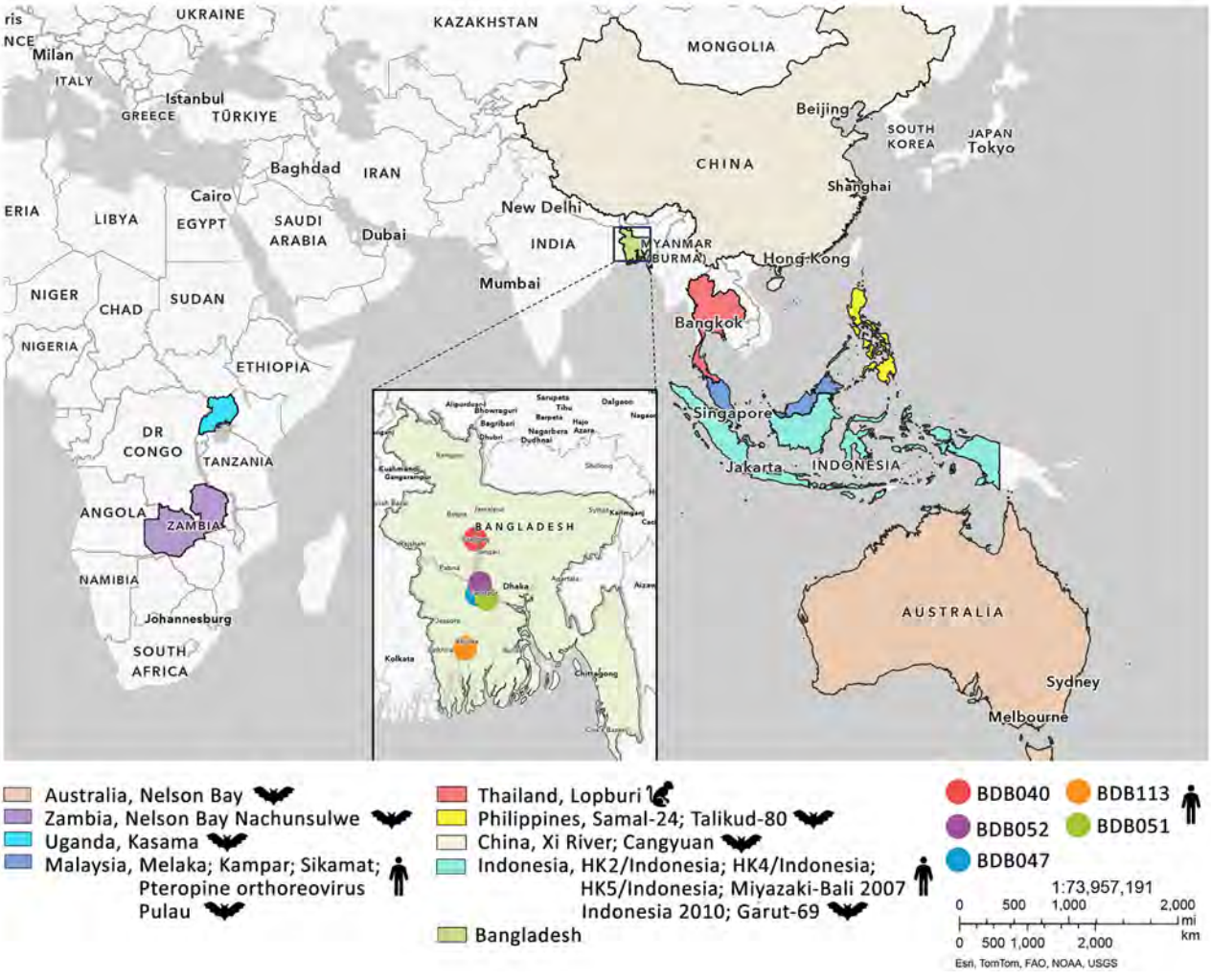

Figure 1. Study locations and locations for related viruses from study of bat reovirus as cause of acute respiratory disease and encephalitis in humans, Bangladesh, 2022–2023. Inset shows Bangladesh with color-coded locations of patients (BDB040, BDB052, BDB047, BDB113, and BDB051) from whom we detected Pteropine orthoreovirus in archived throat swab samples. Larger map shows global locations from which related viruses have been detected in humans, bats, and monkeys.

viral-transport media. We perfomed VCS on NextSeq 2000 (Illumina, https://www.illumina.com), as previously described (*3*). We further used Megablast (MEGA, https://www.megasoftware.net) to compare retrieved sequences to those in GenBank nucleotide databases (Appendix, https://wwwnc.cdc.gov/EID/article/31/12/25-0797-App1.pdf). VCS analysis revealed PRV reads in all patients. We did not identify any other viral or bacterial pathogens in high-throughput sequencing.

We quantified viral load by using an in-house L2-based quantitative PCR (Appendix Table 1). Case-patient BDB051 had the highest viral load, likely due to the short (≈2-day) interval between raw date palm sap consumption and sample collection (Table). Case-patients BDB047 and BDB052 had higher viral loads than did BDB113 and BDB040.

For phylogenetic analysis, we amplified the partial S1 segment encoding the p10 protein (96 aa) by using a consensus PCR (Figure 2; Appendix Table 2). The Bangladesh PRVs clustered at 99.3%–100.0% average nucleotide identity (ANI). Those PRVs showed ≈96% ANI with the Indonesia/2010 detected from a large flying fox (*Pteropus vampyrus*) in Indonesia, ≈85% ANI with the Nachunsulwe-57 detected from an Egyptian fruit bat (*Rousettus aegyptiacus*) in Zambia, and ≈77% ANI with the Kasama strain detected from an Angolan soft-furred fruit bat (*Lissonycteris angolensis*) in Uganda (*10*,*11*). The Bangladesh PRVs also had >77.0% ANI with Xi River virus from a fulvous fruit bat (*R. leschenaultii*) from China, Garut-69 virus from a large flying fox from Indonesia, and the 1968 prototypic NBV from a grey-headed flying fox (*P. policephalus*) in Australia.

To test whether molecular detection (VCS, quantitative PCR, and partial S1 amplicon sequencing) corresponded to infectious virus presence, we inoculated throat swab samples into MDCK cells and examined for cytopathic effects. After 2 MDCK passages, we passaged PRVs once in Vero cells. We successfully cultured virus from 3 swab samples (case-patients BDB047, BDB051, and BDB113) and sequenced on the MiSeq (Illumina) platform. We mapped reads to PRV genomes by using Geneious Prime (https://www.geneious.com) software.

Complete coding sequences of all 10 Bangladesh PRV segments (GenBank accession nos. PP803379–408) showed 91.1%–100% ANI among themselves (Appendix Table 3). S1 segments showed 96.7%–99.9% ANI with each other and clustered with Indonesia/2010 strain, NBV-Australia, NBV-Nachunsulwe-57, and Kasama virus (Figure 3, panel A). Phylogeny of S2 and S3 segments were partially consistent with S1 segments (Figure 3, panels B, C). S4 segments clustered with Kampar and Melaka NBV strains (Figure 3, panel D**)**, previously linked to mild respiratory illness in humans and reported human-to-human transmission (*8*,*12*).

L1, L2, L3, M1, M2, and M3 segments clustered with different PRVs isolated from fruit bats and occasionally from humans in Indonesia and Malaysia (Appendix Figure). That finding suggests unique evolution of each segment from reassortment events among strains circulating in Southeast Asia and long flight ranges of fruit bats. Reassortment is common for segmented RNA virus evolution and enhances risk for zoonotic potential (*13*). All Bangladesh PRV segments showed >76% ANI with NBV-Australia, exceeding the Internationl Committee for Taxonomy of Viruses 2022 species demarcation criteria of <75% ANI (*14*). Thus, the detected PRVs belong to NBV species but are distinct from other mammalian and avian reoviruses.

Conclusions

Humans in Bangladesh commonly consume raw date palm sap, especially in winter. Raw date palm sap is also a food source for fruit bats during winter and is the primary zoonotic route for NiV spillover from bats to humans (*15*). All 5 patients lived within 30–200 km of central Bangladesh but had no known contact with one another. Patients consumed raw date palm sap within 14 days of symptoms developing. Although no contemporaneous sap samples were available for analysis, we speculate that those PRV infections resulted from the consumption of raw date palm sap contaminated with bat excreta. All 5 patients had severe respiratory and neurologic symptoms, but PRV infections in Malaysia, Indonesia, and Vietnam were associated with milder respiratory disease (*5*,*8*,*12*).

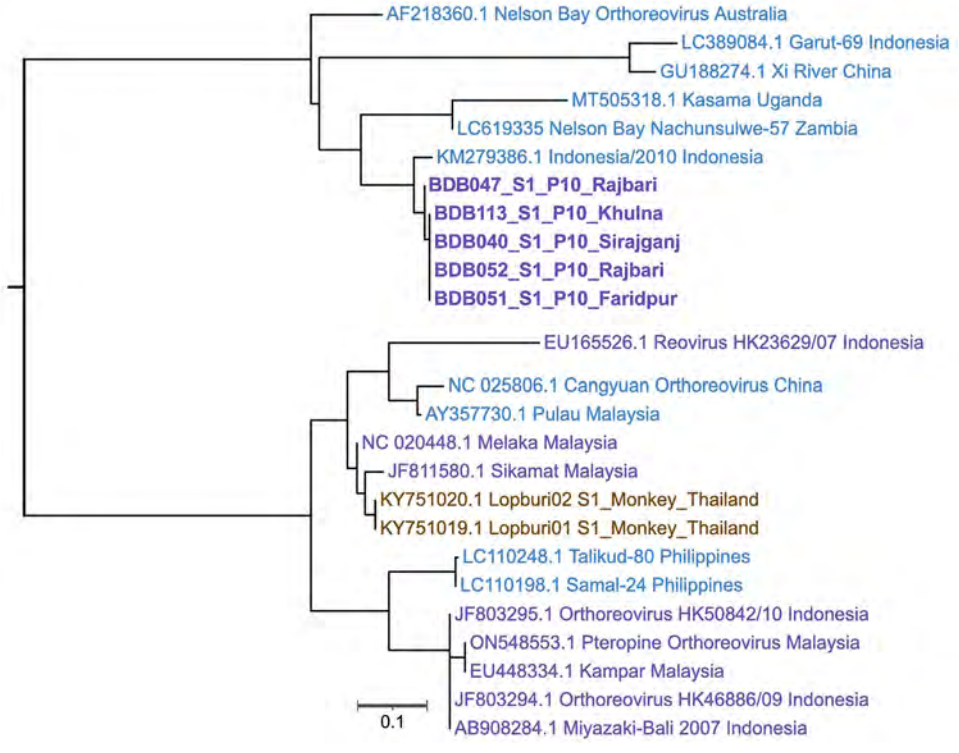

Figure 2. Phylogenic analysis of bat reovirus detected from cases of acute respiratory disease and encephalitis in humans, Bangladesh, 2022–2023. Sequencing of the partial S1 segment showed that Pteropine orthoreovirus from patients in Bangladesh (bold) clustered with 99.3%–100.0% average nucleotide identity (ANI). Bangladesh PRV showed ≈96% ANI with the Indonesia/2010 strain detected from large flying-fox (*Pteropus vampyrus*) in Indonesia (GenBank accession no. KM279386.1) and ≈85% ANI with the Nachunsulwe-57 strain detected from an Egyptian fruit bat (*Rousettus aegyptiacus*) in Zambia (accession no. LC619335) in 2018. GenBank accession numbers are indicated for reference sequences. Scale bar indicates nucleotide substitutions per site.

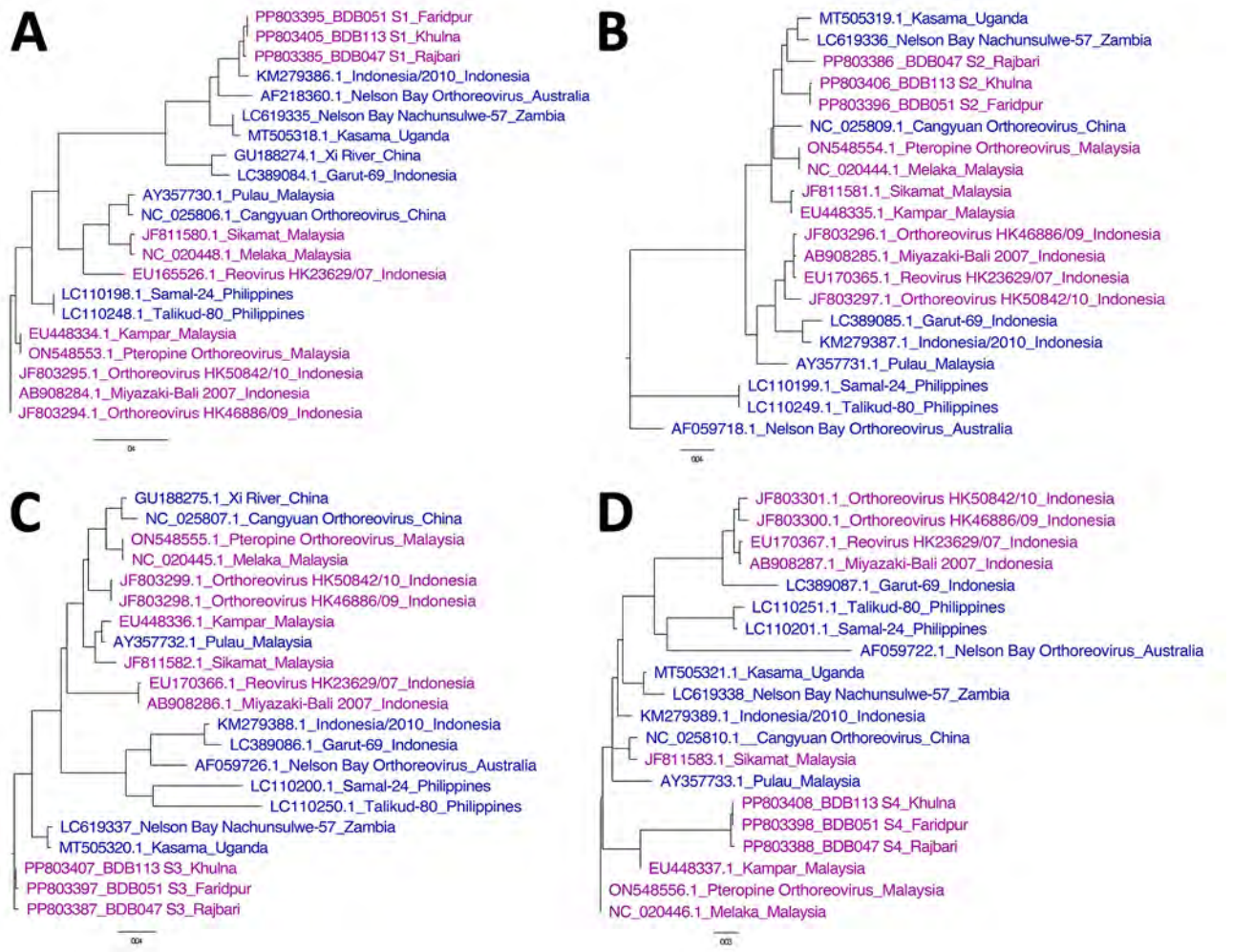

Figure 3. Comparitive phylogeny of bat reovirus as cause of acute respiratory disease and encephalitis in humans, Bangladesh, 2022–2023. A) S1 segment phylogeny showing 96.7%–99.9% average nucleotide identity (ANI) with each other (BDB051, BDB113, and BDB047) and clustered with Indonesia/2010, NBV-Australia, NBV-Nachunsulwe-57, and Kasama virus. B, C) Phylogeny of S2 (B) and S3 (C) segments showing partial consistency with S1 segments. D) S4 segments clustered with Kampar and Melaka strains, previously linked to mild respiratory illness in humans and reported human-to-human transmission. GenBank accession numbers are indicated. Scale bars indicate nucleotide substitutions per site.

Because we focused on severe disease, we cannot exclude the possibility that PRVs in Bangladesh can also cause mild infections.

In summary, human PRV infection can have signs and symptoms similar to those of NiV infection. Like NiV infections, PRV infections can be linked to consumption of date palm sap contaminated with bat excreta. The potential for reassortment in segmented viruses like PRV can result in changes in transmissibility and virulence. Thus, in areas where raw date palm sap is consumed, molecular and serologic surveillance and differential diagnoses of respiratory illnesses with encephalitis and other unexplained febrile illnesses should include PRV, NiV, and other batborne viruses.

Acknowledgments

We highly acknowledge laboratory and field staff from CDC, IEDCR, and icddr,b for collecting specimens from clinical cases, recording metadata, and screening for NiV.

This study was approved by the icddr,b research review committee (approval no. PR-2005-026).

This project was supported with funds provided by United States Department of Agriculture agreements with Columbia University (NACA-58-3022-2-021 and NACA-58-3022-4-053).

About the Authors

Dr. Sultana is an assistant professor of virology and currently serves as a senior scientific officer at the Institute of

Epidemiology, Disease Control and Research (IEDCR) in Bangladesh. Her research focuses on the intersection of human, animal, and environmental health through the One Health approach. Dr. Islam is a One Health epidemiologist at Charles Sturt University, Wagga Wagga, NSW, Australia. His research interests focus on how viruses spill over from wildlife to humans and how we can integrate viral genetics, epidemiology, ecology, and human behaviour to prevent zoonotic disease transmission.

References

1. Letko M, Seifert SN, Olival KJ, Plowright RK, Munster VJ. Bat-borne virus diversity, spillover and emergence. Nat Rev Microbiol. 2020;18:461–71. https://doi.org/10.1038/s41579-020-0394-z
2. Satter SM, Aquib WR, Sultana S, Sharif AR, Nazneen A, Alam MR, et al. Tackling a global epidemic threat: Nipah surveillance in Bangladesh, 2006–2021. PLoS Negl Trop Dis. 2023;17:e0011617. https://doi.org/0.1371/journal.pntd.0011617
3. Briese T, Kapoor A, Mishra N, Jain K, Kumar A, Jabado OJ, et al. Virome capture sequencing enables sensitive viral diagnosis and comprehensive virome analysis. mBio. 2015;6:e01491-15. https://doi.org/10.1128/mBio.01491-15
4. Bennett AJ, Goldberg TL. Pteropine orthoreovirus in an Angolan soft-furred fruit bat (*Lissonycteris angolensis*) in Uganda dramatically expands the global distribution of an emerging bat-borne respiratory virus. Viruses. 2020;12:740. https://doi.org/10.3390/v12070740
5. Tee KK, Chan PQ, Loh AM, Singh S, Teo CH, Iyadorai T, et al. Surveillance, isolation and genomic characterization of *Pteropine orthoreovirus* of probable bat origin among patients with acute respiratory infection in Malaysia. J Med Virol. 2023;95:e28520. https://doi.org/10.1002/jmv.28520
6. Vega-Rodriguez W, Ly H. Emerging *Pteropine* orthoreoviruses and their potential impact on public health. J Med Virol. 2023;95:e28588. https://doi.org/10.1002/jmv.28588
7. Gard GP, Marshall ID. Nelson Bay virus. A novel reovirus. Arch Gesamte Virusforsch. 1973;43:34–42. https://doi.org/10.1007/BF01249346
8. Chua KB, Crameri G, Hyatt A, Yu M, Tompang MR, Rosli J, et al. A previously unknown reovirus of bat origin is associated with an acute respiratory disease in humans. Proc Natl Acad Sci U S A. 2007;104:11424–9. https://doi.org/10.1073/pnas.0701372104
9. Kawagishi T, Kanai Y, Tani H, Shimojima M, Saijo M, Matsuura Y, et al. Reverse genetics for fusogenic bat-borne orthoreovirus associated with acute respiratory tract infections in humans: role of outer capsid protein σC in viral replication and pathogenesis. PLoS Pathog. 2016;12:e1005455. https://doi.org/10.1371/journal.ppat.1005455
10. Harima H, Sasaki M, Orba Y, Okuya K, Qiu Y, Wastika CE, et al. Attenuated infection by a *Pteropine orthoreovirus* isolated from an Egyptian fruit bat in Zambia. PLoS Negl Trop Dis. 2021;15:e0009768. https://doi.org/10.1371/journal.pntd.0009768
11. Lorusso A, Teodori L, Leone A, Marcacci M, Mangone I, Orsini M, et al. A new member of the Pteropine orthoreovirus species isolated from fruit bats imported to Italy. Infect Genet Evol. 2015;30:55–8. https://doi.org/10.1016/j.meegid.2014.12.006
12. Chua KB, Voon K, Crameri G, Tan HS, Rosli J, McEachern JA, et al. Identification and characterization of a new orthoreovirus from patients with acute respiratory infections. PLoS One. 2008;3:e3803. https://doi.org/10.1371/journal.pone.0003803
13. McDonald SM, Nelson MI, Turner PE, Patton JT. Reassortment in segmented RNA viruses: mechanisms and outcomes. Nat Rev Microbiol. 2016;14:448–60. https://doi.org/10.1038/nrmicro.2016.46
14. Matthijnssens J, Attoui H, Bányai K, Brussaard CPD, Danthi P, Del Vas M, et al. ICTV virus taxonomy profile: *Spinareoviridae* 2022. J Gen Virol. 2022;103. https://doi.org/10.1099/jgv.0.001781
15. Luby SP, Rahman M, Hossain MJ, Blum LS, Husain MM, Gurley E, et al. Foodborne transmission of Nipah virus, Bangladesh. Emerg Infect Dis. 2006;12:1888–94. https://doi.org/10.3201/eid1212.060732

Address for correspondence: Nischay Mishra, Mailman School of Public Health, Columbia University, Center for Infection and Immunity, 722 W 168th St, 17th Fl, New York, NY 10032, USA; email: nm2641@cumc.columbia.edu

Pancreatic Schistosomiasis, China, 2020–2024

Long He,[1] Chuanbing Zhao,[1] Yu Lu,[1] Hongzhen Wei, Zanglong Deng, Yunpeng Zhang, Tao Yin

Schistosomiasis is a globally prevalent parasitic infection, but pancreatic involvement is extremely rare. In this article, we report 4 cases of pancreatic schistosomiasis from endemic regions in China. The possible link between schistosomiasis and pancreatic malignancy deserves further study. These cases underscore the diagnostic challenge of pancreatic schistosomiasis.

Schistosomiasis is a parasitic infection caused by trematodes of the genus *Schistosoma* (*1*). Globally, ≈1 billion people are at risk for schistosomiasis and there have been 250 million cases across 78 countries. By 2021, the disease accounted for >1.8 million disability-adjusted life years lost. *Schistosoma* infection is closely linked to impoverished living conditions (*2*).

The *Schistosoma* lifecycle requires an intermediate host, such as *Biomphalaria*, *Bulinus*, and *Oncomelania* snails, before infecting and causing disease in definitive hosts such as humans or other mammals (*3*). The main pathogenic species in humans are *S. hematobium*, *S. japonicum*, and *S. mansoni*. Although adult worms are relatively nonpathogenic, their eggs induce granulomatous inflammation characterized by eosinophilic and lymphocytic infiltration, leading to both acute and chronic disease (*4*).

The clinical manifestations of schistosomiasis are related to infection intensity and duration, and the intestines, liver, and bladder are the most involved organs (*2*). Early infection might manifest as cercarial dermatitis. Acute schistosomiasis is often asymptomatic, but sudden onset of fever, myalgia, fatigue, and abdominal pain lasting 2–10 weeks can occur. Chronic schistosomiasis is typically characterized by nonspecific, intermittent abdominal pain, diarrhea, and rectal bleeding (in *S. mansoni* and *S. japonicum* infections) or hematuria (in *S. hematobium* infection). In advanced chronic cases, complications such as portal hypertension (*S. mansoni* and *S. japonicum*) or hydronephrosis, renal failure, and bladder cancer (*S. hematobium*) can occur (*2*).

Emerging evidence suggests that schistosomiasis is a systemic disease that might also involve the spleen, heart, lungs, nervous system, and other organs (*5*–*7*). However, pancreatic involvement is exceedingly rare. In this article, we report 4 cases of schistosomiasis in China affecting the pancreas (Table). Informed consent was obtained from the patients for the publication of their information.

The Study

Patient 1 was a 49-year-old woman with a 1-year history of intermittent fever (up to 40°C) who was found to have a space-occupying lesion in the pancreatic head during routine examination in October 2020. She resided in Hubei, China, and had a history of untreated schistosomiasis. Computed tomography at Wuhan Union hospital revealed a 4.8 × 3.5 cm mass superior to the pancreatic head, involving the pancreas and associated with enlarged peripancreatic lymph nodes (Figure 1, panels A, B). Tumor markers were unremarkable, but hemoglobin was mildly reduced (93 g/L, reference range 115–150 g/L). To clarify the diagnosis, we conducted an endoscopic ultrasound-guided fine-needle aspiration of the pancreatic head. Pathology demonstrated fibrinous exudate and schistosome eggs (Figure 1, panel C). *S. japonicum* eggs were also found in the stool. The patient was diagnosed with pancreatic schistosomiasis and treated with a 1-day course of praziquantel (60 mg/kg in 3 doses). Two weeks later, her symptoms resolved, and she was discharged. No fever recurrence was observed at 3-month follow-up.

Patient 2 was a 73-year-old man who sought care in November 2024 with 1 day of abdominal pain. Six months prior, he had a history of pancreatitis. He also had a long-term residence in Hubei and a history of

Author affiliation: Union Hospital Department of Pancreatic Surgery, Tongji Medical College, Huazhong University of Science and Technology, Wuhan, China

DOI: https://doi.org/10.3201/eid3112.251098

[1]These authors are co–first authors.

Table. Clinical characteristics of 4 patients with pancreatic schistosomiasis, China, 2020–2024

Case no.	Age, y/sex	Region of infection	Hemaglobin, g/L	*Schistoma japonicum* eggs detected	Stool test	Treatment for *S. japonicum*
1	49/F	Pancreas head	93	Yes	Positive	Praziquantel, 60 mg/kg, 3 doses in 1 day
2	73/M	Pancreatic body	94	Yes	Positive	Praziquantel, 60 mg/kg, 3 doses in 1 day
3	65/M	Pancreatic tail	125	Yes	Positive	NA
4	47/M	Pancreatic tail and spleen	106	Yes	Not available	Praziquantel, 60 mg/kg, 3 doses in 1 day

findings included hemoglobin 94 g/L (reference range 130–175 g/L) and serum amylase 522 U/L (reference range 20–125 U/L); tumor markers were unremarkable. *S. japonicum* eggs were detected in his stool. Abdominal computed tomography scan revealed a nonenhancing, tubular lesion adjacent to the main pancreatic duct in the body of the pancreas, suggesting possible intraductal papillary mucinous neoplasm (IPMN) and an enhancing nodule in the pancreatic tail, suspected to be a neuroendocrine tumor (Figure 1, panels D, E). After fluid replacement, analgesia, and resumption of oral intake, the abdominal pain resolved. We conducted a laparoscopic distal pancreatectomy. Pathology revealed IPMN with

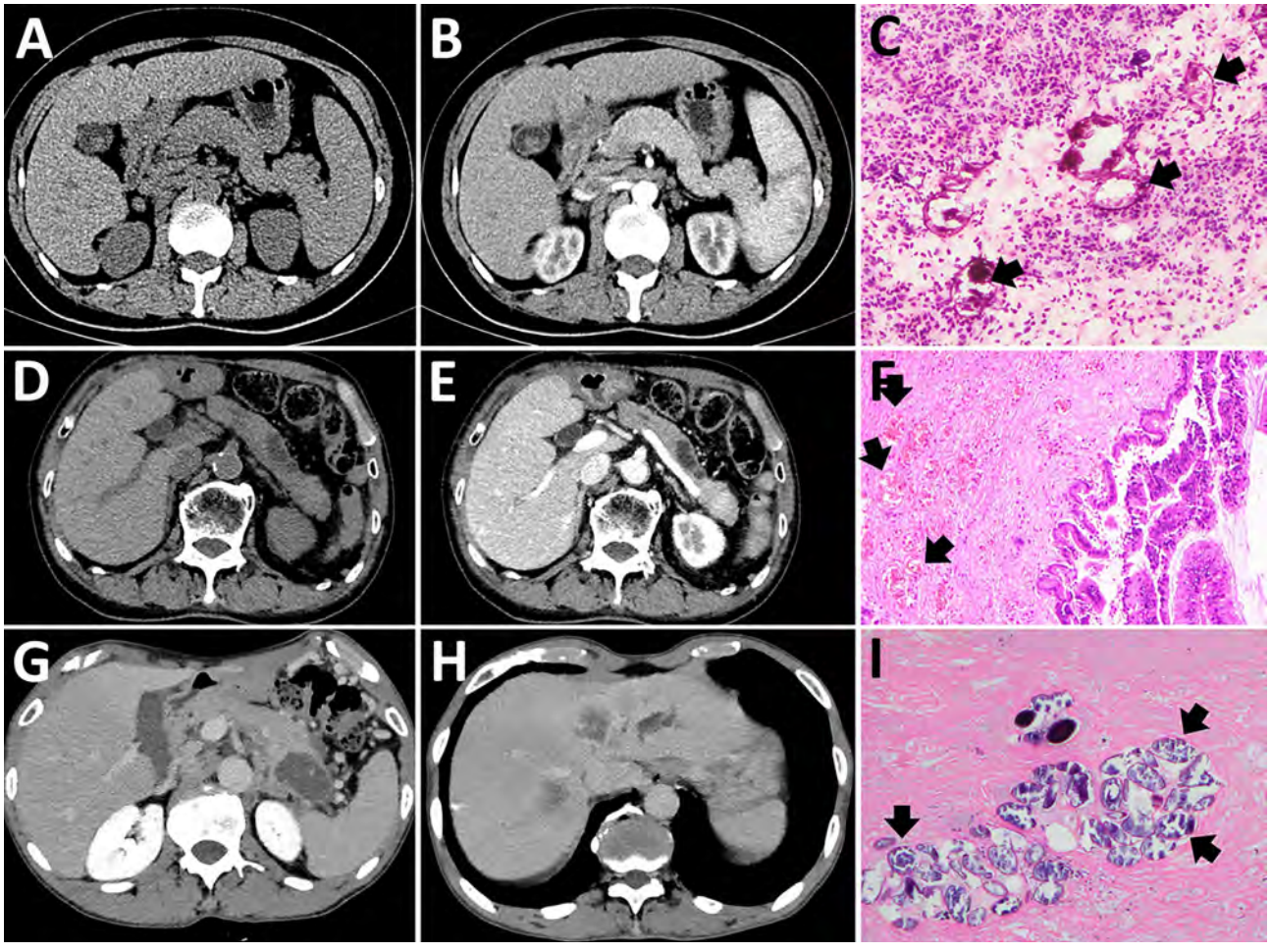

Figure 1. Imaging from 4 cases of pancreatic schistosomiasis, China, 2020–2024. A, B) Computed tomography (CT) images from patient 1 revealing a mass involving the pancreas. C) Pathologic examination from fine-needle aspiration of patient 1 showing fibrinous exudate and schistosome eggs (arrows). D, E) Abdominal CT of patient 2 showing a nonenhancing, tubular lesion adjacent to the main pancreatic duct in the body of the pancreas. F) Pathologic examination of sample from patient 2 showing intraductal papillary mucinous neoplasm with moderate dysplasia and scattered schistosome eggs (arrows). G, H) Abdominal CT of patient 3 revealing a low-density mass in the pancreatic tail and multiple ring-enhancing hepatic nodules. I) Pathologic examination of sample from patient 3 showing schistosome egg deposition (arrows) with associated tissue necrosis.

moderate dysplasia in parts of the glandular epithelium, and scattered schistosome eggs (Figure 1, panel F; Figure 2). We discharged the patient 2 weeks postoperatively and referred him to the infectious diseases department. He was treated with a 1-day course of praziquantel (60 mg/kg in 3 doses). At 3-month follow-up, he remained symptom-free.

Patient 3 was a 65-year-old man who sought care in March 2022 with complaints of left upper abdominal pain lasting 1 month. He had a history of liver cirrhosis and untreated schistosomiasis. Hepatitis B surface antigen, e antigen, and core antibody were all positive. Tumor markers carcino-embryonic antigen, CA125, and CA19-9 were markedly elevated. Hemoglobin measured slightly low at 125 g/L (reference range 130–175 g/L). Contrast-enhanced abdominal computed tomography revealed a low-density mass in the pancreatic tail, highly suggestive of pancreatic cancer, and multiple ring-enhancing hepatic nodules suggestive of metastases (Figure 1, panels G, H). Endoscopic ultrasound-guided biopsy yielded 2 tissue samples: 1 sample showed schistosome egg deposition with tissue necrosis, and the other sample revealed pancreatic carcinoma cells (Figure 1, panel I). We diagnosed the patient with pancreatic schistosomiasis and pancreatic ductal adenocarcinoma with liver metastases. We transferred him to the oncology department for further management. Four months later, follow-up revealed the patient had died.

We published the case of patient 4 last year (*8*). In brief, a 47-year-old man who had had intermittent left upper quadrant abdominal pain for 5 years was found to have a hypodense cystic lesion in the tail of the pancreas on imaging. He subsequently underwent surgery, and the resected specimen's pathology confirmed pancreatic and splenic schistosomiasis. Splenic schistosomiasis was documented previously (*9*).

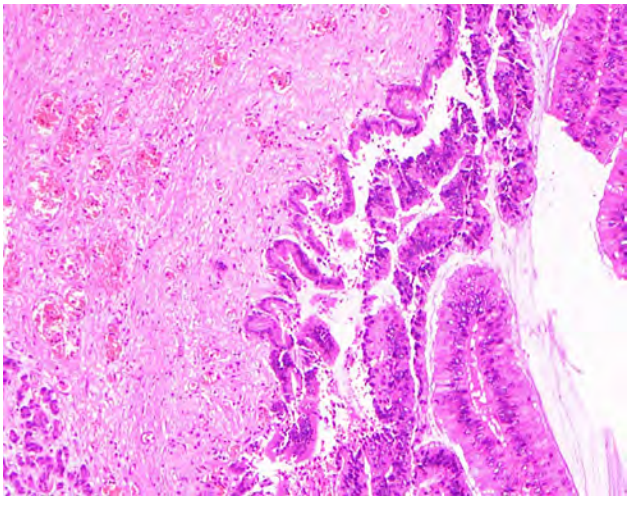

Figure 2. Enlarged image of schistosome eggs in pancreas of patient 2 in report of 4 cases of pancreatic schistosomiasis, China, 2020–2024.

Conclusions

During the past 70 years, China has made remarkable progress in controlling schistosomiasis (caused by *S. japonicum*), resulting in a 99% reduction in prevalence. China is steadily progressing toward the goal of complete schistosomiasis elimination (*10*). However, sporadic cases of schistosomal infection continue to occur in endemic areas such as Hunan, Jiangxi, and Hubei.

Pancreatic schistosomiasis is extremely rare, and we found only 1 known previous report of chronic pancreatitis caused by *S. mansoni* (*11*). Animal studies have shown that schistosome eggs can be deposited in pancreatic tissue (*12*). All 4 patients described in this article lived in endemic areas and had a history of schistosomiasis. Their main symptoms were intermittent abdominal pain and fever, and imaging consistently indicated pancreatic space-occupying lesions that posed diagnostic challenges. Two cases were ultimately diagnosed as inflammatory lesions, 1 as IPMN, and 1 as pancreatic ductal adenocarcinoma with hepatic metastases. Pathology confirmed *S. japonicum* egg deposition in all 4 cases.

Egg deposition in the pancreas induces granuloma formation and chronic inflammation. Of note, in case 3, pancreatic cancer cells and liver metastasis were found at the lesion site. Associations between schistosomiasis and colorectal, liver, and bladder cancers have been previously published (*13*–*15*). Furthermore, schistosome egg deposition in colorectal cancer is linked to a higher rate of the KRAS G12D mutation, which is also a key driver mutation in pancreatic cancer. Therefore, the pancreatic cancer in case 3 might be related to schistosomal infection, rather than being coincidental.

Once pancreatic schistosomiasis is confirmed, praziquantel remains the primary treatment. In this article, patient 1 improved with praziquantel therapy; patients 2 and 4 underwent surgery because of the high suspicion of malignancy and were treated with praziquantel after the diagnosis of pancreatic schistosomiasis; and patient 3 primarily received chemotherapy but died because of advanced disease.

Schistosomiasis involving the pancreas is exceedingly rare and manifests with nonspecific symptoms, making diagnosis challenging. In endemic areas, particularly in patients with a history of schistosomiasis who are found to have pancreatic lesions, pancreatic schistosomiasis should be considered as part of a differential diagnosis. In addition, there is evidence of a potential association between *Schistosoma* infection and pancreatic cancer.

This study was approved by the ethics committee of Union Hospital, Tongji Medical College, Huazhong University of Science and Technology.

This study was supported by the National Natural Science Foundation of China (grant nos. 82173196 and 82472989) and the Key Research and Development Program of Hubei (grant no. 2022BCA012).

Author contributions: data collection and manuscript drafting, L.H., C.Z., and Y.L.; data collection, H.W. and Y.Z.; manuscript revision and study conduction, T.Y.; review and approval of final manuscript, all authors.

About the Author

Dr. He is a surgeon with the Department of Pancreatic Surgery at Union Hospital, Tongji Medical College, Huazhong University of Science and Technology, Wuhan, China. His clinical and research interests include pancreatic diseases.

References

1. Colley DG, Bustinduy AL, Secor WE, King CH. Human schistosomiasis. Lancet. 2014;383:2253–64. https://doi.org/10.1016/S0140-6736(13)61949-2
2. Buonfrate D, Ferrari TCA, Adegnika AA, Russell Stothard J, Gobbi FG. Human schistosomiasis. Lancet. 2025;405:658–70. https://doi.org/10.1016/S0140-6736(24)02814-9
3. Wilson RA. Schistosomiasis then and now: what has changed in the last 100 years? Parasitology. 2020;147:507–15. https://doi.org/10.1017/S0031182020000049
4. Gobbi F, Tamarozzi F, Buonfrate D, van Lieshout L, Bisoffi Z, Bottieau E; TropNet Schisto Task Force. New insights on acute and chronic schistosomiasis: do we need a redefinition? Trends Parasitol. 2020;36:660–7. https://doi.org/10.1016/j.pt.2020.05.009
5. Lambertucci JR. Acute schistosomiasis mansoni: revisited and reconsidered. Mem Inst Oswaldo Cruz. 2010;105:422–35. https://doi.org/10.1590/s0074-02762010000400012
6. Ferrari TC, Moreira PR. Neuroschistosomiasis: clinical symptoms and pathogenesis. Lancet Neurol. 2011;10:853–64. https://doi.org/10.1016/S1474-4422(11)70170-3
7. Gobbi F, Buonfrate D, Angheben A, Beltrame A, Bassetti M, Bertolaccini L, et al. Pulmonary nodules in African migrants caused by chronic schistosomiasis. Lancet Infect Dis. 2017;17:e159–65. https://doi.org/10.1016/S1473-3099(16)30530-8
8. He L, Lu Y, Hu X, Yin T. Schistosomal pancreatitis mimicking pancreatic neoplasm. Dig Liver Dis. 2025;57:342–3. https://doi.org/10.1016/j.dld.2024.10.020
9. Gobbi F, Martelli G, Attard L, Buonfrate D, Angheben A, Marchese V, et al. *Schistosoma mansoni* eggs in spleen and lungs, mimicking other diseases. PLoS Negl Trop Dis. 2015;9:e0003860. https://doi.org/10.1371/journal.pntd.0003860
10. Wang W, Bergquist R, King CH, Yang K. Elimination of schistosomiasis in China: current status and future prospects. PLoS Negl Trop Dis. 2021;15:e0009578. https://doi.org/10.1371/journal.pntd.0009578
11. Shah N, Abrahamian F, Attar B. Recurrent pancreatitis caused by a trematode (*Schistosoma mansoni*) infection. Am J Gastroenterol. 2009;104:S255. https://doi.org/10.14309/00000434-200910003-00688
12. Watanabe K, Kikuchi M, Ohno A, Mohamed RT, Nara T, Ubalee R, et al. The miniature pig: a unique experimental model for *Schistosoma japonicum* infection. Parasitol Int. 2004;53:293–9. https://doi.org/10.1016/j.parint.2004.03.002
13. Gouveia MJ, Santos J, Brindley PJ, Rinaldi G, Lopes C, Santos LL, et al. Estrogen-like metabolites and DNA-adducts in urogenital schistosomiasis-associated bladder cancer. Cancer Lett. 2015;359:226–32. https://doi.org/10.1016/j.canlet.2015.01.018
14. Li X, Liu H, Huang B, Yang M, Fan J, Zhang J, et al. *Schistosoma* infection, KRAS mutation status, and prognosis of colorectal cancer. Chin Med J (Engl). 2024;137:235–7. https://doi.org/10.1097/CM9.0000000000002905
15. Roderfeld M, Padem S, Lichtenberger J, Quack T, Weiskirchen R, Longerich T, et al. *Schistosoma mansoni* egg-secreted antigens activate hepatocellular carcinoma-associated transcription factors c-Jun and STAT3 in hamster and human hepatocytes. Hepatology. 2020;72:626–41. https://doi.org/10.1002/hep.30192

Corresponding author: Tao Yin, Union Hospital, 1277 Jiefang Ave, Wuhan 430022, China; email: ytwhun@hust.edu.cn

Abnormal Prion Protein in Nasal Swab Specimens of Macaques Infected with Creutzfeldt-Jakob Disease

Juraj Cervenak, Oksana Yakovleva, Cyrus Bett, Teresa Pilant, Kelly Rice, Lewis Shankle,[1] David M. Asher,[1] Luisa Gregori, Pedro Piccardo

We transfused 4 macaques with blood of macaques previously infected with variant Creutzfeldt-Jakob disease, transmitting disease to 2 macaques (1 demonstrating clinical signs). Nasal swab specimens from both infected macaques became positive for disease-associated prion protein during the preclinical stage. Such samples are suitable for antemortem diagnosis during long incubation periods.

Variant Creutzfeldt-Jakob disease (vCJD) and sporadic CJD are among a group of rare, always fatal neurodegenerative disorders known as transmissible spongiform encephalopathies (TSEs) or prion diseases (*1*). Researchers have linked vCJD to human dietary exposure to the agent that caused bovine spongiform encephalopathy in cattle (*1*–*3*). The literature documents few transfusion-transmitted cases of vCJD in the early 2000s (*4*,*5*), but no new cases have been reported since 2007. The lack of recent transfusion-transmitted vCJD is reassuring, but a question lingers about the true prevalence of vCJD infections in the population and the iatrogenic risk they pose. This prevalence is difficult to estimate without a validated assay to identify infected persons during the preclinical phase of vCJD, which can last for many decades.

To achieve this goal, we developed a nonhuman primate model of vCJD to collect specimens (blood and nasal swabs) suitable to validate preclinical tests and to detect the presence of abnormal disease-associated prion protein (PrP^{TSE}) in blood (*6*,*7*). We could not conduct studies with human samples because of the rarity of human TSEs and the impossibility of establishing the exact time of most human exposures to the infective agents. To validate the relevance of a macaque model, we attempted to mimic human transmissions of transfusion-transmitted vCJD by blood transfusion from infected to naive macaques and collected biologic samples for testing over a 10-year period.

The Study

We transfused 4 uninfected macaques using blood from 3 macaques (CO7423, CO7422, and C16999) previously infected with vCJD (*6*) (Appendix, https://wwwnc.cdc.gov/EID/article/31/12/25-0679-App1.pdf). We collected 100-mL samples of blood from CO7423, at clinical onset and at terminal phase of illness, and immediately transfused the samples into 2 recipient macaques: CO1619 and 98CO19. Two years later, we transfused 2 macaques, DEIM and DFOO, with red blood cell–depleted blood prepared from whole blood of CO7422 and C16999 (Table 1). We euthanized CO1619 at 58 months posttransfusion (mpt) and euthanized 98CO19 at 104 mpt (8.7 years posttransfusion [ypt]) because of intercurrent illnesses (Table 1). DEIM developed early neurologic signs of mild ataxia and tremors at 104 mpt (8.7 ypt). Those symptoms slowly progressed to marked tremors, unsteadiness on the perch, unkept fur coat, and mild weight loss, all typical signs of vCJD in macaques. We euthanized

Author affiliations: US Food and Drug Administration, Center for Biologics Evaluation and Research, Silver Spring, Maryland, USA (J. Cervenak, O. Yakovleva, C. Bett, T. Pilant, K. Rice, L. Shankle, D.M. Asher, L. Gregori, Unidad Académica de Neuropediátria, Universidad de la República, Montevideo, Uruguay (P. Piccardo)

DOI: http://doi.org/10.3201/eid3112.250679

[1]Retired.

Table 1. Summary of data from study of abnormal prion protein in nasal swab specimens of macaques infected with Creutzfeldt-Jakob disease*

Donor macaque ID	Recipient macaque ID	Transfused sample	Clinical symptoms, ypt (mpt)	Survival time, ypt (mpt)	Age at endpoint, y	Reason for euthanasia
CO7423	CO1619	100 mL whole blood	NA	4.8 (58)	17	Unresectable pelvic tumor
CO7423	98CO19	100 mL whole blood	NA	8.7 (104)	23	Nonreducible inguinal hernia
CO7422	DEIM	Red blood cell–depleted 100 mL whole blood equivalent	8.7 (104)	9 (108)	12	Neurologic signs of vCJD
C16999	DFOO	Red blood cell–depleted 100 mL whole blood equivalent	NA	10 (120)	13	Planned end of study

*Inoculation of these animals was described previously (*6*). mpt, month posttransfusion; NA, not applicable; vCJD, variant Creutzfeld-Jakob disease; ypt, year posttransfusion.

DEIM 4 months after clinical onset. We euthanized DFOO at 120 mpt (10 ypt) when the macaque had reached the preselected experimental endpoint.

We collected blood and nasal swab specimens during and at the end of the study. We harvested brains and other tissues from each macaque. We also collected cerebrospinal fluid from DEIM and DFOO. To detect PrP^{TSE}, the biomarker of TSEs, we used 2 in vitro assays: real-time quaking-induced conversion (RT-QuIC) to assay nasal swab extracts, lymph nodes, and cerebrospinal fluid; and protein misfolding cyclic amplification (PMCA) to assay brain, spleen, and blood samples (*8*,*9*). All tests of tissues and fluids from CO1619 and DFOO were negative for PrP^{TSE}, including neuropathological examinations to show spongiform degeneration and PrP^{TSE} deposits in formalin-fixed paraffin-embedded brain tissue (Table 2). We included samples from vCJD-infected animals and uninfected macaques in each test as controls.

Brain homogenate from 98CO19 was negative for PrP^{TSE} using multiple biochemical detection methods, and the macaque's blood was negative by PMCA as well (Table 2). Neuropathologic studies showed no spongiform degeneration or PrP^{TSE} deposits in 98CO19's brain. However, nasal swab extracts and 2 inguinal lymph node homogenates collected at euthanasia were positive by RT-QuIC (Figure 1) when tested as 1% wt/vol tissue homogenates (4/4 positive wells) but negative in the next 10-fold dilution (0.1% wt/vol), suggesting that very small amounts of PrP^{TSE} were present. PMCA assays of the same 2 tissues were negative. We noted scattered clusters of PrP^{TSE} in sections of the lymph nodes, in the same cells staining for CD21, corresponding to follicular dendritic cells (Figure 2).

We confirmed macaque DEIM to be infected with vCJD by neuropathological and immunohistological examinations of formalin-fixed paraffin-embedded brain tissues and by Western blots of brain suspensions (Appendix Figure, panel A), RT-QuIC of cerebrospinal fluid, and PMCA of blood. PMCA first detected PrP^{TSE} in blood collected at 85 mpt; RT-QuIC showed PrP^{TSE} in nasal swab extracts 7 months later (92 mpt). PrP^{TSE} signals remained positive in both tissues to the end of the study (Appendix Figure). Thus, PrP^{TSE} appeared in those tissues several months before clinical onset, confirming the diagnostic potential of both assays with those materials.

Conclusion

We report the results of blood transfusions from 3 vCJD-infected macaques into 4 recipient macaques. One macaque developed clinical vCJD 9 years after transfusion, an interval consistent with a survival duration of 6.5–8.3 years seen in human recipients transfused with blood from asymptomatic vCJD-infected donors (*5*). One recipient macaque died early in the experiment, and 2 macaques survived ≥9 years with no clinical signs of vCJD. Macaque 98CO19 revealed PrP^{TSE} signals in nasal swab extracts and inguinal lymph node tissues. Researchers have used lymph node tissue previously to identify macaques incubating vCJD before clinical onset of illness (*11*). Our data from RT-QuIC testing showed reactivity that was weak but unequivocal and reproducible. We confirmed the presence of PrP^{TSE} in lymph node tissue by immunohistochemistry of the same tissue. We concluded that 98CO19 died while infected with vCJD.

Previous researchers exploring TTvCJD transfused to macaques reported a fatal neurologic syndrome, described as a myelopathy, that affected 3 of 7 macaques transfused with blood containing low infectivity (determined by low levels of peripheral PrP^{TSE}); the other 4 macaques remained healthy (*12*). The macaques with myelopathy demonstrated clinical signs that included impaired visual acuity and hind limb ataxia, but tests revealed no PrP^{TSE} in brain and other tissues (*12*). Macaque DFOO of our study showed no clinical signs associated with that described myelopathy. Macaque CO1619 died relatively early in the study—too early to know if it had been infected with vCJD or would have developed myelopathy. Our results largely agree with those of

Table 2. Summary of test results from study of abnormal prion protein in nasal swab specimens of macaques infected with Creutzfeldt-Jakob disease*

Recipient macaque ID	Clinical status	Tissue tested	Western blot†	RT-QuIC	PMCA	Histology	Total mice inoculated/ positive results‡
CO1619	Asymptomatic	Brain	Neg	Neg	Neg	Neg	40/0
		Spleen	ND	ND	Neg	ND	10/0
		Ileum	ND	ND	Neg	ND	15/0
		Blood	NA	NA	Neg	N/A	ND
		Nasal swab	ND	Neg	Neg	NA	ND
98CO19	Asymptomatic	Brain	Neg	Neg	Neg	Neg	51/0
		Blood	NA	ND	Neg	NA	ND
		Nasal swab	ND	W pos	Neg	NA	ND
		Lymph node	ND	W pos	Neg	Pos	ND
DEIM	Symptomatic	Brain	Pos	ND	ND	Pos	ND
		Blood	NA	NA	Pos	NA	ND
		Nasal swabs	ND	Pos	Pos	NA	ND
		CSF	ND	Pos	ND	NA	ND
DFOO	Asymptomatic	Brain	Neg	Neg	Neg	Neg	ND
		Blood	NA	NA	Neg	NA	ND
		Nasal swab	ND	Neg	Neg	NA	ND
		CSF	Neg	Neg	Neg	NA	ND

*CSF, cerebrospinal fluid; pos, TSE positive; W pos, weak TSE positive; neg, TSE negative; NA, not applicable; ND, not done; RT-QuIC, real-time quaking-induced conversion; TSE, transmissible spongiform encephalopathy.
†We used 10% homogenates in phosphate-buffered saline, treated with 20 U/mL of benzonase nuclease for 30 minutes at room temperature with constant mixing, followed with 50 µg/mL proteinase K for 1 hour at 37°C to remove normal prion protein. Samples were processed for NuPAGE on 12% Bis-Tris precast gels (Thermo Fisher Scientific, https://www.thermofisher.com), prion protein detected using 3F4 mouse anti-PrP monoclonal antibody (Research Foundation for Mental Hygiene, New York State Institute for Basic Research; https://corporate.rfmh.org/).
‡We inoculated intracerebrally 30-µL aliquots of 1% tissue homogenates into transgenic mice overexpressing the bovine prion protein, TgBo110 (*10*). We monitored mice for 2 years for signs of vCJD and tested the brain of every mouse for PrP^{TSE} with real-time quaking-induced conversion.

Comoy et al., who concluded that not all transfusions transmitted vCJD to macaques (*12*). Similarly, reports from the United Kingdom suggest that not all human recipients surviving 5 years or longer after transfusions developed TTvCJD from a donor with vCJD (*13*). No macaque in our smaller cohort of transfused animals showed evidence of myelopathy.

Over a 10-year period after transfusion, we collected relatively accessible biological materials, such as blood and nasal swab specimens, to test for PrP^{TSE}. We first detected PrP^{TSE} in the blood of macaque DEIM 19 months before onset of overt illness, consistent with results of our previous studies (*6*). Nasal swab extracts from the 2 infected macaques became positive for PrP^{TSE} 12 months before signs of illness for DEIM and at euthanasia for 98CO19 (98CO19's nasal swab specimens were negative 3 months earlier). Those results support potential use of nasal swab specimens as an assay matrix to identify infected persons before clinical onset of vCJD. A caveat is that we do not know how detection of PrP^{TSE} might be affected by prion protein genotype. Research has demonstrated diagnostic accuracy of nasal swab testing for persons with either confirmed or presumed sporadic CJD, but the predictive value of this testing method for detecting cases before onset of neurologic illness remains uncertain (*14*). Acknowledging that our macaques were infected with vCJD, and not sporadic CJD, our results nonetheless suggest that testing nasal swab specimens to detect PrP^{TSE} may be useful in screening persons with family history of CJD, which would enable attempts at early therapeutic intervention (*15*).

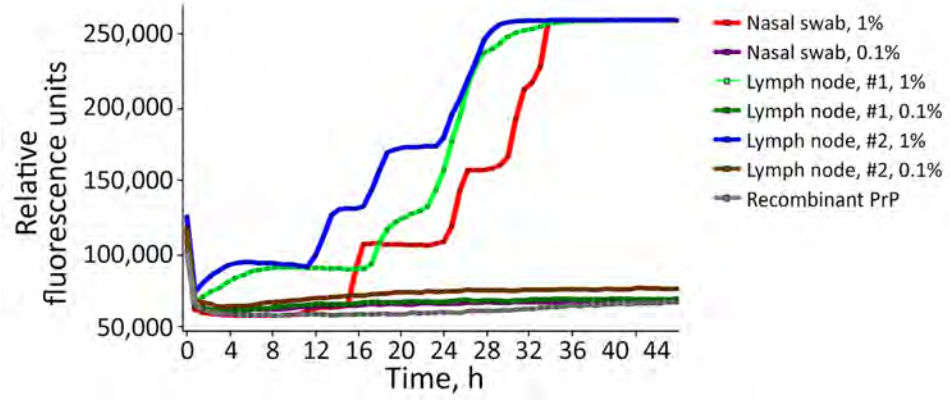

Figure 1. Results of real-time quaking-induced conversion testing of tissue samples from a study of macaques infected with Creutzfeldt-Jakob disease. Data based on nasal swab extracts and lymph nodes 1 and 2 from macaque 98CO19. Each line represents the change in fluorescent signal over time. We tested 1% and 0.1% homogenates; increase in fluorescent signal was observed only with 1% homogenates. PrP, prion protein.

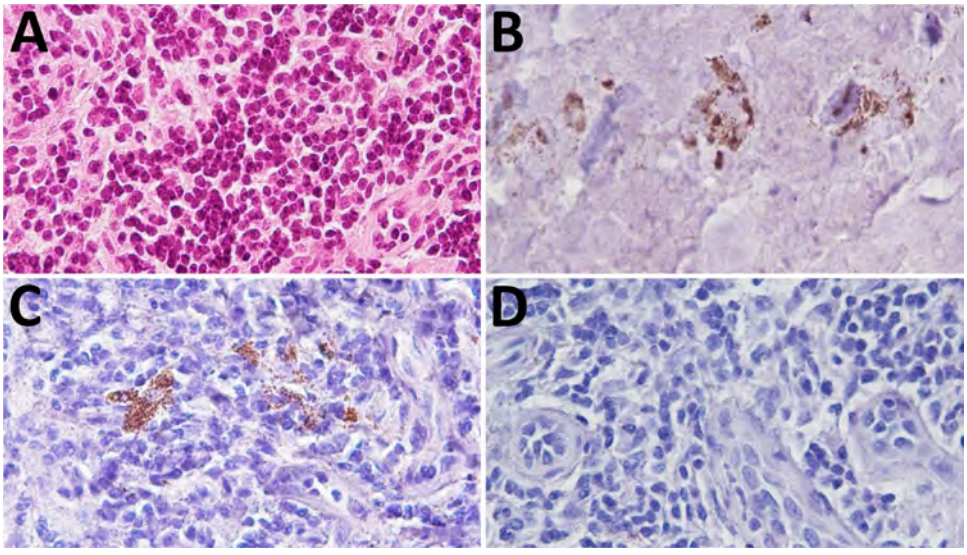

Figure 2. Immunohistochemistry for abnormal disease-associated prion protein (PrP^{TSE}) and CD21 on inguinal lymph node of macaque 98CO19 for study of macaques infected with Creutzfeldt-Jakob disease. Adjacent sections were stained with hematoxylin-eosin (A); immunostained for PrP^{TSE} (B) and CD21 (C); and probed without primary antibody as negative control (D). Original magnification ×40.

Acknowledgments

We thank the technical staff of the Nonhuman Primate Facility at Center for Biologics Evaluation and Research Division of Veterinary Services, for their dedicated and excellent care of the animals. We are particularly indebted to John Dennis for his expertise in performing the macaque transfusions and Ruth Damaris Molano for providing expert veterinary care to the macaques. We also thank members of our laboratory for their support of this project.

The comments and opinions presented in this paper do not bind or obligate the US Food and Drug Administration.

About the Author

Dr. Juraj Cervenak is a biologist at the US Food and Drug Administration, Silver Spring, Maryland, USA. His research focuses on safety of biological products from contamination with transmissible spongiform encephalopathy agents to advance public health.

References

1. Will R. Variant Creutzfeldt-Jakob disease. Folia Neuropathol. 2004;42 Suppl A:77-83.
2. Ironside JW. Variant Creutzfeldt-Jakob disease: an update. Folia Neuropathol. 2012;50:50–6.
3. Belay ED, Schonberger LB. Variant Creutzfeldt-Jakob disease and bovine spongiform encephalopathy. Clin Lab Med. 2002;22:849–62, v–vi.
4. Turner ML, Ludlam CA. An update on the assessment and management of the risk of transmission of variant Creutzfeldt-Jakob disease by blood and plasma products. Br J Haematol. 2009;144:14–23.
5. Seed CR, Hewitt PE, Dodd RY, Houston F, Cervenakova L. Creutzfeldt-Jakob disease and blood transfusion safety. Vox Sang. 2018;113:220–31.
6. Yakovleva O, Bett C, Pilant T, Asher DM, Gregori L. Abnormal prion protein, infectivity and neurofilament light-chain in blood of macaques with experimental variant Creutzfeldt-Jakob disease. J Gen Virol. 2022;103:001764.
7. McDowell KL, Nag N, Franco Z, Bu M, Piccardo P, Cervenak J, et al. Blood reference materials from macaques infected with variant Creutzfeldt-Jakob disease agent. Transfusion. 2015;55:405–12.
8. Atarashi R, Moore RA, Sim VL, Hughson AG, Dorward DW, Onwubiko HA, et al. Ultrasensitive detection of scrapie prion protein using seeded conversion of recombinant prion protein. Nat Methods. 2007;4:645–50.
9. Chen B, Morales R, Barria MA, Soto C. Estimating prion concentration in fluids and tissues by quantitative PMCA. Nat Methods. 2010;7:519–20.
10. Castilla J, Gutiérrez Adán A, Brun A, Pintado B, Ramírez MA, Parra B, et al. Early detection of PrPres in BSE-infected bovine PrP transgenic mice. Arch Virol. 2003;148:677–91.
11. Lescoutra-Etchegaray N, Jaffré N, Sumian C, Durand V, Correia E, Mikol J, et al. Evaluation of the protection of primates transfused with variant Creutzfeldt-Jakob disease-infected blood products filtered with prion removal devices: a 5-year update. Transfusion. 2015;55:1231–41.
12. Comoy EE, Mikol J, Jaffré N, Lebon V, Levavasseur E, Streichenberger N, et al. Experimental transfusion of variant CJD-infected blood reveals previously uncharacterised prion disorder in mice and macaque. Nat Commun. 2017;8:1268.
13. Gregori L, Yang H, Anderson S. Estimation of variant Creutzfeldt-Jakob disease infectivity titers in human blood. Transfusion. 2011;51:2596–602.
14. Fiorini M, Iselle G, Perra D, Bongianni M, Capaldi S, Sacchetto L, et al. High diagnostic accuracy of RT-QuIC assay in a prospective study of patients with suspected sCJD. Int J Mol Sci. 2020;21:880.
15. Vallabh SM, Minikel EV, Schreiber SL, Lander ES. Towards a treatment for genetic prion disease: trials and biomarkers. Lancet Neurol. 2020;19:361–8.

Address for correspondence: Luisa Gregori, US Food and Drug Administration, 10903 New Hampshire Ave, Silver Spring, MD 20903, USA; email: luisa.gregori@fda.hhs.gov

Macrolide Resistance and P1 Cytadhesin Genotyping of *Mycoplasma pneumoniae* during Outbreak, Canada, 2024–2025

Zareen Fatima,[1] Padman Jayaratne,[1] Amjad Arrabi, Candy Rutherford, Daniela Leto, Marek Smieja, Mohammad Rubayet Hasan

We investigated macrolide resistance and P1 genotypes of *Mycoplasma pneumoniae* during the 2024–2025 outbreak in Hamilton, Ontario, Canada. Macrolide resistance remained stable at ≈10%–20%, but significant shifts in P1 genotype distribution and resistance rates in P1 types occurred, indicating notable changes in *M. pneumoniae* molecular epidemiology in Ontario since 2011–2012.

Mycoplasma pneumoniae is a cause of upper and lower respiratory tract infections, particularly in children, and occurs in endemic and epidemic patterns. Although tracheobronchitis is common, pneumonia is the most clinically significant manifestation, accounting for ≈4%–8% of community-acquired bacterial pneumonias during endemic periods (*1*). Macrolides remain the primary therapy for *M. pneumoniae*, but the global rise in clinically relevant resistance is posing increasing challenges to treatment (*2*). Since COVID-19 pandemic restrictions were scaled back during 2023, *M. pneumoniae* incidence and outbreaks have increased substantially worldwide (*3*–*5*). In Ontario, Canada, a delayed but unprecedented rise in detection, reaching up to 30% positivity, has been reported since May 2024 (*6*). We assessed macrolide resistance rates and P1 cytadhesin types of *M. pneumoniae* during the 2024–2025 outbreak in Hamilton, Ontario, Canada, and compared them with strains collected before the COVID-19 pandemic.

Author affiliations: McMaster University, Hamilton, Ontario, Canada (Z. Fatima, P. Jayaratne, D. Leto, M. Smieja, M.R. Hasan); Research Institute of St. Joe's Hamilton, Hamilton (Z. Fatima, A. Arrabi, M. Smieja, M.R. Hasan); Hamilton Regional Laboratory Medicine Program, Hamilton (P. Jayaratne, C. Rutherford, D. Leto, M. Smieja, M.R. Hasan)

DOI: https://doi.org/10.3201/eid3112.250872

The Study

During January 2024–April 2025, a total of 4,297 nasopharyngeal swab (NPS) specimens from 3,717 patients were received by the Microbiology Laboratory of the Hamilton Regional Laboratory Medicine Program in Hamilton for *M. pneumoniae* detection by a laboratory-developed PCR. We screened all *M. pneumoniae*–positive samples (n = 417 after removing duplicates) for macrolide resistance by PCR genotyping and performed P1 cytadhesin typing on a randomly selected ≈25% subset of positive specimens from each month (n = 110) by amplifying the RepMP4 region of P1 cytadhesin gene (*7*) and sequencing with nanopore technology (Oxford Nanopore, https://nanoporetech.com) (Appendix, https://wwwnc.cdc.gov/EID/article/31/12/25-0872-App1.pdf). In addition to specimens received during the postpandemic period, additional *M. pneumoniae*–positive samples received during 2013–2020 were tested for macrolide resistance (n = 45) and P1 types (n = 23). We assessed statistical significance of differences in *M. pneumoniae* detection rates and macrolide resistance among different patient groups using the χ^2 test with Yates correction to adjust for small sample size (Appendix).

On average, 14.2% (381/2,680) of patients tested positive for *M. pneumoniae* in 2024, compared with 0.34% (2/576) in 2022 and 0.36% (2/555) in 2023. Since May 2024, the positivity rate gradually increased, reaching a peak of 22.5% in September 2024. After September, positivity rates steadily declined to <5% by January 2025, despite increased testing volumes through December 2024. Macrolide resistance rates varied by month and accounted for 11.8% of all positive samples during January 2024–April 2025; the highest rate of resistance (50%) was noted in July 2024 (Figure 1, panel

[1]These first authors contributed equally to this article.

A; Appendix Table 2). PCR genotyping identified only 1 single-nucleotide polymorphism (SNP) associated with macrolide resistance: A2063G, which is known to confer high-level macrolide resistance (erythromycin MIC >64 mg/L). This finding is consistent with a study reporting that >90% of isolates from Ontario during 2011–2012 carried the same mutation (*8*).

As expected, *M. pneumoniae* detection rates were much higher (≈20%) in children 5–<18 years of age than in other age groups. The macrolide resistance rate for *M. pneumoniae* in patients in this age group (≈11% of all positives) was not significantly different from the rates of resistance observed in children <5 years of age or adults 18–<65 years of age (Figure 1, panel B). In contrast, 50% of *M. pneumoniae*–positive strains from patients ≥65 years of age were macrolide resistant, a rate that was significantly higher than in children 5–<18 years of age (p = 0.02). Although the specimen number for the >65-year-old group was low (n = 6), the higher rate of macrolide resistance in this group could be related to higher likelihood of macrolide use in elderly patients.

We next compared macrolide resistance rates in *M. pneumoniae* strains during 2013–2020 and 2024–2025 (representing COVID-19 prepandemic and postpandemic periods), which were 17.8% (prepandemic) and 11.8% (postpandemic); the difference was not statistically significant (p = 0.24) (Figure 1, panel C). By P1 typing, 89/110 (81%) *M. pneumoniae* strains belonged to the P1-1 type, and 21/110 (19.1%) belonged to the P1-2 type. The macrolide resistance rate in P1-1–type *M. pneumoniae* strains was 29.9%, significantly higher (p = 0.04) than that in P1-2–type strains (7.7%) (Figure 1, panel D). During 2013–2020, 78.3% of *M. pneumoniae* strains were the P1-1 type, compared with 81% in 2024–2025. The proportions of P1-1 and P1-2 types were not significantly different between the 2 periods (p = 0.85). Among the P1-2 type *M. pneumoniae* strains, 2k, 2b, and 2g/2j variants were detected in specimens collected during

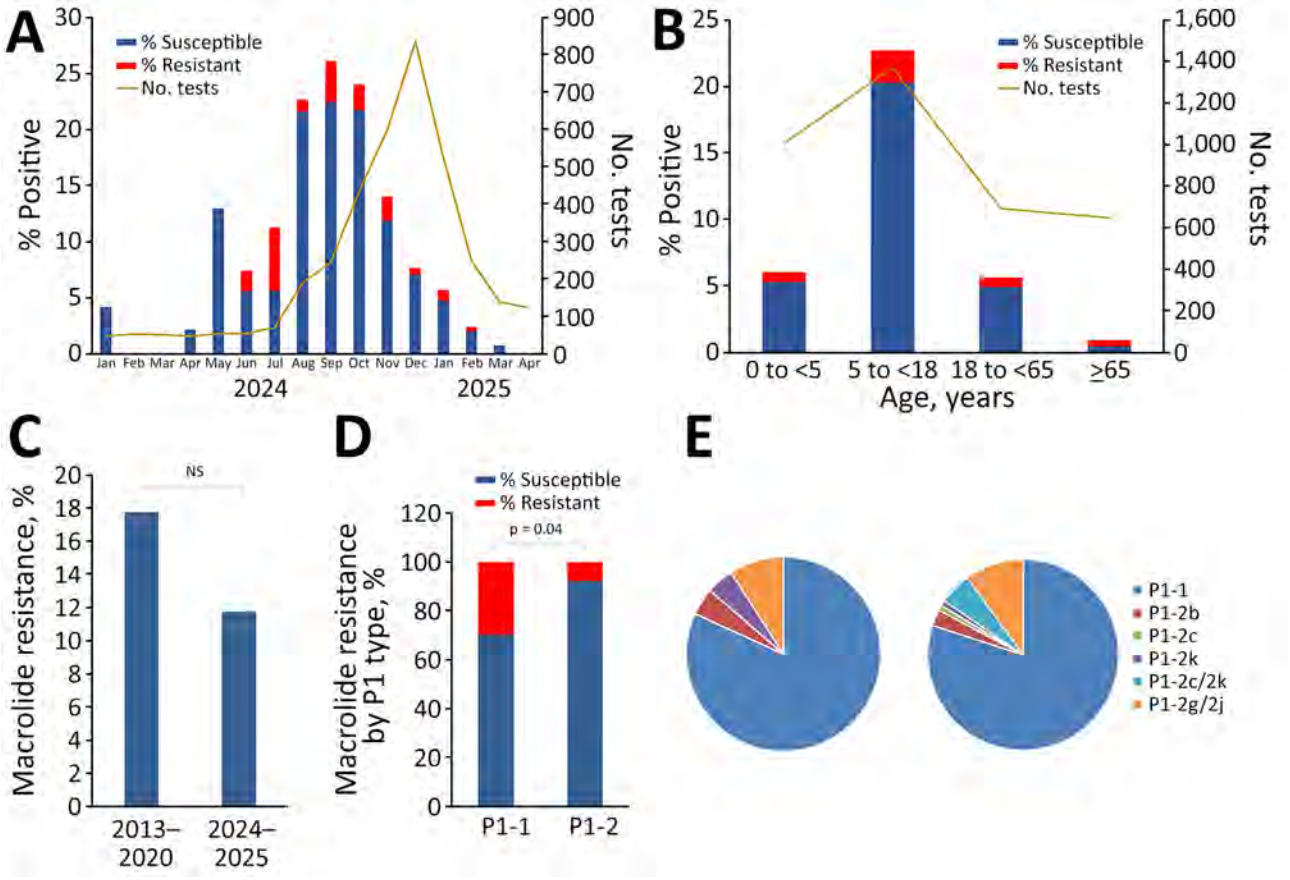

Figure 1. Prevalence, macrolide resistance rates, and P1 genotype distribution of *Mycoplasma pneumoniae* during 2024–2025 outbreak, Hamilton, Ontario, Canada. A) Monthly detection rates of macrolide-susceptible and -resistant *M. pneumoniae* during January 2024–April 2025. B) Detection rates of macrolide-susceptible and -resistant *M. pneumoniae* by age group. C) Comparison of macrolide resistance rates in *M. pneumoniae* before and after primary COVID-19 pandemic years. D) Macrolide resistance rates among different P1 types of *M. pneumoniae*. E) Distribution of P1-1 and P1-2 variant types among *M. pneumoniae* strains before and after primary COVID-19 pandemic years. p value was obtained from χ^2 test with Yates correction. NS, not significant.

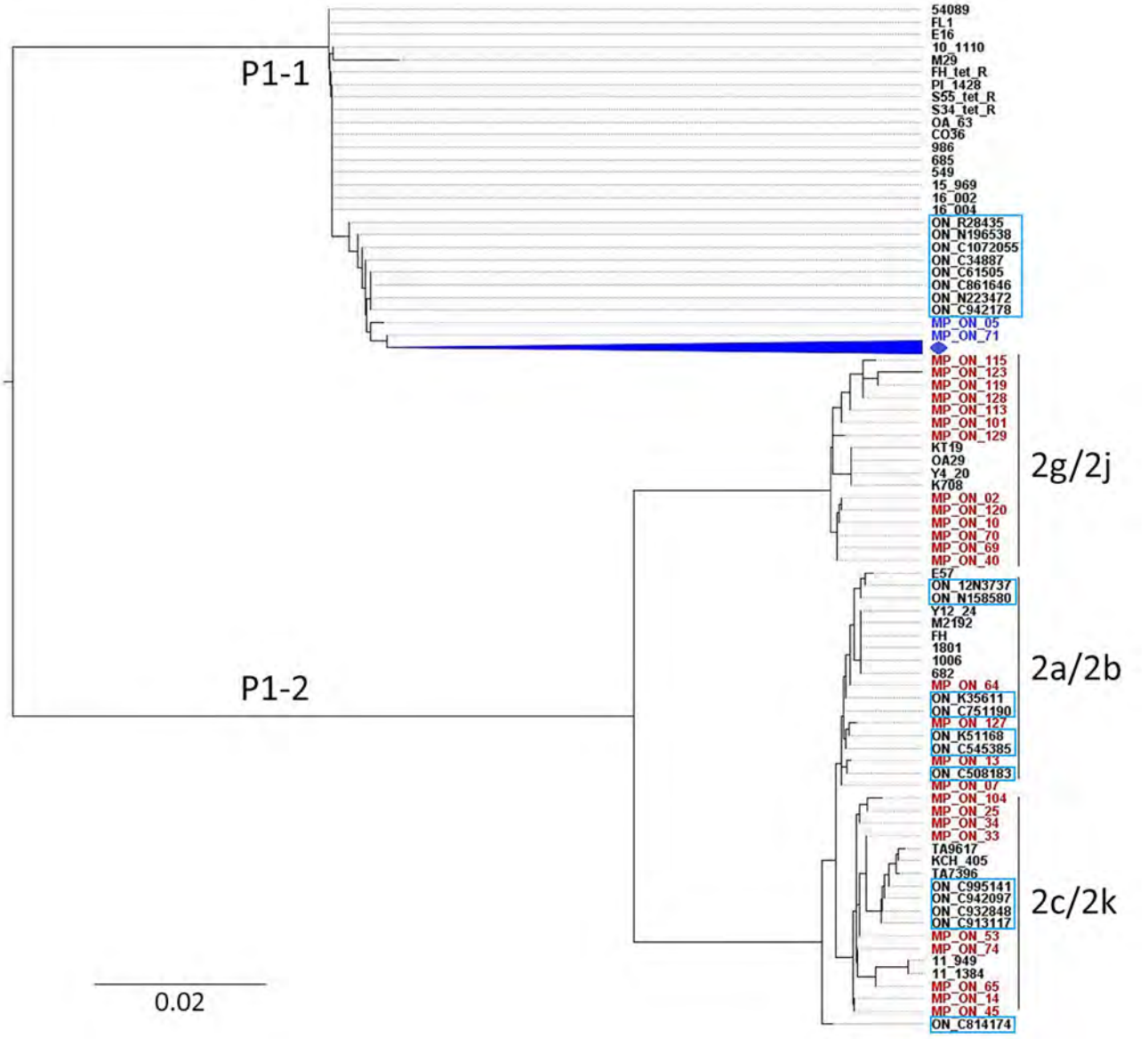

Figure 2. Phylogenetic analysis of *Mycoplasma pneumoniae* based on P1 cytadhesin–RepMP4 genotyping during 2024–2025 outbreak, Hamilton, Ontario, Canada. An unrooted tree was constructed using the neighbor-joining method with the Tamura-Nei model in MEGA X (https://www.megasoftware.net) using aligned sequences generated using Clustal Omega (https://www.ebi.ac.uk/jdispatcher/msa/clustalo). Strains highlighted in blue and red represent the P1-1 and P1-2 type strains assessed in this study. Strains in the light blue boxes indicate previously reported strains from Ontario during 2011–2012 (*8*). Strains shown in black represent reference RepMP4 sequences from *M. pneumoniae* obtained in other countries, representing P1 types and variants (Appendix Table 3, https://wwwnc.cdc.gov/EID/article/31/12/25-0872-App1.pdf). Blue diamond indicates remaining 104 P1-1 strains from this study

2013–2020. There was a predominance of 2g/2j variants (50%) in both periods, but the percentage of 2c/2k variants (36.4%) increased during 2024–2025 (Figure 1, panel E).

Phylogenetic analysis of the RepMP4 region of *M. pneumoniae* strains indicated that all P1-1 type strains (95.1%), including specimens from 2017–2020 (n = 16), clustered together on a distinct branch, separate from previously described strains from Ontario reported >10 years ago (*8*) (Figure 2). That previous study, conducted at the Public Health Ontario Laboratory, included representative specimens from across Ontario, including submissions from the Hamilton region (S.N. Patel, Public Health Ontario, pers. comm., email, 2025 Jul 28). Only 2 strains (MP_ON_05 and MP_ON_71) from the current outbreak showed homology with previously collected strains from Ontario, suggesting the RepMP4 region of P1-1–type

strains has evolved over time while circulating in Ontario. Among the P1-2 types, 4 strains (15.4%) clustered with previously reported P1-2b variants, and 1 strain appeared related to P1-2c variants reported earlier in Ontario. In addition, our study revealed that P1-2 variants 2g/2j were circulating in Ontario as early as 2013, despite not having been previously reported in the region.

The first limitation of our study is that P1 typing was performed on only a subset of samples, and variant analysis relied solely on RepMP4 sequencing. Consequently, some P1-2 variants could only be assigned to variant groups (i.e., 2g/2j and 2c/2k). Moreover, few samples from 2013–2020 were available for P1 genotyping. Nevertheless, despite stable macrolide resistance rates, our findings show a major shift in the molecular epidemiology of *M. pneumoniae* since 2011-2012. Earlier Ontario data (2011–2012) reported P1-1 made up 38.1% of strains and P1-2 61.9% of strains (*8*), whereas in our study, ≈81% of P1-typed strains from the 2024–2025 outbreak were P1-1 type. Furthermore, unlike the previous study, which found no association between macrolide resistance and P1 types, our study shows significantly higher rates of macrolide resistance in the P1-1 group of *M. pneumoniae*. In addition, the distribution of P1-2 variants during the postpandemic period appeared more diverse than in the prepandemic period, and the P1-2c/2k variants expanded postpandemic. Our data, however, represent only the population of the Hamilton region; regional variation elsewhere in Ontario cannot be excluded.

The percentages of P1-1 versus P1-2 types in specimens from 2013–2020 (Figure 1, panel E) differs from previous reports for 2011–2012 (8). That discrepancy reflects that most prepandemic samples in our study (22/23) were collected during 2017–2020; only 1 was from 2013. Those data also suggest that the shift from predominantly P1-2 to P1-1 types might have begun before the pandemic.

Conclusions

Our study provides a snapshot of macrolide resistance rates and P1 genotypes of *M. pneumoniae* strains in Hamilton, Ontario, Canada, nearly a decade after the last provincial report. Macrolide resistance rates appear to have remained stable over that time, but we observed major changes in the P1 cytadhesin types of *M. pneumoniae* circulating in the Hamilton region. Clinicians and other public health professionals should be aware of those changes and their potential effects on clinical and public health management of respiratory infections caused by *M. pneumoniae* in Ontario.

Acknowledgments

We thank all laboratory technologists and technicians at the Virology and Molecular Microbiology Laboratories of the Hamilton Regional Laboratory Medicine Program for conducting routine testing for *M. pneumoniae*.

All sequences analyzed during this study have been submitted to GenBank (accession nos. PX307108–237).

About the Author

Dr. Fatima is a postdoctoral fellow at the Research Institute of St. Joe's and McMaster University. Her research focuses on genomic surveillance of infectious pathogens. Dr. Jayaratne is an associate professor at McMaster University. His primary research interest is the development of molecular diagnostic tests for infectious diseases.

References

1. Waites KB, Xiao L, Liu Y, Balish MF, Atkinson TP. *Mycoplasma pneumoniae* from the respiratory tract and beyond. Clin Microbiol Rev. 2017;30:747–809. https://doi.org/10.1128/CMR.00114-16
2. Chen YC, Hsu WY, Chang TH. Macrolide-resistant *Mycoplasma pneumoniae* infections in pediatric community-acquired pneumonia. Emerg Infect Dis. 2020;26:1382–91. https://doi.org/10.3201/eid2607.200017
3. Upadhyay P, Singh V. *Mycoplasma pneumoniae* outbreak in 2023: post-pandemic resurgence of an atypical bacterial pathogen. Cureus. 2024;16:e58757. https://doi.org/10.7759/cureus.58757
4. Meyer Sauteur PM, Beeton ML; European Society of Clinical Microbiology and Infectious Diseases (ESCMID) Study Group for Mycoplasma and Chlamydia Infections (ESGMAC), and the ESGMAC Mycoplasma pneumoniae Surveillance (MAPS) study group. Mycoplasma pneumoniae: delayed re-emergence after COVID-19 pandemic restrictions. Lancet Microbe. 2024;5:e100–1. https://doi.org/10.1016/S2666-5247(23)00344-0
5. Edouard S, Boughammoura H, Colson P, La Scola B, Fournier PE, Fenollar F. Large-scale outbreak of *Mycoplasma pneumoniae* infection, Marseille, France, 2023–2024. Emerg Infect Dis. 2024;30:1481–4. https://doi.org/10.3201/eid3007.240315
6. Public Health Ontario. *Mycoplasma pneumoniae* testing at Public Health Ontario [cited 2025 Jun 11]. https://www.publichealthontario.ca/-/media/Documents/M/24/mycoplasma-pneumoniae-testing-pho.pdf
7. Jiang FC, Wang RF, Chen P, Dong LY, Wang X, Song Q, et al. Genotype and mutation patterns of macrolide resistance genes of *Mycoplasma pneumoniae* from children with pneumonia in Qingdao, China, in 2019. J Glob Antimicrob Resist. 2021;27:273–8. https://doi.org/10.1016/j.jgar.2021.10.003
8. Eshaghi A, Memari N, Tang P, Olsha R, Farrell DJ, Low DE, et al. Macrolide-resistant *Mycoplasma pneumoniae* in humans, Ontario, Canada, 2010–2011. Emerg Infect Dis. 2013;19:1525–7. https://doi.org/10.3201/eid1909.121466

Address for correspondence: Mohammad Rubayet Hasan, Hamilton Regional Laboratory Medicine Program, Department of Pathology and Molecular Medicine, McMaster University, Hamilton, ON L8N 4A6, Canada; email: hasanm51@mcmaster.ca

Healthcare Worker Attitudes and Perceptions toward Ebola Vaccine, United States, 2024

Rinki Goswami, Anthony Lo Piccolo, Rachel Miller, Maria Frank, Corri Levine, Justin Chan

Our 2024 survey of eligible US healthcare workers found that 48% of unvaccinated healthcare workers are interested in receiving Ebola virus vaccine. The Advisory Committee on Immunization Practices recommended vaccination for healthcare workers at highest risk for occupational exposure to Zaire ebolavirus (*Orthoebolavirus zairense*). Addressing concerns identified by survey respondents might improve vaccine acceptance.

Orthoebolaviruses can be transmitted zoonotically or through exposure to bodily fluids from patients with Ebola disease (*1*). *Orthoebolavirus zairense* (Zaire ebolavirus) is the species most associated with outbreaks (*2*). During the 2014–2016 Zaire ebolavirus epidemic in West Africa, healthcare workers (HCWs) were infected and died from Ebola virus disease (EVD) at much higher rates than the general population (*3*). Four EVD cases were diagnosed in the United States, including 2 nurses involved in the care of an infected patient (*4*).

In 2019, the US Food and Drug Administration approved the Ebola vaccine ERVEBO (Merck, https://www.merck.com). The US Advisory Committee on Immunization Practices (ACIP) recommends the vaccine as a preexposure vaccination for persons at the highest risk of occupational exposure to Zaire ebolavirus (*5*,*6*). Eligible occupational risk groups include those responding to an outbreak, working as personnel at special pathogens treatment centers, or working as laboratorians handling specimens that might contain Zaire ebolavirus.

ERVEBO is highly effective in preventing disease caused by Zaire ebolavirus. The vaccine is a single-dose intramuscular injection that uses a live, attenuated recombinant vesicular stomatitis virus (VSV) to display the Ebola virus (strain Kikwit 1995) surface glycoprotein. An open-label, cluster-randomized ring vaccination trial done in Guinea and Sierra Leone estimated a vaccine efficacy of 100% (95% CI 79.3%–100.0%) (*7*). Subsequent observational studies also demonstrated vaccine effectiveness against Ebola virus transmission and death (*8*,*9*).

The real-world effectiveness of the vaccine in preventing EVD also depends on the willingness of HCWs to receive it. In this article, we describe the perceptions, attitudes, and desire to be vaccinated with ERVEBO among a sample of eligible HCWs from the United States.

The Study

We conducted a cross-sectional online anonymous survey (Appendix, https://wwwnc.cdc.gov/EID/article/31/12/25-1078-App1.pdf) through REDCap (*10*) during March–October 2024. We distributed the survey to HCWs eligible for ERVEBO vaccination on the basis of ACIP guidelines (*5*,*6*) at 3 Regional Emerging Special Pathogen Treatment Centers (RESPTCs): NYC Health + Hospitals/Bellevue (New York, NY, USA); University of Texas Medical Branch (Galveston, TX, USA); and Denver Health and Hospital Authority (Denver, CO, USA) (*11*). We selected those survey sites because they were planning to offer ERVEBO vaccine to eligible staff. The study was approved by the New York University Grossman School of Medicine Institutional Review Board (approval no. i23-00730). We conducted recruitment through email communications (68%) and in-person invitations during optional vaccine education sessions (32%). The cohort we labeled as "interested in receiving vaccine" was made up of respondents who indicated they were already vaccinated or would definitely or probably choose to be vaccinated. The cohort we labeled as "not interested in receiving

Author affiliations: New York University Grossman School of Medicine, New York, New York, USA (R. Goswami, A. Lo Piccolo, J. Chan); NYC Health and Hospitals/Bellevue, New York (A. Lo Piccolo, J. Chan); Denver Health and Hospital Authority, Denver, Colorado, USA (R. Miller, M. Frank); University of Texas Medical Branch, Galveston, Texas, USA (C. Levine)

DOI: https://doi.org/10.3201/eid3112.251078

vaccine or unsure" was made up of respondents who indicated they would definitely or probably not choose to be vaccinated or were unsure. We compared characteristics of the 2 cohorts by using a χ^2 test and considered a p value <0.05 significant.

There were 66 respondents (37% response rate). The largest age group was 30–49 years of age (64%); 63.6% were female and 36.4% male (Table 1). Occupations represented included physicians (42%), nurses (27%), clinical laboratory professionals (24%), emergency medical technicians (5%), and research laboratory professionals (2%). The most represented hospital departments were critical care medicine (27%), hospital medicine (11%), infectious diseases (11%), and pediatric critical care (11%). More than half of participants (56%) had received some form of education on Ebola vaccines, most commonly through informational sheets or pamphlets (33%) or self-study of primary literature or public health guidelines (20%).

Thirty-four respondents (51%) were interested in receiving the vaccine, with a subset of respondents already vaccinated (n = 4) at the time of the survey (Figure, panel A). Among respondents interested and not already vaccinated, 27% would plan to get vaccinated when an EVD case appeared in the United States or their state or region (Figure, panel B).

Among those respondents unsure about or not interested in receiving the vaccine (n = 32), some reported they might be convinced to vaccinate if there were an EVD outbreak in the United States (44%); if they better understood the risks and benefits of vaccination (34%), vaccine safety (31%), or the risk of spreading VSV to others (28%); and if there were an Ebola virus vaccine using a different vaccine technology (19%). In this cohort, the most common reasons for not wanting to receive ERVEBO vaccination or being unsure of their decision included concerns about spreading VSV to others (44%), feeling that the risks of vaccine side effects are not acceptable (31%), not personally knowing enough about the vaccine to make a decision (31%), and not thinking there will be an EVD outbreak in the United States (28%).

Among all respondents, the most common concerns regarding side effects were the potential for serious side effects that lasted a long time or interfered with daily life (62%), the potential increased risk of spreading VSV to others (47%), and the potential increased risk for arthritis (36%). Many respondents expressed desire to learn more about ERVEBO (Table 2). The most selected educational topics of interest included the likelihood and nature of side effects

Table 1. Characteristics of respondents to survey of healthcare worker attitudes and perceptions toward Ebola vaccine, United States, 2024

Characteristic	Total no. (%), n = 66	No. (%) interested in receiving vaccine, n = 34	No. (%) not interested in receiving vaccine or unsure, n = 32	p value*
Age				0.437
18–29	5 (7.6)	2 (40.0)	3 (60.0)	
30–39	22 (33.3)	12 (54.5)	10 (45.5)	
40–49	20 (30.3)	11 (55.0)	9 (45.0)	
50–59	16 (24.2)	9 (56.2)	7 (43.8)	
≥60	3 (4.5)	0	3 (100.0)	
Sex				0.745
F	42 (63.6)	21 (50.0)	21 (50.0)	
M	24 (36.4)	13 (54.2)	11 (45.8)	
Profession				0.225
Clinical laboratory staff	16 (24.2)	5 (31.3)	11 (68.7)	
Research laboratory staff	1 (1.5)	0	1 (100.0)	
Nurse	18 (27.3)	12 (66.7)	6 (33.3)	
Physician	28 (42.4)	15 (53.6)	13 (46.4)	
Emergency medical technician	3 (4.5)	2 (66.7)	1 (33.3)	
Department				0.385
Emergency medicine	6 (9.1)	3 (50.0)	3 (50.0)	
Critical care medicine	18 (27.2)	11 (61.1)	7 (38.9)	
Hospital medicine	7 (10.6)	3 (42.9)	4 (57.1)	
Infectious diseases	7 (10.6)	5 (71.4)	2 (28.6)	
Pediatric critical care	7 (10.6)	5 (71.4)	2 (28.6)	
Other	1 (1.5)	0	1 (100.0)	
Unknown	20 (30.3)	7 (35.0)	13 (65.0)	
Have received Ebola vaccine education				0.463
Y	37 (56.1)	18 (48.6)	19 (51.4)	
N	28 (42.4)	16 (57.1)	12 (42.9)	
Prefer not to answer	1 (1.5)	0	1 (100.0)	

*By using χ^2 test.

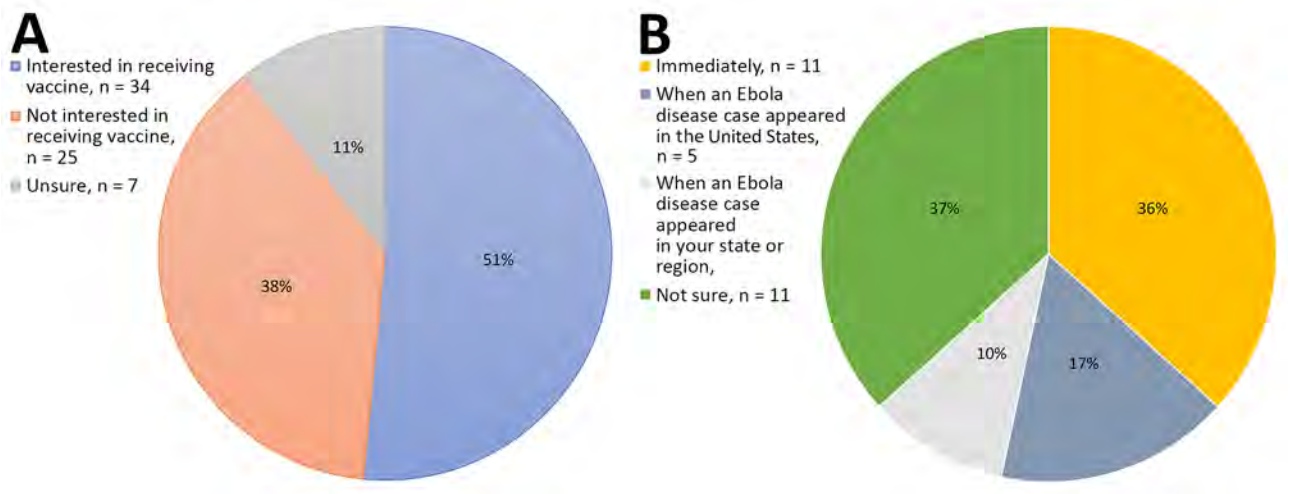

Figure. Survey responses from study of healthcare worker attitudes and perceptions toward the Ebola vaccine, United States, 2024. A) Interest in receiving ERVEBO vaccine (Merck, https://www.merck.com) among eligible healthcare workers at New York City Health + Hospitals/Bellevue (New York, NY, USA); University of Texas Medical Branch (Galveston, TX, USA); and Denver Health and Hospital Authority (Denver, CO, USA) (n = 66). B) Preferred timing for receiving ERVEBO among survey respondents who indicated they were interested in receiving vaccine and not already vaccinated (n = 30).

from vaccination (67%), the likelihood and severity of spreading VSV to others (59%), and what their individual risk of getting EVD was (26%).

In 2022, ACIP expanded their occupational exposure to include laboratory workers within the Laboratory Response Network and staff at SPTCs. They conducted a knowledge, attitudes, and practices survey in October 2020, during an EVD outbreak in the Democratic Republic of the Congo (*6*). Among SPTCs, 54% of respondents reported willingness to be vaccinated. Vaccine willingness increased to 81% if they were given the choice of vaccination timing. Those responses are consistent with our findings that many HCWs interested in ERVEBO vaccination would prefer to wait until an EVD case is imported to the United States. However, the SPTC survey did not report on specific areas of interest for more education or what factors might influence currently uninterested HCWs to get vaccinated in the future.

Surveys conducted in the Democratic Republic of the Congo (*12*) and Uganda (*13*) indicated a strong interest among HCWs to receive an Ebola vaccine. However, those data might not be generalizable to HCWs in the United States because the risk for exposure to Ebola virus is lower. A survey in 2015 during the height of the 2014–2016 Ebola outbreak in West Africa found that only 34% of the US population were interested in receiving an Ebola vaccine (*14*). This survey did not specifically assess HCW interest, and it was performed before the US Food and Drug Administration licensure of ERVEBO.

Table 2. Topics that respondents to survey of healthcare worker attitudes and perceptions toward Ebola vaccine would like to learn more about regarding Ebola virus vaccination, United States, 2024*

Topic	Total no. (%), n = 66	No. (%) interested in receiving vaccine, n = 34	No. (%) not interested in receiving vaccine or unsure, n = 32	p value†
Likelihood and nature of side effects from vaccination	44 (66.7)	23 (67.6)	21 (65.6)	0.862
Likelihood and severity of spreading vaccine virus (vesicular stomatitis virus) to others	39 (59.1)	24 (70.6)	15 (46.9)	0.050
Whether Ebola virus experts or other respected peers are getting vaccinated	14 (21.2)	8 (23.5)	6 (18.8)	0.635
Individual risk of getting Ebola virus disease	17 (25.8)	6 (17.6)	11 (34.4)	0.120
Facts about Ebola virus disease, including infectiousness and risk of severe sickness	13 (19.7)	9 (26.5)	4 (12.5)	0.154
Other‡	5 (7.6)	2 (5.9)	3 (9.4)	0.592
None of the above	8 (12.1)	3 (8.8)	5 (15.6)	0.397

*Survey question: What additional knowledge or education about the Ebola virus vaccine, ERVEBO [Merck, https://www.merck.com], would you like to receive? (Select all that apply).
†By using χ^2 test.
‡Four of 5 respondents indicated "long-term research on this vaccine."

Conclusions

During a period with no EVD outbreaks, 48% (30/62) of eligible unvaccinated HCWs surveyed at 3 US RESPTCs were interested in receiving the ERVEBO Ebola vaccine. Of those interested and not already vaccinated, 27% preferred to postpone vaccination until there is a case of EVD in the United States or their state or region.

One limitation of this study is that only 3 RESPTCs were surveyed, so their attitudes might not be representative of all US HCWs eligible for ERVEBO vaccination. Second, the sample size is too small to analyze for differences between subgroups of respondents. However, we did achieve a 37% survey response rate from a cohort of workers who are most likely to provide ongoing direct care to patients with EVD that require care in the United States.

Deployment of ERVEBO vaccine to eligible HCWs in the United States might be optimized by addressing respondent concerns. Those concerns include improving education on the risks and benefits of ERVEBO vaccination, vaccine safety, and risk of vaccine viral vector transmission.

A.L.P., R.M., M.F., C.L., and J.C. are members of their Regional Emerging Special Pathogen Treatment Center and the National Emerging Special Pathogen Treatment Center, which both receive funding from the Administration for Strategic Preparedness and Response.

About the Author

Dr. Goswami is Medical Director for Travel Medicine at BronxCare Health System and a clinical assistant professor at the Icahn School of Medicine at Mount Sinai. Her clinical and research interests include emerging infectious diseases, biohazardous threats, and travel medicine.

References

1. Jacob ST, Crozier I, Fischer WA II, Hewlett A, Kraft CS, Vega MA, et al. Ebola virus disease. Nat Rev Dis Primers. 2020;6:13. https://doi.org/10.1038/s41572-020-0147-3
2. Centers for Disease Control and Prevention. Ebola (Ebola virus disease): outbreaks [cited 2025 Jun 23]. https://www.cdc.gov/ebola/outbreaks/index.html
3. Evans DK, Goldstein M, Popova A. Health-care worker mortality and the legacy of the Ebola epidemic. Lancet Glob Health. 2015;3:e439–40. https://doi.org/10.1016/S2214-109X(15)00065-0
4. Chevalier MS, Chung W, Smith J, Weil LM, Hughes SM, Joyner SN, et al.; Centers for Disease Control and Prevention. Ebola virus disease cluster in the United States—Dallas County, Texas, 2014. MMWR Morb Mortal Wkly Rep. 2014;63:1087–8.
5. Choi MJ, Cossaboom CM, Whitesell AN, Dyal JW, Joyce A, Morgan RL, et al. Use of Ebola vaccine: recommendations of the advisory committee on immunization practices, United States, 2020. MMWR Recomm Rep. 2021;70:1–12. https://doi.org/10.15585/mmwr.rr7001a1
6. Malenfant JH, Joyce A, Choi MJ, Cossaboom CM, Whitesell AN, Harcourt BH, et al. Use of Ebola vaccine: expansion of recommendations of the advisory committee on immunization practices to include two additional populations—United States, 2021. MMWR Morb Mortal Wkly Rep. 2022;71:290–2. https://doi.org/10.15585/mmwr.mm7108a2
7. Henao-Restrepo AM, Camacho A, Longini IM, Watson CH, Edmunds WJ, Egger M, et al. Efficacy and effectiveness of an rVSV-vectored vaccine in preventing Ebola virus disease: final results from the Guinea ring vaccination, open-label, cluster-randomised trial (Ebola Ça Suffit!). Lancet. 2017;389:505–18. https://doi.org/10.1016/S0140-6736(16)32621-6
8. Meakin S, Nsio J, Camacho A, Kitenge R, Coulborn RM, Gignoux E, et al.; Epicentre-MSF EVD Working Group. Effectiveness of rVSV-ZEBOV vaccination during the 2018–20 Ebola virus disease epidemic in the Democratic Republic of the Congo: a retrospective test-negative study. Lancet Infect Dis. 2024;24:1357–65. https://doi.org/10.1016/S1473-3099(24)00419-5
9. Coulborn RM, Bastard M, Peyraud N, Gignoux E, Luquero F, Guai B, et al. Case fatality risk among individuals vaccinated with rVSVΔG-ZEBOV-GP: a retrospective cohort analysis of patients with confirmed Ebola virus disease in the Democratic Republic of the Congo. Lancet Infect Dis. 2024;24:602–10. https://doi.org/10.1016/S1473-3099(23)00819-8
10. Harris PA, Taylor R, Thielke R, Payne J, Gonzalez N, Conde JG. Research electronic data capture (REDCap)—a metadata-driven methodology and workflow process for providing translational research informatics support. J Biomed Inform. 2009;42:377–81. https://doi.org/10.1016/j.jbi.2008.08.010
11. National Emerging Special Pathogens Training and Education Center. Partners and regional contacts [cited 2025 Jun 23]. https://netec.org/about-netec/partners-regional-contacts
12. Doshi RH, Garbern SC, Kulkarni S, Perera SM, Fleming MK, Muhayangabo RF, et al. Ebola vaccine uptake and attitudes among healthcare workers in North Kivu, Democratic Republic of the Congo, 2021. Front Public Health. 2023;11:1080700. https://doi.org/10.3389/fpubh.2023.1080700
13. Waltenburg MA, Kainulainen MH, Whitesell A, Nyakarahuka L, Baluku J, Kyondo J, et al. Knowledge, attitudes, and practices and long-term immune response after rVSVΔG-ZEBOV-GP Ebola vaccination in healthcare workers in high-risk districts in Uganda. Vaccine. 2024;42:126031. https://doi.org/10.1016/j.vaccine.2024.05.079
14. Painter JE, DiClemente RJ, von Fricken ME. Interest in an Ebola vaccine among a U.S. national sample during the height of the 2014–2016 Ebola outbreak in West Africa. Vaccine. 2017;35:508–12. https://doi.org/10.1016/j.vaccine.2016.11.093

Address for correspondence: Justin Chan, NYC Health + Hospitals/Bellevue, 462 1st Ave, H-building 6W57, New York, NY 10016, USA; email: justin.chan@nyulangone.org

Persistent Infection in Harbor Seals 12–13 Years after Phocine Distemper Virus Epizootics in 1988 and 2002, North Sea

Marco W.G. van de Bildt, Jolianne M. Rijks, Trine Hammer Jensen, Sophie M.J.M. Brasseur, Marja J.L. Kik, Albert D.M.E. Osterhaus, Andrea Gröne, Thijs Kuiken, Jooske IJzer

Phocine distemper virus caused epizootics of fatal pneumonia in North Sea harbor seals in 1988 and 2002. Two seals that stranded years later were infected with defective phocine distemper virus variants that caused severe encephalomyelitis. Old seal encephalitis resembled subacute sclerosing panencephalitis in humans and old dog encephalitis in canines.

Phocine distemper virus (PDV) epizootics among harbor seals (*Phoca vitulina*) in Europe caused the deaths of ≈23,000 seals in 1988 and ≈30,000 in 2002 (*1*). Infected animals had marked lymphoid depletion and necrosis, broncho-interstitial pneumonia, and, in some cases, nonsuppurative encephalitis (*2*). For other members of the genus *Morbillivirus*, family *Paramyxoviridae*, including measles virus of humans and canine distemper virus of dogs, rare occasions of persistent central nervous system (CNS) infections have been reported that caused neurologic signs 3–20 years after the primary infection (*3*,*4*), characterized by nonsuppurative encephalitis, demyelination, and intranuclear inclusion bodies, and result in subacute sclerosing panencephalitis (SSPE) in humans and old dog encephalitis (ODE) in dogs. We report comparable persistent PDV in harbor seals, for which we propose the name old seal encephalitis.

Author affiliations: Erasmus University Medical Centre, Rotterdam, the Netherlands (M.W.G. van de Bildt, T. Kuiken); Dutch Wildlife Health Centre, Utrecht, the Netherlands (J.M. Rijks, M.J.L. Kik, J. IJzer); Aalborg University, Aalborg, Denmark (T. Hammer Jensen); Wageningen Marine Research, Den Helder, the Netherlands (S.M.J.M. Brasseur); Utrecht University, Utrecht (M.J.L. Kik, A. Gröne, J. IJzer); University of Veterinary Medicine, Hannover, Germany (A.D.M.E. Osterhaus)

DOI: https://doi.org/10.3201/eid3112.250329

The Study

We found 2 harbor seals from the North Sea stranded alive along the Netherlands coast in 2001 and 2014. The stranding of the first seal (case 1) was 13 years after the 1988 PDV epizootic and of the second seal (case 2) was 12 years after the 2002 PDV epizootic. We admitted the first seal for rehabilitation but had to euthanize it 3 weeks later because of progressive paresis of its hind limbs and weight loss. After postmortem examination, we estimated its age as 19 years, based on cementum layers in one of its upper canine teeth (*5*). We estimated the second seal as 15 years of age based on cementum layers; the animal was stranded during an influenza A(H10N7) outbreak. We euthanized it on the day of stranding because of emaciation and apathy.

We performed postmortem examinations on seal carcasses and collected samples of major organs for pathologic and virologic analyses. We performed pathologic analysis on tissues fixed in 10% neutral-buffered formalin and embedded in paraffin blocks. We cut sections 4 microns thick and stained them with hematoxylin and eosin or with luxol fast blue for histopathologic examination. We stained sequential tissue sections for virus antigen detection by an immunohistochemical technique, either using a monoclonal canine distemper virus antibody known to cross-react with PDV (VMRD, https://www.vmrd.com) for morbillivirus antigen detection or a hemagglutinin-specific mouse monoclonal antibody HB65 (ATTC H16-L10-4R5) for influenza virus antigen detection.

We performed virologic analysis for morbillivirus as described previously (*6*). In brief, we used tissue samples that had been stored frozen to test for morbillivirus by reverse-transcription PCR (RT-PCR) using universal morbillivirus primers, based on conserved sequences in the phosphoprotein,

hemagglutinin (HA), or matrix (M) genes (*7*). We sequenced selected HA gene fragments for phylogenetic comparison. To isolate morbillivirus, we inoculated 10% tissue homogenate samples of seal brain (case 1 and case 2), liver, spleen, kidney, and urinary bladder (case 2) onto Vero.DogSLAMtag cells (*8*). We made 3 consecutive passages and checked for cytopathic changes daily. We tested cells for the presence of morbillivirus by immunofluorescence (IFA) (*9*) and tested cells and supernatants by RT-PCR. We also tested tissue samples for influenza A virus by RT-PCR using specific primers (*10*).

We observed no gross lesions in brain, spinal cord, or sciatic nerves of either seal during postmortem examination. Both seals had multifocal nonsuppurative encephalomyelitis with perivascular lymphoplasmacytic cuffing (Figure 1, panel A) and rare neuronal necrosis, characterized by shrunken cells, hypereosinophilic cytoplasm, and loss of nuclei. We found lesions in the cerebrum of both seals and the cerebellum and spinal cord in case 1. In case 1, we observed demyelination in cerebellum and in ventral (Figure 1, panel B) and lateral funiculi of the spinal cord, whereas the dorsal funiculi were relatively spared. In case 2, demyelination was absent. We did not observe inclusion bodies in either case. Immunohistochemistry for morbillivirus showed staining of neurons at the sites of CNS lesions (Figure 1, panels C, D). We detected no other major lesions in case 1. In case 2, we detected avian influenza A(H10N7) virus in the lungs by RT-PCR. We did not detect influenza A antigen in the cerebrum, lung, or pulmonary lymph node in case 2. We detected the presence of PDV in the brains, but not lungs, of both animals by RT-PCR for morbillivirus and sequencing of the amplicon. We designated the strains PDV/NL/2001 (case 1) and PDV/NL/2014 (case 2). Phylogenetic analysis of the HA gene revealed that PDV/NL/2001 was most closely related to the virus from 1988, whereas PDV/NL/2014 clustered together with PDV isolated during the outbreak of 2002 (Figure 2). The M and HA genes of both PDV strains had a region with numerous uracil-to-cytosine substitutions; we identified 19 substitutions in the cytoplasmic domain and the anchor sequence of the HA gene of PDV/NL/2001 and 5 substitutions in those of PDV/NL/2014. We also observed in PDV/NL/2014 a putative truncation of the M gene. We were unable to isolate morbillivirus from tissue samples and detected no morbillivirus with IFA or RT-PCR.

Conclusions

In this study, we demonstrated marked multifocal nonsuppurative encephalomyelitis associated with

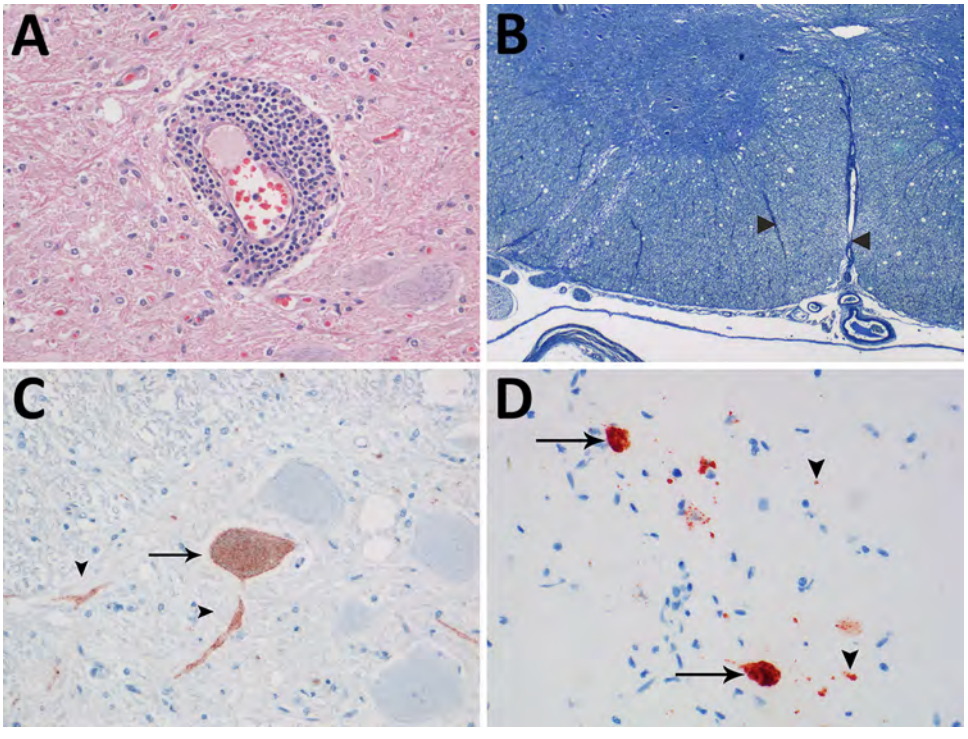

Figure 1. Evidence of persistent infection in 2 harbor seals stranded in the North Sea region years after phocine distemper virus epizootics. A) Marked perivascular accumulation of lymphocytes and plasma cells stained with hematoxylin and eosin from a seal infected in the 1988 epizootic outbreak (case 1). Original magnification ×200. B) Vacuolation and demyelination (between arrowheads) in the cervical spinal cord in case 1, stained with Kluver luxol fast blue. Original magnification ×20. C) Phocine distemper virus antigen expression in neuronal cell body (arrows) and axons or dendrites (arrowheads) of the spinal cord in case 1 by immunohistochemistry using monoclonal antibody against canine distemper virus. Original magnification ×400. D) Phocine distemper virus antigen expression in neuronal cell bodies (arrows) and axons or dendrites (arrowheads) of the spinal cord of a seal infected in the 2002 epizootic outbreak (case 2) by immunohistochemistry using monoclonal antibody against canine distemper virus. Original magnification ×400.

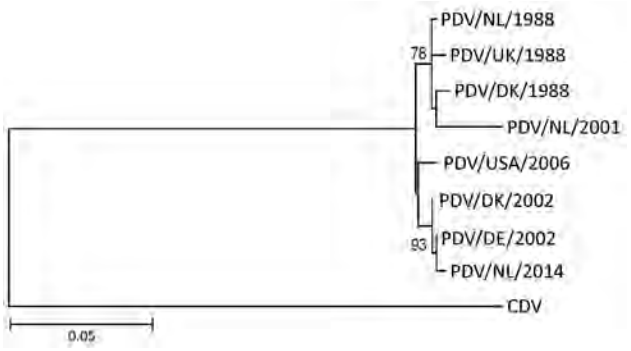

Figure 2. Phylogenetic maximum-likelihood tree based on the deduced amino acid sequence of the hemagglutinin gene (1824 nt) in study of persistent infection in 2 harbor seals stranded in the North Sea region years after phocine distemper virus epizootics. Tree was constructed using the Jones-Taylor-Thornton substitution model with invariant sites and gamma distributed rate variation with 1,000 bootstrap replicates in MEGA 6.0 (https://www.megasoftware.net). Bootstrap values >70% are shown at nodes. GenBank accession numbers for each isolate were as follows: PDV/NL/1988, NC 028249.1; PDV/UK/1988, D10371.1; PDV/DK/1988, Z36979.1; PDV/USA/2006, HQ007902.1; PDV/DK/2002, FJ648456.1; PDV/DE/2002, KU342692.1; CDV, NC 001921.1. Isolates from this study were deposited under accession nos. KY681679.1 (PDV/NL/2001) and KU342688.1 (PDV/NL/2014). Scale bar indicates nucleotide substitutions per site. CDV, canine distemper virus; PDV, phocine distemper virus.

PDV infection in 2 harbor seals that stranded several years after PDV epizootics had occurred. The seal in case 1 would have been 6 years of age during the PDV epizootic in the Northeast Atlantic harbor seal population in 1988; it was stranded in 2001 (13 years later) with an infection of PDV that clustered with those from the 1988 epizootic. The seal in case 2 would have been 3 years of age during the second PDV epizootic in 2002; it was stranded in 2014 (12 years later) with an infection of PDV that clustered with those from the 2002 epizootic. In the years after the PDV epizootics in 1988 and 2002, PDV antibody prevalence progressively declined in the Northeast Atlantic harbor seal population, indicating that PDV was no longer circulating in the population (*1*,*11*). Taking those results together, the simplest explanation is that the case 1 seal was infected during the 1988 and the case 2 seal during the 2002 PDV epizootic.

The viruses involved had multiple mutations in the HA and M genes, which resemble the biased hypermutation observed in measles virus sequences from SSPE cases (*12*). Together with the putative truncation of the M gene observed in PDV/NL/14, those mutations might result in aberrant viral protein expression. Those genetic changes, together with the failure to isolate PDV from tissue samples of cases 1 and 2, are consistent with the presence of defective and noninfectious viruses in the brains of those seals as described for persistent measles virus and canine distemper virus in the brain (*3*,*13*).

We conclude that PDV can cause persistent infection in the brains of harbor seals, with a pathogenesis similar to that of SSPE in humans from persistent measles virus infection and ODE in domestic dogs from persistent canine distemper virus infection. The characteristics of the 2 cases in harbor seals fit with those of ODE in domestic dogs and SSPE in humans in the timing (several years after presumed infection), organ distribution (limited to the CNS), level of inflammation (marked perivascular aggregation of lymphoid cells), presence of viral inclusions (variable frequency, absent in some cases), and virus properties (defective, noninfectious virus) (*3*,*4*). The presence of typical lesions in the spinal cord in case 1 is different from the distribution of lesions of ODE, which are typically restricted to the forebrain (*4*). We found no previous evidence for an ODE-like syndrome in PDV infections of pinnipeds (*14*). In line with the nomenclature in dogs, we propose the name old seal encephalitis.

The effect of PDV on the North Sea harbor seal population was thought to be limited to the periods of the 1988 and 2002 epizootics. However, the persistent infections of PDV in harbor seals causing severe neurologic disease implied that its effect extends into the interepizootic period. Our findings suggest a potential for delayed-onset encephalitis (i.e., SSPE) as a result of the current measles epidemic in the United States and Europe (*15*).

Acknowledgments

We thank Ecomare and the Seal Rehabilitation and Research Centre for taking care of the seals; Arnold Gronert and Jaap van de Hiele for seal collection and transport; Ton Richter and Fiona Read for helping to determine the seals' age; Marsha de Coo, Hélène Verheije, Steven van Beurden, Alphons van Asten, and Geert de Vrieze for technical assistance; and Ursula Siebert for providing positive control tissue.

About the Author

Mr. van de Bildt is employed at the Department of Viroscience, Erasmus University Medical Centre, the Netherlands. His research interests include emerging viral diseases, with a focus on morbillivirus infections in marine mammals.

References

1. Ludes-Wehrmeister E, Dupke C, Harder TC, Baumgärtner W, Haas L, Teilmann J, et al. Phocine distemper virus (PDV) seroprevalence as predictor for future outbreaks in harbour seals. Vet Microbiol. 2016;183:43–9. https://doi.org/10.1016/j.vetmic.2015.11.017
2. Stimmer L, Siebert U, Wohlsein P, Fontaine JJ, Baumgärtner W, Beineke A. Viral protein expression and phenotyping of inflammatory responses in the central nervous system of phocine distemper virus-infected harbor seals (*Phoca vitulina*). Vet Microbiol. 2010;145:23–33. https://doi.org/10.1016/j.vetmic.2010.02.034
3. Buchanan R, Bonthius DJ. Measles virus and associated central nervous system sequelae. Semin Pediatr Neurol. 2012;19:107–14. https://doi.org/10.1016/j.spen.2012.02.003
4. Headley SA, Amude AM, Alfieri AF, Bracarense AP, Alfieri AA, Summers BA. Molecular detection of canine distemper virus and the immunohistochemical characterization of the neurologic lesions in naturally occurring old dog encephalitis. J Vet Diagn Invest. 2009; 21:588–97. https://doi.org/10.1177/104063870902100502
5. Dietz R, Heide-Jorgensen M-P, Harkonen T, Teilmann J, Valentin N. Age determination of European harbour seal, *Phoca vitulina* L. Sarsia. 1991;76:17–21. https://doi.org/10.1080/00364827.1991.10413461
6. Daoust PY, McBurney SR, Godson DL, van de Bildt MWG, Osterhaus ADME. Canine distemper virus-associated encephalitis in free-living lynx (*Lynx canadensis*) and bobcats (*Lynx rufus*) of eastern Canada. J Wildl Dis. 2009;45:611–24. https://doi.org/10.7589/0090-3558-45.3.611
7. De Vries RD, Verburgh J, Van de Bildt MWG, Osterhaus ADME, de Swart RL. Complete genome sequence of phocine distemper virus isolated from a harbor seal (*Phoca vitulina*) during the 1988 North Sea epidemic. Genome Announce. 2013;1:e00291–13. https://doi.org/10.1128/genomeA.00291-13
8. Seki F, Ono N, Yamaguchi R, Yanagi Y. Efficient isolation of wild strains of canine distemper virus in Vero cells expressing canine SLAM (CD150) and their adaptability to marmoset B95a cells. J Virol. 2003;77:9943–50. https://doi.org/10.1128/JVI.77.18.9943-9950.2003
9. Visser IKG, Van Bressem MF, de Swart RL, van de Bildt MWG, Vos HW, van der Heijden RWJ, et al. Characterization of morbilliviruses isolated from dolphins and porpoises in Europe. J Gen Virol. 1993;74:631–41. https://doi.org/10.1099/0022-1317-74-4-631
10. Munster VJ, Baas C, Lexmond P, Waldenström J, Wallensten A, Fransson T, et al. Spatial, temporal, and species variation in prevalence of influenza A viruses in wild migratory birds. PLoS Pathog. 2007;3:e61. https://doi.org/10.1371/journal.ppat.0030061
11. Bodewes R, Morick D, van de Bildt MWG, Osinga N, Rubio García A, Sánchez Contreras GJ, et al. Prevalence of phocine distemper virus specific antibodies: bracing for the next seal epizootic in north-western Europe. Emerg Microbes Infect. 2013;2:1–5. https://doi.org/10.1038/emi.2013.2
12. Cattaneo R, Schmid A, Billeter MA, Sheppard RD, Udem SA. Multiple viral mutations rather than host factors cause defective measles virus gene expression in a subacute sclerosing panencephalitis cell line. J Virol. 1988;62:1388–97. https://doi.org/10.1128/jvi.62.4.1388-1397.1988
13. Wyss-Fluehmann G, Zurbriggen A, Vandevelde M, Plattet P. Canine distemper virus persistence in demyelinating encephalitis by swift intracellular cell-to-cell spread in astrocytes is controlled by the viral attachment protein. Acta Neuropathol. 2010;119:617–30. https://doi.org/10.1007/s00401-010-0644-7
14. Duignan PJ, Van Bressem MF, Baker JD, Barbieri M, Colegrove KM, De Guise S, et al. Phocine distemper virus: current knowledge and future directions. Viruses. 2014;6:5093–134. https://doi.org/10.3390/v6125093
15. Mathis AD, Raines K, Filardo TD, Wiley N, Leung J, Rota PA, et al. Measles update—United States, January 1–April 17, 2025. MMWR Morb Mortal Wkly Rep. 2025;74:232–8. https://doi.org/10.15585/mmwr.mm7414a1

Address for correspondence: Thijs Kuiken, Department of Viroscience, Erasmus University Medical Centre, P.O. Box 2040, 3000 CA Rotterdam, the Netherlands; email: t.kuiken@erasmusmc.nl